AN ABSTRACT OF THE THESIS OF

Jakob R. Walter for the degree of Honors Baccalaureate of Science in Civil Engineering presented on May 13, 2016. Title: Numerical Investigation of Aggregate Trench-Reinforced Clay Ground Improvement to Increase Bearing Capacity of Continuous Strip Foundations.

Abstract Approved: _____

Dr. Armin W. Stuedlein, P.E.

Compacted aggregate trenches are a method of soil improvement that could be substituted for commonly used aggregate piers in certain geometrical arrangements of shallow foundations. However, this type of ground improvement has little research to support the understanding of their contribution to improved strength of an unimproved clay soil. This study uses numerical simulations to address the current shortcomings in our understanding of the impact of compacted aggregate trench ground improvement on the bearing capacity of shallow foundations. Numerical models have been constructed in commonly-used software, *FLAC 7.0,* to conduct a parametric study of 92 different compacted aggregate trench configurations to determine their improvement relative to 15 different unimproved clay soil simulations. Typical construction equipment has been considered to establish the magnitude of various construction parameters to inform the parametric study. In the unimproved cases, different undrained shear strengths and footing embedment depths have been considered. The aggregate trench-improved models evaluate different compacted aggregate trench lengths, widths, and placement beneath a 3 meter wide strip footing in the same varying clay strength and footing embedment depths. The study demonstrates that the most significant impact to soil improvement is the placement location of the aggregate trench beneath the strip footing. Additionally, the parameter of aggregate trench length is found to have a greater contribution to soil improvement compared to trench width.

**Key Words:** Aggregate, Construction, Geotechnical, Improvement, Numerical, Trench

**Corresponding e-mail address:** waltejak@oregonstate.edu

**Numerical Investigation of Aggregate Trench-Reinforced Clay Ground Improvement to Increase Bearing Capacity of Continuous Strip Foundations**

**By**

**Jakob R. Walter**

**A PROJECT**

**Submitted to**

**Oregon State University**

**University Honors College**

**In partial fulfillment of the requirements for the degree of**

**Honors Baccalaureate of Science in Civil Engineering (Honors Scholar)**

**Presented May 13, 2016**

**Commencement June 2016**

Honors Baccalaureate of Science in Civil Engineering project of Jakob R. Walter presented on May 13, 2016.

APPROVED:

Armin Stuedlein, Ph.D., P.E.
Mentor, representing Civil and Construction Engineering

T. Matthew Evans, Ph.D.
Committee Member, representing Civil and Construction Engineering

Ben Leshchinsky, Ph.D.
Committee Member, representing Forest Engineering, Resources, and Management

Head, School of Civil and Construction Engineering

Dean, University Honors College

I understand that my project will become part of the permanent collection of Oregon State University, University Honors College. My signature below authorized release of my project to any reader upon request.

Jakob R. Walter, Author

**Acknowledgements**

I will be forever thankful to Dr. Armin Stuedlein for this research opportunity that he provided to me as an undergraduate student at Oregon State University. Through his guidance and mentorship I am pleased to have accomplished this University Honors College Thesis. His assistance and instruction within the geotechnical engineering discipline and technical writing have been an invaluable experience for which I am exceedingly grateful. I also wish to extend my gratitude to those professors, Dr. Ben Leshchinsky and Dr. Matt Evans, who accepted to fill the roles of committee members. Your contributions both further stimulated my development and understanding to this field into which I hope to continue my learning.

In addition to those professors who supported me throughout this project, I must also thank PhD candidate Andrew Strahler who provided assistance with *FLAC* on multiple occasions. His direct assistance to my models and understanding of the software was crucial to my success. Lastly, I wish to also thank MS candidate Sam Conklin for his assistance with MATLAB programing that drastically reduced the time required for data processing at the end of my project.

## TABLE OF CONTENTS

**LIST OF FIGURES** ..... **VII**

**LIST OF TABLES** ..... **XI**

**1.0 INTRODUCTION** ..... **1**

**2.0 LITERATURE REVIEW** ..... **3**

2.1 BEARING CAPACITY ..... 3

2.2 AGGREGATE PIER GROUND IMPROVEMENT ..... 4

*2.2.1 General Overview* ..... *5*

*2.2.2 Impact of Aggregate Pier Ground Improvement on Bearing Capacity* ..... *8*

2.3 SUMMARY ..... 14

**3.0 RESEARCH OBJECTIVES AND METHODOLOGY** ..... **15**

3.1 RESEARCH OBJECTIVES ..... 15

*3.1.1 Construction Constraints* ..... *15*

*3.1.2 Parametric Study* ..... *17*

3.2 RESEARCH METHODOLOGY ..... 18

**4.0 BEARING CAPACITY CALCULATIONS FOR THE CONTROL SCENARIO** ..... **20**

**5.0 *FLAC* 7.0 ANALYSIS PROGRAM** ..... **23**

5.1 SOFTWARE DESCRIPTION ..... 23

5.2 DEVELOPMENT OF FINITE DIFFERENCE MESH ..... 24

5.3 CALIBRATION OF CONSTITUTIVE MODELS ..... 28

*5.3.1 Native Ground: Elastic Perfectly-Plastic* ..... *28*

*5.3.2 Compacted Aggregate: CYSOIL Hardening Model* ..... *30*

5.4 MODELING METHODOLOGY ..... 32

*5.4.1 Parametric Study* ..... *38*

*5.4.2 Output and Data Analysis* ..... *40*

5.5 SUMMARY ..... 44

**6.0 RESULTS OF THE PARAMETRIC STUDY ..... 45**

6.1 BEARING CAPACITY VERSUS FOOTING DISPLACEMENT ..... 45

*6.1.1 Comparison to Control Scenarios ..... 45*

*6.1.2 Factors Affecting the Bearing Capacity of Improved Soil ..... 55*

6.2 CONTACT PRESSURE DISTRIBUTION BENEATH FOOTING ..... 65

*6.2.1 Comparison to Control Scenarios ..... 65*

*6.2.2 Impact of Trench Dimensions on Contact Pressure Distribution ..... 67*

6.3 SUMMARY OF RESULTS ..... 70

**7.0 SUMMARY, CONCLUSIONS, AND SUGGESTIONS FOR FURTHER STUDY ..... 72**

7.1 SUMMARY OF RESEARCH PERFORMED ..... 72

7.2 CONCLUSIONS ..... 73

7.3 SUGGESTIONS FOR FURTHER STUDY ..... 74

**REFERENCES ..... 76**

**A. APPENDIX: BEARING CAPACITY CALCULATIONS OF CONTROL SCENARIOS ..... 78**

**B. APPENDIX: TABLE OF PARAMETRIC STUDY FOR TRENCH IMPROVED CLAY SOIL ..... 87**

**C. APPENDIX: BEARING CAPACITY VS DISPLACEMENT FIGURES – ALL TRENCH IMPROVED CASES ..... 91**

**D. APPENDIX: MATLAB SCRIPT FOR THE EXTRAPOLATION OF RELEVANT CONTACT PRESSURE DATA ..... 197**

**E. APPENDIX: CONTACT PRESSURE DISTRIBUTION – ALL TRENCH IMPROVED CASES ..... 198**

## LIST OF FIGURES

Figure 2-1: Installation of aggregate piers (Hayward Baker, 2016) ..... 5

Figure 2-2: General shear failure of aggregate pier ..... 7

Figure 2-3: Localized bulging failure of aggregate pier ..... 7

Figure 2-4: Punching shear failure of aggregate pier ..... 7

Figure 2-5: Example test setup for aggregate pier: (a) schematic; (b) photograph (Stuedlein and Holtz, 2012) ..... 9

Figure 2-6: Possible aggregate pier configurations below footing: (a) single isolated pier; (b) intermediate single pier; (c) intermediate group of piers; (d) ground of piers (Stuedlein and Holtz, 2013) ..... 12

Figure 2-7: Typical experimental test setup for large footing: (a) schematic; (b) photo (Stuedlein and Holtz, 2012) ..... 13

Figure 3-1: CAT 390 excavator (left) & Komatsu PC30MR-3 mini excavator (right) ..... 16

Figure 3-2: CAT 390 with extended reach boom ..... 17

Figure 5-1: FLAC basic explicit calculation cycle (Itasca “Theory and Background,” 2011) ..... 24

Figure 5-2: FLAC clay soil finite difference mesh ..... 26

Figure 5-3: Discretization of FLAC elements into sub-elements: a) overlaid quadrilateral elements used in FLAC, b) typical triangular element with velocity vectors, c) nodal force vector (Itasca “Theory and Background,” 2011) ..... 27

Figure 5-4: FLAC Mohr-Coulomb failure criteria (Itasca “Constitutive Models” 2011) ..... 29

Figure 5-5: Formulation of model parameters for c-y soil hardening model (a) reference bulk (kref) and shear moduli (gref) (b) friction and dilation angles ..... 31

Figure 5-6: Triaxial aggregate soil data compared with FLAC CY soil hardening model..... 32

Figure 5-7: 6 meter long, 1.5 meter wide aggregate trench modeled in FLAC..... 33

Figure 5-8: 6 meter long, 1.5 meter wide aggregate trench with embedment modeled in FLAC 35

Figure 5-9: 3 meter long, 1.5 meter wide centered aggregate trench modeled in FLAC ..... 37

Figure 5-10: 3 meter long, 1.5 meter wide split edge aggregate trench modelled in FLAC ..... 38

Figure 5-11: Bearing pressure vs displacement curve of centered 3m long, 1.5m wide trench improved 40kPa clay soil profile..... 41

Figure 5-12: Contact pressure distribution of centered 3m Long, 1.5m wide trench beneath footing in 40kPa clay soil profile..... 42

Figure 5-13: Contact pressure distribution of two trenches 3m long, 0.75m wide beneath each edge of footing in 40kPa clay soil profile..... 43

Figure 6-1: Bearing pressure versus displacement with no embedment (unimproved native clay) ..... 46

Figure 6-2: Bearing pressure versus displacement (3 meter long, 1.5 meter wide trench centered beneath footing in 20 kPa, 40 kPa, and 80 kPa clay with no embedment)..... 47

Figure 6-3: Bearing pressure versus displacement (40 kPa clay improved with four different trench compacted aggregate trench configurations) ..... 49

Figure 6-4: Ultimate bearing pressure versus depth of footing embedment (no soil improvement) ..... 50

Figure 6-5: Ultimate bearing pressure versus depth of footing embedment (40 kPa native clay and single trench centered beneath footing) ..... 51

Figure 6-6: Ultimate bearing pressure versus depth of footing embedment (40 kPa native clay and two trenches along sides beneath footing) ..... 52
Figure 6-7: Effect of area replacement ratio on ultimate bearing pressure with no embedment depth (40 kPa native clay and single trench centered beneath footing)..... 53
Figure 6-8: Effect of area replacement ratio on ultimate bearing pressure with no embedment depth (40 kPa native clay and two trenches along sides beneath footing)..... 54
Figure 6-9: Ultimate bearing pressure versus trench width with no embedment depth (20 kPa native clay and single trench centered beneath footing)..... 56
Figure 6-10: Ultimate bearing pressure versus trench width with no embedment depth (40 kPa native clay and single trench centered beneath footing)..... 57
Figure 6-11: Ultimate bearing pressure versus trench width with no embedment depth (80 kPa native clay and single trench centered beneath footing)..... 58
Figure 6-12: Ultimate bearing pressure versus trench width with no embedment depth (40 kPa native clay and two trenches along sides beneath footing)..... 59
Figure 6-13: Ultimate bearing pressure versus trench length with no embedment depth (20 kPa native clay and single trench centered beneath footing)..... 60
Figure 6-14: Ultimate bearing pressure versus trench length with no embedment depth (40 kPa native clay and single trench centered beneath footing)..... 61
Figure 6-15: Ultimate bearing pressure versus trench length with no embedment depth (80 kPa native clay and single trench centered beneath footing)..... 62
Figure 6-16: Ultimate bearing pressure versus trench length with no embedment depth (40 kPa native clay and two trenches along sides beneath footing)..... 63

Figure 6-17: Contact pressure distribution of 3 m wide strip footing with no embedment over 40 kPa native clay (bearing capacity equals 214 kPa) ..... 66
Figure 6-18: Contact pressure distribution of 3m wide strip footing with 3m embedment depth over 40 kPa native clay (bearing capacity equals 300 kPa) ..... 67
Figure 6-19: Contact pressure distribution of 3m long, 1.5m wide compacted aggregate trench (40 kPa native clay and single trench centered beneath footing) ..... 68
Figure 6-20: Contact pressure distribution of 3m long, 1.5m wide compacted aggregate trench (40 kPa native clay and two trenches along sides beneath footing) ..... 69

## LIST OF TABLES

Table 3-1: Confining aggregate trench parameters ..... 16

Table 4-1: Control soil scenarios with no improvement ..... 20

Table 4-2: Calculated bearing capacity of control scenarios ..... 22

Table 5-1: Factors proposed for variation in the parametric study ..... 39

Table 6-1: Comparison of ultimate bearing pressure of trench improved soil to native unimproved soil (3m long trenches in 40kPa clay) ..... 55

Table 6-2: Resistance increase compared to unimproved 40 kPa clay per unit volume of trench improved soil profiles in 40 kPa clay ..... 64

# NUMERICAL INVESTIGATION OF AGGREGATE TRENCH-REINFORCED CLAY GROUND IMPROVEMENT TO INCREASE BEARING CAPACITY OF CONTINUOUS STRIP FOUNDATIONS

## 1.0 INTRODUCTION

With the continuous expansion of civil infrastructure in the present day, the need for site development in locations typically considered impractical is growing. As a result, projects will face new challenges as construction must be completed on soil profiles that may have previously been considered unsuitable. Methods such as aggregate pier construction currently exist to improve such soil profiles, but require specialized construction equipment that may be costly. Because of this reality the need for more simplified, but equally effective soil improvement techniques has arisen.

Aggregate pier construction involves the removal of undesirable soil using relatively uncommon auger-drilling techniques. The drilled cavity is then filled using lifts of a stronger soil material such as gravel. This procedure will be carried out in several locations to develop a grid of piers within the footprint of a proposed shallow foundation. The purpose of this is to increase the overall bearing capacity of the foundation, and thus allow for greater loads upon the foundation from the superstructure. The scope of this project is to investigate the possibility of replacing the aggregate piers in the previous example with trenches that are dug using conventional excavators and then replaced with compacted aggregate. Digging a trench with an excavator along the base of a proposed continuous shallow foundation and compacting it with gravel would be faster and more cost effective than the traditional aggregate pier soil improvement method.

A systematic study was conducted to investigate the feasibility of this ground improvement alternative. Chapter 2 begins with a review of literature on the aggregate pier ground improvement alternative. Chapter 3 presents the objectives and methodology of the research conducted on clayey soil improvement with compacted aggregate trenches. Chapter 4 will explain the control scenarios calculated for a basis of comparison for the research, and Chapter 5 details the use of the software used for numerical modeling that forms the basis of this research. Chapter 6 will present the results of the study, followed by a summary of the work completed with suggestions for future research in Chapter 7. A bibliography and appendices follow the summary.

# 2.0 LITERATURE REVIEW

## *2.1 Bearing Capacity*

The concept of bearing capacity refers to a soils ability to support an amount of bearing pressure associated with bearing failure. Terzaghi (1943) proposed the framework for the current theory for the bearing capacity of a soil. The equation developed by Terzaghi (1943) related the strength parameters of the soil, such as the cohesion and friction angle, and the unit weight of the soil, along with geometric characteristics of a footing such as the depth of embedment and width to the bearing capacity (Cerato & Lutenegger, 2007). The original formula developed by Terzaghi (1943) is given by:

$$q_{ult} = c'N_c + \sigma'_{zD}N_q + \frac{1}{2}\gamma' B N_\gamma \qquad (2\text{-}1)$$

In Equation 1-1 above, $N_c$, $N_q$, and $N_\gamma$ correspond to bearing capacity factors determined by Terzaghi (1943) and developed as a function of $\phi$', the soil friction angle. While this method of establishing the ultimate bearing capacity for a soil deposit provides a good approximation, many researchers such as Meyerhof (1953, 1963), Brinch Hansen (1970), and Vesić (1973, 1975) have contributed extensive work to improve upon this method (Coduto, 2001). Additional factors to account for impacts due to footing shape, depth of embedment, load inclination, base inclination, and ground inclination have been developed to form an expanded expression for bearing capacity, expressed as:

$$q_{ult} = c'N_c s_c d_c i_c b_c g_c + \sigma'_{zD}N_q s_q d_q i_q b_q g_q + \frac{1}{2}\gamma' B N_\gamma s_\gamma d_\gamma i_\gamma b_\gamma g_\gamma \qquad (2\text{-}2)$$

where

$c'$ = soil cohesion

$\sigma'_{zD}$ = vertical effective stress at depth of footing

$\gamma'$ = unit weight of soil

$B$ = width of footing

$s_c, s_q, \& \, s_\gamma$ = footing shape factors

$d_c, d_q, \& \, d_\gamma$ = footing depth factors

$i_c, i_q, \& \, i_\gamma$ = load inclination factors

$b_c, b_q, \& \, b_\gamma$ = base inclination factors

$g_c, g_q, \& \, g_\gamma$ = ground inclination factors

This expanded expression for bearing capacity provides a more general framework for evaluating the factors affecting the capacity provided by the soil to the footing under consideration. However, one limitation of this expression is that it is limited to the application of a footing resting on a single, uniform or homogeneous soil deposit and is thus inappropriate for use in determining the bearing capacity of a soil composite such as native soil improved with compacted gravel aggregate.

### *2.2 Aggregate Pier Ground Improvement*

A common method of increasing the bearing capacity of a relatively weak soil stratum is the installation of a single or grouping of aggregate piers under a structure footprint (Stuedlein and Holtz, 2013). The following sections discuss this method along with the benefits and draw backs to this type of engineered fill as means for soil improvement.

### 2.2.1 General Overview

An aggregate pier is a column of compacted coarse aggregate that is placed within a native or pre-existing soil deposit, and is also referred to as a stone column. Stone columns are used to not only reinforce the surrounding soil in stiffness and strength, but also increase drainage and rate of consolidation of compressible soils (Stuedlein and Holtz, 2013). A variety of installation techniques have been developed for aggregate piers. However, is has been proven that the construction method has little impact on the soil improvement characteristics of the piers, given that the aggregate is compacted with modern methods (Stuedlein and Holtz, 2012). Figure 2-1 below illustrates the installation of a series of aggregate piers. The first stage involves drilling or excavating a cavity, and the second stage fills the cavity in multiple lifts with gravel aggregate and compacting the material with compaction equipment. The resulting product is then a profile of reinforced, composite soil for which a shallow foundation can be constructed upon.

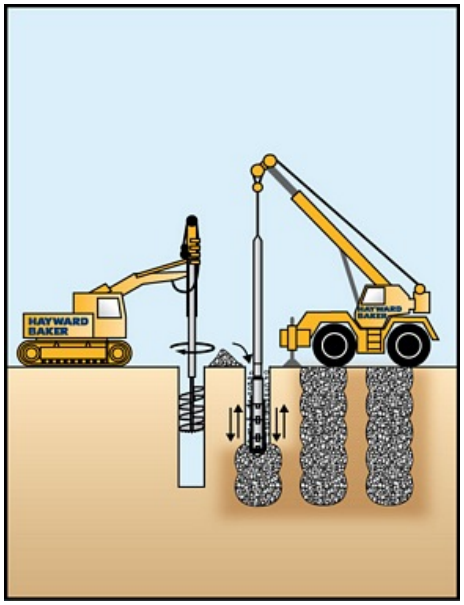


*Figure 2-1: Installation of aggregate piers (Hayward Baker, 2016)*

For many decades, researches have been working to establish suitable methods for identifying an accurate bearing capacity of aggregate reinforced soil. Early investigations by Hughes and Withers (1974) developed predictions of the capacity of a single stone column from the use of the unit cell and pressuremeter test analog. In present day, researchers such as Etezad et al. (2015), utilize numerical methods to analyze column groupings through a multitude of analytical models in an effort to produce design charts with modified bearing capacity factors.

While the analytical methods have varied over the years and between those conducting research projects, three methods of failure associated with stone column reinforced soil have become widely agreed upon. These modes of failure can be observed in Figure 2-2 through Figure 2-4 on the following page.

The failure mechanisms shown on the next page were developed using numerical methods reported by Hanna et al. (2013). Figure 2-2 depicts a scenario in which the full side friction of the aggregate pier has been mobilized. In this case, the failure plane develops into a continuous surface through the sides of the pier up to the ground surface. Figure 2-3 presents the case in which the lateral earth pressure in the aggregate pier exceeds the capacity of the confining clay soil. In this scenario the sides of the pier will bulge out into the clay stratum. Figure 2-4 illustrates the failure of the clay soil surrounding the aggregate pier as if it were a stiff columnar element, similar to a pile foundation. This case is extremely rare and inappropriate for use since aggregate piers are never as stiff as a steel or concrete pile (Madhav and Vitkar, 1978).

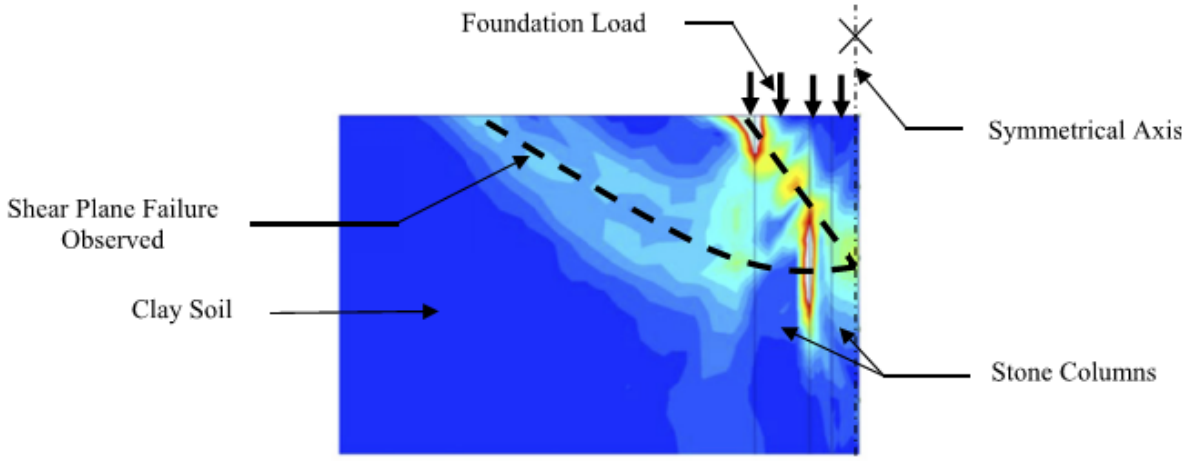


*Figure 2-2: General shear failure of aggregate pier*

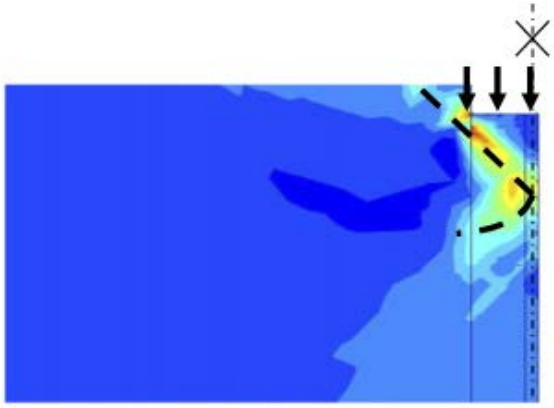

*Figure 2-3: Localized bulging failure of aggregate pier*

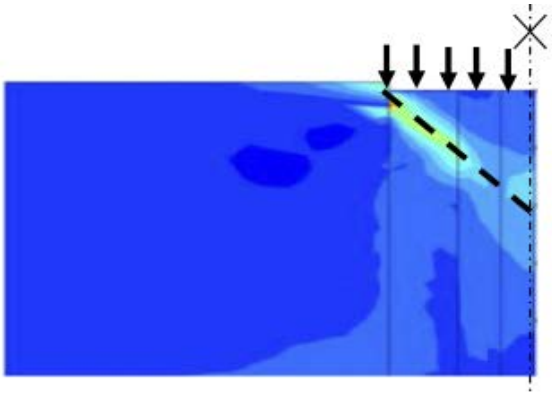

*Figure 2-4: Punching shear failure of aggregate pier*

Previous research has been conducted by Stuedlein and Holtz (2012) to better understand the occurrence of different failure mechanisms of rammed aggregate piers. It has been generally identified that in the case of a single, isolated pier, short profiles with a slenderness ratio less than 3 will experience a toe plunging failure. Conversely, in the case of a long aggregate pier, failure is governed by the bulging case (Stuedlein and Holtz, 2013).

### 2.2.2 Impact of Aggregate Pier Ground Improvement on Bearing Capacity

The dimensions of an aggregate pier or trench within a soil profile controls the performance of the supported footing as proven through experimental research conducted by White et al. (2007), Stuedlein and Holtz (2012), and others. An example experiment for a small footing above an improved profile with a single aggregate pier can be seen in Figure 2-5. This schematic and photograph is exemplary of the testing conducted by Stuedlein and Holtz (2012). In the schematic it can be observed how a footing would be constructed over a single aggregate pier to increase soil bearing capacity.

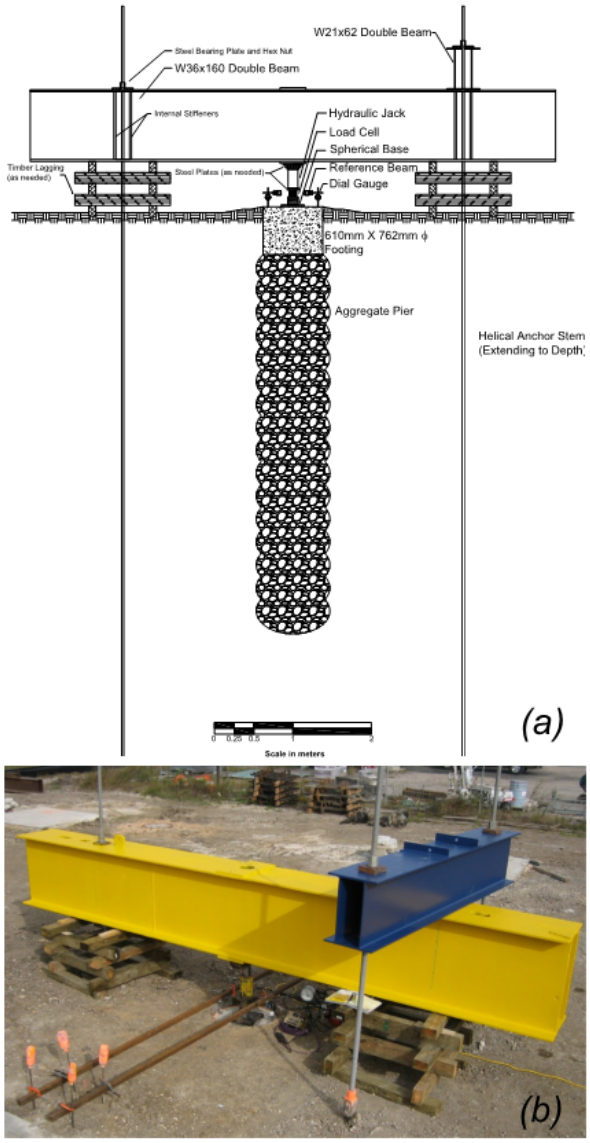


*Figure 2-5: Example test setup for aggregate pier: (a) schematic; (b) photograph (Stuedlein and Holtz, 2012)*

In the case of general shear, the width of the aggregate ground improvement relative to the loaded region or footing is the primary factor impacting bearing capacity over and above other factors, such as the native soil properties. The impact of an aggregate pier trench on

bearing capacity of a soft soil was investigated by Madhav et al., (1979), who proposed that the ultimate bearing of the reinforced soil, $q_{ult}$, can be given by:

$$q_{ult} = \frac{1+sin\phi_1}{1-sin\phi_1}(4c_2 + \sigma'_{ro} + k_0 q_s) - \frac{d^2 p}{B^2} + (1 - \frac{d^2 p}{B^2})q_s \qquad (2\text{-}3)$$

where

$q_s$ = is 2/3 the bearing capacity of unreinforced soil;

$\phi_1$ = is the friction angle of aggregate;

$c_2$ = is the cohesion of soft soil;

$k_0$ = is the at rest lateral earth pressure of soft soil;

$d_p$ = is the width of aggregate pier or trench;

$B$ = is the width of footing or loaded area.

It is important to note that the replacement ratio, $\frac{d_p}{B}$, is restricted to the range of 0 to 1. In addition to this equation, Madhav et al., (1979) also developed design charts for Terzaghi's bearing capacity factors using plasticity theory and confirmation from experimental results. This work resulted in correlations between strength properties of the two soil stratums and replacement ratio to modified bearing capacity factors. Applications of these charts however, are limited to specific strength property ratios between the two types of soil.

Since this early development of bearing capacity calculations to estimate the improvement of soil performance with the introduction of a granular fill by Madhav et al. (1979) additional, recent research has been conducted. The topic has been investigated though experimental testing by White et al. (2007), with laboratory model tests by Nazir and Azzam (2010), and by assessment of analytical models such as those of Etezad et al. (2015). Stuedlein

and Holtz (2013) conducted some of the most recent work to improve existing models with empirical modifications. This included applying all relevant past models to a test sample consisting of 30 different footing loading tests on stone columns to determine the accuracy and uncertainty for each method. Ultimately the Modified Hughes et al. (1975) method was deemed preferable for estimating the bearing capacity of an aggregate pier supported shallow foundation. The resulting equation of this model is given by:

$$q_{ult} = \left[\sigma_{ro} + k_p * s_u\right] * \frac{1+sin(\phi_P)}{1-sin(\phi_P)} \qquad (2\text{-}4)$$

where

$\sigma_{ro}$ = is the ultimate total in situ lateral stress;

$s_u$ = is the surrounding soil cohesion;

$\phi_P$ = is the friction angle of the aggregate;

$k_p$ = is the modified cavity expansion factor and defined by:

$$k_p = -1.45 * ln(s_u) + 8.52 \qquad (2\text{-}5)$$

Equation (2-4) was also modified to account for a group of aggregate piers installed beneath a footing. Typical unimproved soil bearing capacity factors may be applied to account for depth of embedment of the footing and square or circular profiles. Figure 2-6 demonstrates some of the possible aggregate pier configurations below a footing for which the modified equation could be applicable.

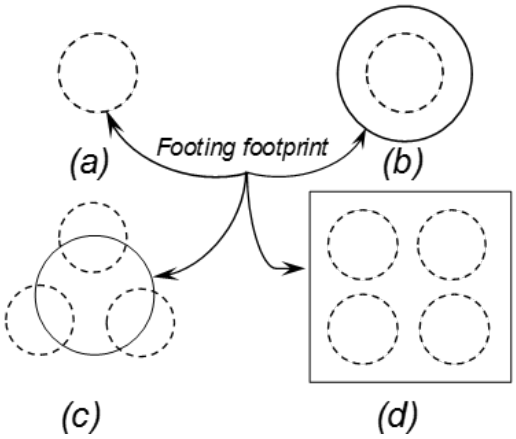


*Figure 2-6: Possible aggregate pier configurations below footing: (a) single isolated pier; (b) intermediate single pier; (c) intermediate group of piers; (d) ground of piers (Stuedlein and Holtz, 2013)*

The form of this modified equation is given by:

$$q_{ult} = \left[\sigma_{ro} + k_p * s_u\right] * \frac{1+sin(\phi_P)}{1-sin(\phi_P)} + \lambda_c d_c N_c s_u * (1 - a_r) \qquad (2\text{-}6)$$

where

$\lambda_c$ = is a footing shape factor;

$d_c$ = is a footing depth correction factor;

$a_r$ = is the area replacement ratio defined as the ratio of aggregate pier area versus total area under the footing.

Figure 2-7 below demonstrates the typical test set up for a footing supported by multiple aggregate piers as conducted by Stuedlein and Holtz (2012). This figure shows that the aggregate piers only account for a portion of the area under the square footing.

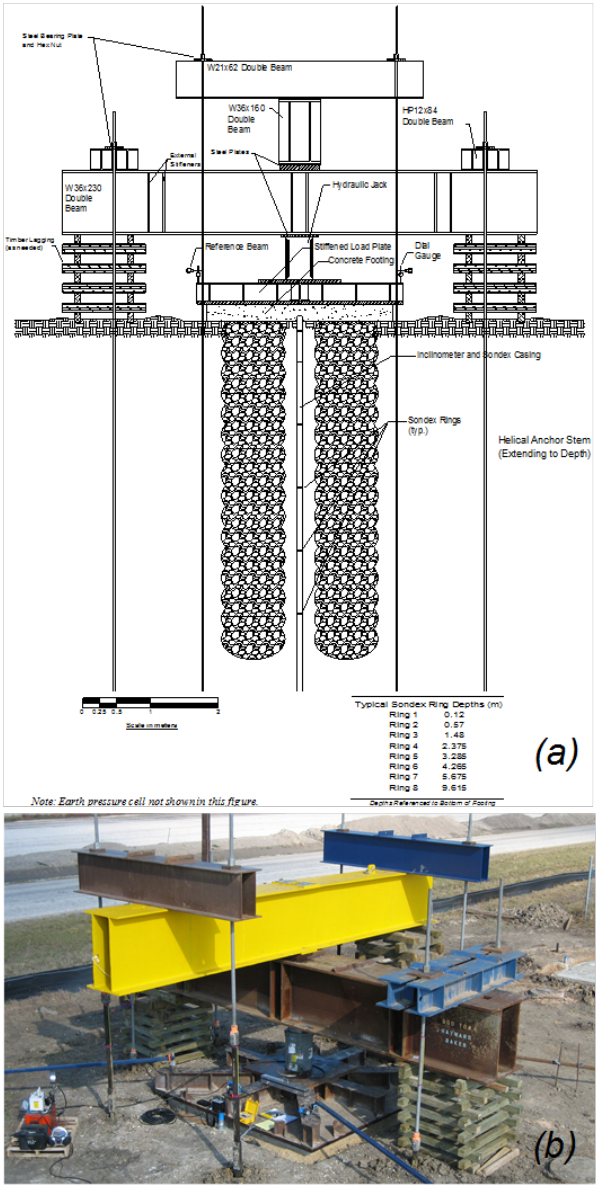


*Figure 2-7: Typical experimental test setup for large footing: (a) schematic; (b) photo (Stuedlein and Holtz, 2012)*

The research completed by Stuedlein and Holtz (2013) provides the basis for the development of the Modified Hughes et al. (1975) method for calculating aggregate pier improved soil capacity. An improved understanding of aggregate pier bearing capacity has been

established as a result. However, this work is not appropriate for aggregate trench-improved ground.

### *2.3 Summary*

For many decades the impact of rammed aggregate piers installed in soft soils on the bearing capacity of the overall soil system has been researched. With established models such as the Modified Hughes et al. (1975) method, a reliable calculation can be made to estimate the bearing capacity of an aggregate pier reinforced soil. These methods consider more soil and pier parameters and result in less error than methods ever used before.

With the lack of validated methods for aggregate trenches, the study of the deformation and bearing capacity of compacted aggregate trenches seems warranted. Methods for estimating the bearing capacities of soil profiles such as these are relatively under-developed and date back to methods developed by Madhav and Vitkar (1978). As a result, further research is warranted to improve our understanding of the bearing capacity improvements through the use of compacted aggregate trenches. The other aspect of compacted aggregate trenches that has not been investigated is the magnitude of footing settlements as a function of other possible design variables; this area of research would also be warranted in future research.

# 3.0 Research Objectives and Methodology

The primary goal of this research project is to investigate the application of compacted aggregate trenches as an alternative for aggregate piers to improve the bearing capacity of a clay soil stratum. In order to determine the suitability of this alternative, a study of different trench design parameters will be conducted and evaluated on the basis of footing performance.

## *3.1 Research Objectives*

The effect of a compacted granular aggregate trench installed in a plastic, fine-grained soil on bearing capacity is relatively unknown when compared to that of aggregate piers. For this reason, the first objective of the project was to establish what trench dimensions should be evaluated. With an understanding of what trench dimensions may vary due to construction constraints, the parameters of the study can be established. Compacted granular aggregate trench improved soil profiles within a plastic, fine-grained soil will then be evaluated using numerical methods to determine bearing capacity and compared with unimproved soil bearing capacity. Iterations to this process will then be made to determine what compacted aggregate trench parameters are most significant for improving the bearing capacity of a plastic, fine-grained soil.

### 3.1.1 Construction Constraints

It was important to consider the types of equipment that would be used in this type of construction and the constraints associated with the use of such equipment. Figure 3-1 on the following page depicts two possible pieces of equipment for trench excavation representing minimum and maximum reach and bucket width.

*Figure 3-1: CAT 390 excavator (left) & Komatsu PC30MR-3 mini excavator (right)*

Excavators in size ranging between those shown in Figure 3-1 can be paired with a wide range in bucket sizes to achieve a number of possible trench widths and depths. The corresponding bounds in trench dimensions are listed in Table 3-1.

*Table 3-1: Confining aggregate trench parameters*

| | **Depth of Trench** *(meters)* | **Width of Trench** *(meters)* | **Equipment** |
|---|---|---|---|
| **Minimum** | 0 | 0.3 | Komatsu |
| **Maximum** | 8.3 | ∞ | CAT |

The parameters shown in Table 3-1 were established by considering the Komatsu Mini Excavator with a minimum bucket width of 0.3 meters, and the CAT with a maximum bucket width of 2.35 meters. The maximum depth for digging a vertical wall was also found to be 8.3 meters and 2.4 meters for the CAT and Komatsu excavators respectively. Deeper depths can be reached with specialized extended reach arms such as the CAT in Figure 3-2 below.

*Figure 3-2: CAT 390 with extended reach boom*

Attachements such as these however would not be considered common on a construction site and are thus not considered in this study. Minimum trench depth and maximum trench width would not be of concern since any equipment could dig a shallow excavation or make multiple digging passes to expand width.

### 3.1.2 Parametric Study

A parametric study may now be developed to encompass the ranges in realistic dimensions of trench construction possible with common excavators and compaction equipment. This study investigated the effect of geometrical parameters including the trench width and depth, and depth of footing embedment. Additionally the undrained shear strength of the native or existing clayey soil was also varied.

### *3.2 Research Methodology*

This study included the assessment of the bearing capacity of the unreinforced clayey subgrade in order to develop a suitable control scenario for each corresponding aggregate trench scenario. The control scenarios evaluated are presented in Table 4-1 in the following chapter. The purpose of these unreinforced scenarios is to provide a standard basis of comparison for all further models with a trench improvement. The bearing capacity of these conditions was first evaluated with an equation similar to that represented in Equation (2-2), as described in greater detail in Chapter 4. The control scenarios were then also evaluated using the finite difference numerical modelling software selected for evaluation of the reinforced soil, described in detail in Chapter 5. The use of bearing capacity calculations and numerical modelling software make it possible to determine the relative degree of accuracy of the simplified calculations.

The next step was to generate numerical models of the trench reinforced soil composite. The results of the numerical simulations included the mobilization of bearing capacity as a function of the imposed displacement of the footing, and the development and distribution of contact pressure below of the footing. The simulations also provide a means to identify the progression of failure within the soil composite and improve our understanding of reinforced soil behavior. The results of the simulations were synthesized by comparing the effect of trench width, length, depth of footing embedment, and area replacement ratio on the bearing capacity. These results are presented in Chapter 6.

The computational server used for the numerical modeling portion of the project is named “Terzaghi,” and runs a Microsoft Windows Server 2008 R2 Enterprise operating system.

This computer runs on a 64 bit operating system and is installed with two Intel Xeon X5690 processors that operate at 3.46 GHz. The installed memory (RAM) of the computer is 32GB.

The finite difference software implemented for the analysis of the parametric study is *FLAC* 7.0 by Itasca. This program allows simulation of two dimensional geotechnical analyses and in this case is used to simulate the behavior of soil before, during and after yielding conditions. The program allows for the generation of a finite difference grid that represents the soil profiles as a continuum. Further explanation of the program and its application in this study can be found in Chapter 5.

## 4.0 Bearing Capacity Calculations for the Control Scenario

Before any soil models would be evaluated in *FLAC 7.0* a series of soil control scenarios was established. The calculated bearing capacity of these scenarios would be the basis of comparison for all improved soil cases to determine degree of improvement. This comparison allows for the possibility of formulating a bearing capacity factor to account for the soil improvement effects generated by an aggregate trench later in the study.

The soil conditions established for the control scenario can be observed in Table 4-1 below. In all of these cases, the footing being modeled is 3 meters in width and near-infinite to represent the long dimension of a continuous strip footing.

*Table 4-1: Control soil scenarios with no improvement*

| Undrained Shear Strength *(kPa)* | Unit Weight *($kN/m^3$)* | Depth of Footing Embedment *(m)* |
|---|---|---|
| 80 | 17.65 | 0 |
| 80 | 17.65 | 1 |
| 80 | 17.65 | 1.5 |
| 80 | 17.65 | 2 |
| 80 | 17.65 | 3 |
| 40 | 17.65 | 0 |
| 40 | 17.65 | 1 |
| 40 | 17.65 | 1.5 |
| 40 | 17.65 | 2 |
| 40 | 17.65 | 3 |
| 20 | 17.65 | 0 |
| 20 | 17.65 | 1 |
| 20 | 17.65 | 1.5 |
| 20 | 17.65 | 2 |
| 20 | 17.65 | 3 |

The bearing capacity of the above soil conditions was evaluated with the general bearing capacity equation improved with Meyerhof (1963) correction factors. The form of this equation is as follows

$$q_{ult} = c'N_c f_{cd} + \sigma' N_q f_{qd} + 0.5B\gamma N_\gamma f_{\gamma d} \quad (4\text{-}1)$$

where

$c'$ = cohesion of soil;

$\sigma'$ = vertical effective stress at base of footing;

$B$ = width of footing;

$\gamma$ = unit weight of soil;

$N_c, N_q, N_\gamma$ = bearing capacity factors;

$f_{cd}, f_{qd}, f_{\gamma d}$ = Meyerhof depth correction factors.

Bearing capacity factors used with this equation are defined as follows:

$$N_c = \pi + 2 \quad (4\text{-}2)$$
$$N_q = e^{\pi tan(\phi')} K_p \quad (4\text{-}3)$$
$$N_\gamma = 2\left(N_q + 1\right) tan(\phi') \quad (4\text{-}4)$$

Meyerhof depth correction factors applied to Equation (4-1) are defined as the following:

$$f_{cd} = 1 + 0.2\sqrt{K_p}\,\frac{d_F}{B} \quad (4\text{-}5)$$
$$f_{qd} = 1 \quad (4\text{-}6)$$
$$f_{\gamma d} = 1 \quad (4\text{-}7)$$

where

$K_p$ = passive lateral earth pressure coefficient;

$d_F$ = depth of embedment of footing.

The full evaluation of bearing capacity for each of the 15 control scenarios are represented in Appendix A. The results of the bearing capacity calculations for each selected undrained shear strength and possible depth of embedment for the study is summarized in Table 4-2 below.

*Table 4-2: Calculated bearing capacity of control scenarios*

| Undrained Shear Strength *(kPa)* | Unit Weight *($kN/m^3$)* | Depth of Footing Embedment *(m)* | Ultimate Bearing Capacity *(kPa)* |
|---|---|---|---|
| 80 | 17.65 | 0 | 411 |
| 80 | 17.65 | 1 | 456 |
| 80 | 17.65 | 1.5 | 479 |
| 80 | 17.65 | 2 | 501 |
| 80 | 17.65 | 3 | 547 |
| 40 | 17.65 | 0 | 206 |
| 40 | 17.65 | 1 | 237 |
| 40 | 17.65 | 1.5 | 253 |
| 40 | 17.65 | 2 | 268 |
| 40 | 17.65 | 3 | 300 |
| 20 | 17.65 | 0 | 103 |
| 20 | 17.65 | 1 | 127 |
| 20 | 17.65 | 1.5 | 140 |
| 20 | 17.65 | 2 | 152 |
| 20 | 17.65 | 3 | 176 |

## 5.0 *FLAC* 7.0 Analysis Program

The program Fast Lagrangian Analysis of Continua (*FLAC*) was used to conduct the numerical analysis of the various soil and footing conditions of the parametric study. This chapter describes the program and how it operates in detail, the models specific to the parametric study, and the output developed using *FLAC 7.0*.

### *5.1 Software Description*

*FLAC* is a finite difference program that conducts a two-dimensional engineering analysis of soil, rock, or other specific material within a Lagrangian formulation. To define a model for analysis, a grid or mesh of nodes at which deformation and forces are computed is created and the areas bounded by nodes define soil elements. These elements deform and respond to the user prescribed constitutive relationships and applied boundary conditions following adjustment of the grid to fit desired model geometry. Nodal forces, deformations, pressures, and/or velocities can then be applied to the grid or mesh and result in deformations and stresses as in accordance with the specified constitutive relationship.

The Lagrangian analysis conducted by *FLAC* does not require the formulation of a global stiffness matrix like finite element analysis programs. Alternatively, incremental displacements are added to defined coordinates within the grid. This method thus allows for the finite difference mesh to move in conjunction with the deformation of the soil profile unlike an Eulerian formulation where the grid is held fixed in relation to the material deformations. In order to make this type of analysis possible, the *FLAC* user defines a velocity upon the soil mesh at specific step intervals to reach an ultimate displacement. At each step of the velocity

application the software uses the new displacements to calculate the stress and strain relationship using a chosen constitutive model. This calculation will result in new stresses within the elements of the material and require a recalculation of equilibrium for the entire mesh. A visual representation of this calculation series can be seen below in Figure 5-1.

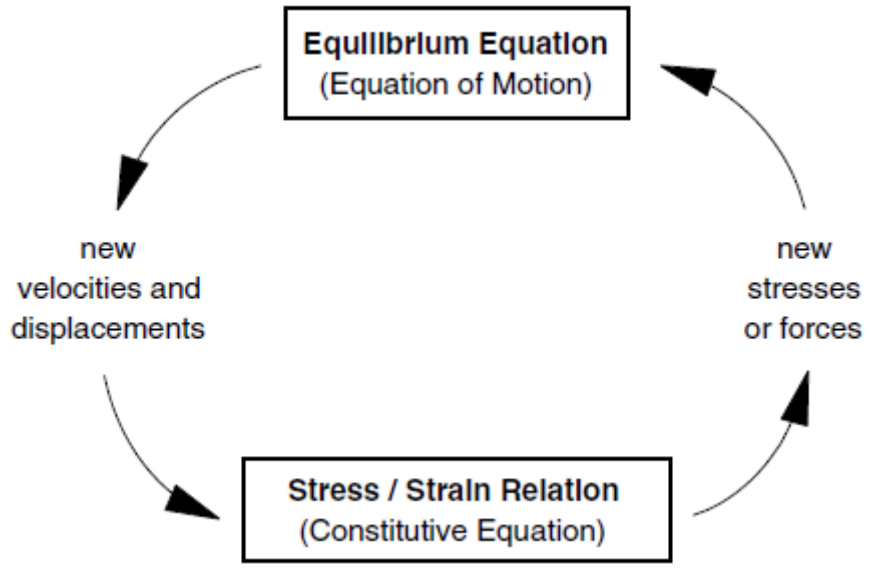


*Figure 5-1: FLAC basic explicit calculation cycle (Itasca "Theory and Background," 2011)*

### *5.2 Development of Finite Difference Mesh*

To analyze the desired soil profile, the *FLAC* user will create a mesh as discussed in Section 5.1. The Lagrangian formulation is then conducted using the finite difference method. A finite difference solution substitutes the series of differential equations needed to model the soil behavior, such as stress and strain, with an algebraic expression. The finite difference method used by *FLAC* is considered to be explicit because of the formulation of new algebraic expressions for each time step of loading. This method can be contrasted with the implicit matrix-based solutions of finite element programs. The explicit finite difference method is

advantageous for geotechnical applications as it requires no iterations to follow nonlinear constitutive models, and a comparatively small amount of computational effort is required for each time step. The disadvantage to this form however is the need for very small time steps in order to produce accurate results and prevent "noise" in the analysis output data.

To begin modeling of the soil profile for analysis, the finite difference mesh was first generated with the properties of clay as the native soil. The principle of symmetry was used to generate a mesh that represented one half of the actual ground profile to be considered (Figure 5-2). This means that half the width of the footing is modeled (placed in the top left corner of the mesh as described subsequently), and only half the width of the improved soil (i.e., the aggregate trench) would be installed prior to conducting the parametric study.

The mesh shown in Figure 5-2 consists of a square, 60 element by 60 element grid (3,600 elements in total). The mesh was generated to be finest in the top left corner and least fine in the bottom right corner with a constant rate of incremental gradation moving from the left to the right and top to the bottom. This means that soil elements nearest the zone of loading are smallest, while those furthest from loading are the largest. The advantage to this arrangement is that the regions with the highest gradients in stress and displacements will have the highest density of unbalanced force convergence requirements, thus reducing the error in the final output. Figure 5-2 also shows that boundary conditions were established on the soil mesh. The vertical sides of the soil profile are restrained from movement in the horizontal ($x$) directions as denoted by an "X" at each mesh node of both sides. The bottom of the mesh is also restrained in the vertical ($y$) direction as if there were a layer of rigid bedrock as denoted by a "B" at each mesh node along the bottom of the soil profile.

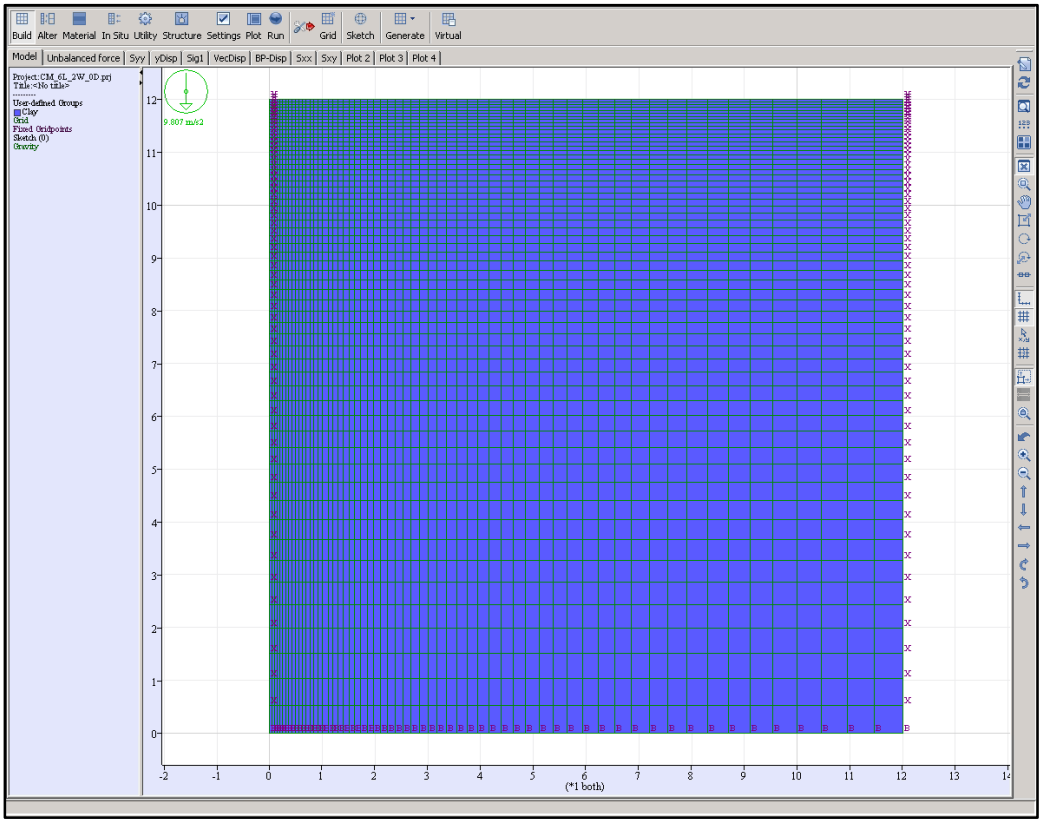


*Figure 5-2: FLAC clay soil finite difference mesh*

While the mesh in Figure 5-2 above depicts quadrilateral soil elements, *FLAC* actually conducts a finite difference analysis upon four separate triangular elements within each visible quadrilateral. These four sub-elements are formed by separately dividing a quadrilateral in half diagonally in opposing cuts as shown in Figure 5-3 below.

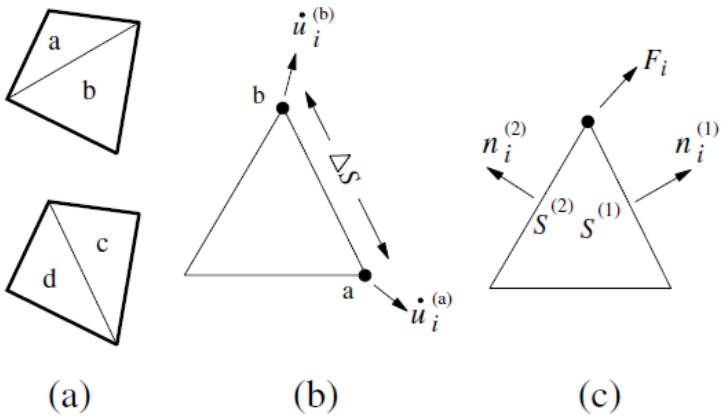


*Figure 5-3: Discretization of FLAC elements into sub-elements: a) overlaid quadrilateral elements used in FLAC, b) typical triangular element with velocity vectors, c) nodal force vector (Itasca "Theory and Background," 2011)*

Each coupled triangle (a & b, c & d) set is analyzed separately for the stress components $\sigma_{xx}, \sigma_{yy}, \sigma_{zz},$ and $\sigma_{xy}$. The stress components for the quadrilateral element is then the average of the differing stress components from each coupled triangle pair. The result of the stresses within a single element is thus formulated from 16 different values for increased accuracy. If the triangles of one set become badly distorted the force vectors of the set are not considered in the representative forces for the overall element. If both sets of triangular sub-elements become distorted, an error message results and the analysis is terminated. This error can occur when a mesh is not refined adequately for the level of deformation in the soil at a specific location, poorly set boundary conditions, or other reasons. The governing finite difference equation used to analyze each sub-element triangle is given by:

$$< \frac{\partial f}{\partial x_i} > = \frac{1}{A} \sum_s < f > n_i \Delta s \qquad (5\text{-}1)$$

where

A = is the surface area of the triangular sub-element;

$< f >$ = is the vector or tensor averaged over the triangle side length;

$n_i$ = is the unit normal to the surface, s;

$\Delta s$ = is the length of a side of the triangle.

This summation is evaluated for each side length of the four triangles within the 60 by 60 quadrilateral element mesh, resulting in 43,200 calculations for each time step in the model.

## *5.3 Calibration of Constitutive Models*

In order to effectively model accurate soil behavior within *FLAC*, appropriate constitutive models must be chosen and calibrated to meet the intended soil response. The following sections discuss the constitutive models selected to represent the clay and compacted aggregate.

### 5.3.1 Native Ground: Elastic Perfectly-Plastic

The constitutive model selected for the native clay soil was an elastic, perfectly-plastic stress-strain model with a Mohr-Coulomb failure criterion, the latter of which is shown in Figure 5-4. In this first order model, both the elastic and plastic behavior of the soil is defined linearly; slope of elastic behavior is defined by the soil modulus of elasticity and Poisson's ratio, which are calculated from the bulk and shear moduli. The assumed values for the native soil bulk and shear moduli are 5 MPa and 3 MPa respectively. The failure criteria for the soil is defined using a specified friction angle and/or cohesion intercept. In all cases of this study, the clay soil is modeled assuming undrained conditions (given the rapidity with which the loading is applied). Therefore, the strength of the clayey native subgrade is modeled with cohesions, but no a friction

angle with corresponding dilation angle. As described earlier, the undrained shear strength (i.e. cohesions) was selected equal to 20, 40, and 80 kPa.

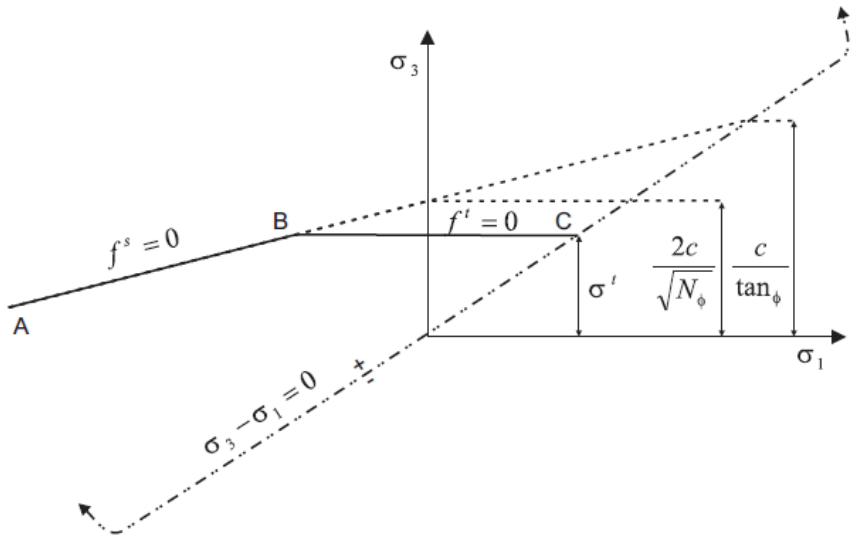


*Figure 5-4: FLAC Mohr-Coulomb failure criteria (Itasca "Constitutive Models" 2011)*

In the case of undrained conditions, the value of $f^s$, which represents the failure criterion is given by:

$$f^s = \sigma_1 - \sigma_3 + 2c \qquad (5\text{-}2)$$

where

$\sigma_1$ = major principle stress;

$\sigma_3$ = minor principle stress;

$c$ = cohesion or undrained shear strength of the clay.

This equation is simplified from its original form because the value of $N_\phi$ is equal to 1 for undrained conditions. The sign convention accompanying Figure 5-4 and Eq. (5-2) considers compressive stresses to be negative. Although the elastic-perfectly plastic constitutive model

with Mohr-Coulomb failure criterion is not the most robust formulation of soil behavior, it is a conventional and accepted model for representing failure mechanisms in soil.

### 5.3.2 Compacted Aggregate: CYSOIL Hardening Model

The constitutive model selected for the compacted aggregate material placed within the aggregate trenches within the parametric study is a cap-yield (c-y) relationship. The selection of this model was driven by the need for an accurate deviatoric and volumetric response of the aggregate. The model uses shear and volumetric hardening/softening laws to model the behavior of a soil under loaded conditions. The more accurate response is a product of the cap-yield model accounting for possible grain crushing that would be expected in an aggregate soil at high effective confining stresses. The accuracy of the cap-yield relationship is dependent on the user-defined parameters that control the soil hardening conditions. The model parameters chosen for the compacted aggregate in *FLAC* simulations were obtained through comparison to triaxial test data of a dense aggregate sample. The variation in reference bulk modulus (Kref) and reference shear modulus (Gref) that was required to reproduce the pressure dependence of the aggregate modeled is shown in Figure 5-5(a) for five different effective confining pressures, whereas the variation of friction and dilation angle with confining pressure is shown in Figure 5-5(b).

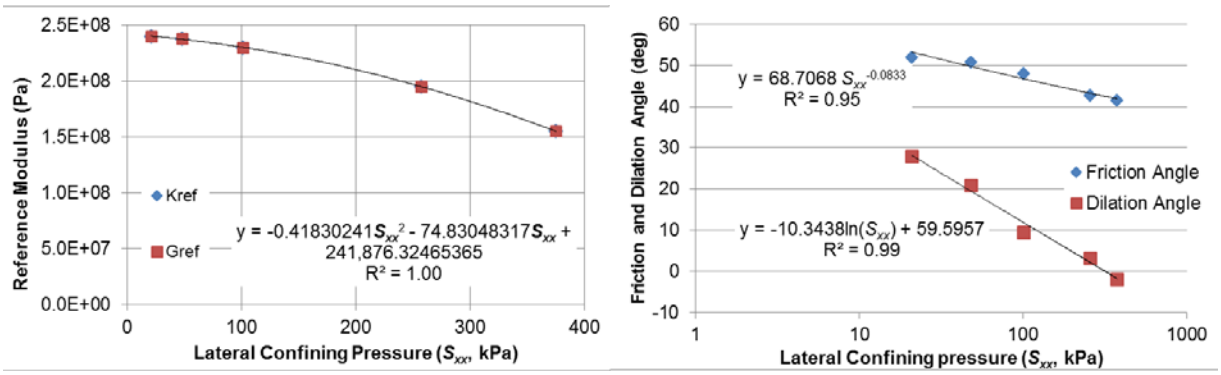


(a) (b)

*Figure 5-5: Formulation of model parameters for c-y soil hardening model (a) reference bulk (kref) and shear moduli (gref) (b) friction and dilation angles*

Constitutive model parameters selected to fit the measured response of the compacted aggregate in this study invoke those fitted parameters that correspond to an effective confining pressure of 100 kPa. The corresponding reference bulk modulus (Kref) of 230 MPa and reference shear modulus (Gref) of 230 MPa that was required to reproduce the desired response at 100 kPa. The corresponding friction and dilation angle for 100 kPa confining pressure was set at 48 and 10 degrees, respectively. Figure 5-6 below compares the measured consolidated drained triaxial test data with the simulated aggregate response using the CYSOIL constitutive model. It can be observed that the simulation closely follows the measured lab data, and therefore this model was considered suitably calibrated. It is noted that the initial volumetric contraction under small shear strains is captured, as is the subsequent development of dilation as axial strains accumulate.

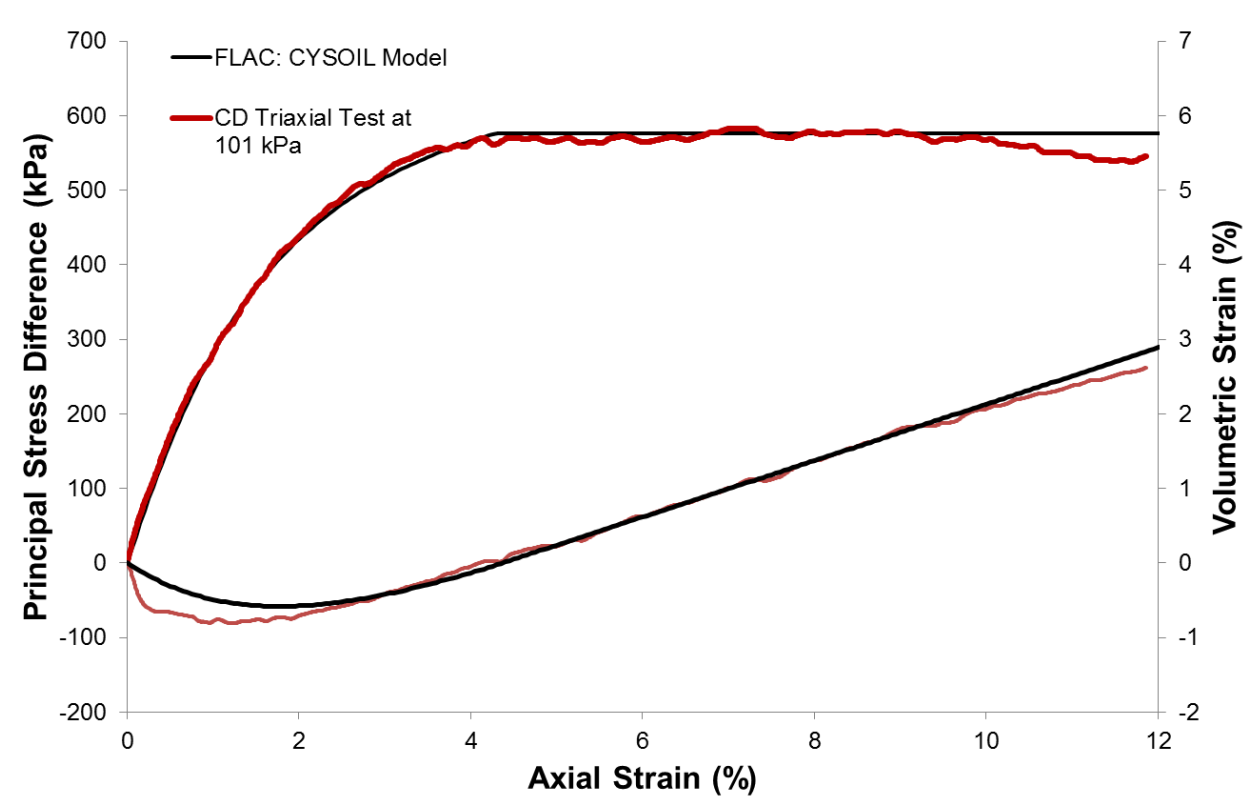


*Figure 5-6: Triaxial aggregate soil data compared with FLAC CY soil hardening model*

### *5.4 Modeling Methodology*

In order to model the aggregate trench surrounded by the native soil, a portion of the native soil in the top left corner of the mesh was removed and replaced with the aggregate characteristics described in Section 5.3.2. The trench parameters established by the parametric study are described in section 5.4.1. It is important to note that by using symmetry, the compacted aggregate trenches modelled in *FLAC* are only half of the total trench width. By modelling only half the trench and footing width, accurate values of pressure can be obtained

while reducing the necessary number of calculations (and thus time required for each model) by 50%. An example of trench placed within a native soil profile is presented in Figure 5-7 below.

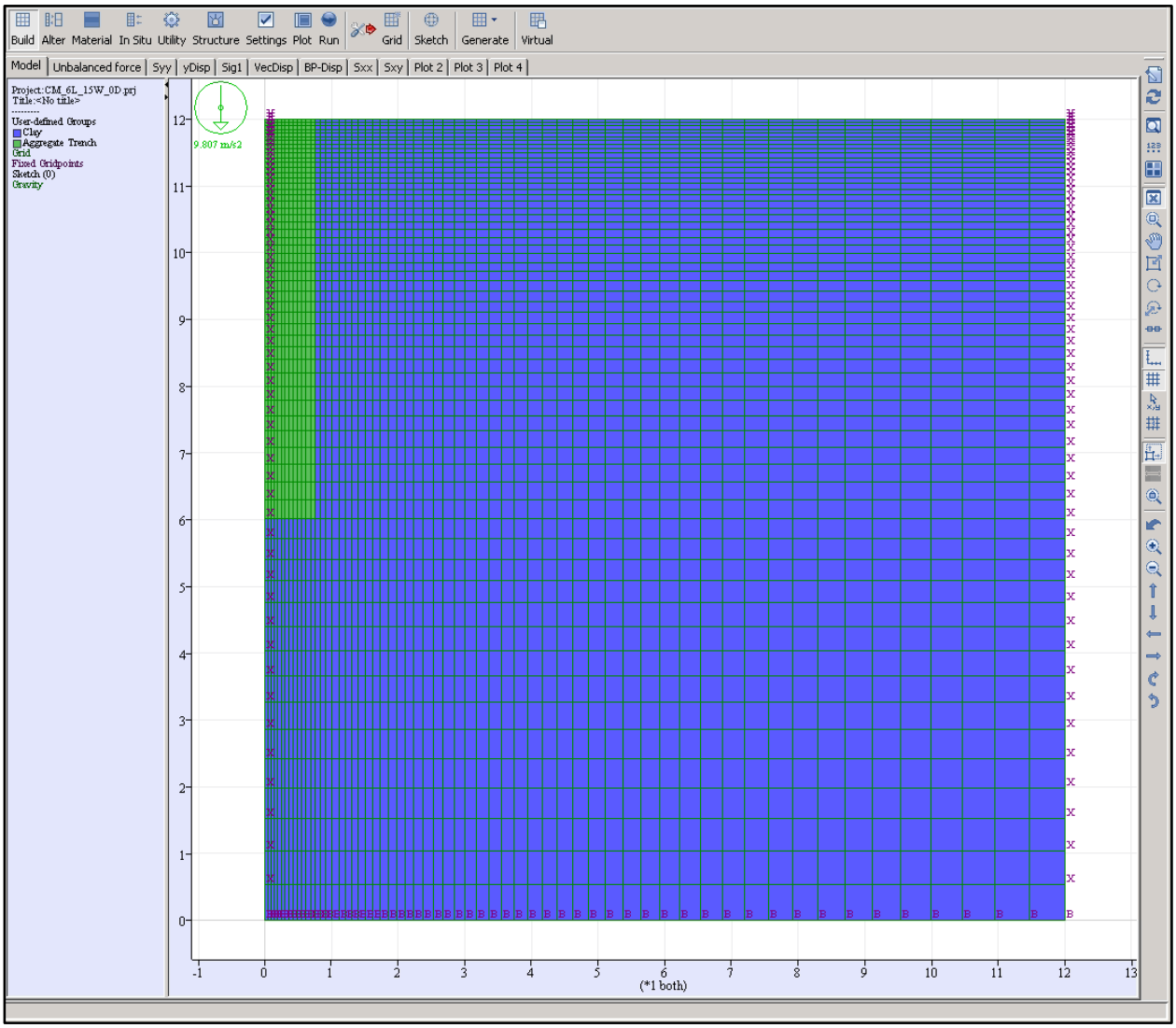


*Figure 5-7: 6 meter long, 1.5 meter wide aggregate trench modeled in FLAC*

Figure 5-7 illustrates the example of a 6 meter long trench measuring 1.5 meters in width shown in green with no footing embedment. This soil profile is specified as Trial Number 16 in

Appendix Table B-2. All other model trials were modeled in a similar fashion, and cases which required footing embedment were modeled as shown in Figure 5-8. Figure 5-8 shows the same case as in Figure 5-7, but with an embedment depth of 3 meters. This model corresponds to Trial Number 18 in Appendix Table B-2. To accommodate the change in shear mechanism within the soil in this scenario, additional boundary restraints were applied to the vertical plane that is coincident of the edge of the footing area. The restriction of horizontal movements is depicted by an "X" at each element node, and assumes that the soil would be constrained by the concrete footing.

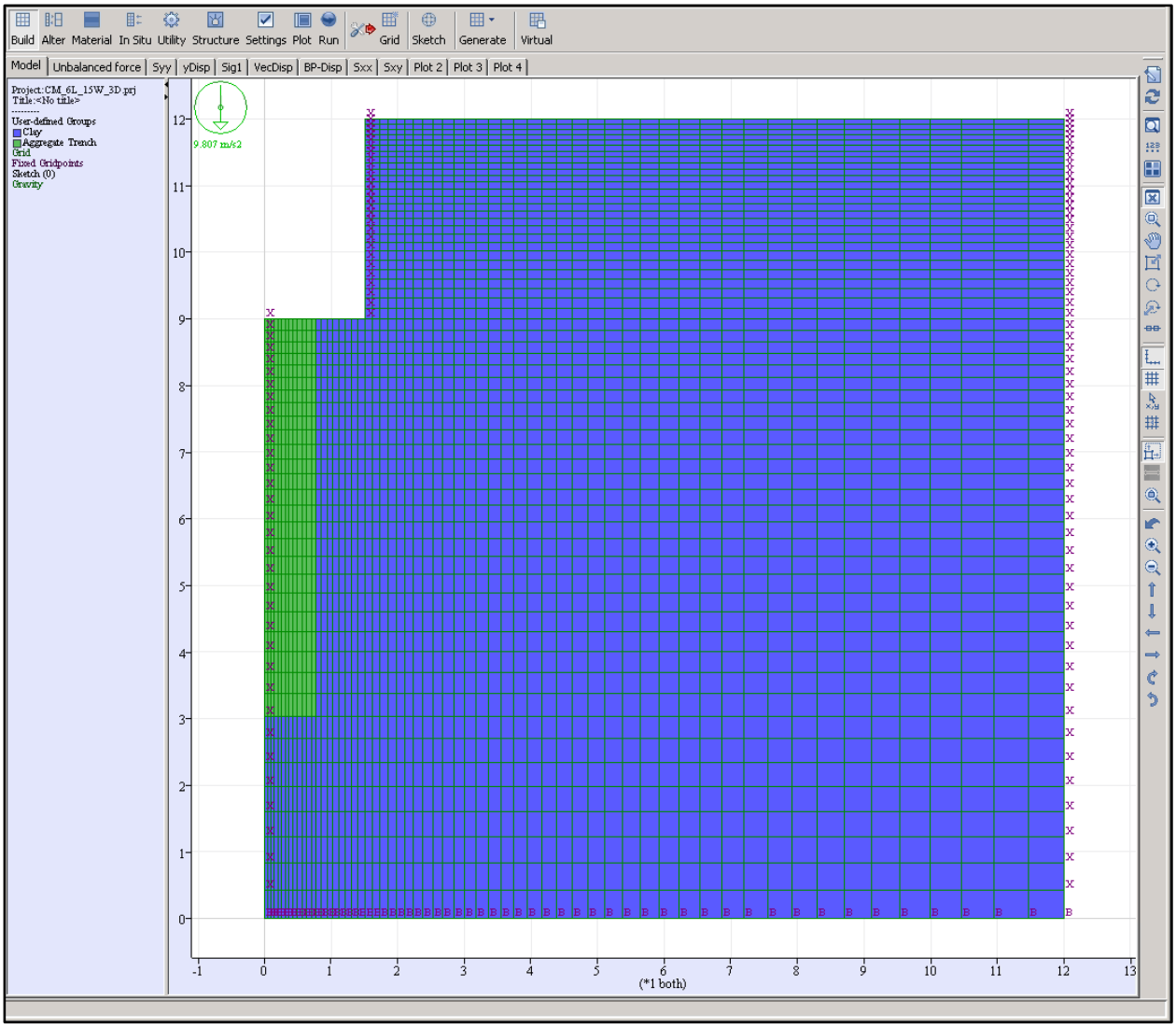


*Figure 5-8: 6 meter long, 1.5 meter wide aggregate trench with embedment modeled in FLAC*

The loading associated with the continuous strip footing was modeled by applying a constant velocity that would act in specified increments (time steps) until reaching a chosen displacement. In this study the applied velocity was one-one thousandth of a millimeter per second and was applied for 2,000,000 seconds to achieve an ultimate displacement of two meters. The rate of displacement (applied velocity) was chosen to be a value slow enough so as

to allow for the calculations described in Sections 5.1 and 5.2 to be conducted without significant "noise". The reduction in "noise" is represented by less transient unbalanced force convergence and thus a smoother acquisition of footing displacements is obtained. The corresponding value of displacement was chosen as a threshold at which it was expected for all improved soil scenarios to be failed in a "collapse" failure (as opposed to some arbitrary displacement criterion). In several trials for those cases where the undrained strength of the native soil equal to 80 kPa, 3 meters (3,000,000 seconds) was required to reach the bearing capacity of the soil profile. The *FLAC* representation of an applied velocity is shown in Figure 5-9 below. Note that for this figure, the screen has been zoomed in on the trench to make the applied velocity more visible to the reader. Figure 5-9 shows that the applied nodal velocity of one-one thousandth of a millimeter is indicated with the "Y" symbols in the upper left section of the mesh. The numbers under each "Y" ranging from 1 to 22 correspond to the nodes at which displacement and pressure are being recorded. The output files from the data collected at the nodes numbered 1 through 22 in the previous figures were then later used to create plots of bearing pressure versus displacement and contact pressure distribution underneath the footings. After the analysis of trenches such as those depicted in Figure 5-7, Figure 5-8, and Figure 5-9, an additional improved ground scenario was determined to be of interest. Because of the high concentrations of stress at the edges of a footing, analyses where an aggregate trench was placed at each of the footing edge locations could indicate a more effective improvement strategy. Figure 5-10 below illustrates in *FLAC* the arrangement of trenches, again using symmetry to simplify the model, at opposing edges of the strip footing.

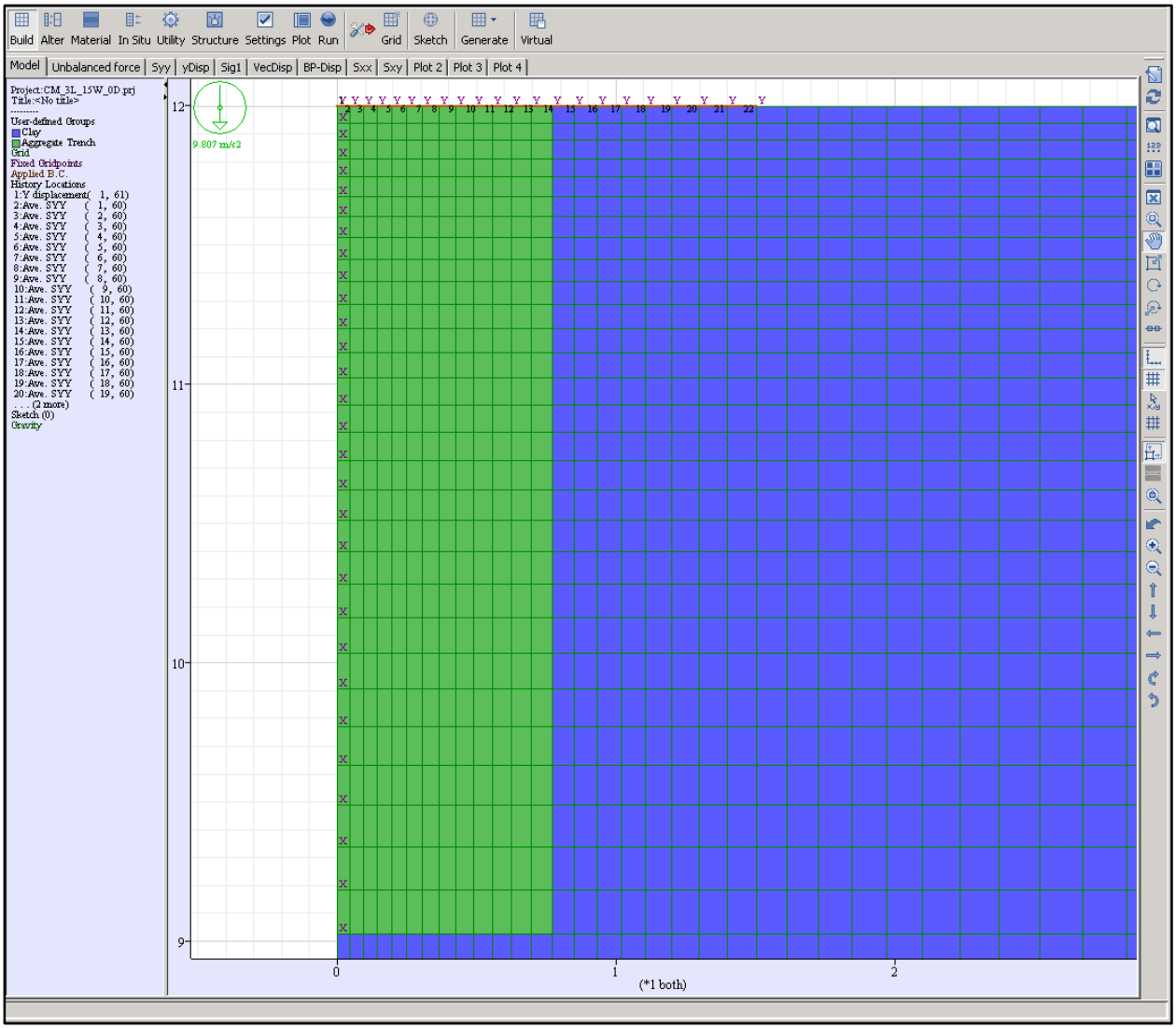


*Figure 5-9: 3 meter long, 1.5 meter wide centered aggregate trench modeled in FLAC*

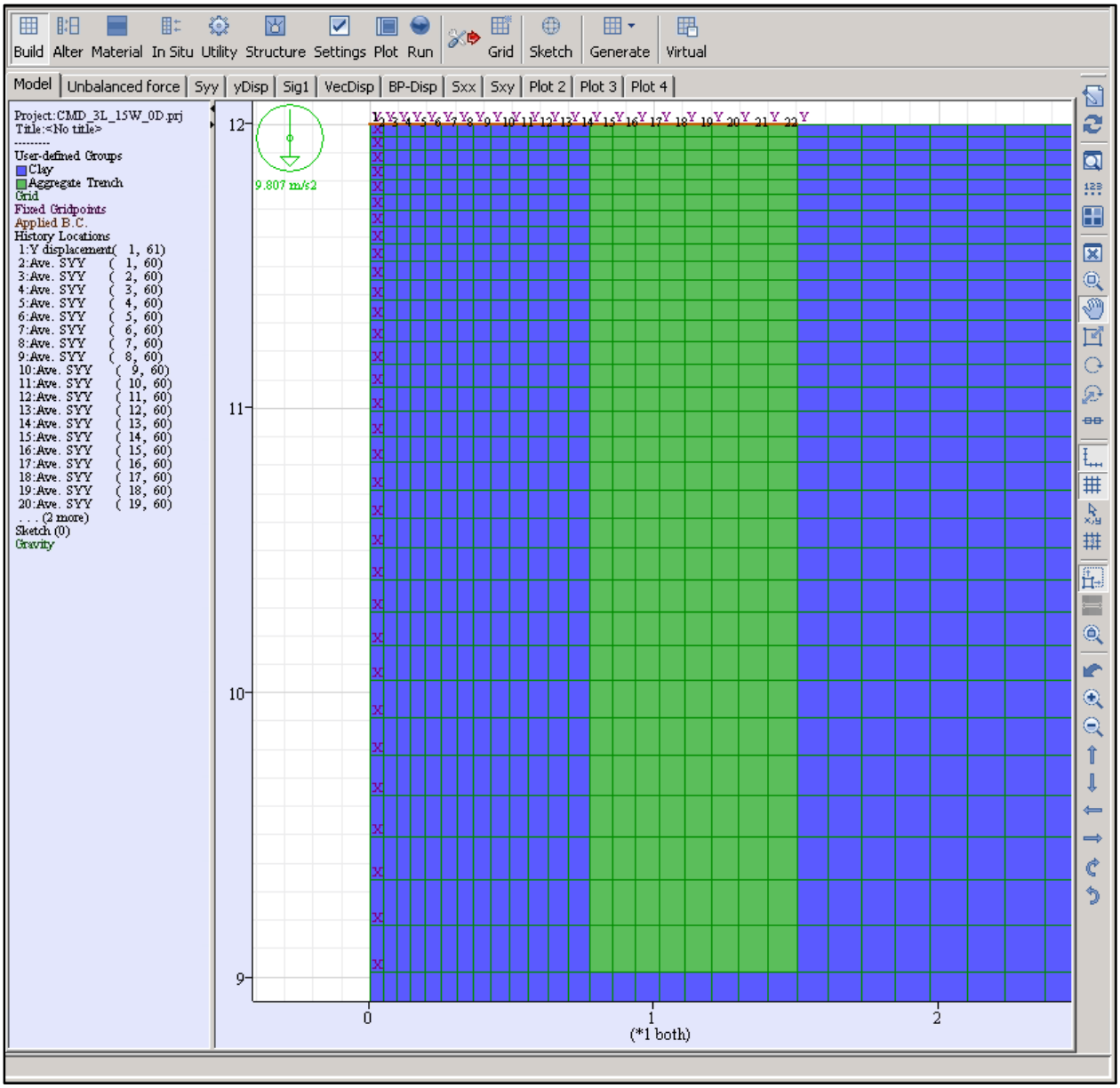


*Figure 5-10: 3 meter long, 1.5 meter wide split edge aggregate trench modelled in FLAC*

### 5.4.1 Parametric Study

In order to create a sufficient basis for comparison, many trials are necessary in a parametric study. A critical task comprises the determination of what dimensions (parameters)

of the trench are most important for improving the soil. Normalized geometrical relationships of footing width ($B_F$), footing depth ($d_F$), trench width ($W_T$), and trench length ($L_T$) were selected to create an adequate basis for drawing conclusions of parametric sensitivity. Table 5-1 below shows the geometrical relationships that were selected to guide the parametric study.

*Table 5-1: Factors proposed for variation in the parametric study*

| $L_T/W_T$ | $B_F/W_T$ | $d_F/B_F$ | Clay $S_u$ | Configuration |
|---|---|---|---|---|
| 2 | 1 | 0 | 20 kPa | Single Trench in Middle |
| 3 | 1.15 | 0.33 | 40 kPa | |
| 5 | 1.33 | 0.67 | 80 kPa | Two Trenches on Each Edge |
| 8 | 1.5 | 1 | | |
| | 2 | | | |

When considering the parametric study tabulated above, it can be observed that there are 480 different combinations of trench scenarios in addition to the previous 15 control cases. Considering the extent of such a study, refinement in the number of trials was pursued to limit the number of trials to those that would be most beneficial for drawing relevant conclusions. The process for which was iterative and involved the running of multiple trials before finalizing the final quantity necessary for drawing relevant conclusions. Ultimately the trials that were selected totaled 107, and the combinations of parameters for each are presented within the tables of Appendix B. It was also established that the native clay soil of 40 kPa undrained strength would be considered the “base case”. More parametric studies were conducted with models with 40 kPa undrained shear strength than with others in order to investigate the full range in possible parametric trends.

### 5.4.2 Output and Data Analysis

The output files provided by *FLAC* for each trench analysis include two separate *.fis files. The first is titled “bp_disp.fis” and contains the displacement from each velocity increment and the average soil pressure beneath the footing at each increment. The second file is titled “contact.fis” and includes the pressure at each of the nodes numbered 1 through 22 in Figure 5-9 at each velocity increment.

The “bp_disp.fis” files were analyzed entirely in Microsoft Excel to create plots of bearing pressure versus displacement of each trench improved soil profile. An example plot is presented in Figure 5-11. This scenario depicts the bearing pressure displacement curve for the model shown in Figure 5-9. The black line of this figure illustrates the raw output data, while the red line depicts a smoothed version of the data. The smoothed values at each increment were calculated using a running geometric mean. Smoothing the data in this way was necessary to eliminate “noise” in many of the plots representing soil pressure development.

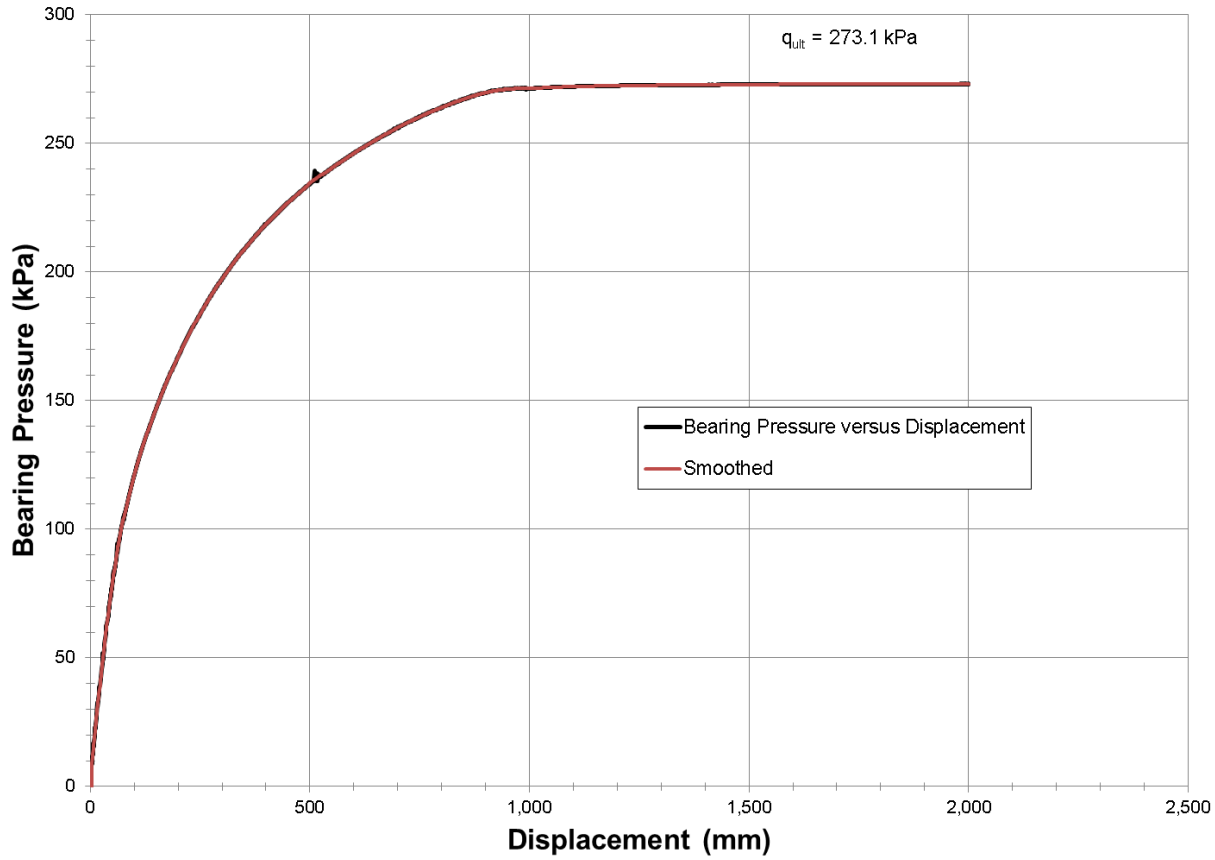


*Figure 5-11: Bearing pressure vs displacement curve of centered 3m long, 1.5m wide trench improved 40kPa clay soil profile*

Figures such as Figure 5-11 were generated for each of the modeled soil profiles in *FLAC;* all model bearing pressure displacement curves are presented in Appendix C. The mobilization of bearing pressure with footing displacement provides an understanding of the evolution of stresses in a soil profile with a specific trench improvement.

The second type of plot that was created for all scenarios within the "base case" of 40 kPa undrained shear strength for the native clay was footing contact pressure distribution at specified displacements. Since the "contact.fis" output files contained over 40,000 data points, a MATLAB script was used to quickly extract the necessary data points. The script employed for

this purpose is presented in Appendix D. The data points extracted were the pressure values beneath the footing at 100, 500, and 1,500 millimeters of displacement. Figures with this extracted data were then created in Excel, and an example of which being Figure 5-12 below. The figure below depicts an example contact pressure distribution figure from the same *FLAC* trial illustrated in Figure 5-11. The pressure distribution of this figure is common of all the cases analyzed in which the trench was centered under the continuous strip footing.

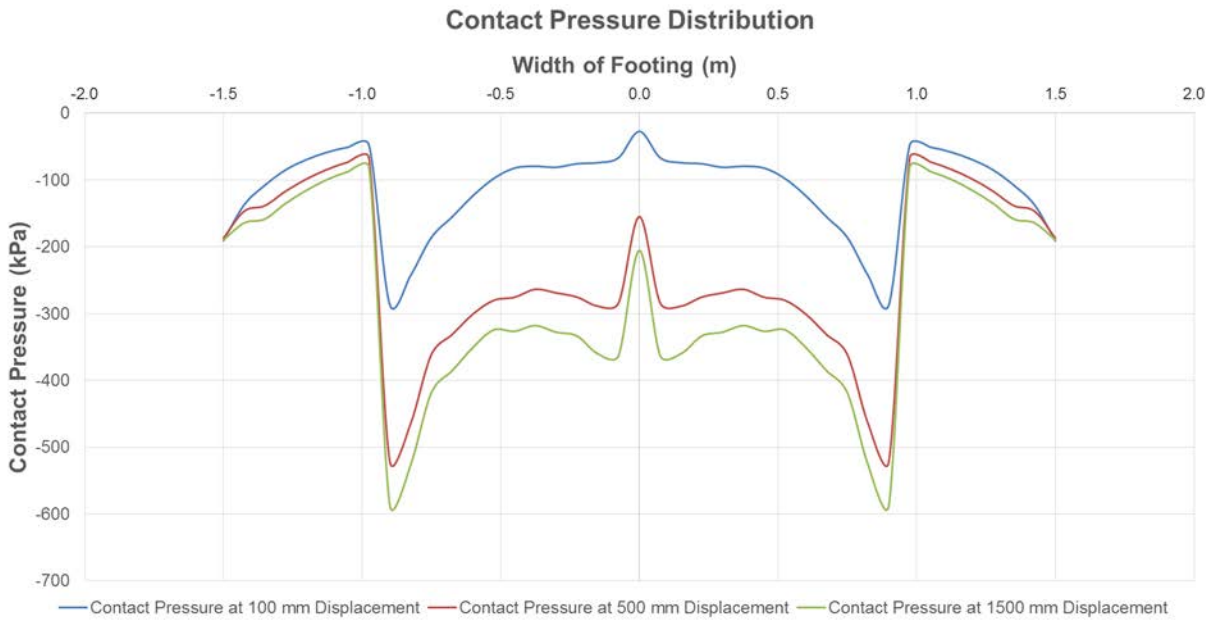


*Figure 5-12: Contact pressure distribution of centered 3m Long, 1.5m wide trench beneath footing in 40kPa clay soil profile*

The other relevant case analyzed in *FLAC* entails a soil profile improved with trenches placed at the opposing edges of the continuous strip footing. The contact pressure distribution for this type of soil improvement takes a much different form, an example of which can be seen in Figure 5-13 below. In this figure, the area replacement ratio of the compacted aggregate trench relative to the footing area is the same as that of Figure 5-12. The pressure distribution

however is much different because there are two separate trenches of 0.75 meters wide along each side of the strip footing as opposed to one 1.5 meter wide trench down the center of the strip footing. Contact pressure distribution figures for all cases of 40 kPa undrained shear strength native clay can be viewed in Appendix E.

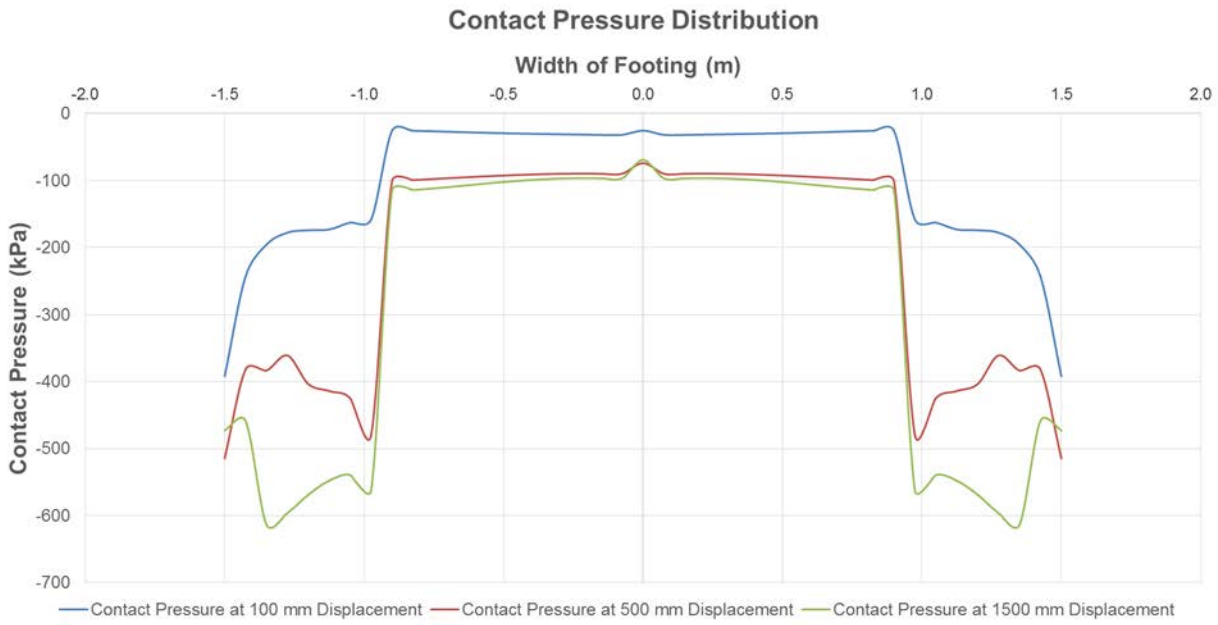


*Figure 5-13: Contact pressure distribution of two trenches 3m long, 0.75m wide beneath each edge of footing in 40kPa clay soil profile*

The significance of output data from all *FLAC* trials is discussed in greater detail in Chapter 6. Specifically, the values of bearing capacity for each trial are compared to determine the trench parameters that have the greatest impact on the improved bearing pressure performance.

### *5.5 Summary*

Numerical models were employed to develop simulated data to determine the efficacy of aggregate trench improved clay ground to increase the bearing capacity of a continuous strip footing. The software utilized to conduct these models was *FLAC 7.0*, from which output data was received and analyzed with MATLAB and Microsoft Excel. The clay soil was modeled using an elastic-perfectly plastic behavior, while the compacted aggregate trenches were modelled with cap-yield soil hardening behavior.

Output data received from *FLAC* was used to create plots of bearing pressure versus displacement of the continuous strip footing, and the contact pressure distribution beneath the footing at specified settlements. With these plots, bearing pressures at failure from each soil profile can be compared to the control scenarios discussed in Chapter 4. The distribution of contact pressures can also be considered in determining the most preferable trench ground improvement configurations. The profiles analyzed in *FLAC* provide a sufficient amount of data to determine the most significant trench parameters for improving the bearing capacity of a clay soil.

# 6.0 Results of the Parametric Study

The parametric study conducted with numerical models provides a large set of simulated data. Analysis of the derived data is required to better quantify the impact of each parameter investigated on the improvement of a clayey soil. The following sections of this chapter presents the results of the study in concise figures that depict the impact of various aggregate trench design parameters that were adjusted throughout the study. Both bearing capacity improvements and changes in contact pressure distribution beneath the footing as a result of a compacted aggregate trench are considered.

## *6.1 Bearing Capacity versus Footing Displacement*

### 6.1.1 Comparison to Control Scenarios

Bearing pressure versus displacement of the analyzed soil was the first relationship observed for each *FLAC* model. Figure 6-1 depicts this relationship for the unimproved cases of 20 kPa, 40 kPa, and 80 kPa. In the figure below, a higher bearing capacity is observed with increased undrained shear strength of the native clay. Clearly defined points of soil yielding are shown to be more apparent with an increase in shear strength as well. The bearing capacity demonstrated by these models match that of the calculated bearing capacities in Chapter 4 for every case. Figure 6-2 depicts the case of a 3 meter wide strip footing above native clay with varying undrained shear strength. The bearing capacity of the soil in the cases of 20 kPa, 40 kPa, and 80 kPa undrained shear strength were found to be 107 kPa, 214 kPa, and 428 kPa respectively. It is observed that increasing the undrained shear strength of the clay by 100% results in a 100% increase in bearing capacity of the soil.

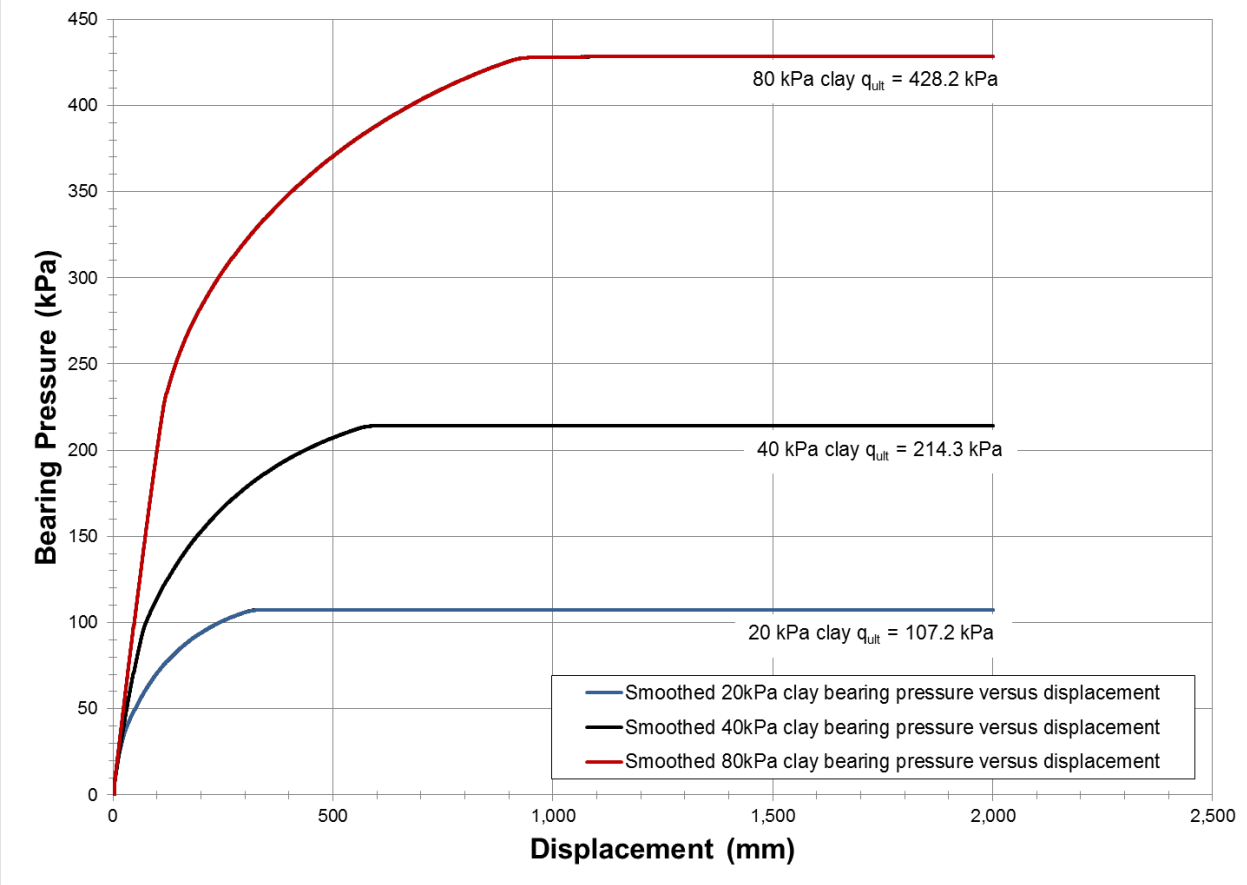


*Figure 6-1: Bearing pressure versus displacement with no embedment (unimproved native clay)*

Figure 6-2 below depicts the bearing pressure versus displacement curve for a 3 meter long, 1.5 meter wide compacted aggregate trench beneath the center of a 3 meter wide footing in 20 kPa, 40 kPa, and 80 kPa clay. In these cases, the soil reaches an ultimate pressure of 138 kPa, 273 kPa, and 547 kPa respectively. All simulations represent a greater capacity when compared to the unimproved cases in Figure 6-1. The bearing capacity of each profile was also realized at a greater displacement in each simulation. Each improved soil profile represented in Figure 6-2 demonstrate a 28% increase in bearing capacity when compared to the unimproved cases depicted in Figure 6-1. It is thus observed that the percentage increase in bearing capacity with a

given compacted aggregate trench is constant regardless of the undrained shear strength of the native clay.

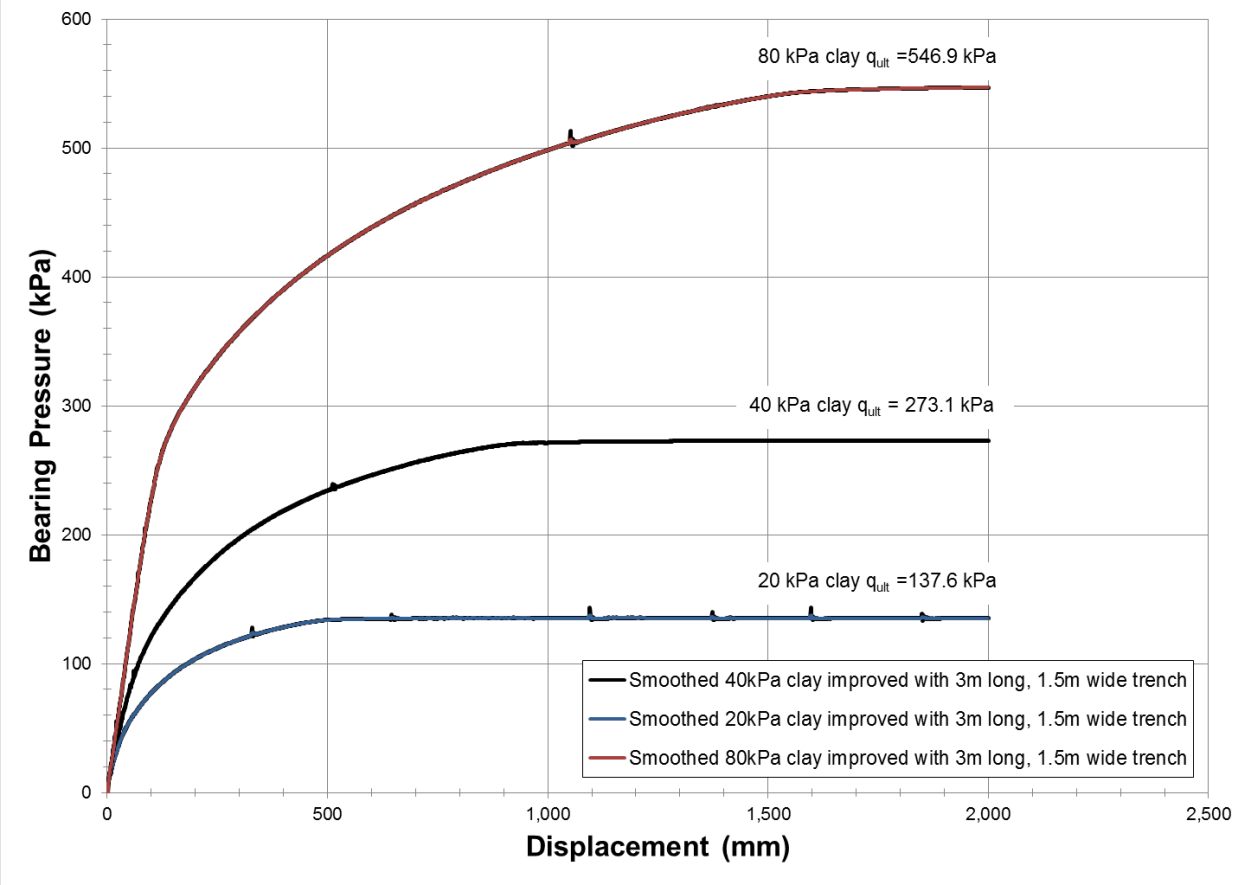


*Figure 6-2: Bearing pressure versus displacement (3 meter long, 1.5 meter wide trench centered beneath footing in 20 kPa, 40 kPa, and 80 kPa clay with no embedment)*

Figure 6-3 below illustrates the impact of increasing different parameters of the compacted aggregate trench. In the models represented by this bearing pressure versus displacement cure, the "base case" of 40 kPa native clay is further investigated. The 3 meter long, 1.5 meter wide trench has been adjusted in three different ways to compare the percentage of improvement to bearing capacity relative to the unimproved clay simulation. In these models, the trench investigated in Figure 6-2 has been adjusted by decreasing the width from 1.5 meters

to 0.6 meters (a 60% reduction in aggregate), increasing the length from 3 meters to 4.5 meters (a 50% increase in aggregate), and by splitting lengthwise to place to trenches of half width beneath each edge of the footing as opposed to one beneath the center of the footing. In the simulation where trench width has been reduced, the bearing capacity of the soil is 248 kPa, which corresponds to a 12% loss of bearing capacity improvement relative to the unimproved 40 kPa clay when compared to the 1.5 meter long trench shown in Figure 6-2. The increase in trench length improved the bearing capacity of the soil to 321 kPa, which corresponds to a 22% gain in bearing capacity improvement relative to the unimproved 40 kPa clay when compared to the 3 meter long trench. This trend suggests that compacted aggregate trench length has a greater impact on bearing capacity improvement compared to trench width. The final bearing pressure versus displacement curve represents a simulation with the same quantity of aggregate as the 3 meter long, 1.5 meter wide trench shown in Figure 6-2. In this case however, there are two trenches beneath the edges of the footing measuring 3 meters long and 0.75 meters wide. The resulting bearing capacity of this improved soil is 330 kPa, which corresponds to a 26% gain in bearing capacity improvement relative to the unimproved 40 kPa clay when compared to the 3 meter long, 1.5 meter wide trench centered beneath the center of the footing. The total bearing capacity improvement relative to the unimproved case is 54% in this simulation, which represents the greatest soil improvement of the four aggregate improved soil profiles shown in Figure 6-3. This finding indicates that placing two trenches of half the width beneath the edges of a footing is more efficient than a single trench beneath the center of a footing.

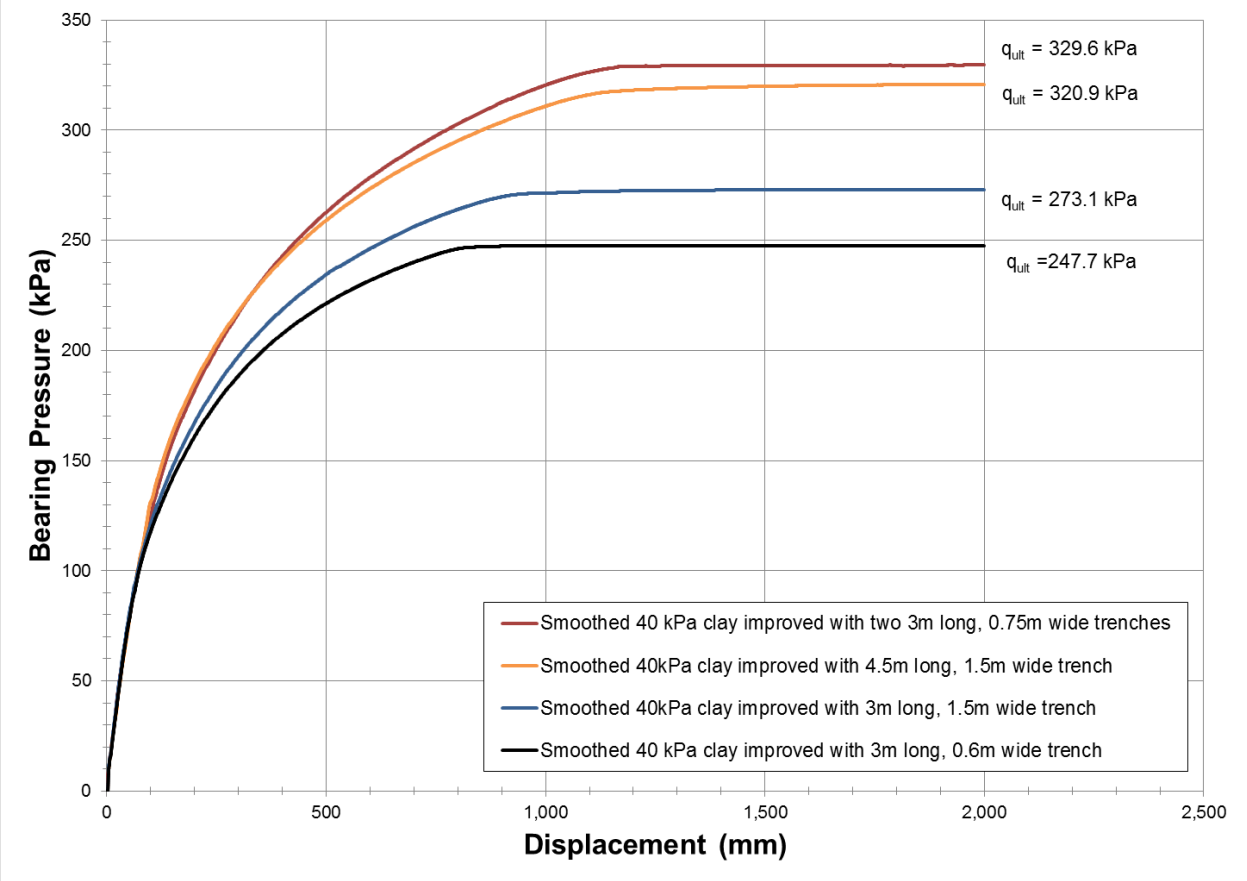


*Figure 6-3: Bearing pressure versus displacement (40 kPa clay improved with four different trench compacted aggregate trench configurations)*

One of the first trends observed across all unimproved soil trials was the relationship of maximum bearing pressure and depth of embedment for the footing. Figure 6-4 below demonstrates that this relationship is nearly linear. In this figure, the variation of bearing capacity with depth of footing embedment is plotted for the three varied undrained shear strengths that composed the unimproved control cases of the study. The observation of the linear approximation for bearing capacity of a trench improved soil relative to footing embedment depth was one factor that led to a reduction in trials during the study. With a proven near-linear relationship, the necessary trials for a given trench arrangement could be reduced to the

minimum and maximum embedment depths of concern. Intermediate depths could then be simulated solely for verification of the linear trend. Figure 6-4 demonstrates a high coefficient of determination ($R^2$) for the linear approximation of maximum bearing pressure versus depth of footing embedment. With this information, it was determined that the maximum and minimum footing embedment depths were of highest importance to the study.

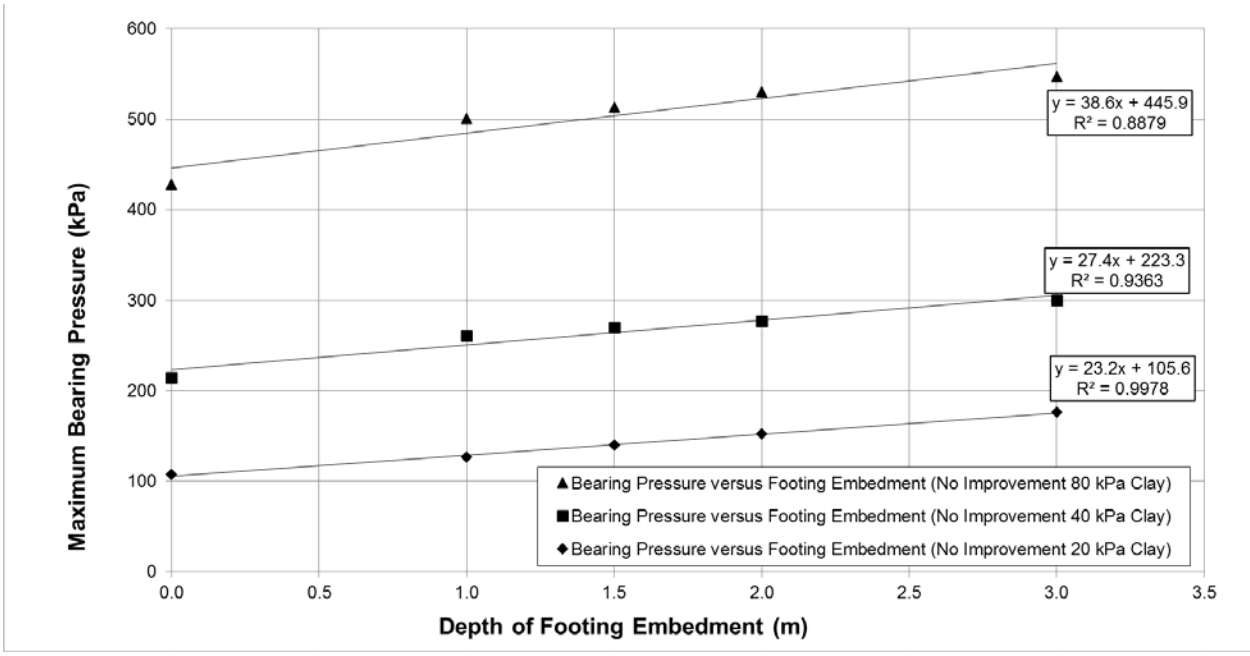


*Figure 6-4: Ultimate bearing pressure versus depth of footing embedment (no soil improvement)*

With an established near linear relationship of footing embedment for the unimproved soil cases, a similar relationship was expected for the aggregate trench improved simulations. Figure 6-5 depicts four different aggregate trench improved cases in which trenches have been centered beneath the strip footing within a 40 kPa undrained shear strength native clay. It is observed that the relationship of bearing capacity to depth of footing embedment remains linear

for a specific aggregate trench case, but the trend of this relationship is very different for each type of compacted aggregate trench improved case shown.

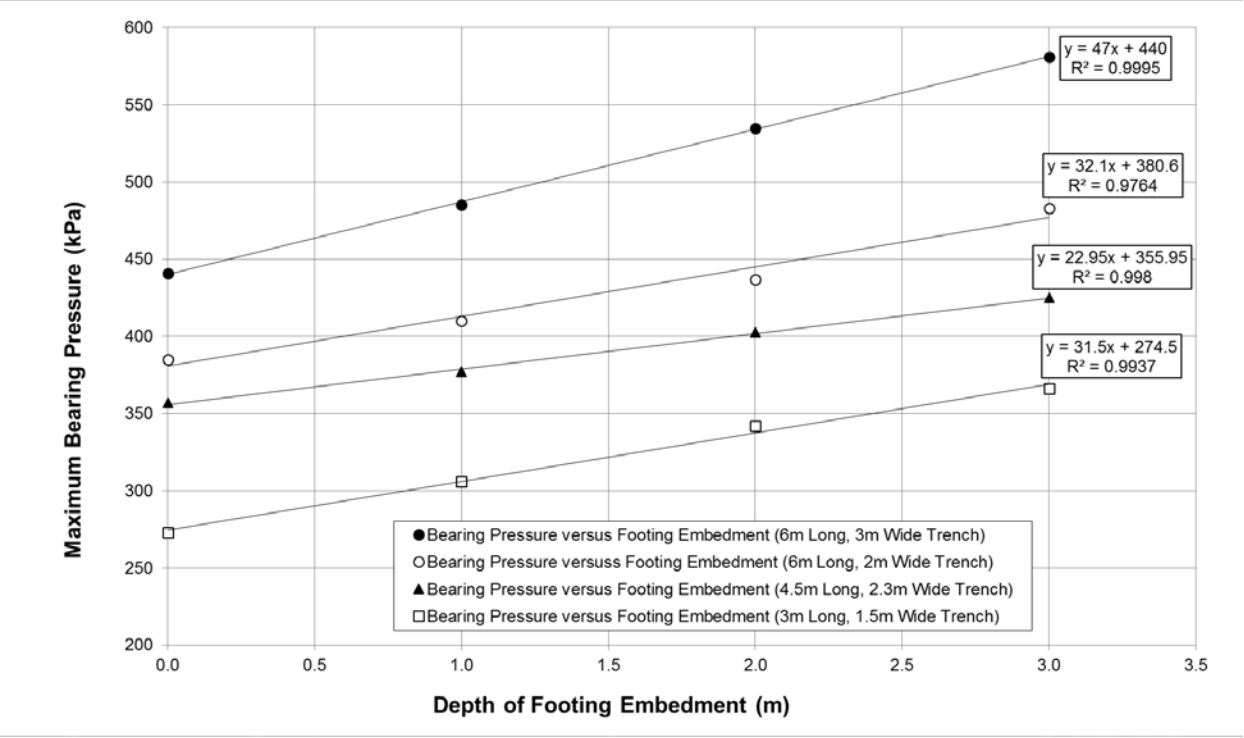


*Figure 6-5: Ultimate bearing pressure versus depth of footing embedment (40 kPa native clay and single trench centered beneath footing)*

The linear relationship of bearing capacity versus footing embedment was also investigated for the case of two compacted aggregate trenches beneath the two side lengths of a continuous strip footing. Figure 6-6 below illustrates aggregate trench improved soil cases with two trenches beneath each side of a continuous strip footing in a native soil of 40 kPa undrained shear strength clay. Figure 6-6 further supports the claim that the trend of the linear relationship of bearing capacity and footing embedment depth is variable depending on the parameters of the compacted aggregate trench improving the clay soil.

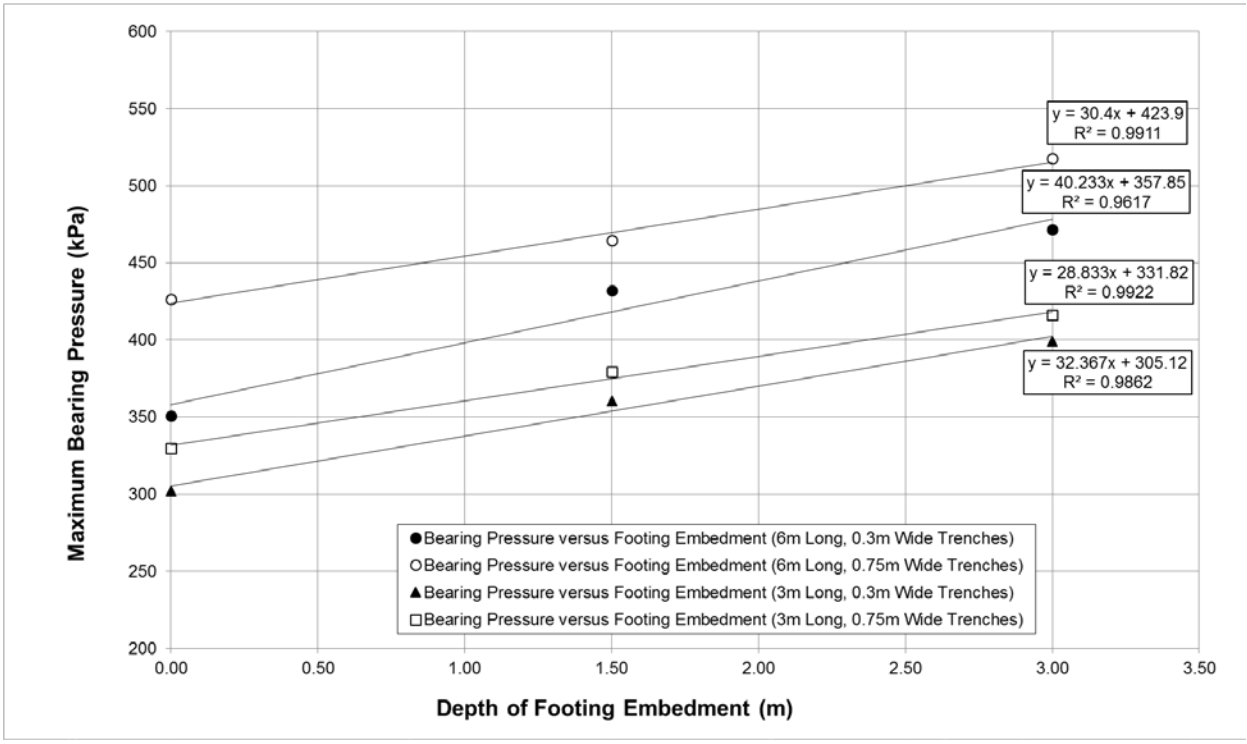


*Figure 6-6: Ultimate bearing pressure versus depth of footing embedment (40 kPa native clay and two trenches along sides beneath footing)*

Another compacted aggregate trench parameter expected to have a great impact on bearing capacity was the area replacement ratio. This ratio is defined as the percent plan surface area of trench of the total footprint area of the footing. Figure 6-7 below demonstrates how increasing the area replacement ratio of a trench with constant length increases the maximum bearing capacity of the footing. It can also be observed that the rate of improvement by increasing this ratio (demonstrated by the fitted slope coefficient in each equation) is greater for high values of initial area replacement ratio. This finding suggests that increasing the area replacement ratio of a compacted aggregate trench from 80% to 90% is more significant than increasing the area replacement ratio from 10% to 20%. Therefore, the effect on bearing capacity by increasing the area replacement ratio is non-linear and shows increasing returns.

Since the width of a trench is directly related to the area replacement ratio, this finding suggests that the compacted aggregate trench width has a great impact on bearing capacity. Figure 6-7 however, also takes in to account the length of trench, which is different for each set of increasing footing area replacement ratio. Parameters of trench length and width thus need to be independently isolated to determine which has the greatest impact on bearing capacity of a compacted aggregate trench improved clay soil.

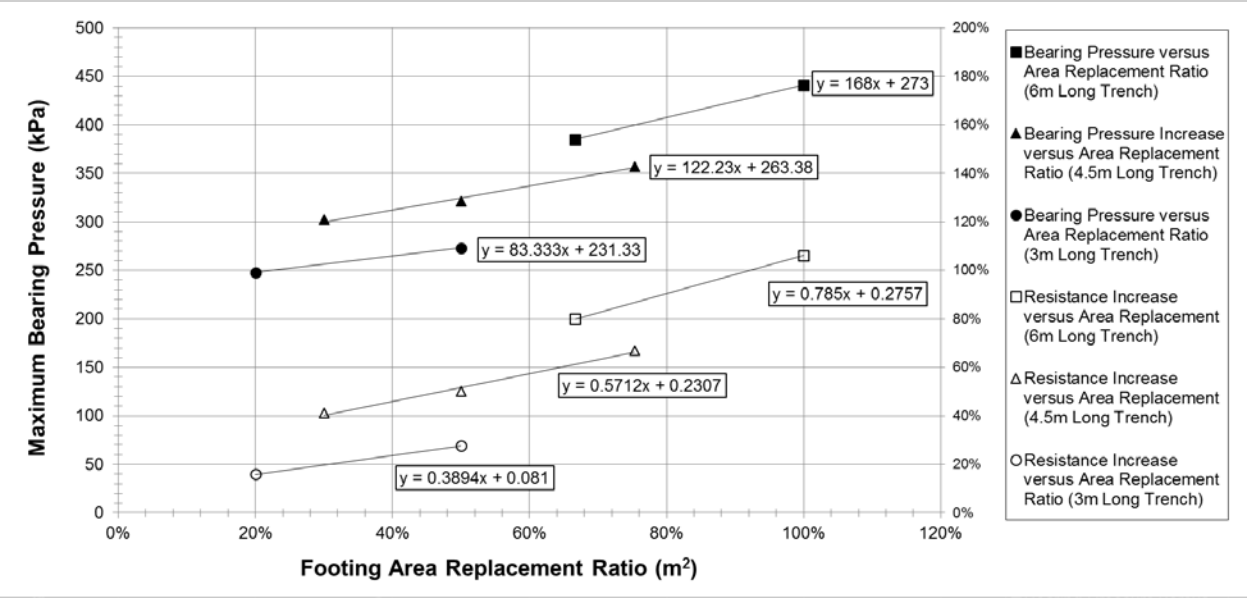


*Figure 6-7: Effect of area replacement ratio on ultimate bearing pressure with no embedment depth (40 kPa native clay and single trench centered beneath footing)*

The comparison of maximum bearing pressure versus footing area replacement ratio is compared in Figure 6-8 for the case of two trenches along both sides beneath a continuous strip footing. In this case 3 m and 6 m long trenches have been considered. The increasing in the rate of ultimate bearing pressure increases by a greater magnitude as compared to the simulations presented in Figure 6-7. It can also be observed from this figure that the configuration of two compacted aggregate trenches beneath the two sides of a strip footing will provide a greater

increase to bearing capacity of a clay soil when compared to a single trench beneath the middle of the footing with the same area replacement ratio.

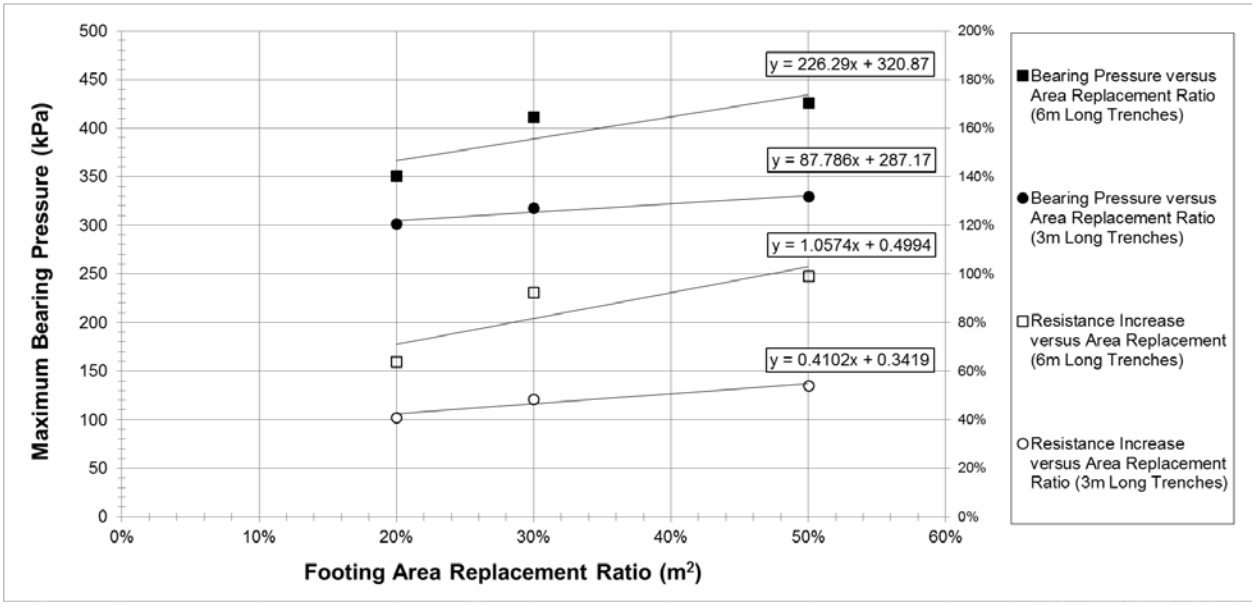


*Figure 6-8: Effect of area replacement ratio on ultimate bearing pressure with no embedment depth (40 kPa native clay and two trenches along sides beneath footing)*

Table 6-1 below demonstrates that the use of two separate trenches beneath the footing edges resulting in a greater impact to bearing capacity of the native soil when compared to a centered single trench with the same area replacement ratio. The example cases used to make this comparison consist of cases with 3 meter long trenches beneath a strip footing with an area replacement ratio of 50%. The use of two trenches of half the width, but placed at the edges of the footing, provides nearly double the increase in soil resistance than the single trench alternative.

*Table 6-1: Comparison of ultimate bearing pressure of trench improved soil to native unimproved soil (3m long trenches in 40kPa clay)*

| Trench Configuration | Trench Length (m) | Trench Width (m) | Footing Width (m) | Footing Depth (m) | Shear Strength ($S_u$) | Maximum Pressure (kPa) | Resistance Increase (%) | Slenderness Ratio | Area Replacement $A_r$ |
|---|---|---|---|---|---|---|---|---|---|
| Unimproved Soil | 0.00 | 0.00 | 3.00 | 0.00 | 40.0 | 214 | | | |
| | 0.00 | 0.00 | 3.00 | 1.00 | 40.0 | 261 | | | |
| | 0.00 | 0.00 | 3.00 | 1.50 | 40.0 | 270 | | | |
| | 0.00 | 0.00 | 3.00 | 2.00 | 40.0 | 277 | | | |
| | 0.00 | 0.00 | 3.00 | 3.00 | 40.0 | 300 | | | |
| Single Trench Centered Beneath Footing | 3.00 | 1.50 | 3.00 | 0.00 | 40.0 | 273 | 28% | 2 | 50% |
| | 3.00 | 1.50 | 3.00 | 1.00 | 40.0 | 306 | 17% | 2 | 50% |
| | 3.00 | 1.50 | 3.00 | 2.00 | 40.0 | 342 | 23% | 2 | 50% |
| | 3.00 | 1.50 | 3.00 | 3.00 | 40.0 | 366 | 22% | 2 | 50% |
| Two Trenches Under Each Edge of Footing | 3.00 | 0.75 | 3.00 | 0.00 | 40.0 | 330 | 54% | 4 | 50% |
| | 3.00 | 0.75 | 3.00 | 1.50 | 40.0 | 380 | 41% | 4 | 50% |
| | 3.00 | 0.75 | 3.00 | 3.00 | 40.0 | 416 | 39% | 4 | 50% |

These results have demonstrated that the placement of a compacted aggregate trench within a clay soil will improve ultimate bearing pressure. More interpretation of the trials however, is necessary to understand the parameters most impactful to the improvement of a native clay soil. Section 6.1.2 includes figures depicting the impact of these parameters on bearing capacity to better determine the efficacy of aggregate trench-reinforced clay ground improvement.

### 6.1.2 Factors Affecting the Bearing Capacity of Improved Soil

Compacted aggregate trench width is the first parameter isolated to compare the bearing capacity improvement to a native clay soil. This has been done for all native clay soil cases of 20 kPa, 40 kPa, and 80 kPa undrained shear strength. Figure 6-9 below depicts the case of a 20 kPa undrained shear strength clay in which both 3 meter and 6 meter long compacted aggregate trenches centered beneath the continuous strip footing are considered. The figure below demonstrates that a longer footing results in a more significant increase in bearing capacity with increasing compacted aggregate trench width. Furthermore, it can be observed that the

percentage increase in bearing capacity with a 6 meter long trench is over double that of a 3 meter long trench at all equal trench widths.

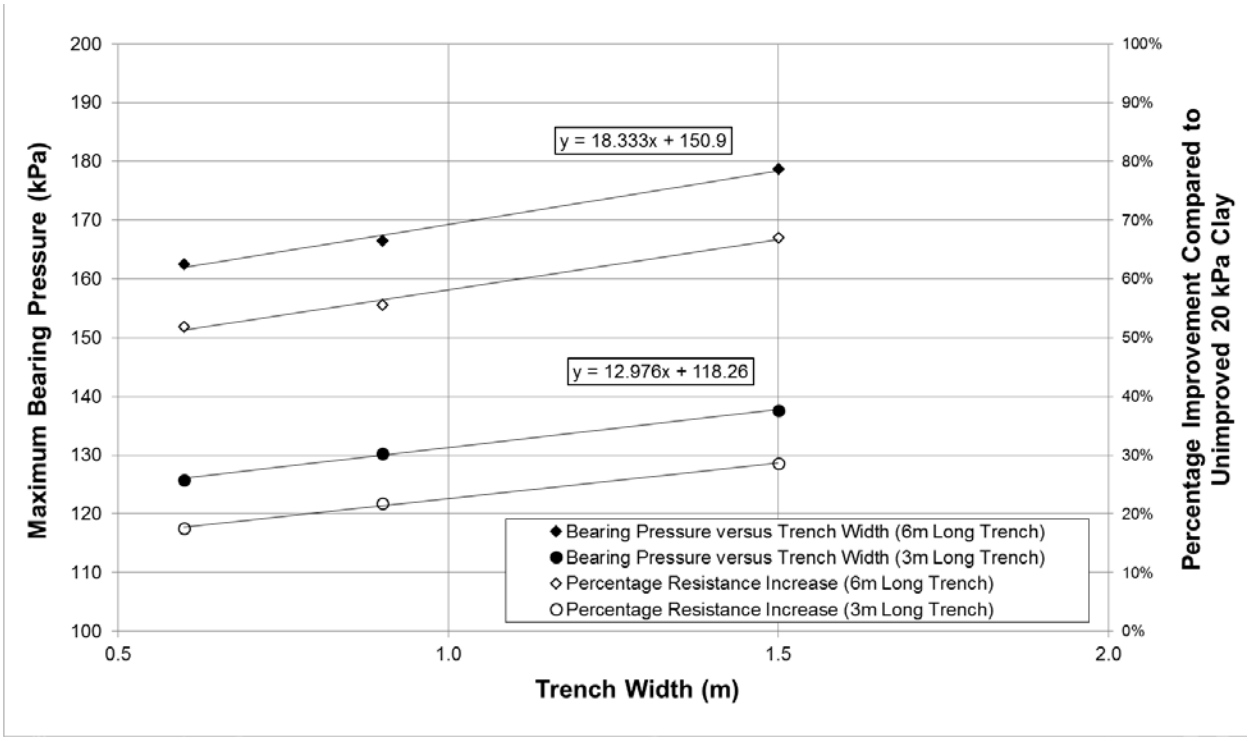


*Figure 6-9: Ultimate bearing pressure versus trench width with no embedment depth (20 kPa native clay and single trench centered beneath footing)*

The difference in bearing capacity increase compared to the unimproved 20 kPa clay soil case reveals that doubling the length, and therefore overall trench volume, more than doubles the resistance increase with all considered widths. Figure 6-10 below illustrates the same relationship of maximum bearing pressure versus trench width in the case of 40 kPa undrained shear strength native clay. The increase in native clay undrained shear strength results in overall higher ultimate bearing pressures as was expected. Additionally, the rate of bearing capacity increase with increasing trench width is higher when compared to that of a weaker clay soil. The same general trend of increased bearing capacity compared to the unimproved soil case with

increasing aggregate length is also observed. In this figure the increase in bearing capacity of a 3 meter long aggregate trench improved 40 kPa clay soil to a 4.5 meter long aggregate trench (50% increase in length) results in a bearing capacity improvement of 28% to 50% respectively compared to the unimproved case (a 79% increase in improvement).

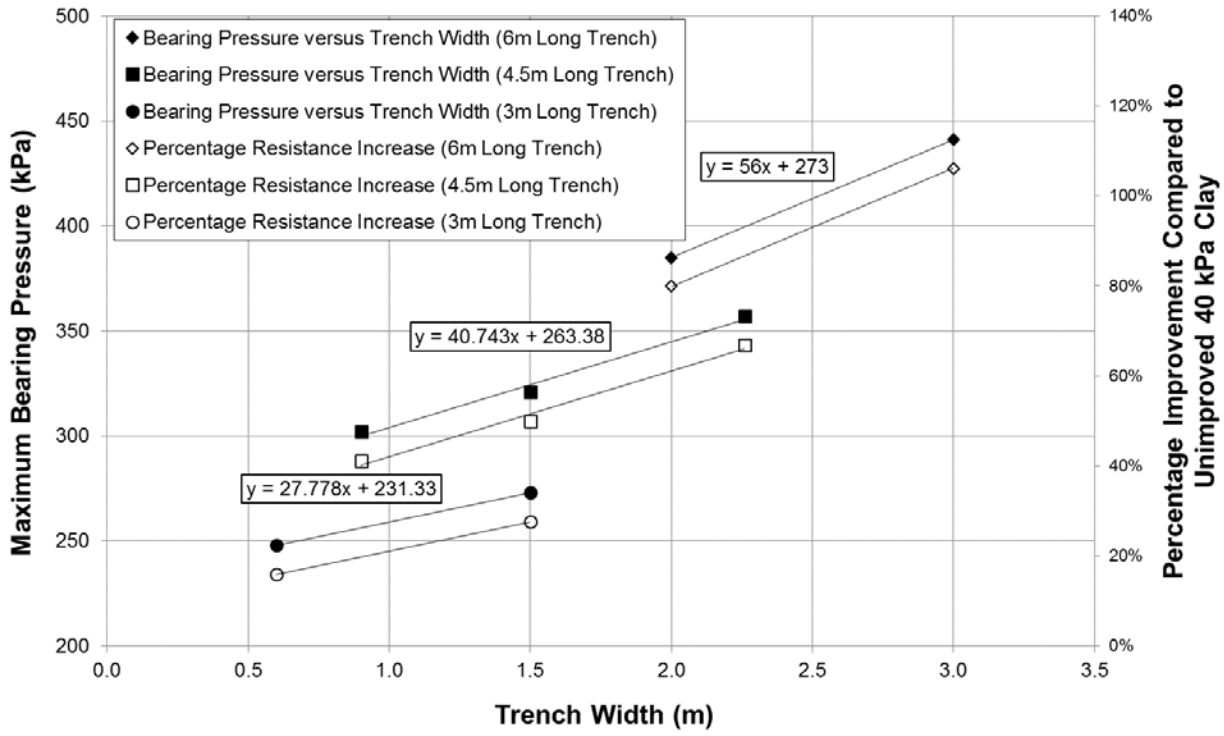


*Figure 6-10: Ultimate bearing pressure versus trench width with no embedment depth (40 kPa native clay and single trench centered beneath footing)*

The cases of maximum bearing capacity versus trench width in an 80 kPa undrained shear strength native clay are show in Figure 6-11 below. Again, a more rapid increase in maximum bearing pressure compared to the unimproved 80 kPa clay is the result of a higher undrained shear strength of the native clay as supported by Figure 6-11. The improvement percentages still follow the same trends as before, however it is observed that increasing the

strength of the native clay alone did not result in a greater percentage capacity improvement. These percentage values shown on the minor ordinate (right side of the figure) are nearly the same as those for the 3 and 6 meter long trenches in a 20 kPa undrained shear strength clay.

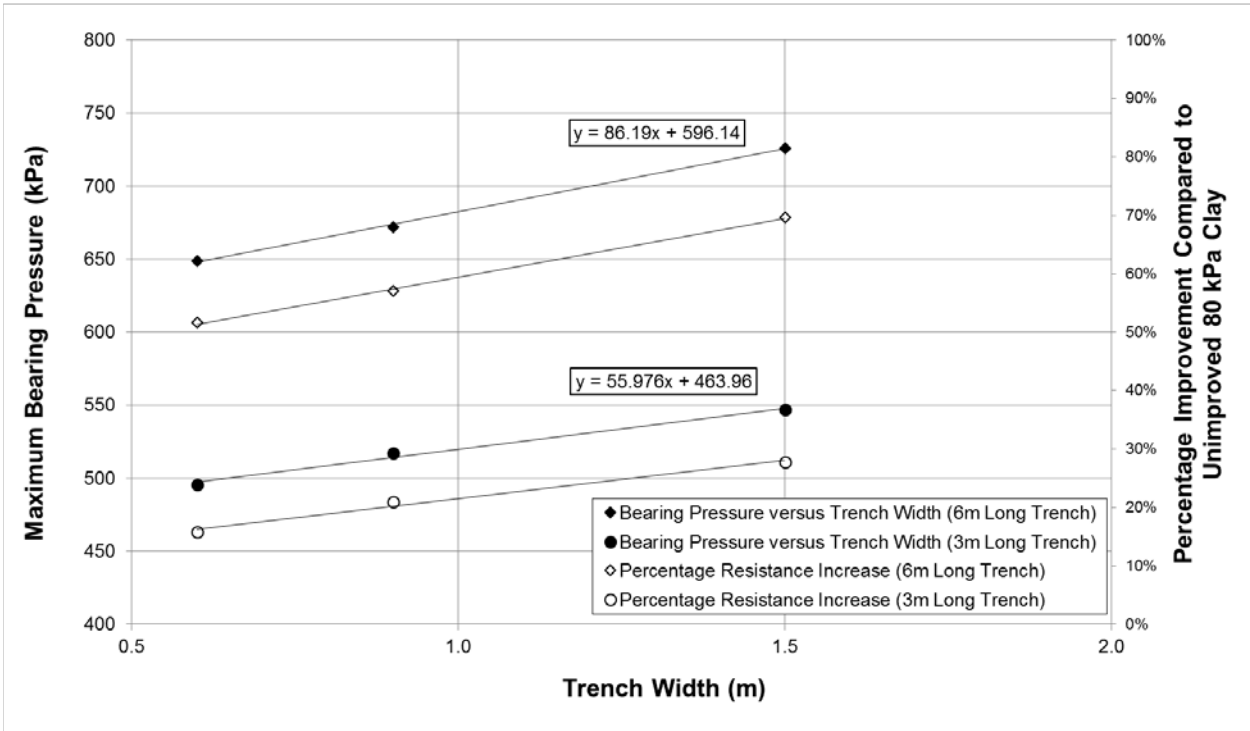


*Figure 6-11: Ultimate bearing pressure versus trench width with no embedment depth (80 kPa native clay and single trench centered beneath footing)*

Figure 6-12 below depicts data from the investigation of effect of increased bearing capacity of a clayey soil improved with two compacted aggregate trenches as a function of trench width. In this case the two trenches would be installed below the sides of the strip footing. Placing two trenches of half the original single trench width along both side lengths beneath the footing results in a higher bearing capacity as compared to the single aggregate trench cases in Figure 6-10. This configuration also results in a greater increase in capacity with increasing trench

width. Thus, it can be concluded that the effect of trench width on bearing capacity is stronger for the case of two trenches.

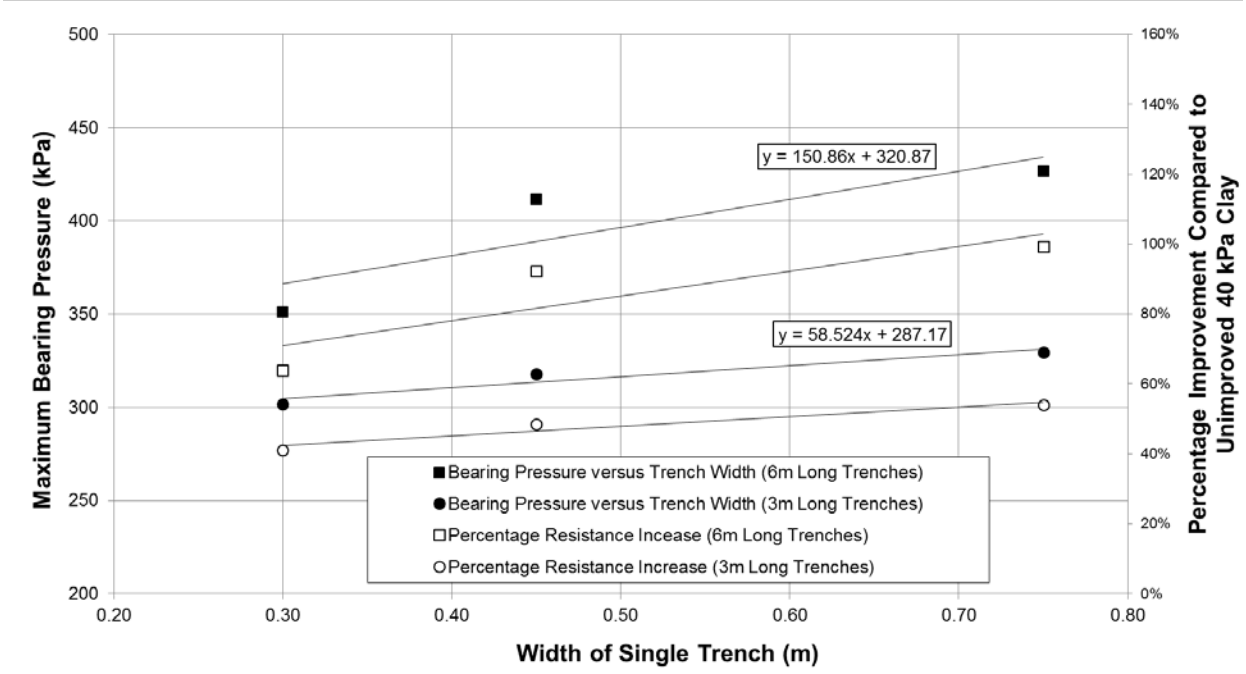


*Figure 6-12: Ultimate bearing pressure versus trench width with no embedment depth (40 kPa native clay and two trenches along sides beneath footing)*

To continue the investigation of which compacted aggregate trench parameter has a greater impact on improvement to soil bearing capacity, the trench length was isolated. This was done for the following four figures that compare maximum bearing pressure versus trench length. Figure 6-13 below depicts data from the trials modeled in a 20 kPa native clay soil. In the figure below it can be observed that increasing the length of the aggregate trench will have a strong impact on the bearing capacity of an improved soil profiled. In the case of a 1.5 meter wide trench, doubling the length from 3 to 6 meters increases the percentage resistance increase from 29% to 67% relative to the unimproved 20 kPa clayey soil. Therefore, doubling the size of

the trench in length results in over twice the resistance increase percentage with respect to an unimproved clay soil profile. This is likely because the increase in length for these cases has transitioned the failure mechanism of the soil to one that more fully mobilizes the strength of the compacted aggregate. The finding related to compacted aggregate trench length reveals a more significant impact to bearing capacity of the soil when compared to increasing the trench width in the 20 kPa native clay cases.

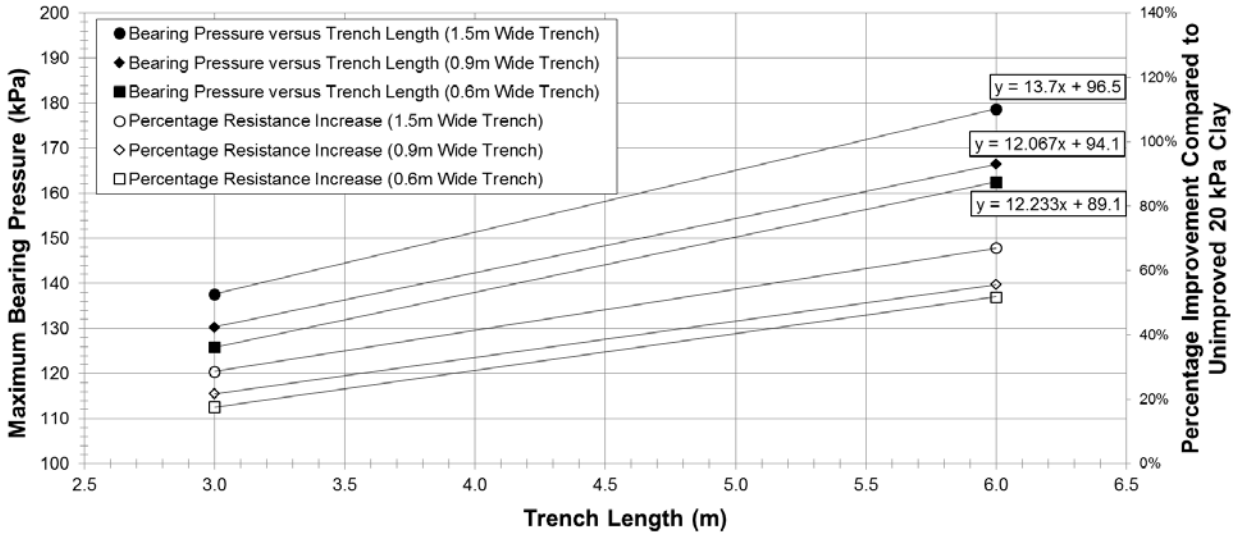


*Figure 6-13: Ultimate bearing pressure versus trench length with no embedment depth (20 kPa native clay and single trench centered beneath footing)*

Figure 6-14 below depicts the impact of increasing compacted aggregate trench length within a 40 kPa undrained shear strength native clay. In this 40 kPa clayey soil condition more compacted aggregate trench widths were modeled. In Figure 6-14 it can be observed that the rate of bearing capacity increase with respect to increasing trench length remains relatively constant across all trench widths. Consistent coefficients of the first term in each line equation verify this observation. It should also be noted that again, the percentage of resistance increase

compared to control scenarios increases at a faster rate with trench length as compared to trench width.

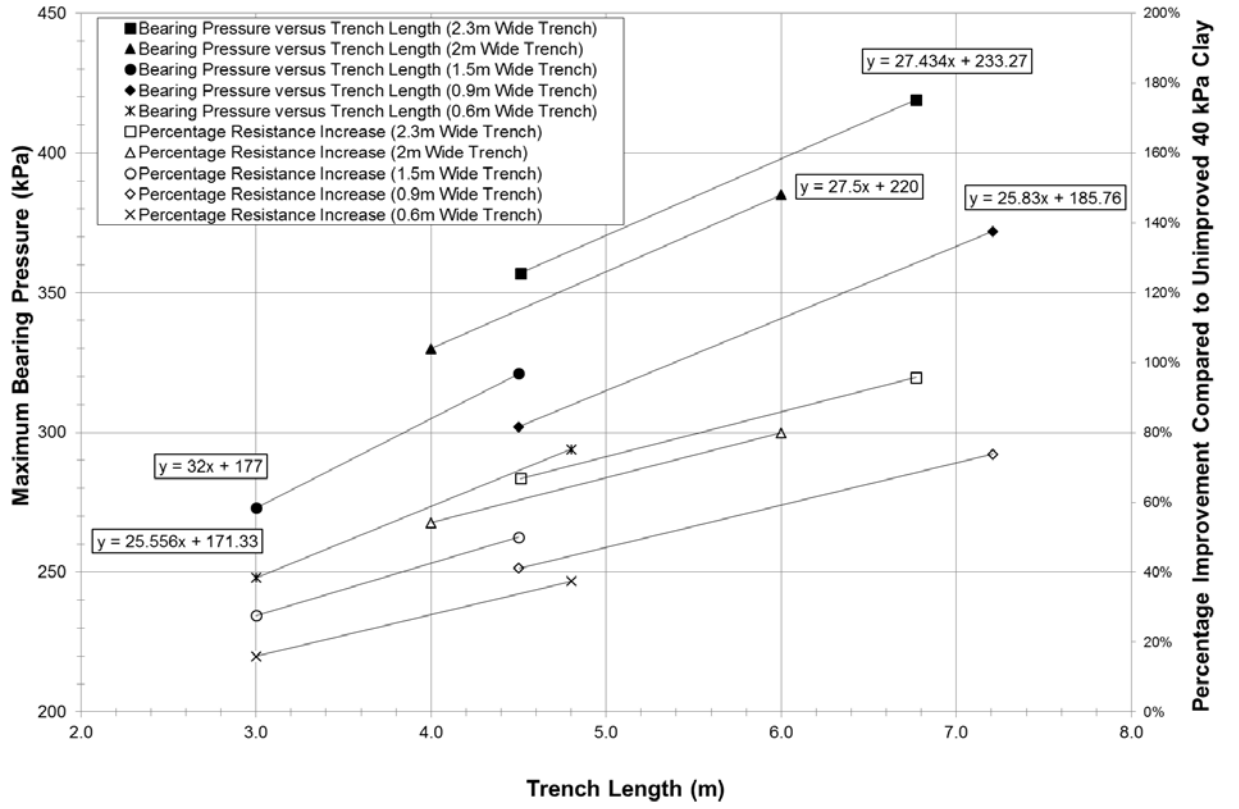


*Figure 6-14: Ultimate bearing pressure versus trench length with no embedment depth (40 kPa native clay and single trench centered beneath footing)*

Figure 6-15 below compares the results of increasing compacted aggregate trench length within a native clay of 80 kPa undrained shear strength. Figure 6-15 shows that the general trends of increasing bearing capacity with increasing length and undrained shear strength are maintained. The percentage resistance increase in bearing pressure from the control case of an unimproved 80 kPa clayey soil however, is almost the same compared to the 20 kPa undrained

shear strength native clay in which compacted aggregate trenches of the exact same dimensions were modeled.

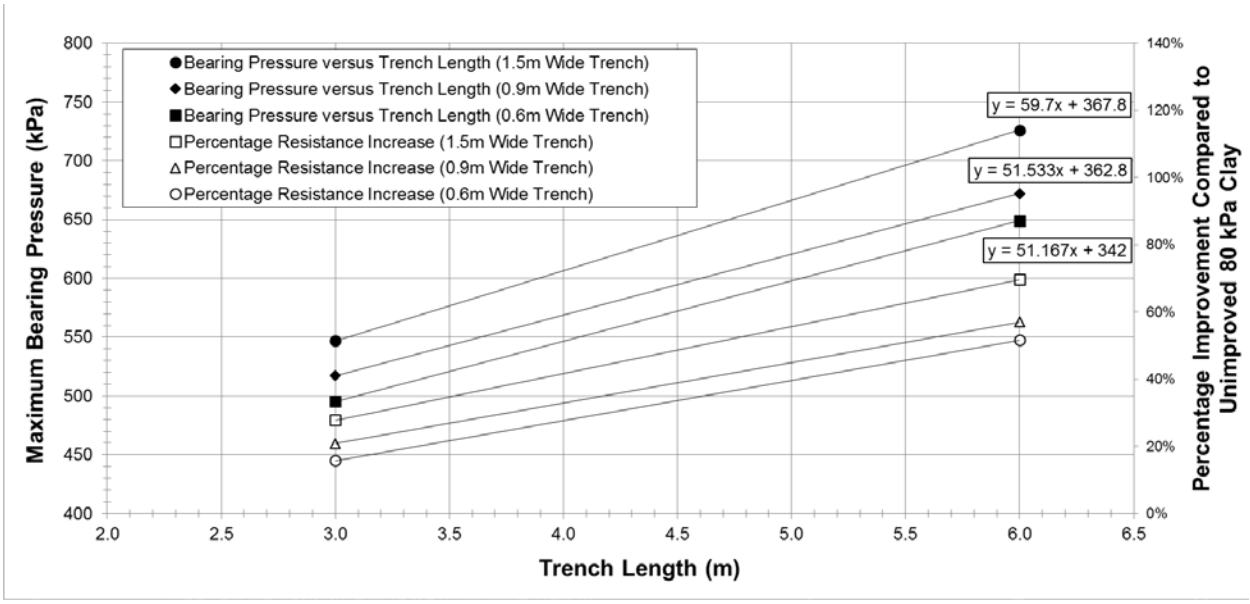


*Figure 6-15: Ultimate bearing pressure versus trench length with no embedment depth (80 kPa native clay and single trench centered beneath footing)*

Overall, in the case of a single compacted aggregate trench beneath the center of a strip footing, increasing trench length with have the greatest impact on soil improvement relative to a native clay soil bearing capacity. This relationship is particularly true in the case of wide trenches as increasing length will thus add more compacted aggregate to the soil profile per unit length. The relationship does not appear to be impacted significantly by the undrained shear strength of the native clay. Figure 6-16 was created to draw conclusions on this hypothesis in the case of two compacted aggregate trenches along both sides beneath a strip footing. Figure 6-16 should be been compared to Figure 6-12 to determine if trench length or width has a greater impact on soil improvement. Figure 6-16 demonstrates that increasing the length of two

compacted aggregate trenches beneath a strip footing has an approximately same effect when compared to a single aggregate trench beneath the center of the footing with double the width. Doubling the length of these trenches does not result in as great of a percentage resistance increase as the single trench cases, but it is greater than the increase as a result of doubling the width as observed previously in Figure 6-12. While this double trench configuration is a more efficient use of aggregate, it may be more costly to construct, which could detract from the soil improvement in overall design economics.

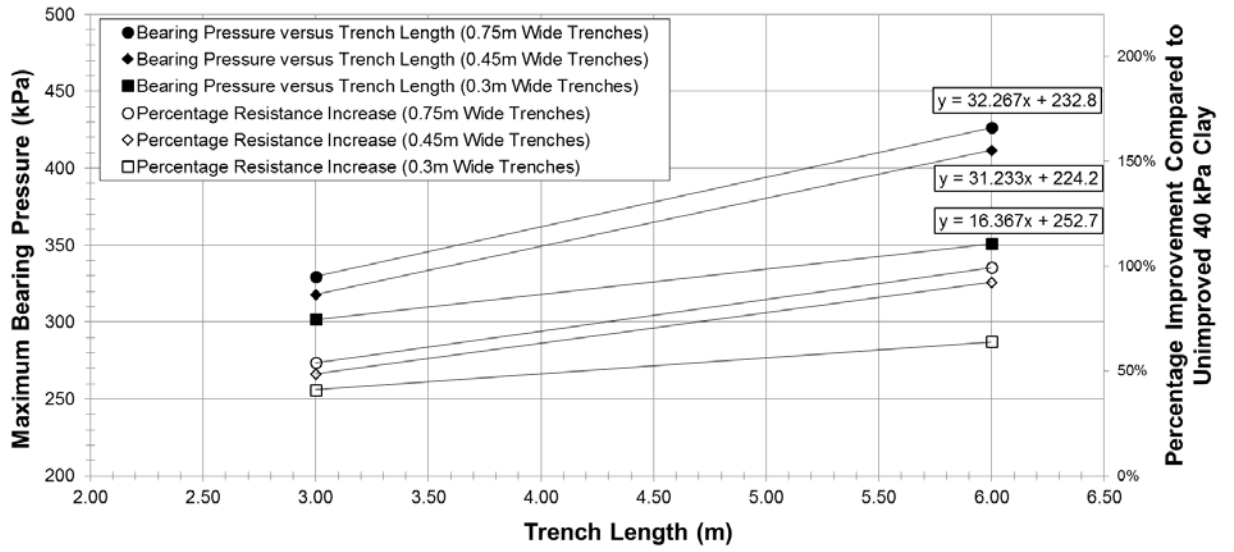


*Figure 6-16: Ultimate bearing pressure versus trench length with no embedment depth (40 kPa native clay and two trenches along sides beneath footing)*

The trends in increasing bearing capacity shown in the previous four figures indicates that increasing compacted aggregate trench length has a large impact on soil improvement. The impact from increasing trench length is in fact greater then increasing trench width in all configurations and native clay soil conditions within the study. Table 6-2 further illustrates the impact of ultimate bearing pressure improvement through adjustment of trench parameters. In

this table, the efficiency of a compacted aggregate trench is explored by calculating the soil resistance increase, compared to unimproved soil cases, and relative to the total amount of aggregate used to reinforce the soil per unit length. Table 6-2 demonstrates that the most efficient compacted aggregate trench configuration the use of two short and narrow trenches. These improvement in bearing capacity is superior to increases in bearing capacity when compared to a single compacted aggregate trench. Furthermore, it can be observed that in all cases, increasing the width of the trench reduces the efficiency of the trench, while increasing the length increases efficiency in the single trench case. It should also be noted that there are diminishing returns on soil improvement as the footing is set deeper into the native soil. In these cases, the improvement in capacity from embedment of the footing has a greater effect than improvement from the use of a compacted aggregate trench.

*Table 6-2: Resistance increase compared to unimproved 40 kPa clay per unit volume of trench improved soil profiles in 40 kPa clay*

| Trench Configuration | Trench Length *(m)* | Trench Width *(m)* | Footing Width *(m)* | Footing Depth *(m)* | Shear Strength *($S_u$)* | Maximum Pressure *(kPa)* | Resistance Increase *(%)* | Trench Volume per Unit Length *($m^3$)* | Resistance Increase per Unit Volume |
|---|---|---|---|---|---|---|---|---|---|
| Unimproved Soil | 0.00 | 0.00 | 3.00 | 0.00 | 40.0 | 214 | | | |
| | 0.00 | 0.00 | 3.00 | 3.00 | 40.0 | 300 | | | |
| Single Trench Centered Beneath Footing | 4.50 | 2.26 | 3.00 | 0.00 | 40.0 | 357 | 67% | 10.2 | 6.6% |
| | 4.50 | 2.26 | 3.00 | 3.00 | 40.0 | 425 | 42% | 10.2 | 4.1% |
| | 4.50 | 1.50 | 3.00 | 0.00 | 40.0 | 321 | 50% | 6.8 | 7.4% |
| | 4.50 | 1.50 | 3.00 | 3.00 | 40.0 | 391 | 30% | 6.8 | 4.5% |
| | 3.00 | 1.50 | 3.00 | 0.00 | 40.0 | 273 | 28% | 4.5 | 6.1% |
| | 3.00 | 1.50 | 3.00 | 3.00 | 40.0 | 366 | 22% | 4.5 | 4.9% |
| Two Trenches Under Each Edge of Footing | 6.00 | 0.75 | 3.00 | 0.00 | 40.0 | 426 | 99% | 9.0 | 11.0% |
| | 6.00 | 0.75 | 3.00 | 3.00 | 40.0 | 518 | 73% | 9.0 | 8.1% |
| | 3.00 | 0.75 | 3.00 | 0.00 | 40.0 | 330 | 54% | 4.5 | 12.0% |
| | 3.00 | 0.75 | 3.00 | 3.00 | 40.0 | 416 | 39% | 4.5 | 8.6% |
| | 3.00 | 0.30 | 3.00 | 0.00 | 40.0 | 302 | 41% | 1.8 | 22.8% |
| | 3.00 | 0.30 | 3.00 | 3.00 | 40.0 | 399 | 33% | 1.8 | 18.3% |

## *6.2 Contact Pressure Distribution beneath Footing*

### 6.2.1 Comparison to Control Scenarios

The use of a numerical code such as *FLAC 7.0* allows the observation of the simulated contact pressure distribution of the footing on the soil during all steps of displacement in the soil profile. Figure 6-17 presents an example of such a contact pressure distribution, in which the pressure directly beneath the continuous strip footing has been plotted at 100, 500, and 1,500 millimeters of footing displacement into a soil profile. In this case the 3 m wide strip footing has been compressed into an un-reinforced clay soil profile with an undrained shear strength of 40 kPa and no footing embedment depth. Figure 6-17 typifies the unimproved footing case. Contact pressure beneath the footing in this case is initially greatest along the edges of the footing. Upon displacement to soil failure however (500 mm and 1,500 mm displacements on the figure below), the distribution of pressure becomes more consistent beneath the footing. Contact pressure quickly increases to maximum within 25 centimeters from the center line of the footing and remains relatively constant from this location to the edge of the footing. Judging from the shape of the contact pressure distribution in Figure 6-17, the soil would have failed first along the edge of the footing where contact pressures are greatest at low displacements.

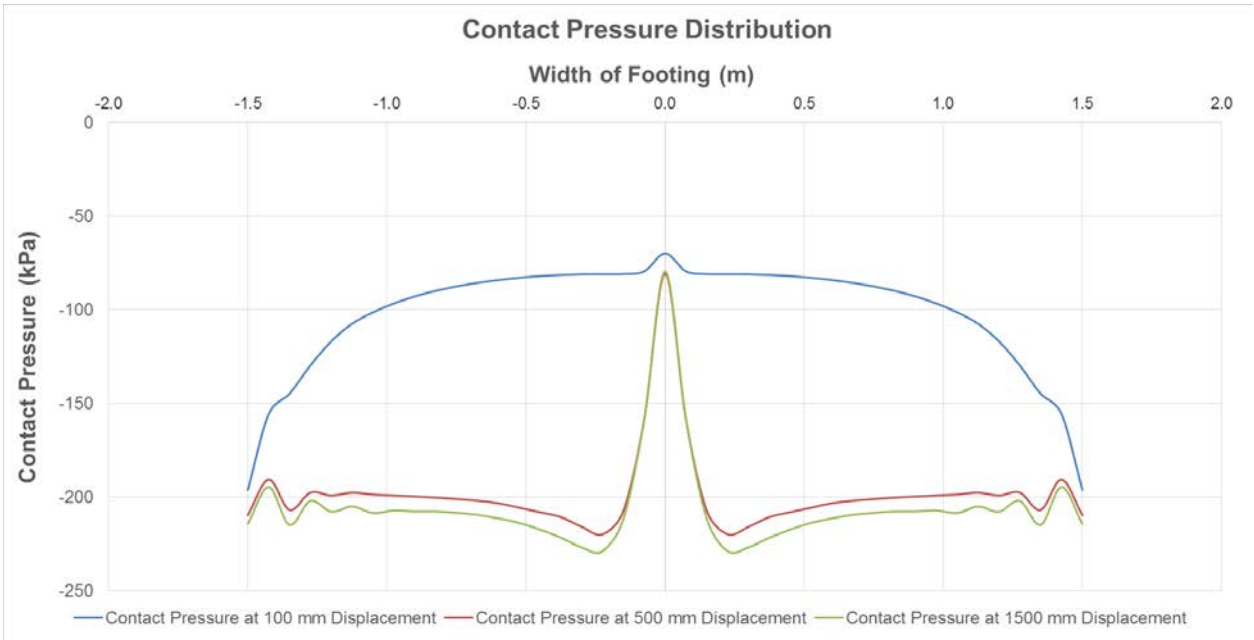


*Figure 6-17: Contact pressure distribution of 3 m wide strip footing with no embedment over 40 kPa native clay (bearing capacity equals 214 kPa)*

Figure 6-18 below represents the same 3 meter wide strip footing resting on the same 40 kPa native clay. In this scenario however, the footing has been placed into the soil with a 3 meter depth of embedment, which in all cases increased the bearing capacity of the soil profile. In the figure below, a similar distribution of pressure at 100 millimeters of displacement is observed as was in Figure 6-17. The 3 meter embedment depth providing a higher maximum bearing pressure results in a less uniform distribution of pressure beneath the footing at greater displacements. It can be observed that the soil again failed at the edges of the footing, however pressure beneath the footing from the center to outside edges appeared more linear compared to a relatively constant distribution in the case of no footing embedment.

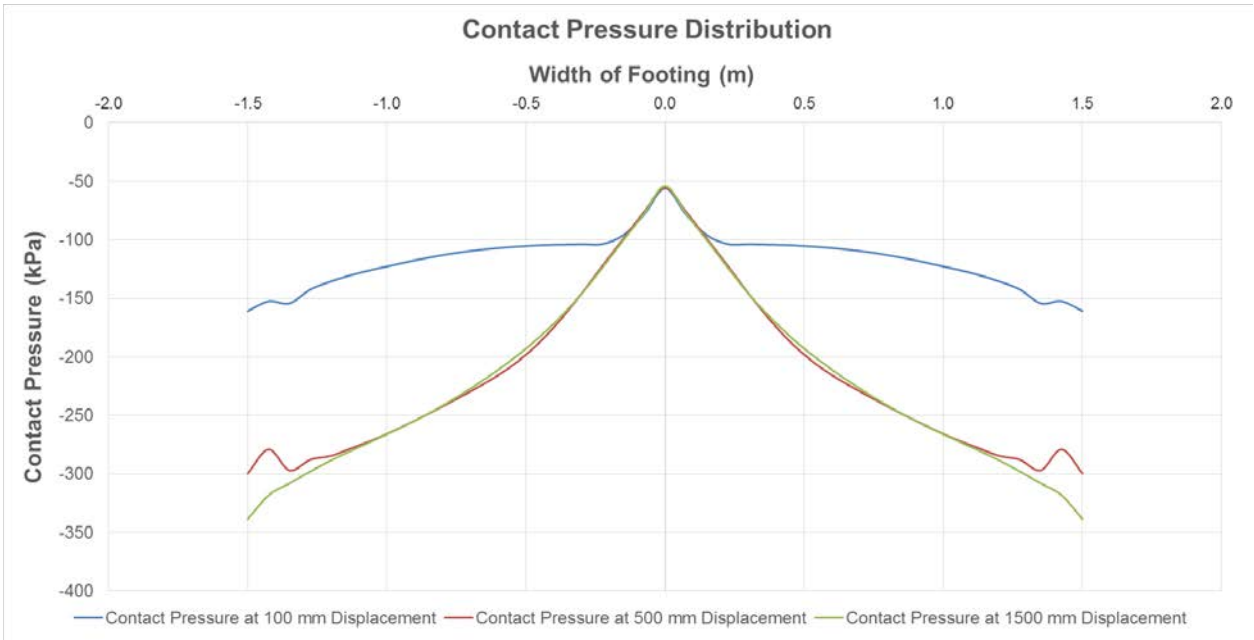


*Figure 6-18: Contact pressure distribution of 3m wide strip footing with 3m embedment depth over 40 kPa native clay (bearing capacity equals 300 kPa)*

The following section explores how different compacted aggregate trench configurations alter the contact pressure distribution beneath the footing.

### 6.2.2 Impact of Trench Dimensions on Contact Pressure Distribution

The pressure distribution beneath a footing has been plotted in the following figures to better understand how a compacted aggregate trench increases the overall bearing capacity of a clay soil profile. The distribution of pressure beneath a continuous strip footing show little difference when considering the variation in the undrained shear strength of the native clay. Thus, only 40 kPa undrained shear strength native soil cases have been considered for the purpose of investigating a compacted aggregate trench impact on contact pressure distribution.

Figure 6-19 below demonstrates a case in which the native clay has been improved with a single compacted aggregate trench beneath the center of a continuous strip footing. Most all of the cases with a single trench have taken this form relative to the width of the compacted aggregate trench. The figure below shows that the maximum contact pressure manifests at the far edges of the trench, 0.75 meters from the center of the footing in this case. Figure 6-19 demonstrates how a compacted aggregate trench beneath the center of the footing redistributes the contact pressure when compared to the non-improved soil case in Figure 6-17. The soil experiences failure at a higher pressure and that pressure occurs at the interface between the compacted aggregate trench and the native clay soil. There is then a sharp reduction of pressure in the native clay beyond the aggregate trench because of the lower capacity in this type of soil compared to the stone within the trench.

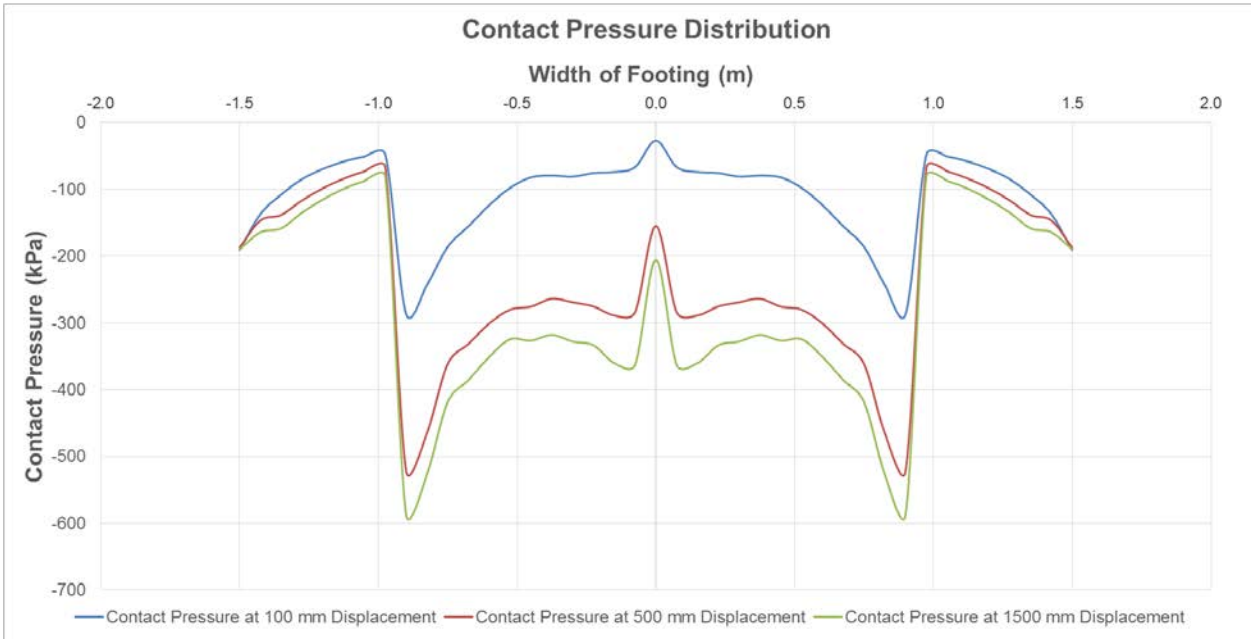


*Figure 6-19: Contact pressure distribution of 3m long, 1.5m wide compacted aggregate trench (40 kPa native clay and single trench centered beneath footing)*

The contact pressure beneath the continuous strip footing is distributed completely differently in the case of two compacted aggregate trenches under each end of the footing. Figure 6-20 below illustrates how the contact pressures reach a maximum at the far ends of the footing when the aggregate trenches are in this location. The area replacement ratio of compacted aggregate in Figure 6-20 is the same as the configuration in Figure 6-19. This is achieved by having two trenches of half the width and equal length as the one modeled for Figure 6-19. In Figure 6-20 the contact pressures on the footing-native clay interface are relatively constant and low in magnitude. The maximum contact pressures are reached at the extreme edges of the footing as was observed in the non-improved clay soil trials, but this time with a much higher pressure gradient.

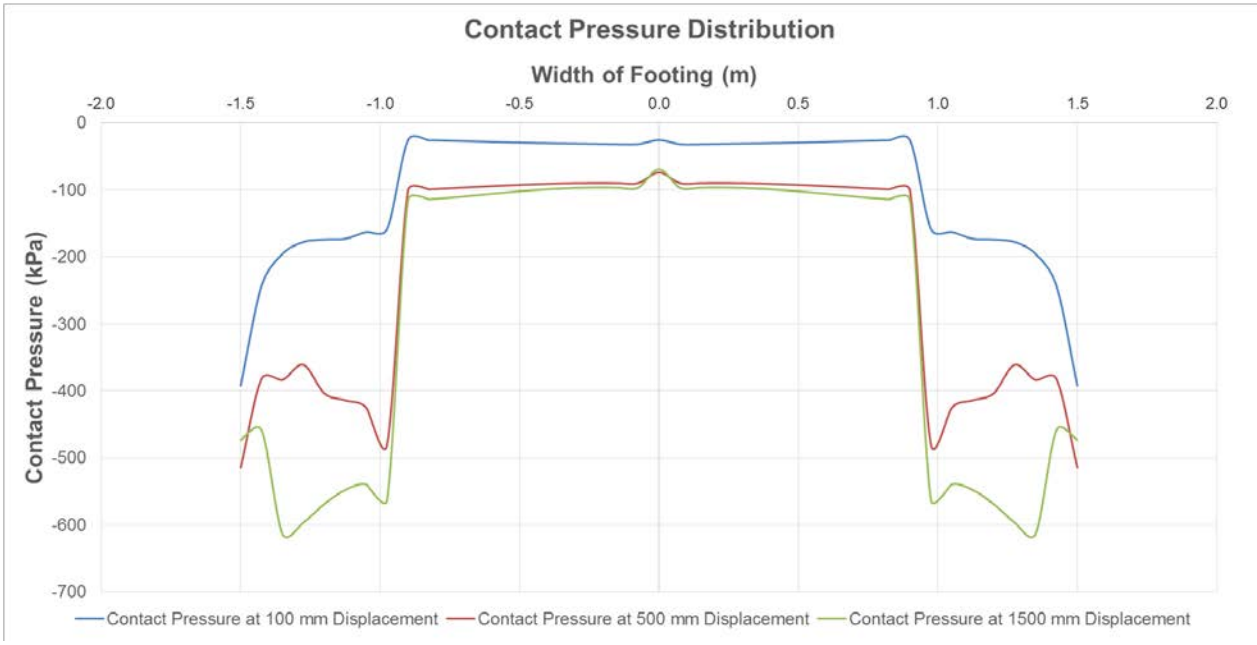


*Figure 6-20: Contact pressure distribution of 3m long, 1.5m wide compacted aggregate trench (40 kPa native clay and two trenches along sides beneath footing)*

It was previously shown that placing compacted aggregate trenches at the edges of the footing was more effective at increasing bearing capacity of the soil profile. This is because the weaker clay material is being replaced in the regions beneath the footing most prone to high pressure with a more competent soil, compacted stone. The pressure distributions of Figure 6-19 and Figure 6-20 substantiates the previous observations that less wide aggregate trenches placed at the ends of a continuous strip footing provide a more significant increase in bearing capacity as compared to a single trench of double the width in the center of the footing.

### *6.3 Summary of Results*

It can be concluded that a clay soil of any undrained shear strength can be improved with a compacted aggregate trench by the comparison of the results of the numerical simulations. The percentage increase in bearing capacity relative to the native clay soil with a compacted aggregate trench reduces with increasing depth of footing embedment. Furthermore it was shown that increasing the length of a compacted aggregate trench compared to width is a more efficient way of enhancing the improvement of the soil relative to the unimproved native clay. Increasing the width of the trench requires a greater volume of additional aggregate in order to produce the same percentage increase in bearing capacity. Another finding of the study demonstrated that two separate trenches, each along the edges of a continuous strip footing, more significantly increases the bearing capacity of the soil compared to the single trench case of equal area replacement ratio. Higher bearing pressures for an improved soil profile can be achieved with the same trench length and area replacement ratio of compacted aggregate to native soil by separating the improvement into two trenches at each end of the footing. This

method of soil improvement may however be more costly to construct since it consists of two separate excavations. More information would be required to determine if the enhanced soil improvement realized by two separate compacted aggregate trenches would be more economical when compared to a single aggregate trench.

## 7.0 Summary, Conclusions, and Suggestions for Further Study

The following sections of this chapter highlight the steps taken for research into the efficacy of aggregate trench-reinforced clay ground improvement to increase bearing capacity of continuous strip foundations. Additionally, the key findings of the research are discussed and suggestions for further study are provided.

### *7.1 Summary of Research Performed*

The study to investigate compacted aggregate trenches began with a review of the literature available regarding related topics. Chapter 2 presented a brief survey of some current computational models used to evaluate the bearing capacity of a soil profile as well as aggregate pier improvements for a weak native soil. After consulting the literature, the research objectives were established to investigate the potential of improving a clay soil with compacted aggregate trenches, rather than the typical aggregate piers. This goal was driven by the types of construction equipment that are most commonly available. The excavators that would construct the proposed compacted aggregate trenches are considered preferable to the drilling machines necessary for rammed aggregate piers because they are more common and widely available. While considering the constraints for construction, a parametric study was devised to encompass a wide range of compacted aggregate trenches that could be used to improve a clay soil.

The first analysis performed were calculations of bearing capacity for unimproved native clay of 20, 40, and 80 kPa undrained shear strength at various footing depths of embedment. The calculated values were then verified with numerical models generated in *FLAC 7.0*. Next, the parametric study of various aggregate trench-improved soil cases was conducted with numerical

models in *FLAC 7.0*. The compacted aggregate trench models addressed a variety of trench dimensions, area replacement ratios beneath the footing, and two different trench configurations. Output data from all of these models was used to generate bearing pressure versus displacement figures (Appendix C) as well as contact pressure distribution figures for all cases in 40 kPa undrained shear strength clay (Appendix E). Results were presented regarding the soil improvement generated by introducing compacted aggregate trenches to the native clay.

### *7.2 Conclusions*

Numerical models of unimproved clay soil profiles demonstrated that a near-linear relationship exists between soil bearing capacity and depth of embedment of the footing. This relationship however, was altered by the introduction of a compacted aggregate trench. In an aggregate trench improved soil profile, the percentage increase in bearing capacity is reduced as the footing is embedded deeper into the soil. The relationship of area replacement ratio of the compacted aggregate trench relative to the native soil beneath a footing was also found to be non-linear. As the area replacement ratio is increased, diminishing returns are observed for the increase in bearing capacity relative to an unimproved clay soil profile.

The simulations performed in *FLAC* reveal that the most significant compacted aggregate trench design parameter for single trenches is length. Increasing the length of a compacted aggregate trench will result in a greater improvement to the soil bearing capacity then increasing width. The most significant overall design factor, however, was found to be the configuration of trenches beneath the footing. By using the same volume of aggregate, two trenches of half the width can be installed along the edges of a strip footing. This will provide a significantly larger

improvement to bearing capacity compared to a single trench. Thus, the most effective way within the bounds of this study to improve a clay soil is with two long and relatively narrow compacted aggregate trenches beneath the two edges of a continuous strip footing. While this method provides the greatest improvement to a clay soil, it may not however be the most economical to construct.

### *7.3 Suggestions for Further Study*

Since the cases with two compacted aggregate trenches provided the greatest improvement to a clay soil profile, it is suggested to further investigate this configuration. A recommended first step would be to evaluate soil improved with two trenches of equal parameters at different locations beneath the footing. Placing the trenches closer and further apart from the edges of the footing would be necessary to pin down the exact configuration that provides the highest increase to the native clay bearing capacity. Once the optimal trench placement was determined, a new parametric study with a larger range of trench lengths and widths should be conducted. This would ideally reveal a strong relationship between compacted aggregate trench sizes and bearing capacity of the improved soil profile. With this additional data, it would be recommended to formulate bearing capacity factors that could be applied to Equation (4-1) used in Chapter 4 to compute the bearing capacity of the native soil. Additionally, it is assumed that at some point there will be convergence in soil improvement with increasing trench length. Finding this length with the use of more numerical models would be advantageous to determining when it would be necessary to increase trench width in order to further increase bearing capacity.

Although further simulations could be performed to provide the basis for proposing new bearing capacity factors, it is also suggested that field tests be performed to confirm the suitability of such factors. A variety of the analyzed soil improvement cases could be constructed and tested to large displacements to approach the bearing capacity of trench-improved soil. This field testing would provide a set of data that could allow definite statements regarding the actual improvement gained by the use of compacted aggregate trenches to be made. Experience in constructing these trenches would also provide insight to the costs associated with excavating and filling two trenches beneath a footing as opposed to a single aggregate trench of double the width. This experience along with construction estimating research could reveal the most economically feasible way to improve the bearing capacity of a clay soil.

## References


Caterpillar Inc. *390D L Hydraulic Excavators*. Caterpillar, 2013.

Cerato, Amy B., and Alan J. Lutenegger. (2007) "Scale Effects of Shallow Foundation Bearing Capacity on Granular Material." *Journal of Geotechnical and Geoenvironmental Engineering* 133.10: 1192-202.

Coduto, Donald P. (2001) *Foundation Design: Principles and Practices*. 2nd ed. Upper Saddle River, NJ: Prentice Hall.

Etezad, M., A. M. Hanna, and T. Ayadat. (2015) "Bearing Capacity of a Group of Stone Columns in Soft Soil." *International Journal of Geomechanics* 15.2: 04014043-1 4014043-15.

Hanna, A. M., Etezad, M., and Ayadat, T. (2013) “Mode of Failure of a Group of Stone Columns in Soft Soil.” *International Journal of Geomechanics*, 10.1061/(ASCE) GM.1943 5622.0000175, 87-96

Hayward Baker, (2016) "Vibro Pier Sample Specifications." <http://www.haywardbaker.com/WhatWeDo/Techniques/GroundImprovement/VibroPiers/Specifications/default.aspx>

Itasca Consulting Group Inc. (2011) “User’s Guide” *Fast Lagrangian Analysis of Continua.* 1-3.

Itasca Consulting Group Inc. (2011) “Theory and Background” *Fast Lagrangian Analysis of Continua*. 1-12.

Itasca Consulting Group Inc. (2011) “Constitutive Models” *Fast Lagrangian Analysis of Continua*. 30-145.

Komatsu Europe. *Mini Excavator PC30MR-3*. Japan: Komatsu Europe, 2012. Print.

Madhav, M. R., N.G. R. Iyengar, P. P. Vitkar, and A. Nandia. (1979) "Increased Bearing Capacity and Reduced Settlements Due to Inclusions in Soil." Proc. of International Conference on Soil Reinforcement, France, Paris. Kampur, India: Indian Institute of Technology. 329-33.

Madhav, M. R., and P. P. Vitkar. (1978) "Strip Footing on Weak Clay Stabilized with a Granular Trench or Pile." *Canadian Geotechnical Journal* 15.4: 605-09.

Nazir, Ashraf Kamal, and Wasim R. Azzam. (2010) “Improving the Bearing Capacity of Footing on Soft Clay with Sand Pile With/without Skirts.” *Alexandria Engineering Journal* 49.4: 371-77

Stuedlein, Armin W., and Robert D. Holtz. (2012) "Analysis of Footing Load Tests on Aggregate Pier Reinforced Clay." *Journal of Geotechnical and Geoenvironmental Engineering* 138.9: 1091-103.

Stuedlein, Armin W., and Robert D. Holtz. (2013) "Bearing Capacity of Spread Footings on Aggregate Pier Reinforced Clay." *Journal of Geotechnical and Geoenvironmental Engineering* 139: 49-58

Terzaghi, K. (1943) *Theoretical Soil Mechanics.* New York: J. Wiley and Sons.

White, David J., Ha T. V. Pham, and Kenneth K. Hoevelkamp. (2007) “Support Mechanisms of Rammed Aggregate Piers. I: Experimental Results.” *Journal of Geotechnical and Geoenvironmental Engineering* 133.12: 1503-511.

# A. Appendix: Bearing Capacity Calculations of Control Scenarios

Calculation verification of ultimate bearing capacity of soil profile to be reinforced and analyzed in FLAC 7.0. Values taken from soil properties are as follows:

prop density: $\rho := 1800$ cohesion: $c := 80000$ friction: $\phi' := 0\ deg$

Analysis of non-reinforced clay profile - Bearing Capacity with no embedment

$s_u := 80\ kPa$ $\gamma := 17.65\ \frac{kN}{m^3}$ $D_f := 0\ m$ $B := 3\ m$ $k_p := \tan\left(45\ deg + \frac{\phi'}{2}\right)^2$

| | | |
|---|---|---|
| Meyerhof corrections | $f_{qd} := 1$ | $f_{qd} = 1$ |
| | $f_{\gamma d} := 1$ | $f_{\gamma d} = 1$ |
| | $f_{cd} := 1 + 0.2 \cdot \sqrt{k_p} \cdot \left(\frac{D_f}{B}\right)$ | $f_{cd} = 1$ |
| Bearing coefficients | $N_q := e^{\pi \cdot \tan(\phi')} \cdot k_p$ | $N_q = 1$ |
| | $N_\gamma := 2 \cdot (N_q + 1) \cdot \tan(\phi')$ | $N_\gamma = 0$ |
| | $N_c := \pi + 2$ | $N_c = 5.14$ |
| Vertical effective stress | $\sigma' := D_f \cdot \gamma$ | $\sigma' = 0\ kPa$ |
| Cohesion value | $c' := s_u - \sigma' \cdot \tan(\phi')$ | $c' = 80\ kPa$ |

Ultimate bearing capacity

$$q_{ult.0} := c' \cdot N_c \cdot f_{cd} + \sigma' \cdot N_q \cdot f_{qd} + \frac{1}{2} \cdot B \cdot \gamma \cdot N_\gamma \cdot f_{\gamma d}$$

Analysis of non-reinforced clay profile - Bearing Capacity with 1m embedment

$s_u := 80\ kPa$ $\gamma := 17.65\ \frac{kN}{m^3}$ $D_f := 1\ m$ $B := 3\ m$ $k_p := \tan\left(45\ deg + \frac{\phi'}{2}\right)^2$

| | | |
|---|---|---|
| Meyerhof corrections | $f_{qd} := 1$ | $f_{qd} = 1$ |
| | $f_{\gamma d} := 1$ | $f_{\gamma d} = 1$ |
| | $f_{cd} := 1 + 0.2 \cdot \sqrt{k_p} \cdot \left(\frac{D_f}{B}\right)$ | $f_{cd} = 1.067$ |
| Bearing coefficients | $N_q := e^{\pi \cdot \tan(\phi')} \cdot k_p$ | $N_q = 1$ |
| | $N_\gamma := 2 \cdot (N_q + 1) \cdot \tan(\phi')$ | $N_\gamma = 0$ |
| | $N_c := \pi + 2$ | $N_c = 5.14$ |
| Vertical effective stress | $\sigma' := D_f \cdot \gamma$ | $\sigma' = 17.65\ kPa$ |
| Cohesion value | $c' := s_u - \sigma' \cdot \tan(\phi')$ | $c' = 80\ kPa$ |

Ultimate bearing capacity

$$q_{ult.1} := c' \cdot N_c \cdot f_{cd} + \sigma' \cdot N_q \cdot f_{qd} + \frac{1}{2} \cdot B \cdot \gamma \cdot N_\gamma \cdot f_{\gamma d}$$

Analysis of non-reinforced clay profile - Bearing Capacity with 1.5m embedment

$s_u := 80\ kPa \qquad \gamma := 17.65\ \frac{kN}{m^3} \qquad D_f := 1.5\ m \qquad B := 3\ m \qquad k_p := \tan\left(45\ deg + \frac{\phi'}{2}\right)^2$

Meyerhof corrections

$f_{qd} := 1 \qquad f_{qd} = 1$

$f_{\gamma d} := 1 \qquad f_{\gamma d} = 1$

$f_{cd} := 1 + 0.2 \cdot \sqrt{k_p} \cdot \left(\frac{D_f}{B}\right) \qquad f_{cd} = 1.1$

Bearing coefficients

$N_q := e^{\pi \cdot \tan(\phi')} \cdot k_p \qquad N_q = 1$

$N_\gamma := 2 \cdot (N_q + 1) \cdot \tan(\phi') \qquad N_\gamma = 0$

$N_c := \pi + 2 \qquad N_c = 5.14$

Vertical effective stress $\sigma' := D_f \cdot \gamma \qquad \sigma' = 26.475\ kPa$

Cohesion value $c' := s_u - \sigma' \cdot \tan(\phi') \qquad c' = 80\ kPa$

Ultimate bearing capacity

$$q_{ult.1.5} := c' \cdot N_c \cdot f_{cd} + \sigma' \cdot N_q \cdot f_{qd} + \frac{1}{2} \cdot B \cdot \gamma \cdot N_\gamma \cdot f_{\gamma d}$$

Analysis of non-reinforced clay profile - Bearing Capacity with 2m embedment

$s_u := 80\ kPa \qquad \gamma := 17.65\ \frac{kN}{m^3} \qquad D_f := 2\ m \qquad B := 3\ m \qquad k_p := \tan\left(45\ deg + \frac{\phi'}{2}\right)^2$

Meyerhof corrections

$f_{qd} := 1 \qquad f_{qd} = 1$

$f_{\gamma d} := 1 \qquad f_{\gamma d} = 1$

$f_{cd} := 1 + 0.2 \cdot \sqrt{k_p} \cdot \left(\frac{D_f}{B}\right) \qquad f_{cd} = 1.133$

Bearing coefficients

$N_q := e^{\pi \cdot \tan(\phi')} \cdot k_p \qquad N_q = 1$

$N_\gamma := 2 \cdot (N_q + 1) \cdot \tan(\phi') \qquad N_\gamma = 0$

$N_c := \pi + 2 \qquad N_c = 5.14$

Vertical effective stress $\sigma' := D_f \cdot \gamma \qquad \sigma' = 35.3\ kPa$

Cohesion value $c' := s_u - \sigma' \cdot \tan(\phi') \qquad c' = 80\ kPa$

Ultimate bearing capacity

$$q_{ult.2} := c' \cdot N_c \cdot f_{cd} + \sigma' \cdot N_q \cdot f_{qd} + \frac{1}{2} \cdot B \cdot \gamma \cdot N_\gamma \cdot f_{\gamma d}$$

Analysis of non-reinforced clay profile - Bearing Capacity with 3m embedment

$s_u := 80\ kPa$ $\gamma := 17.65\ \frac{kN}{m^3}$ $D_f := 3\ m$ $B := 3\ m$ $k_p := \tan\left(45\ deg + \frac{\phi'}{2}\right)^2$

Meyerhof corrections

$f_{qd} := 1$ $f_{qd} = 1$

$f_{\gamma d} := 1$ $f_{\gamma d} = 1$

$f_{cd} := 1 + 0.2 \cdot \sqrt{k_p} \cdot \left(\frac{D_f}{B}\right)$ $f_{cd} = 1.2$

Bearing coefficients

$N_q := e^{\pi \cdot \tan(\phi')} \cdot k_p$ $N_q = 1$

$N_\gamma := 2 \cdot (N_q + 1) \cdot \tan(\phi')$ $N_\gamma = 0$

$N_c := \pi + 2$ $N_c = 5.14$

Vertical effective stress $\sigma' := D_f \cdot \gamma$ $\sigma' = 52.95\ kPa$

Cohesion value $c' := s_u - \sigma' \cdot \tan(\phi')$ $c' = 80\ kPa$

Ultimate bearing capacity

$$q_{ult.3} := c' \cdot N_c \cdot f_{cd} + \sigma' \cdot N_q \cdot f_{qd} + \frac{1}{2} \cdot B \cdot \gamma \cdot N_\gamma \cdot f_{\gamma d}$$

Bearing capacity of clay soil with cohesion of 80kPa

Bearing Capacity with no embedment: $q_{ult.0} = 411\ kPa$

Bearing Capacity with 1m embedment: $q_{ult.1} = 456\ kPa$

Bearing Capacity with 1.5m embedment: $q_{ult.1.5} = 479\ kPa$

Bearing Capacity with 2m embedment: $q_{ult.2} = 501\ kPa$

Bearing Capacity with 3m embedment: $q_{ult.3} = 547\ kPa$

Calculation verification of ultimate bearing capacity of soil profile to be reinforced and analyzed in FLAC 7.0. Values taken from soil properties are as follows:

prop density: $\rho := 1800$ cohesion: $c := 40000$ friction: $\phi' := 0\ deg$

Analysis of non-reinforced clay profile - Bearing Capacity with no embedment

$s_u := 40\ kPa$ $\gamma := 17.65\ \frac{kN}{m^3}$ $D_f := 0\ m$ $B := 3\ m$ $k_p := \tan\left(45\ deg + \frac{\phi'}{2}\right)^2$

Meyerhof corrections

$f_{qd} := 1$ $f_{qd} = 1$

$f_{\gamma d} := 1$ $f_{\gamma d} = 1$

$f_{cd} := 1 + 0.2 \cdot \sqrt{k_p} \cdot \left(\frac{D_f}{B}\right)$ $f_{cd} = 1$

Bearing coefficients

$N_q := e^{\pi \cdot \tan(\phi')} \cdot k_p$ $N_q = 1$

$N_\gamma := 2 \cdot (N_q + 1) \cdot \tan(\phi')$ $N_\gamma = 0$

$N_c := \pi + 2$ $N_c = 5.14$

Vertical effective stress $\sigma' := D_f \cdot \gamma$ $\sigma' = 0\ kPa$

Cohesion value $c' := s_u - \sigma' \cdot \tan(\phi')$ $c' = 40\ kPa$

Ultimate bearing capacity

$$q_{ult.0} := c' \cdot N_c \cdot f_{cd} + \sigma' \cdot N_q \cdot f_{qd} + \frac{1}{2} \cdot B \cdot \gamma \cdot N_\gamma \cdot f_{\gamma d}$$

Analysis of non-reinforced clay profile - Bearing Capacity with 1m embedment

$s_u := 40\ kPa$ $\gamma := 17.65\ \frac{kN}{m^3}$ $D_f := 1\ m$ $B := 3\ m$ $k_p := \tan\left(45\ deg + \frac{\phi'}{2}\right)^2$

Meyerhof corrections

$f_{qd} := 1$ $f_{qd} = 1$

$f_{\gamma d} := 1$ $f_{\gamma d} = 1$

$f_{cd} := 1 + 0.2 \cdot \sqrt{k_p} \cdot \left(\frac{D_f}{B}\right)$ $f_{cd} = 1.067$

Bearing coefficients

$N_q := e^{\pi \cdot \tan(\phi')} \cdot k_p$ $N_q = 1$

$N_\gamma := 2 \cdot (N_q + 1) \cdot \tan(\phi')$ $N_\gamma = 0$

$N_c := \pi + 2$ $N_c = 5.14$

Vertical effective stress $\sigma' := D_f \cdot \gamma$ $\sigma' = 17.65\ kPa$

Cohesion value $c' := s_u - \sigma' \cdot \tan(\phi')$ $c' = 40\ kPa$

Ultimate bearing capacity

$$q_{ult.1} := c' \cdot N_c \cdot f_{cd} + \sigma' \cdot N_q \cdot f_{qd} + \frac{1}{2} \cdot B \cdot \gamma \cdot N_\gamma \cdot f_{\gamma d}$$

Analysis of non-reinforced clay profile - Bearing Capacity with 1.5m embedment

$s_u := 40\ kPa \qquad \gamma := 17.65\ \frac{kN}{m^3} \qquad D_f := 1.5\ m \qquad B := 3\ m \qquad k_p := \tan\left(45\ deg + \frac{\phi'}{2}\right)^2$

Meyerhof corrections

$f_{qd} := 1 \qquad f_{qd} = 1$

$f_{\gamma d} := 1 \qquad f_{\gamma d} = 1$

$f_{cd} := 1 + 0.2 \cdot \sqrt{k_p} \cdot \left(\frac{D_f}{B}\right) \qquad f_{cd} = 1.1$

Bearing coefficients

$N_q := e^{\pi \cdot \tan(\phi')} \cdot k_p \qquad N_q = 1$

$N_\gamma := 2 \cdot (N_q + 1) \cdot \tan(\phi') \qquad N_\gamma = 0$

$N_c := \pi + 2 \qquad N_c = 5.14$

Vertical effective stress $\sigma' := D_f \cdot \gamma \qquad \sigma' = 26.475\ kPa$

Cohesion value $c' := s_u - \sigma' \cdot \tan(\phi') \qquad c' = 40\ kPa$

Ultimate bearing capacity

$$q_{ult.1.5} := c' \cdot N_c \cdot f_{cd} + \sigma' \cdot N_q \cdot f_{qd} + \frac{1}{2} \cdot B \cdot \gamma \cdot N_\gamma \cdot f_{\gamma d}$$

Analysis of non-reinforced clay profile - Bearing Capacity with 2m embedment

$s_u := 40\ kPa \qquad \gamma := 17.65\ \frac{kN}{m^3} \qquad D_f := 2\ m \qquad B := 3\ m \qquad k_p := \tan\left(45\ deg + \frac{\phi'}{2}\right)^2$

Meyerhof corrections

$f_{qd} := 1 \qquad f_{qd} = 1$

$f_{\gamma d} := 1 \qquad f_{\gamma d} = 1$

$f_{cd} := 1 + 0.2 \cdot \sqrt{k_p} \cdot \left(\frac{D_f}{B}\right) \qquad f_{cd} = 1.133$

Bearing coefficients

$N_q := e^{\pi \cdot \tan(\phi')} \cdot k_p \qquad N_q = 1$

$N_\gamma := 2 \cdot (N_q + 1) \cdot \tan(\phi') \qquad N_\gamma = 0$

$N_c := \pi + 2 \qquad N_c = 5.14$

Vertical effective stress $\sigma' := D_f \cdot \gamma \qquad \sigma' = 35.3\ kPa$

Cohesion value $c' := s_u - \sigma' \cdot \tan(\phi') \qquad c' = 40\ kPa$

Ultimate bearing capacity

$$q_{ult.2} := c' \cdot N_c \cdot f_{cd} + \sigma' \cdot N_q \cdot f_{qd} + \frac{1}{2} \cdot B \cdot \gamma \cdot N_\gamma \cdot f_{\gamma d}$$

Analysis of non-reinforced clay profile - Bearing Capacity with 3m embedment

$s_u := 40\ kPa$ $\gamma := 17.65\ \frac{kN}{m^3}$ $D_f := 3\ m$ $B := 3\ m$ $k_p := \tan\left(45\ deg + \frac{\phi'}{2}\right)^2$

Meyerhof corrections

$f_{qd} := 1$ $f_{qd} = 1$

$f_{\gamma d} := 1$ $f_{\gamma d} = 1$

$f_{cd} := 1 + 0.2 \cdot \sqrt{k_p} \cdot \left(\frac{D_f}{B}\right)$ $f_{cd} = 1.2$

Bearing coefficients

$N_q := e^{\pi \cdot \tan(\phi')} \cdot k_p$ $N_q = 1$

$N_\gamma := 2 \cdot (N_q + 1) \cdot \tan(\phi')$ $N_\gamma = 0$

$N_c := \pi + 2$ $N_c = 5.14$

Vertical effective stress $\sigma' := D_f \cdot \gamma$ $\sigma' = 52.95\ kPa$

Cohesion value $c' := s_u - \sigma' \cdot \tan(\phi')$ $c' = 40\ kPa$

Ultimate bearing capacity

$$q_{ult.3} := c' \cdot N_c \cdot f_{cd} + \sigma' \cdot N_q \cdot f_{qd} + \frac{1}{2} \cdot B \cdot \gamma \cdot N_\gamma \cdot f_{\gamma d}$$

Bearing capacity of clay soil with cohesion of 40kPa

Bearing Capacity with no embedment: $q_{ult.0} = 206\ kPa$

Bearing Capacity with 1m embedment: $q_{ult.1} = 237\ kPa$

Bearing Capacity with 1.5m embedment: $q_{ult.1.5} = 253\ kPa$

Bearing Capacity with 2m embedment: $q_{ult.2} = 268\ kPa$

Bearing Capacity with 3m embedment: $q_{ult.3} = 300\ kPa$

Calculation verification of ultimate bearing capacity of soil profile to be reinforced and analyzed in FLAC 7.0. Values taken from soil properties are as follows:

prop density: $\rho := 1800$ cohesion: $c := 20000$ friction: $\phi' := 0\ deg$

Analysis of non-reinforced clay profile - Bearing Capacity with no embedment

$s_u := 20\ kPa$ $\gamma := 17.65\ \frac{kN}{m^3}$ $D_f := 0\ m$ $B := 3\ m$ $k_p := \tan\left(45\ deg + \frac{\phi'}{2}\right)^2$

Meyerhof corrections

$f_{qd} := 1$ $f_{qd} = 1$

$f_{\gamma d} := 1$ $f_{\gamma d} = 1$

$f_{cd} := 1 + 0.2 \cdot \sqrt{k_p} \cdot \left(\frac{D_f}{B}\right)$ $f_{cd} = 1$

Bearing coefficients

$N_q := e^{\pi \cdot \tan(\phi')} \cdot k_p$ $N_q = 1$

$N_\gamma := 2 \cdot (N_q + 1) \cdot \tan(\phi')$ $N_\gamma = 0$

$N_c := \pi + 2$ $N_c = 5.14$

Vertical effective stress $\sigma' := D_f \cdot \gamma$ $\sigma' = 0\ kPa$

Cohesion value $c' := s_u - \sigma' \cdot \tan(\phi')$ $c' = 20\ kPa$

Ultimate bearing capacity

$$q_{ult.0} := c' \cdot N_c \cdot f_{cd} + \sigma' \cdot N_q \cdot f_{qd} + \frac{1}{2} \cdot B \cdot \gamma \cdot N_\gamma \cdot f_{\gamma d}$$

Analysis of non-reinforced clay profile - Bearing Capacity with 1m embedment

$s_u := 20\ kPa$ $\gamma := 17.65\ \frac{kN}{m^3}$ $D_f := 1\ m$ $B := 3\ m$ $k_p := \tan\left(45\ deg + \frac{\phi'}{2}\right)^2$

Meyerhof corrections

$f_{qd} := 1$ $f_{qd} = 1$

$f_{\gamma d} := 1$ $f_{\gamma d} = 1$

$f_{cd} := 1 + 0.2 \cdot \sqrt{k_p} \cdot \left(\frac{D_f}{B}\right)$ $f_{cd} = 1.067$

Bearing coefficients

$N_q := e^{\pi \cdot \tan(\phi')} \cdot k_p$ $N_q = 1$

$N_\gamma := 2 \cdot (N_q + 1) \cdot \tan(\phi')$ $N_\gamma = 0$

$N_c := \pi + 2$ $N_c = 5.14$

Vertical effective stress $\sigma' := D_f \cdot \gamma$ $\sigma' = 17.65\ kPa$

Cohesion value $c' := s_u - \sigma' \cdot \tan(\phi')$ $c' = 20\ kPa$

Ultimate bearing capacity

$$q_{ult.1} := c' \cdot N_c \cdot f_{cd} + \sigma' \cdot N_q \cdot f_{qd} + \frac{1}{2} \cdot B \cdot \gamma \cdot N_\gamma \cdot f_{\gamma d}$$

Analysis of non-reinforced clay profile - Bearing Capacity with 1.5m embedment

$s_u := 20\ kPa$ $\gamma := 17.65\ \frac{kN}{m^3}$ $D_f := 1.5\ m$ $B := 3\ m$ $k_p := \tan\left(45\ deg + \frac{\phi'}{2}\right)^2$

Meyerhof corrections

$f_{qd} := 1$ $f_{qd} = 1$

$f_{\gamma d} := 1$ $f_{\gamma d} = 1$

$f_{cd} := 1 + 0.2 \cdot \sqrt{k_p} \cdot \left(\frac{D_f}{B}\right)$ $f_{cd} = 1.1$

Bearing coefficients

$N_q := e^{\pi \cdot \tan(\phi')} \cdot k_p$ $N_q = 1$

$N_\gamma := 2 \cdot (N_q + 1) \cdot \tan(\phi')$ $N_\gamma = 0$

$N_c := \pi + 2$ $N_c = 5.14$

Vertical effective stress $\sigma' := D_f \cdot \gamma$ $\sigma' = 26.475\ kPa$

Cohesion value $c' := s_u - \sigma' \cdot \tan(\phi')$ $c' = 20\ kPa$

Ultimate bearing capacity

$$q_{ult.1.5} := c' \cdot N_c \cdot f_{cd} + \sigma' \cdot N_q \cdot f_{qd} + \frac{1}{2} \cdot B \cdot \gamma \cdot N_\gamma \cdot f_{\gamma d}$$

Analysis of non-reinforced clay profile - Bearing Capacity with 2m embedment

$s_u := 20\ kPa$ $\gamma := 17.65\ \frac{kN}{m^3}$ $D_f := 2\ m$ $B := 3\ m$ $k_p := \tan\left(45\ deg + \frac{\phi'}{2}\right)^2$

Meyerhof corrections

$f_{qd} := 1$ $f_{qd} = 1$

$f_{\gamma d} := 1$ $f_{\gamma d} = 1$

$f_{cd} := 1 + 0.2 \cdot \sqrt{k_p} \cdot \left(\frac{D_f}{B}\right)$ $f_{cd} = 1.133$

Bearing coefficients

$N_q := e^{\pi \cdot \tan(\phi')} \cdot k_p$ $N_q = 1$

$N_\gamma := 2 \cdot (N_q + 1) \cdot \tan(\phi')$ $N_\gamma = 0$

$N_c := \pi + 2$ $N_c = 5.14$

Vertical effective stress $\sigma' := D_f \cdot \gamma$ $\sigma' = 35.3\ kPa$

Cohesion value $c' := s_u - \sigma' \cdot \tan(\phi')$ $c' = 20\ kPa$

Ultimate bearing capacity

$$q_{ult.2} := c' \cdot N_c \cdot f_{cd} + \sigma' \cdot N_q \cdot f_{qd} + \frac{1}{2} \cdot B \cdot \gamma \cdot N_\gamma \cdot f_{\gamma d}$$

Analysis of non-reinforced clay profile - Bearing Capacity with 3m embedment

$s_u := 20\ kPa$ $\gamma := 17.65\ \frac{kN}{m^3}$ $D_f := 3\ m$ $B := 3\ m$ $k_p := \tan\left(45\ deg + \frac{\phi'}{2}\right)^2$

Meyerhof corrections

$f_{qd} := 1$ $f_{qd} = 1$

$f_{\gamma d} := 1$ $f_{\gamma d} = 1$

$f_{cd} := 1 + 0.2 \cdot \sqrt{k_p} \cdot \left(\frac{D_f}{B}\right)$ $f_{cd} = 1.2$

Bearing coefficients

$N_q := e^{\pi \cdot \tan(\phi')} \cdot k_p$ $N_q = 1$

$N_\gamma := 2 \cdot (N_q + 1) \cdot \tan(\phi')$ $N_\gamma = 0$

$N_c := \pi + 2$ $N_c = 5.14$

Vertical effective stress $\sigma' := D_f \cdot \gamma$ $\sigma' = 52.95\ kPa$

Cohesion value $c' := s_u - \sigma' \cdot \tan(\phi')$ $c' = 20\ kPa$

Ultimate bearing capacity

$$q_{ult.3} := c' \cdot N_c \cdot f_{cd} + \sigma' \cdot N_q \cdot f_{qd} + \frac{1}{2} \cdot B \cdot \gamma \cdot N_\gamma \cdot f_{\gamma d}$$

Bearing capacity of clay soil with cohesion of 20kPa

Bearing Capacity with no embedment: $q_{ult.0} = 103\ kPa$

Bearing Capacity with 1m embedment: $q_{ult.1} = 127\ kPa$

Bearing Capacity with 1.5m embedment: $q_{ult.1.5} = 140\ kPa$

Bearing Capacity with 2m embedment: $q_{ult.2} = 152\ kPa$

Bearing Capacity with 3m embedment: $q_{ult.3} = 176\ kPa$

## B. Appendix: Table of Parametric Study for Trench Improved Clay Soil

*Table B-1: Control models of parametric study*

| No Trench Under Footing | | | | | | |
|---|---|---|---|---|---|---|
| Trial # | Trench Length $L_T$ *(m)* | Trench Width $W_T$ *(m)* | Footing Width $B_F$ *(m)* | Footing Depth $d_F$ *(m)* | Area Replacement $A_r$ *(%)* | Clay Cohesion $S_u$ *(kPa)* |
| 1 | 0.0 | 0.0 | 3.0 | 0.0 | 0% | 20.0 |
| 2 | 0.0 | 0.0 | 3.0 | 1.0 | 0% | 20.0 |
| 3 | 0.0 | 0.0 | 3.0 | 1.5 | 0% | 20.0 |
| 4 | 0.0 | 0.0 | 3.0 | 2.0 | 0% | 20.0 |
| 5 | 0.0 | 0.0 | 3.0 | 3.0 | 0% | 20.0 |
| 6 | 0.0 | 0.0 | 3.0 | 0.0 | 0% | 40.0 |
| 7 | 0.0 | 0.0 | 3.0 | 1.0 | 0% | 40.0 |
| 8 | 0.0 | 0.0 | 3.0 | 1.5 | 0% | 40.0 |
| 9 | 0.0 | 0.0 | 3.0 | 2.0 | 0% | 40.0 |
| 10 | 0.0 | 0.0 | 3.0 | 3.0 | 0% | 40.0 |
| 11 | 0.0 | 0.0 | 3.0 | 0.0 | 0% | 80.0 |
| 12 | 0.0 | 0.0 | 3.0 | 1.0 | 0% | 80.0 |
| 13 | 0.0 | 0.0 | 3.0 | 1.5 | 0% | 80.0 |
| 14 | 0.0 | 0.0 | 3.0 | 2.0 | 0% | 80.0 |
| 15 | 0.0 | 0.0 | 3.0 | 3.0 | 0% | 80.0 |

*Table B-2: Single trench models of parametric study*

| Single Trench Centered Under Footing | | | | | | |
|---|---|---|---|---|---|---|
| Trial # | Trench Length $L_T$ *(m)* | Trench Width $W_T$ *(m)* | Footing Width $B_F$ *(m)* | Footing Depth $d_F$ *(m)* | Area Replacement $A_r$ *(%)* | Clay Cohesion $S_u$ *(kPa)* |
| 16 | 6.0 | 1.5 | 3.0 | 0.0 | 50% | 20.0 |
| 17 | 6.0 | 1.5 | 3.0 | 1.5 | 50% | 20.0 |
| 18 | 6.0 | 1.5 | 3.0 | 3.0 | 50% | 20.0 |
| 19 | 6.0 | 0.9 | 3.0 | 0.0 | 30% | 20.0 |
| 20 | 6.0 | 0.9 | 3.0 | 1.5 | 30% | 20.0 |
| 21 | 6.0 | 0.9 | 3.0 | 3.0 | 30% | 20.0 |
| 22 | 6.0 | 0.6 | 3.0 | 0.0 | 20% | 20.0 |
| 23 | 6.0 | 0.6 | 3.0 | 1.5 | 20% | 20.0 |
| 24 | 6.0 | 0.6 | 3.0 | 3.0 | 20% | 20.0 |
| 25 | 3.0 | 1.5 | 3.0 | 0.0 | 50% | 20.0 |
| 26 | 3.0 | 1.5 | 3.0 | 1.5 | 50% | 20.0 |
| 27 | 3.0 | 1.5 | 3.0 | 3.0 | 50% | 20.0 |
| 28 | 3.0 | 0.9 | 3.0 | 0.0 | 30% | 20.0 |
| 29 | 3.0 | 0.9 | 3.0 | 1.5 | 30% | 20.0 |
| 30 | 3.0 | 0.9 | 3.0 | 3.0 | 30% | 20.0 |
| 31 | 3.0 | 0.6 | 3.0 | 0.0 | 20% | 20.0 |
| 32 | 3.0 | 0.6 | 3.0 | 1.5 | 20% | 20.0 |
| 33 | 3.0 | 0.6 | 3.0 | 3.0 | 20% | 20.0 |
| 34 | 7.2 | 0.9 | 3.0 | 0.0 | 30% | 40.0 |
| 35 | 7.2 | 0.9 | 3.0 | 3.0 | 30% | 40.0 |
| 36 | 6.8 | 2.3 | 3.0 | 0.0 | 75% | 40.0 |
| 37 | 6.8 | 2.3 | 3.0 | 3.0 | 75% | 40.0 |
| 38 | 6.0 | 3.0 | 3.0 | 0.0 | 100% | 40.0 |
| 39 | 6.0 | 3.0 | 3.0 | 1.0 | 100% | 40.0 |
| 40 | 6.0 | 3.0 | 3.0 | 2.0 | 100% | 40.0 |
| 41 | 6.0 | 3.0 | 3.0 | 3.0 | 100% | 40.0 |
| 42 | 6.0 | 2.0 | 3.0 | 0.0 | 67% | 40.0 |
| 43 | 6.0 | 2.0 | 3.0 | 1.0 | 67% | 40.0 |
| 44 | 6.0 | 2.0 | 3.0 | 2.0 | 67% | 40.0 |
| 45 | 6.0 | 2.0 | 3.0 | 3.0 | 67% | 40.0 |
| 46 | 5.2 | 2.6 | 3.0 | 0.0 | 87% | 40.0 |
| 47 | 5.2 | 2.6 | 3.0 | 1.0 | 87% | 40.0 |
| 48 | 5.2 | 2.6 | 3.0 | 2.0 | 87% | 40.0 |
| 49 | 5.2 | 2.6 | 3.0 | 3.0 | 87% | 40.0 |
| 50 | 4.8 | 0.6 | 3.0 | 0.0 | 20% | 40.0 |
| 51 | 4.8 | 0.6 | 3.0 | 1.0 | 20% | 40.0 |
| 52 | 4.8 | 0.6 | 3.0 | 2.0 | 20% | 40.0 |
| 53 | 4.8 | 0.6 | 3.0 | 3.0 | 20% | 40.0 |

| Single Trench Centered Under Footing | | | | | | |
|---|---|---|---|---|---|---|
| Trial # | Trench Length $L_T$ *(m)* | Trench Width $W_T$ *(m)* | Footing Width $B_F$ *(m)* | Footing Depth $d_F$ *(m)* | Area Replacement $A_r$ *(%)* | Clay Cohesion $S_u$ *(kPa)* |
| 54 | 4.51 | 2.26 | 3.0 | 0.0 | 75% | 40.0 |
| 55 | 4.51 | 2.26 | 3.0 | 1.0 | 75% | 40.0 |
| 56 | 4.5 | 2.3 | 3.0 | 2.0 | 75% | 40.0 |
| 57 | 4.5 | 2.3 | 3.0 | 3.0 | 75% | 40.0 |
| 58 | 4.5 | 1.5 | 3.0 | 0.0 | 50% | 40.0 |
| 59 | 4.5 | 1.5 | 3.0 | 3.0 | 50% | 40.0 |
| 60 | 4.5 | 0.9 | 3.0 | 0.0 | 30% | 40.0 |
| 61 | 4.5 | 0.9 | 3.0 | 3.0 | 30% | 40.0 |
| 62 | 4.0 | 2.0 | 3.0 | 0.0 | 67% | 40.0 |
| 63 | 4.0 | 2.0 | 3.0 | 1.0 | 67% | 40.0 |
| 64 | 4.0 | 2.0 | 3.0 | 2.0 | 67% | 40.0 |
| 65 | 4.0 | 2.0 | 3.0 | 3.0 | 67% | 40.0 |
| 66 | 3.0 | 1.5 | 3.0 | 0.0 | 50% | 40.0 |
| 67 | 3.0 | 1.5 | 3.0 | 1.0 | 50% | 40.0 |
| 68 | 3.0 | 1.5 | 3.0 | 2.0 | 50% | 40.0 |
| 69 | 3.0 | 1.5 | 3.0 | 3.0 | 50% | 40.0 |
| 70 | 3.0 | 0.6 | 3.0 | 0.0 | 20% | 40.0 |
| 71 | 3.0 | 0.6 | 3.0 | 3.0 | 20% | 40.0 |
| 72 | 6.0 | 1.5 | 3.0 | 0.0 | 50% | 80.0 |
| 73 | 6.0 | 1.5 | 3.0 | 1.5 | 50% | 80.0 |
| 74 | 6.0 | 1.5 | 3.0 | 3.0 | 50% | 80.0 |
| 75 | 6.0 | 0.9 | 3.0 | 0.0 | 30% | 80.0 |
| 76 | 6.0 | 0.9 | 3.0 | 1.5 | 30% | 80.0 |
| 77 | 6.0 | 0.9 | 3.0 | 3.0 | 30% | 80.0 |
| 78 | 6.0 | 0.6 | 3.0 | 0.0 | 20% | 80.0 |
| 79 | 6.0 | 0.6 | 3.0 | 1.5 | 20% | 80.0 |
| 80 | 6.0 | 0.6 | 3.0 | 3.0 | 20% | 80.0 |
| 81 | 3.0 | 1.5 | 3.0 | 0.0 | 50% | 80.0 |
| 82 | 3.0 | 1.5 | 3.0 | 1.5 | 50% | 80.0 |
| 83 | 3.0 | 1.5 | 3.0 | 3.0 | 50% | 80.0 |
| 84 | 3.0 | 0.9 | 3.0 | 0.0 | 30% | 80.0 |
| 85 | 3.0 | 0.9 | 3.0 | 1.5 | 30% | 80.0 |
| 86 | 3.0 | 0.9 | 3.0 | 3.0 | 30% | 80.0 |
| 87 | 3.0 | 0.6 | 3.0 | 0.0 | 20% | 80.0 |
| 88 | 3.0 | 0.6 | 3.0 | 1.5 | 20% | 80.0 |
| 89 | 3.0 | 0.6 | 3.0 | 3.0 | 20% | 80.0 |

*Table B-3: Double trench models of parametric study*

| Double Trench Each Under Edges of Footing | | | | | | |
|---|---|---|---|---|---|---|
| Trial # | Trench Length $L_T$ *(m)* | Trench Width $W_T$ *(m)* | Footing Width $B_F$ *(m)* | Footing Depth $d_F$ *(m)* | Area Replacement $A_r$ *(%)* | Clay Cohesion $S_u$ *(kPa)* |
| 90 | 6.0 | 0.75 | 3.0 | 0.0 | 50% | 40.0 |
| 91 | 6.0 | 0.75 | 3.0 | 1.5 | 50% | 40.0 |
| 92 | 6.0 | 0.75 | 3.0 | 3.0 | 50% | 40.0 |
| 93 | 6.0 | 0.45 | 3.0 | 0.0 | 30% | 40.0 |
| 94 | 6.0 | 0.45 | 3.0 | 1.5 | 30% | 40.0 |
| 95 | 6.0 | 0.45 | 3.0 | 3.0 | 30% | 40.0 |
| 96 | 6.0 | 0.30 | 3.0 | 0.0 | 20% | 40.0 |
| 97 | 6.0 | 0.30 | 3.0 | 1.5 | 20% | 40.0 |
| 98 | 6.0 | 0.30 | 3.0 | 3.0 | 20% | 40.0 |
| 99 | 3.0 | 0.75 | 3.0 | 0.0 | 50% | 40.0 |
| 100 | 3.0 | 0.75 | 3.0 | 1.5 | 50% | 40.0 |
| 101 | 3.0 | 0.75 | 3.0 | 3.0 | 50% | 40.0 |
| 102 | 3.0 | 0.45 | 3.0 | 0.0 | 30% | 40.0 |
| 103 | 3.0 | 0.45 | 3.0 | 1.5 | 30% | 40.0 |
| 104 | 3.0 | 0.45 | 3.0 | 3.0 | 30% | 40.0 |
| 105 | 3.0 | 0.30 | 3.0 | 0.0 | 20% | 40.0 |
| 106 | 3.0 | 0.30 | 3.0 | 1.5 | 20% | 40.0 |
| 107 | 3.0 | 0.30 | 3.0 | 3.0 | 20% | 40.0 |

## C. Appendix: Bearing Capacity vs Displacement Figures – All Trench Improved Cases

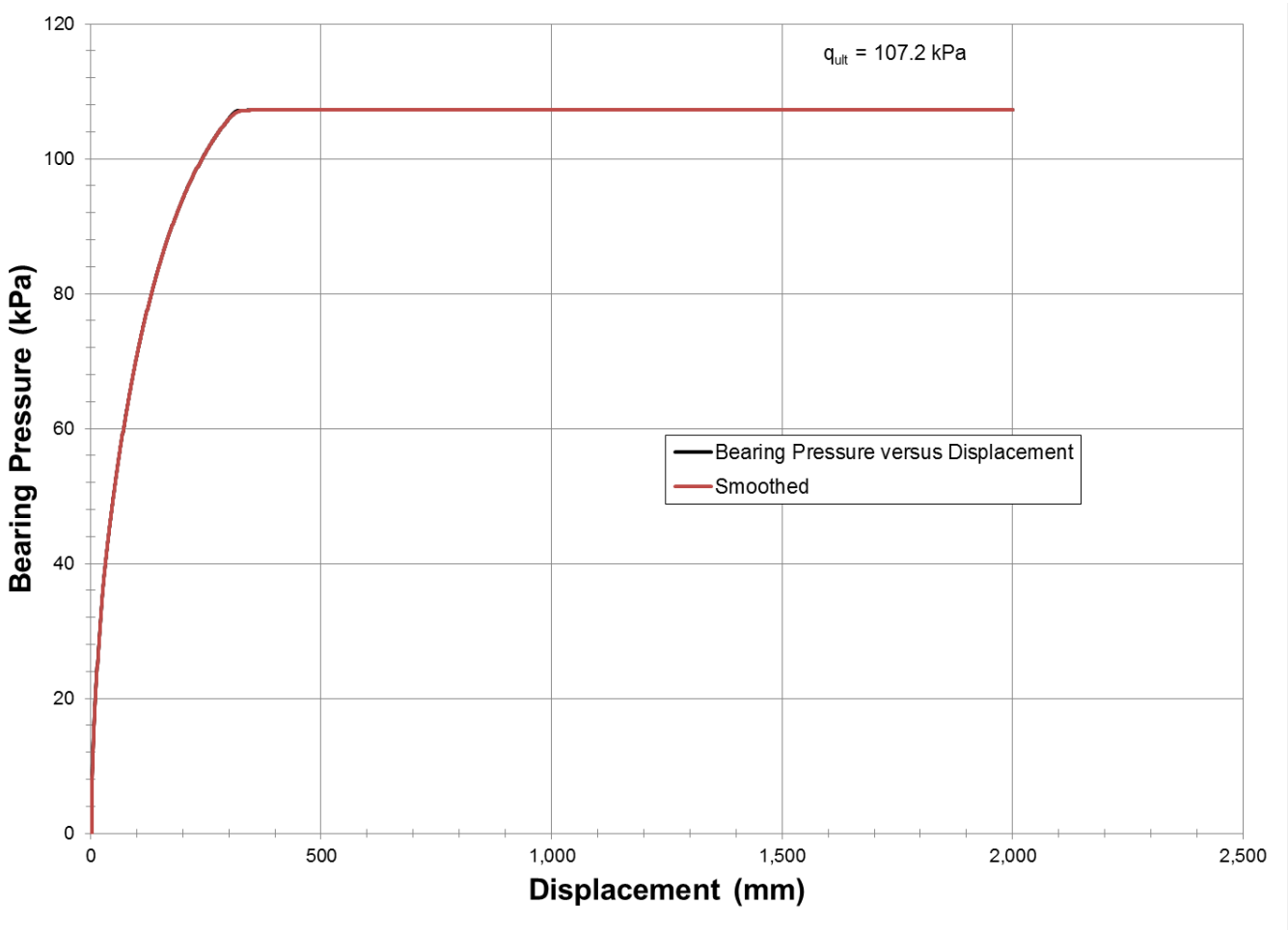


*Figure C-1: Bearing pressure versus displacement (unimproved 20 kPa native clay; no embedment depth)*

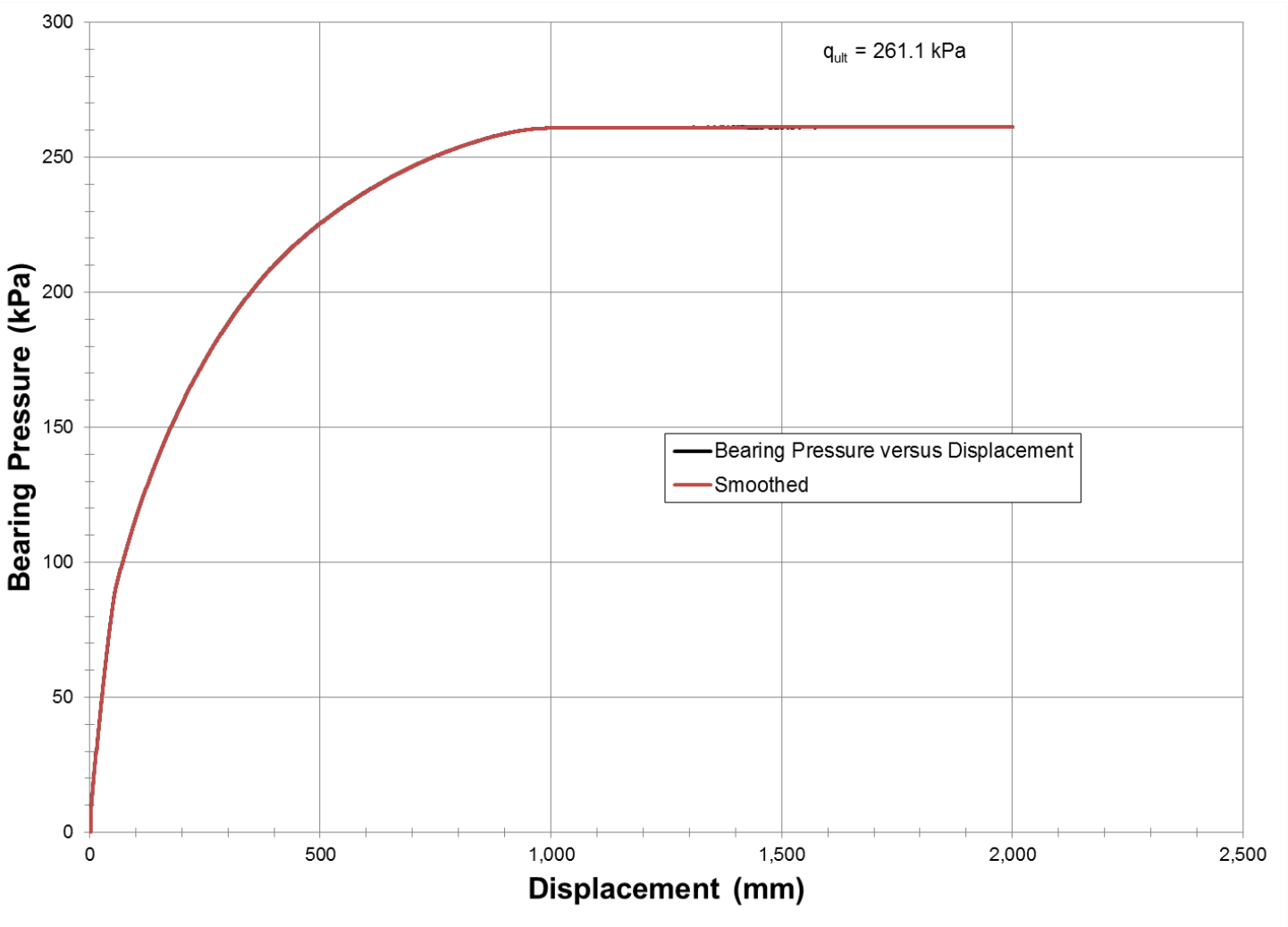


*Figure C-2: Bearing pressure versus displacement (unimproved 20 kPa native clay; 1 m embedment depth)*

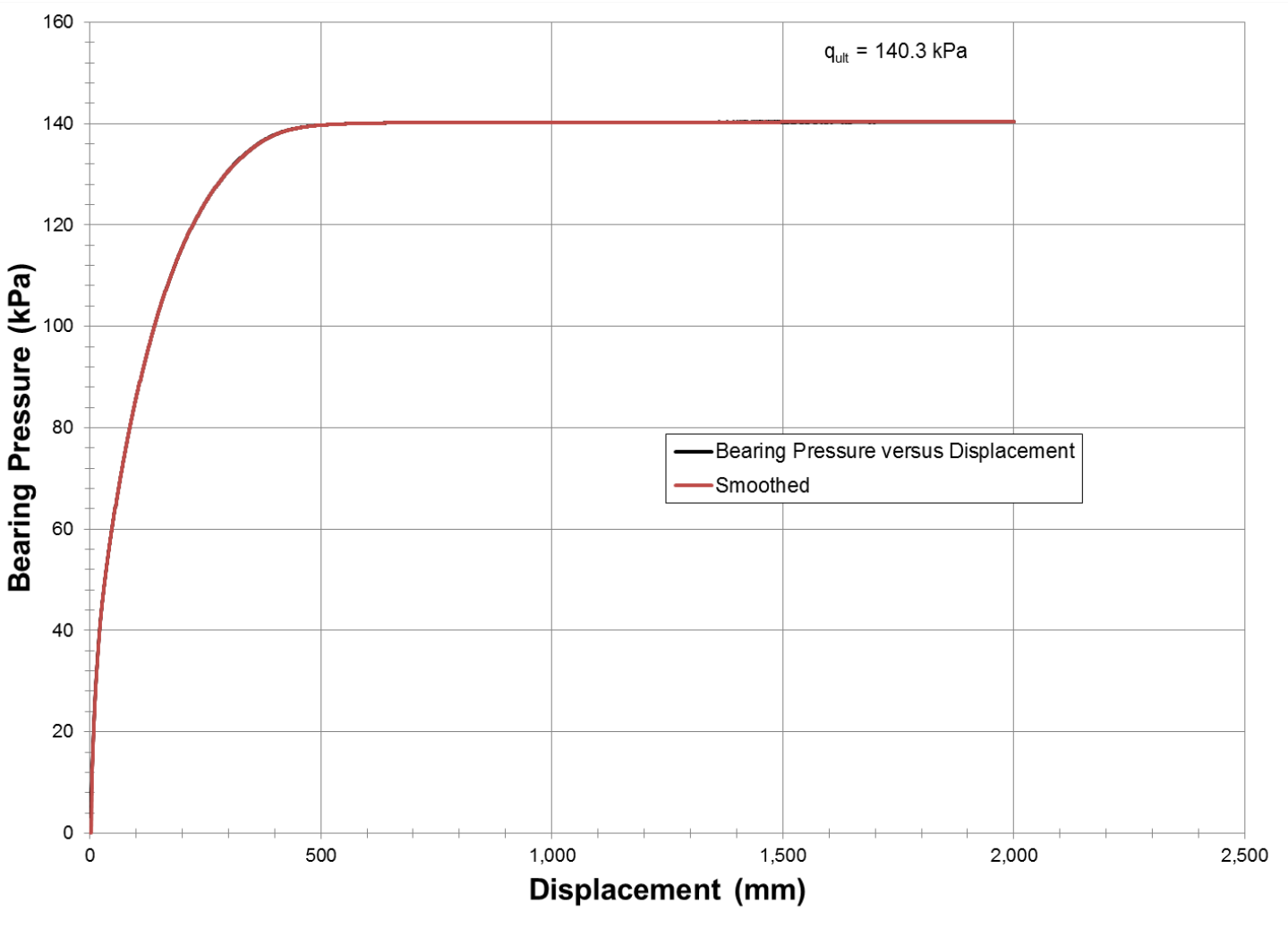


*Figure C-3: Bearing pressure versus displacement (unimproved 20 kPa native clay; 1.5 m embedment depth)*

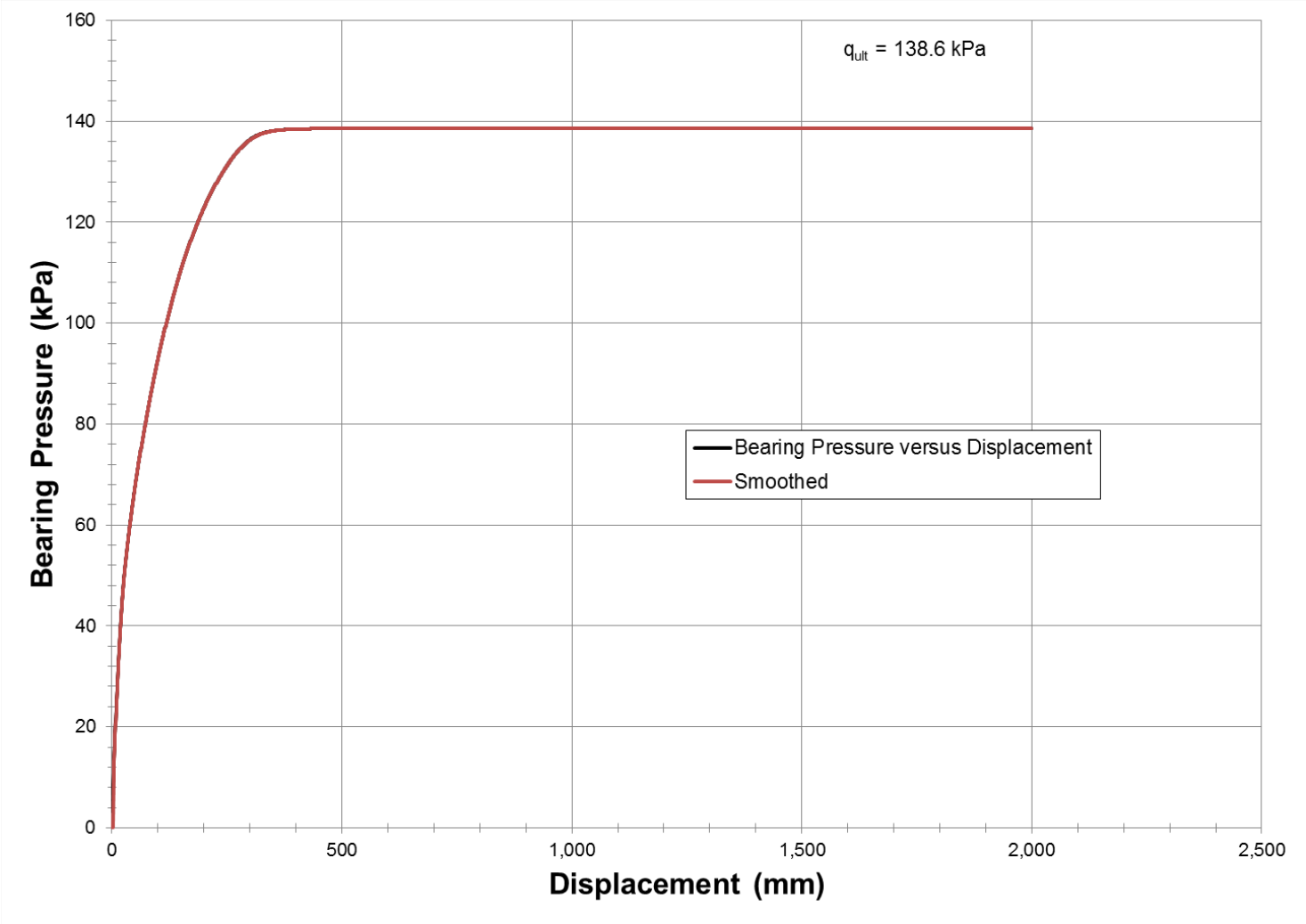


*Figure C-4: Bearing pressure versus displacement (unimproved 20 kPa native clay; 2 m embedment depth)*

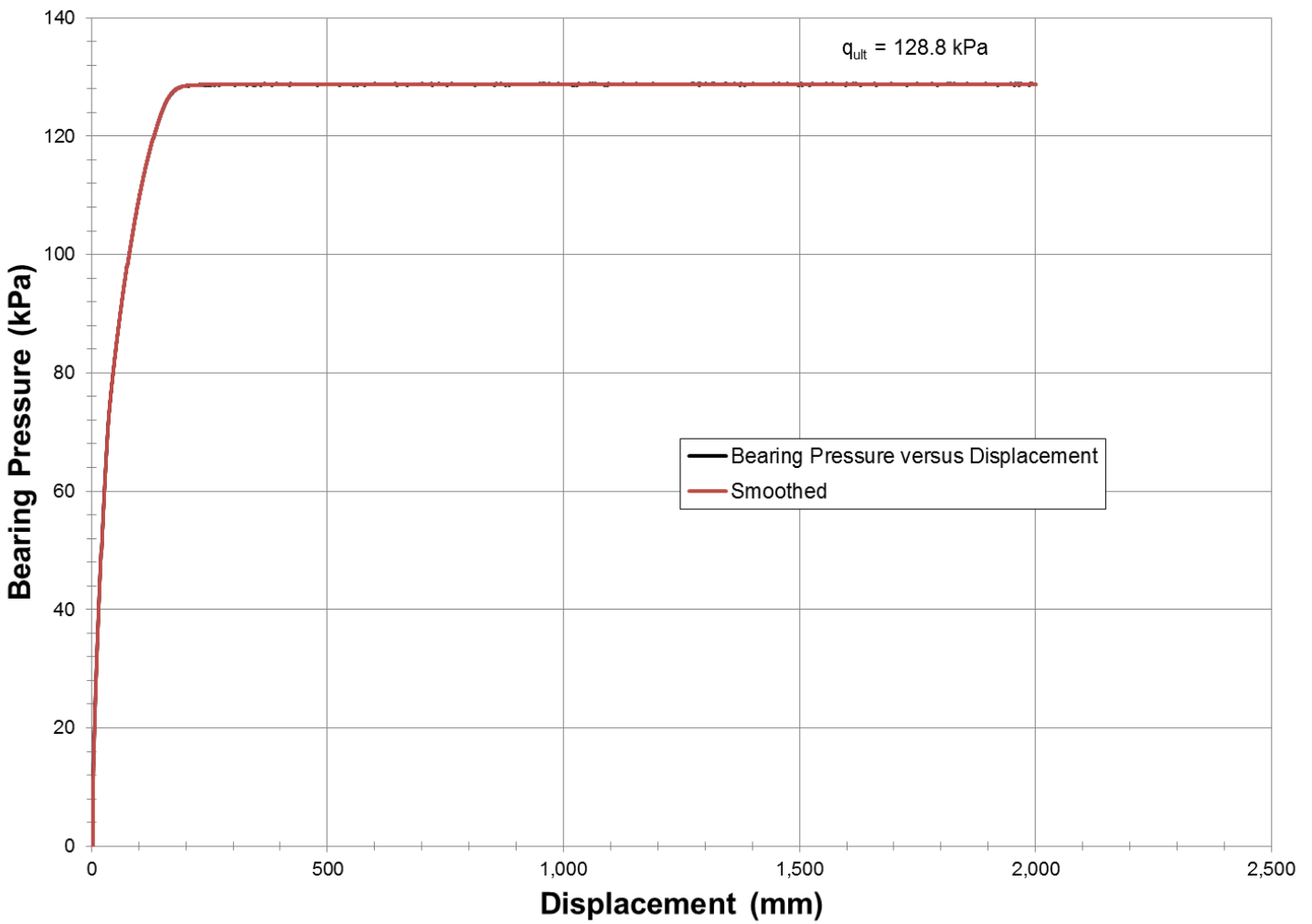


*Figure C-5: Bearing pressure versus displacement (unimproved 20 kPa native clay; 3 m embedment depth)*

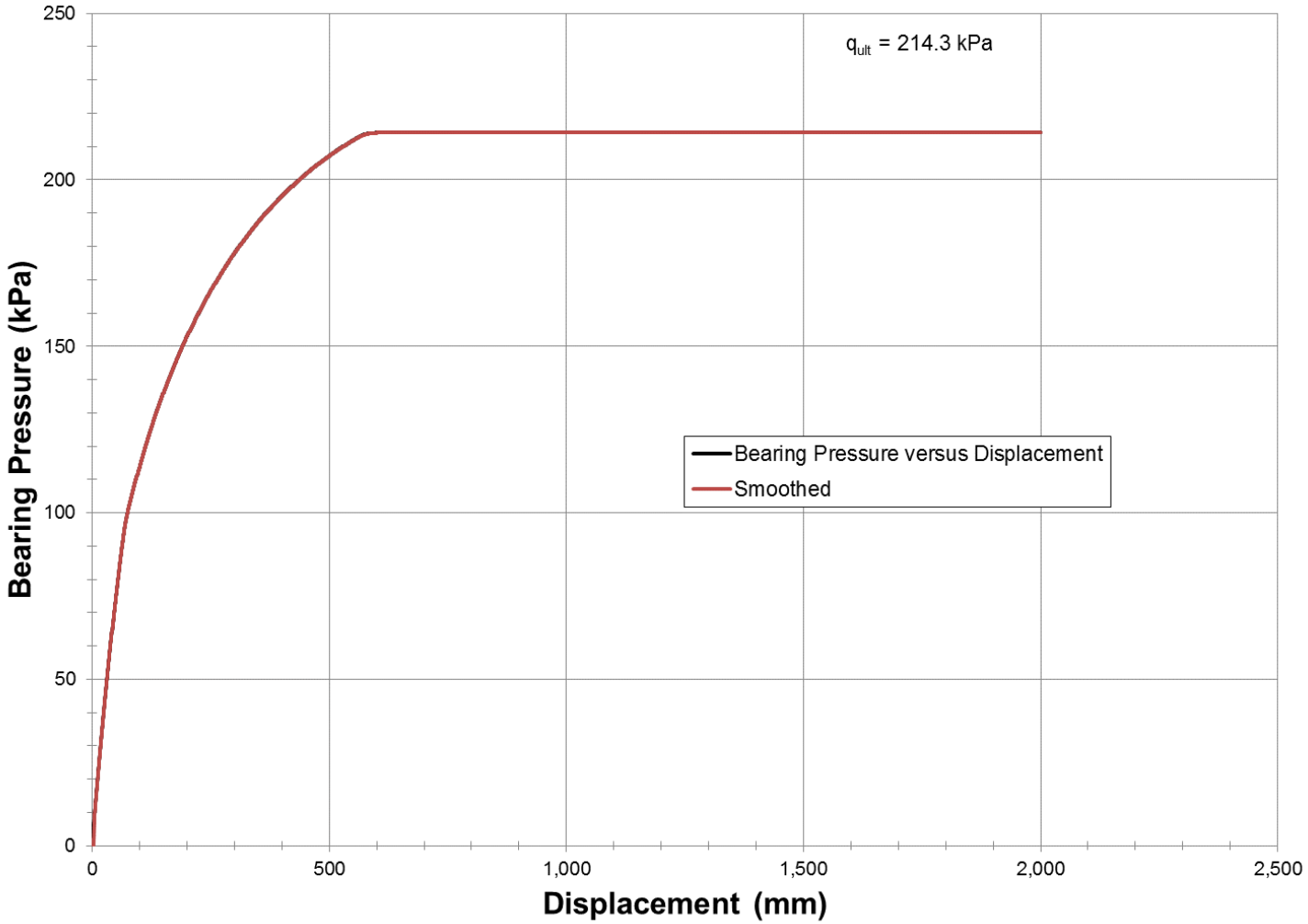


*Figure C-6: Bearing pressure versus displacement (unimproved 40 kPa native clay; no embedment depth)*

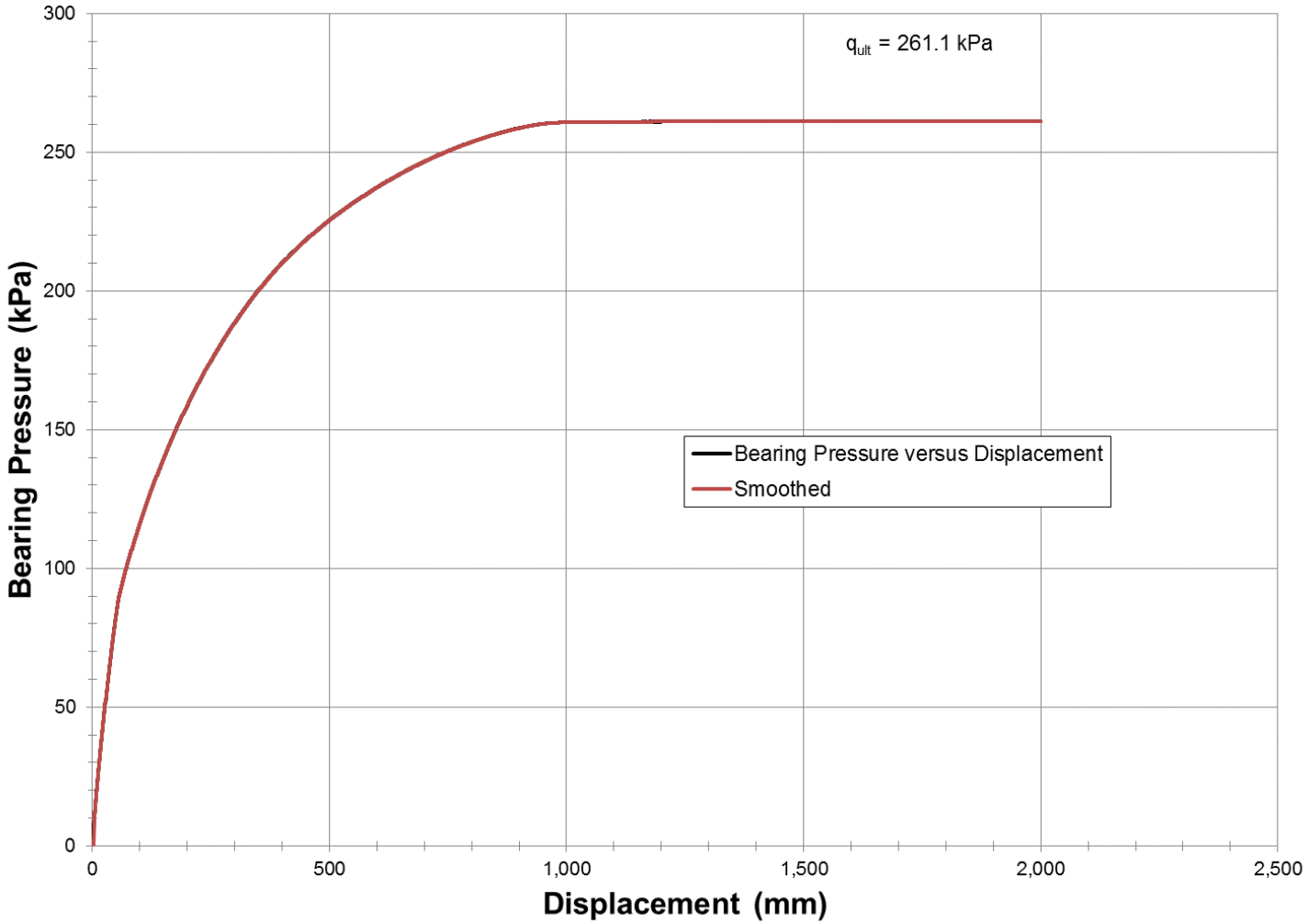


*Figure C-7: Bearing pressure versus displacement (unimproved 40 kPa native clay; 1 m embedment depth)*

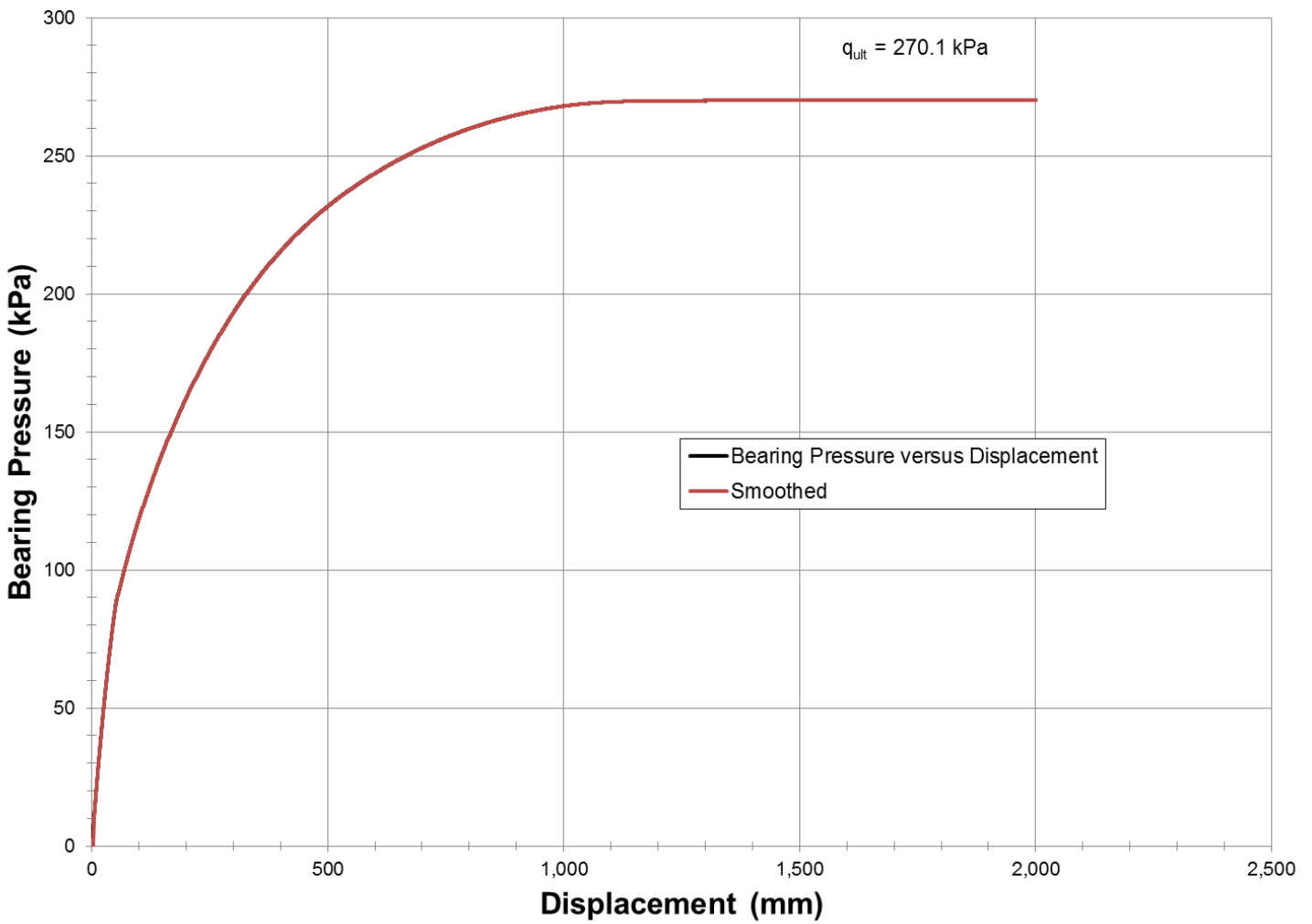


*Figure C-8: Bearing pressure versus displacement (unimproved 40 kPa native clay; 1.5 m embedment depth)*

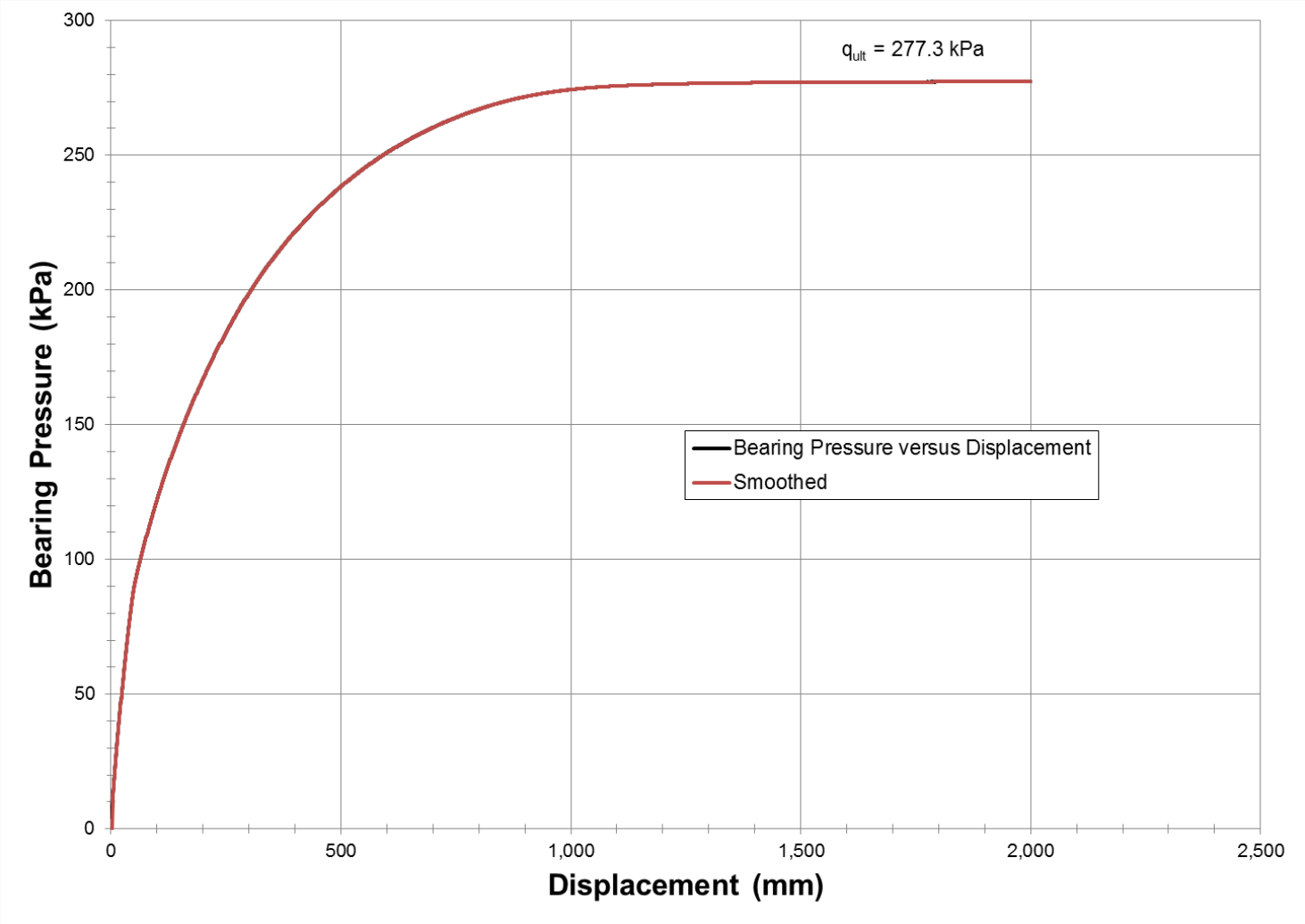


*Figure C-9: Bearing pressure versus displacement (unimproved 40 kPa native clay; 2 m embedment depth)*

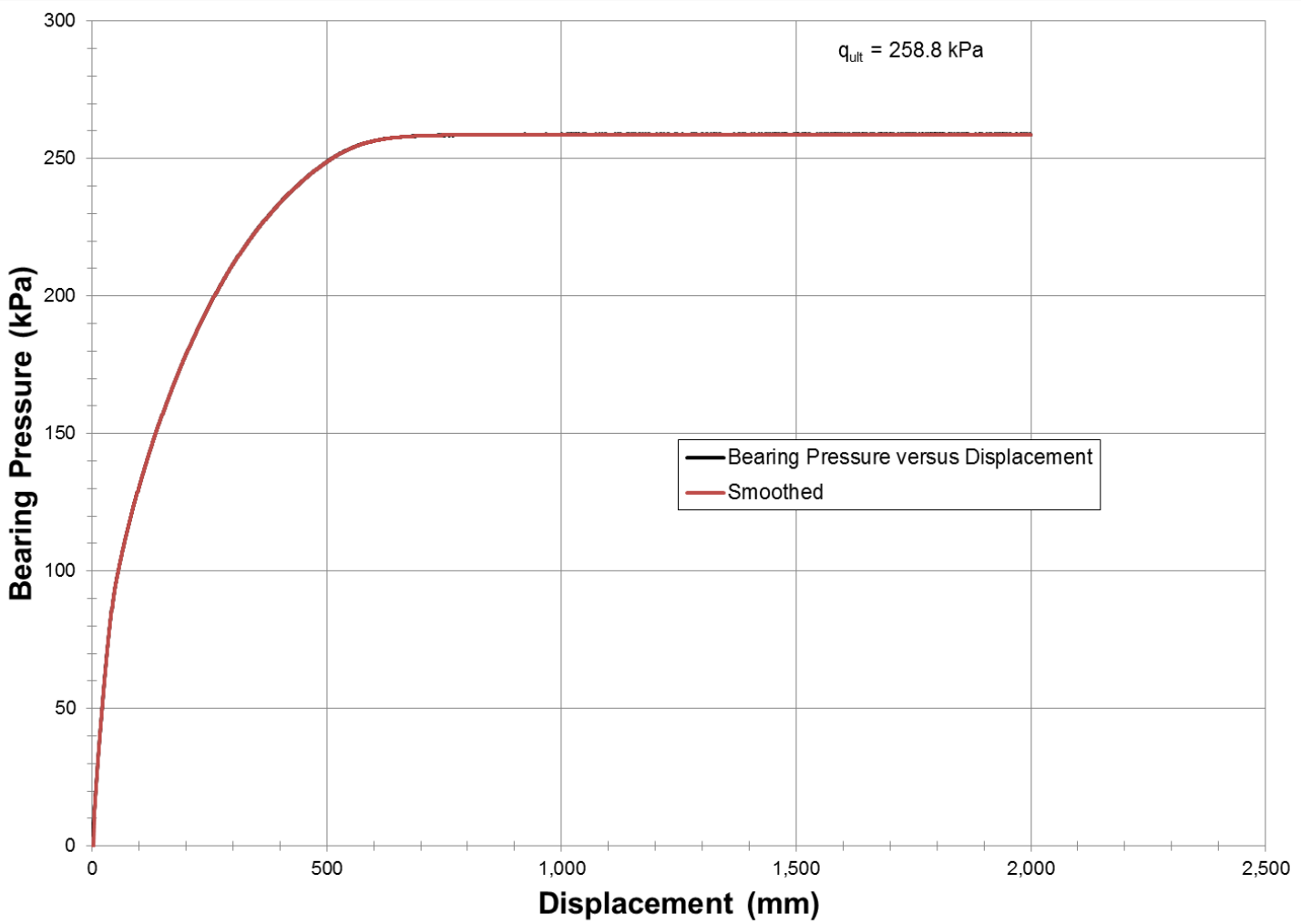


*Figure C-10: Bearing pressure versus displacement (unimproved 40 kPa native clay; 3 m embedment depth)*

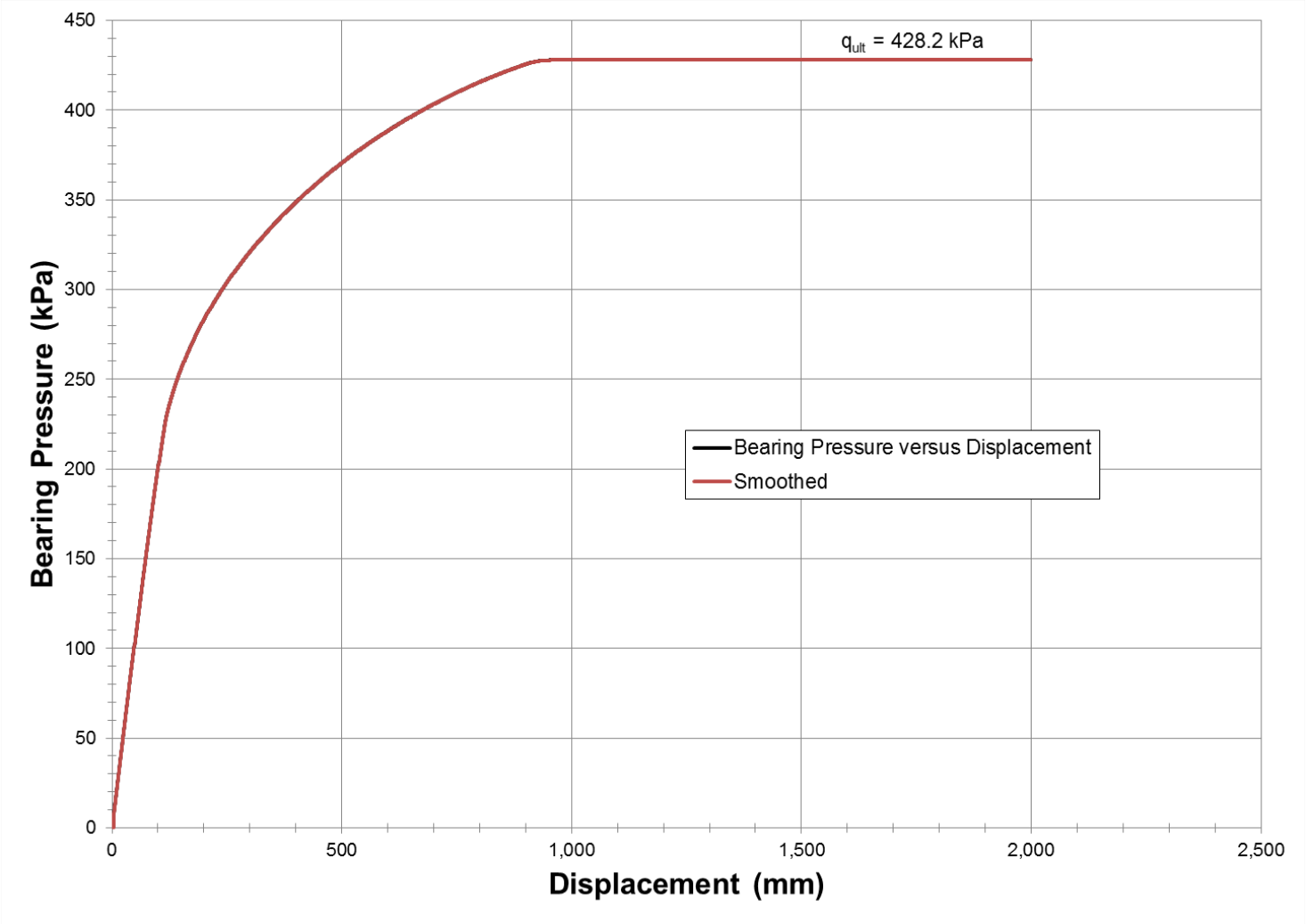


*Figure C-11: Bearing pressure versus displacement (unimproved 80 kPa native clay; no embedment depth)*

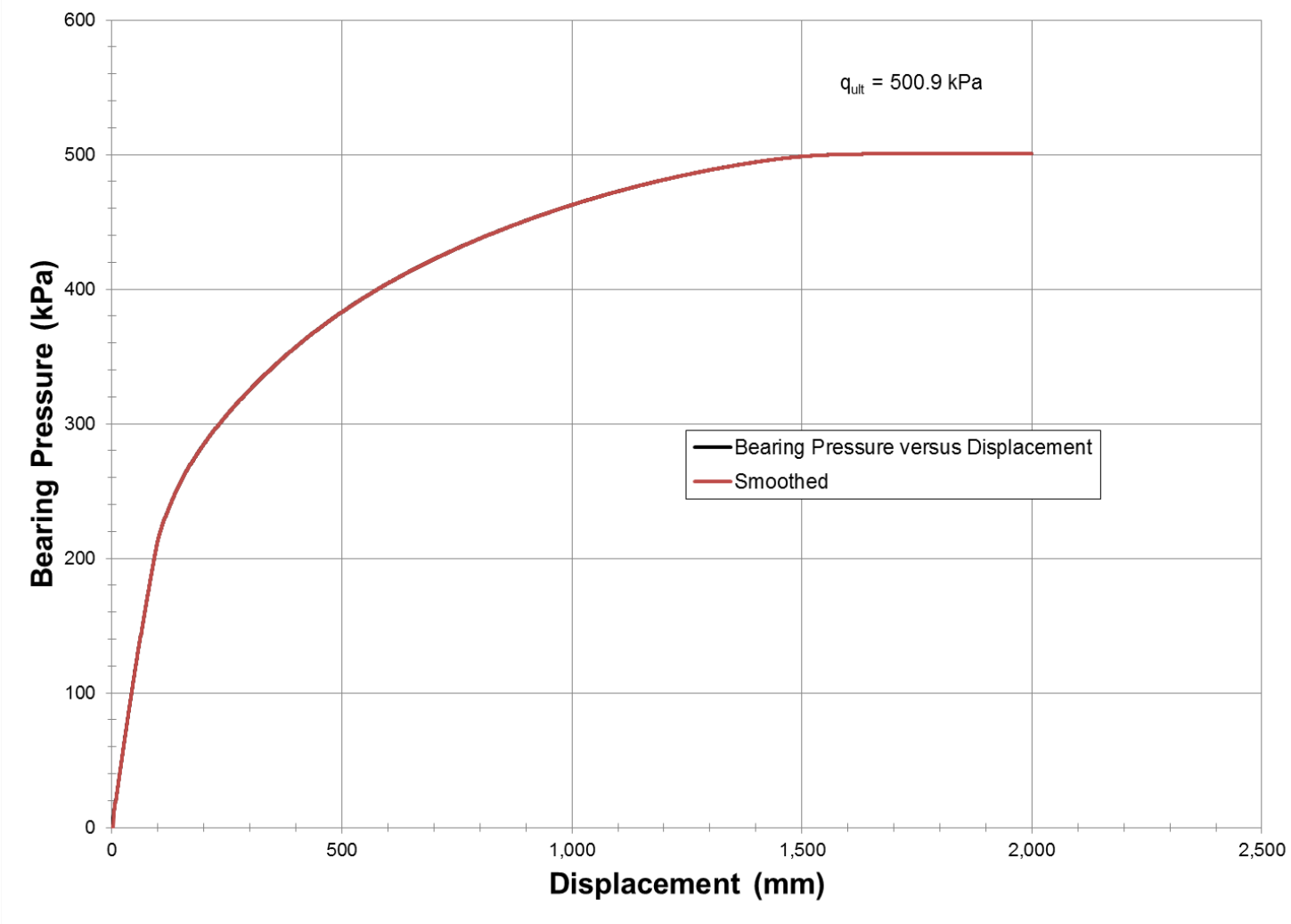


*Figure C-12: Bearing pressure versus displacement (unimproved 80 kPa native clay; 1 m embedment depth)*

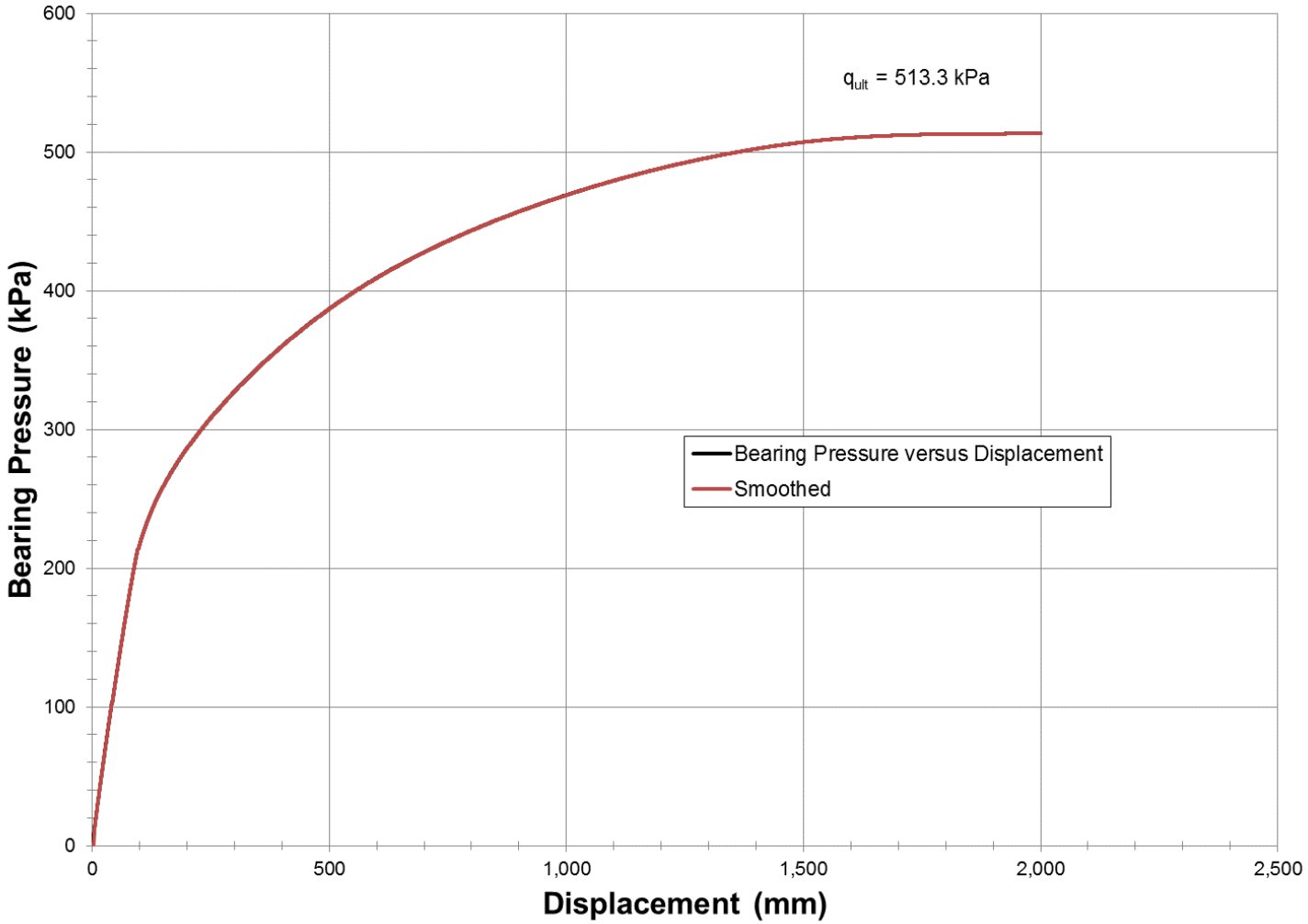


*Figure C-13: Bearing pressure versus displacement (unimproved 80 kPa native clay; 1.5 m embedment depth)*

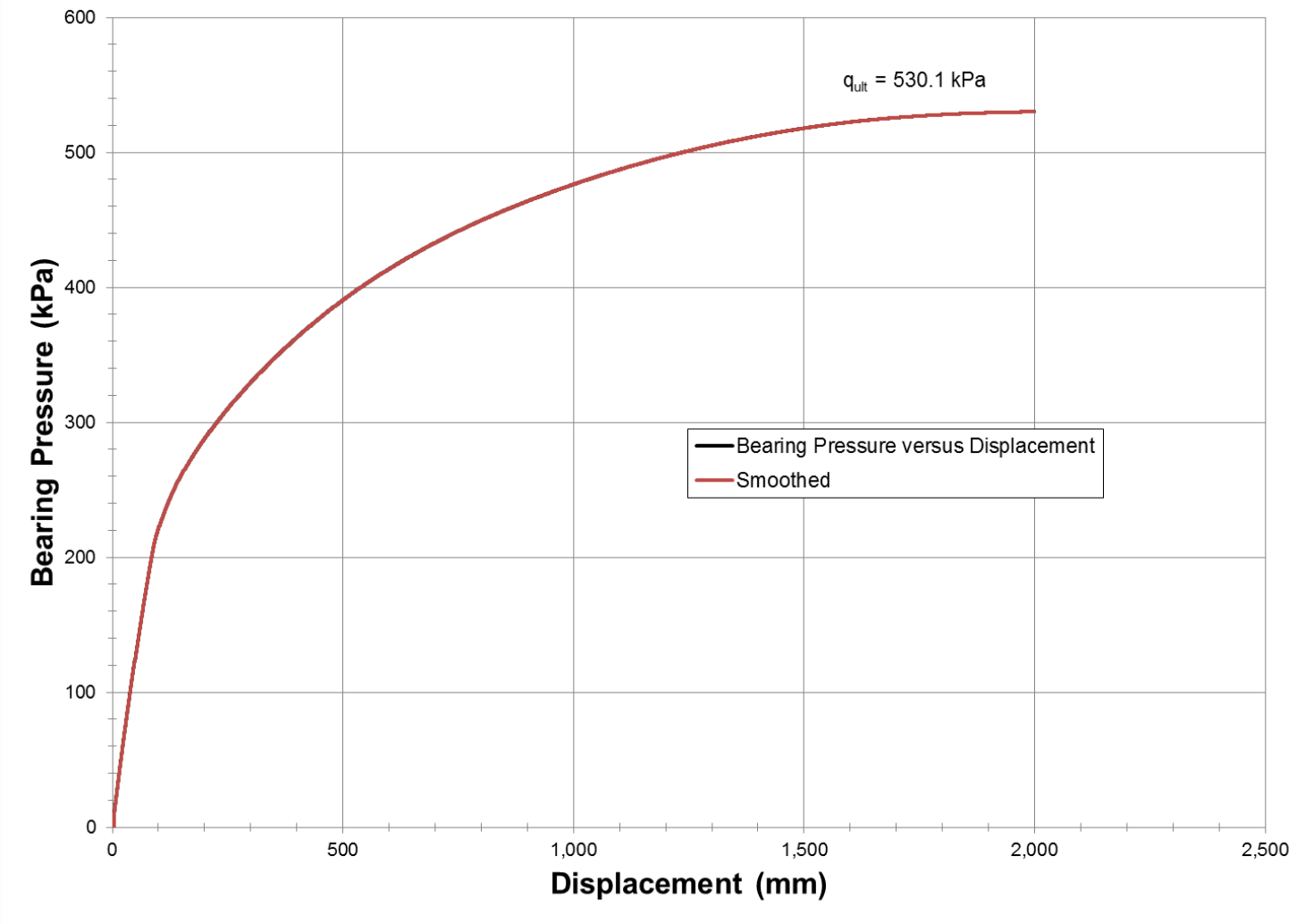


*Figure C-14: Bearing pressure versus displacement (unimproved 80 kPa native clay; 2 m embedment depth)*

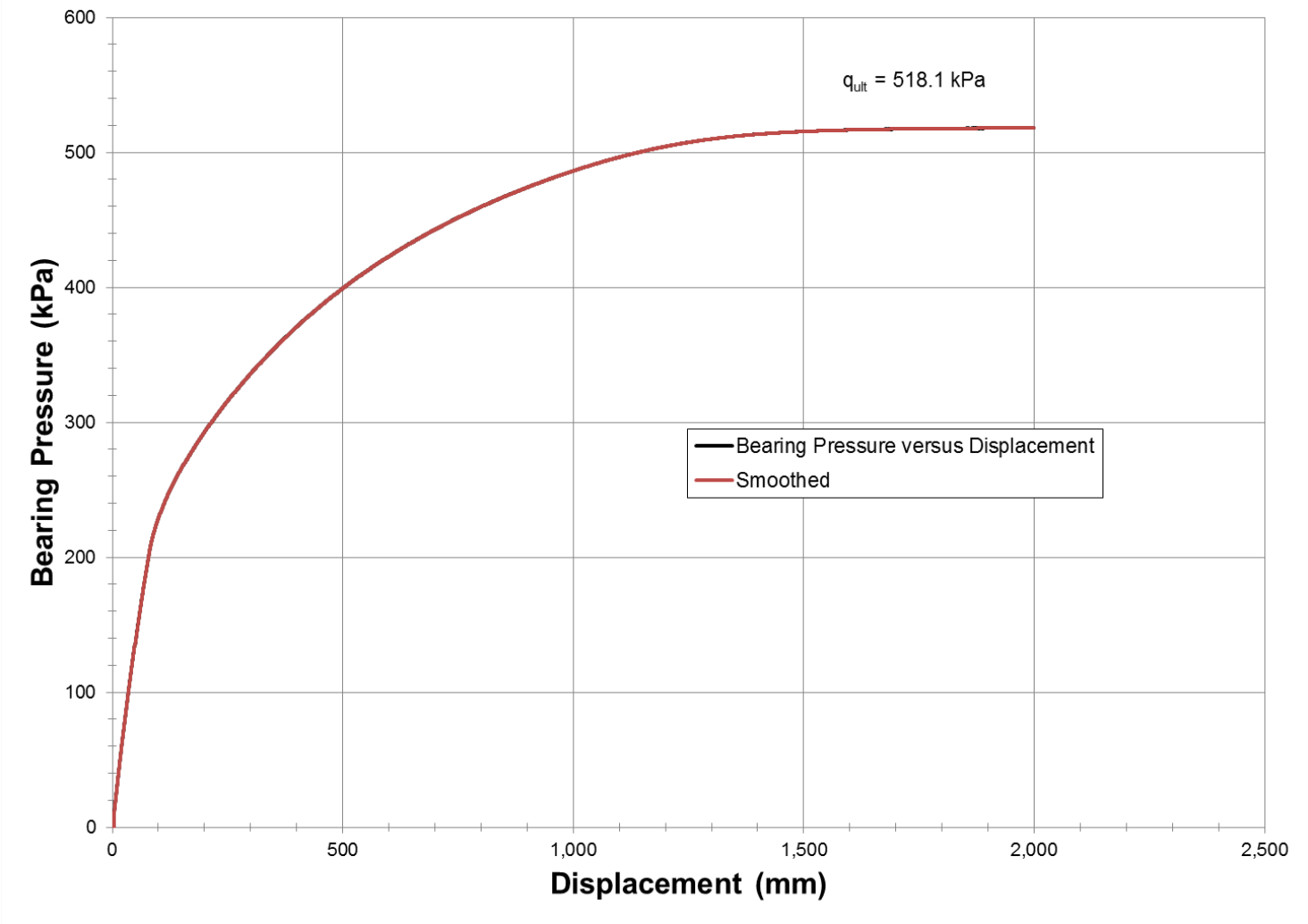


*Figure C-15: Bearing pressure versus displacement (unimproved 80 kPa native clay; 3 m embedment depth)*

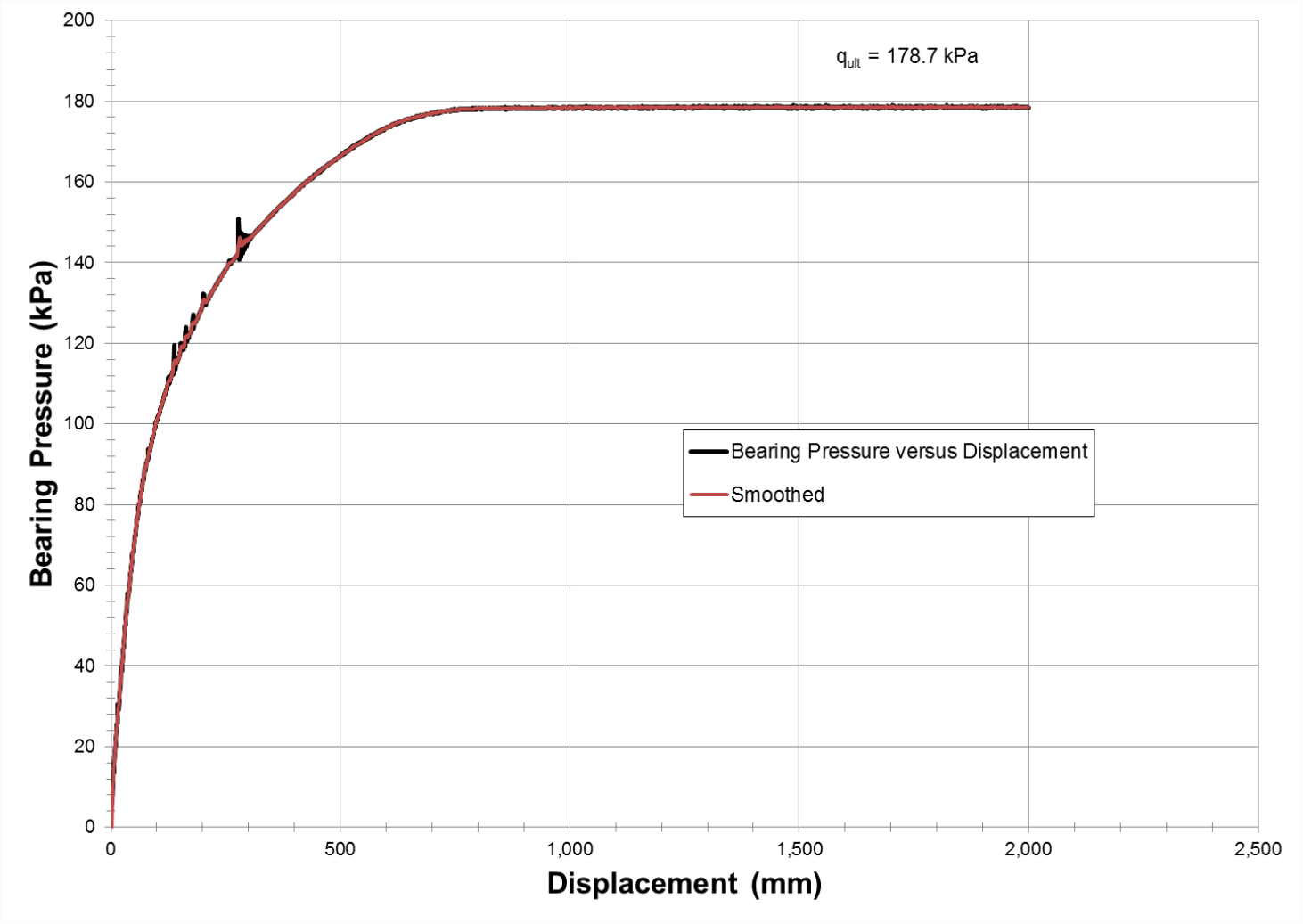


*Figure C-16: Bearing pressure versus displacement (single 6 m long, 1.5 m wide trench in 20 kPa native clay; no embedment depth)*

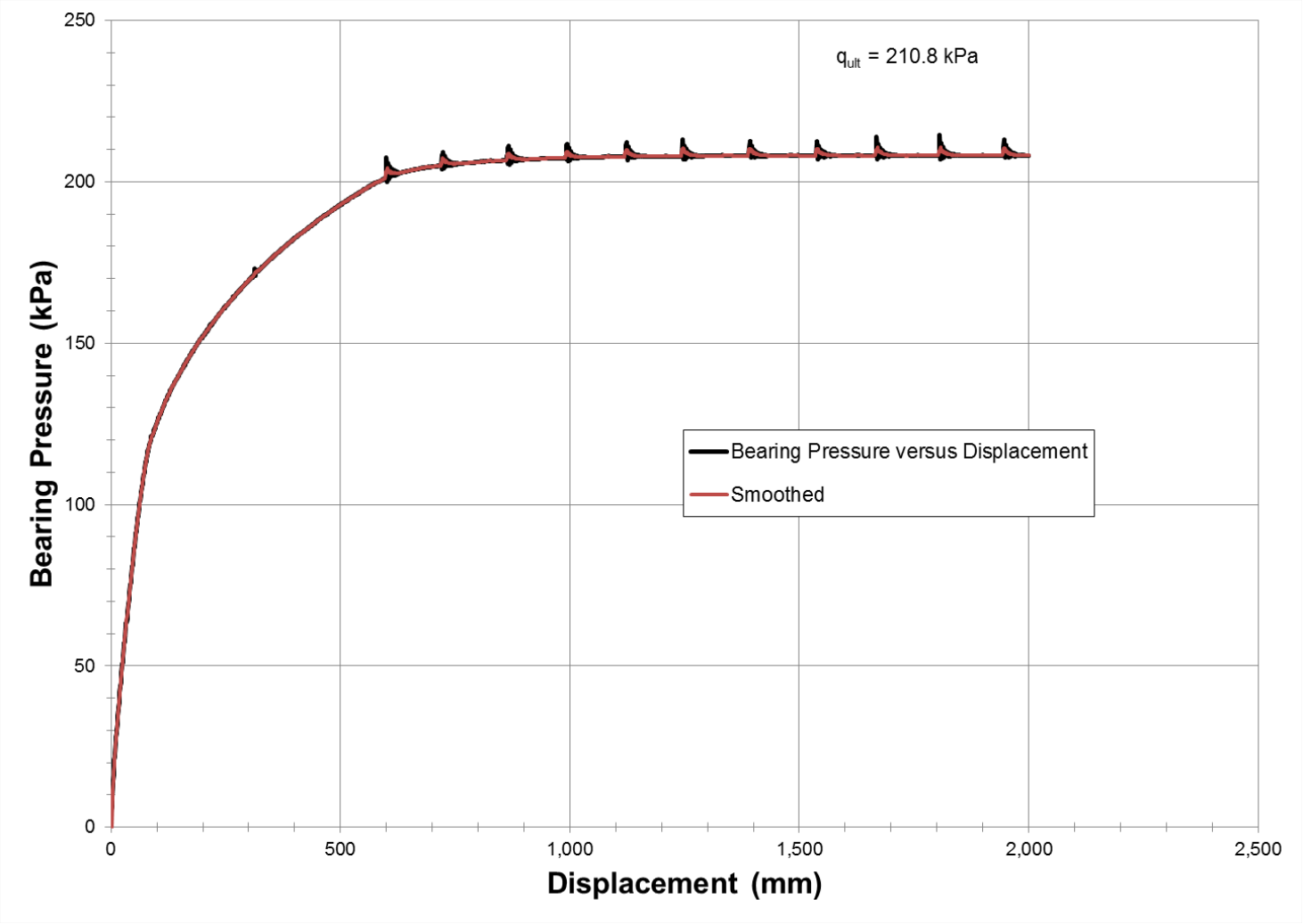


*Figure C-17: Bearing pressure versus displacement (single 6 m long, 1.5 m wide trench in 20 kPa native clay; 1.5 m embedment depth)*

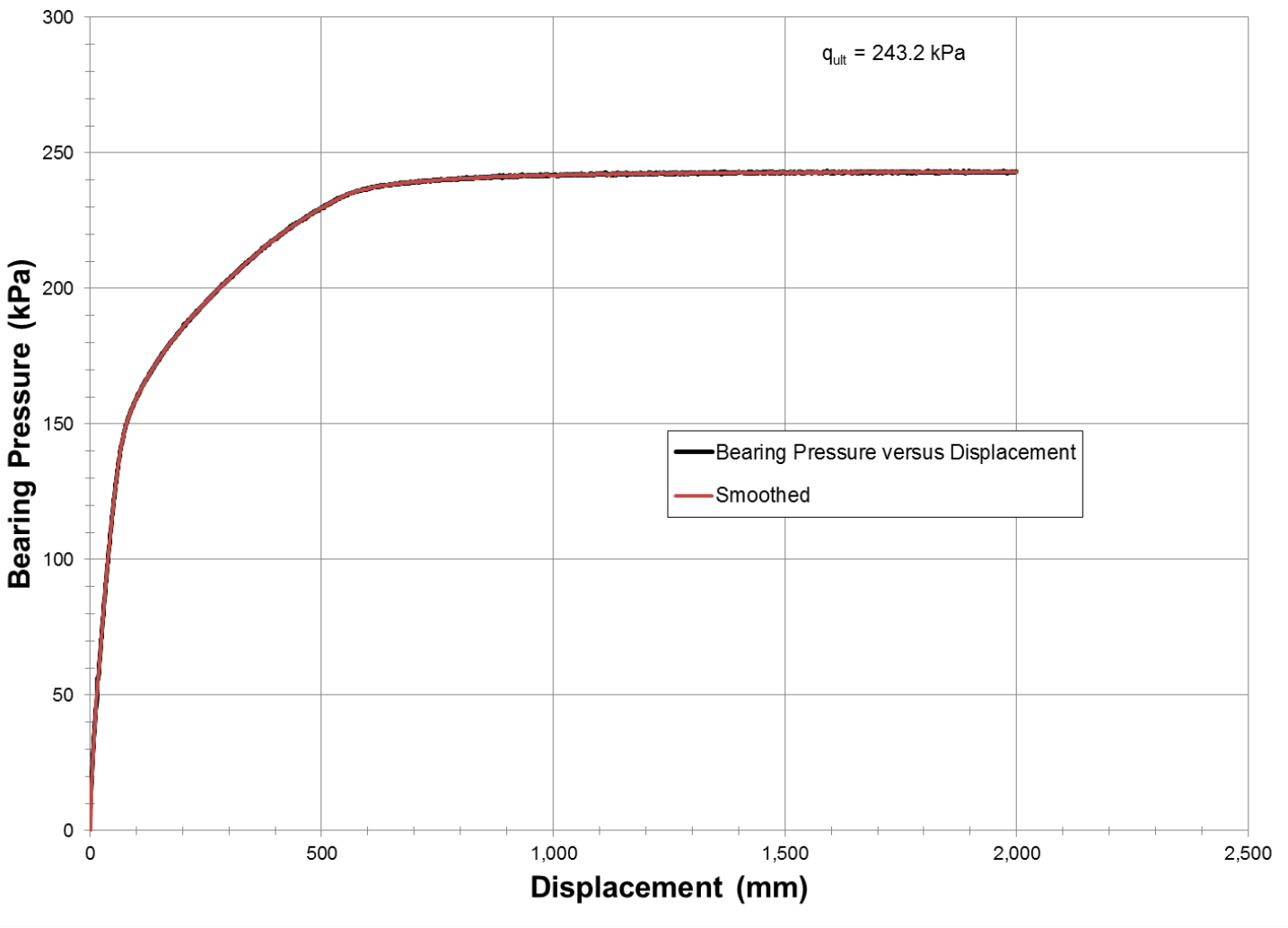


*Figure C-18: Bearing pressure versus displacement (single 6 m long, 1.5 m wide trench in 20 kPa native clay; 3 m embedment depth)*

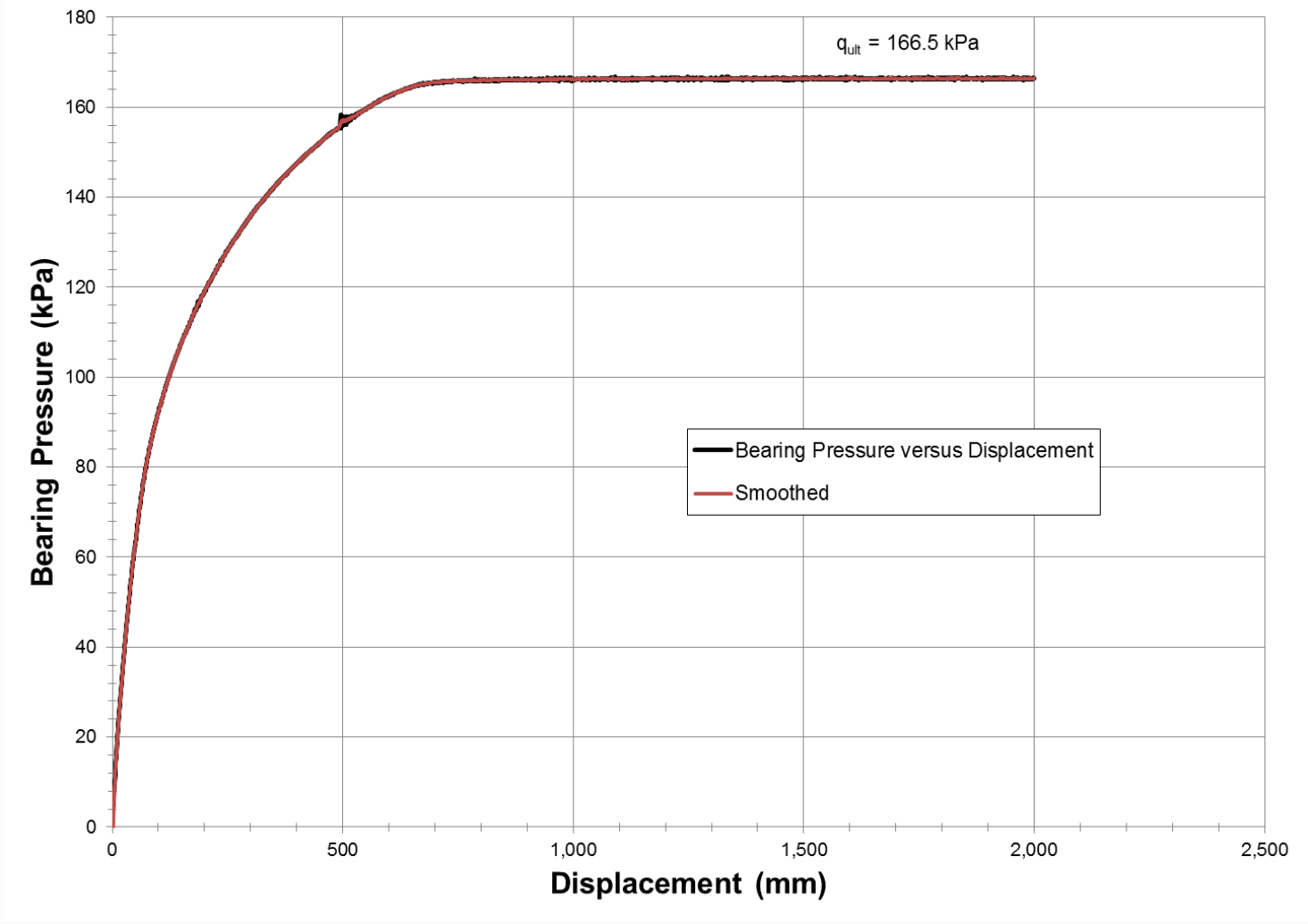


*Figure C-19: Bearing pressure versus displacement (single 6 m long, 0.9 m wide trench in 20 kPa native clay; no embedment depth)*

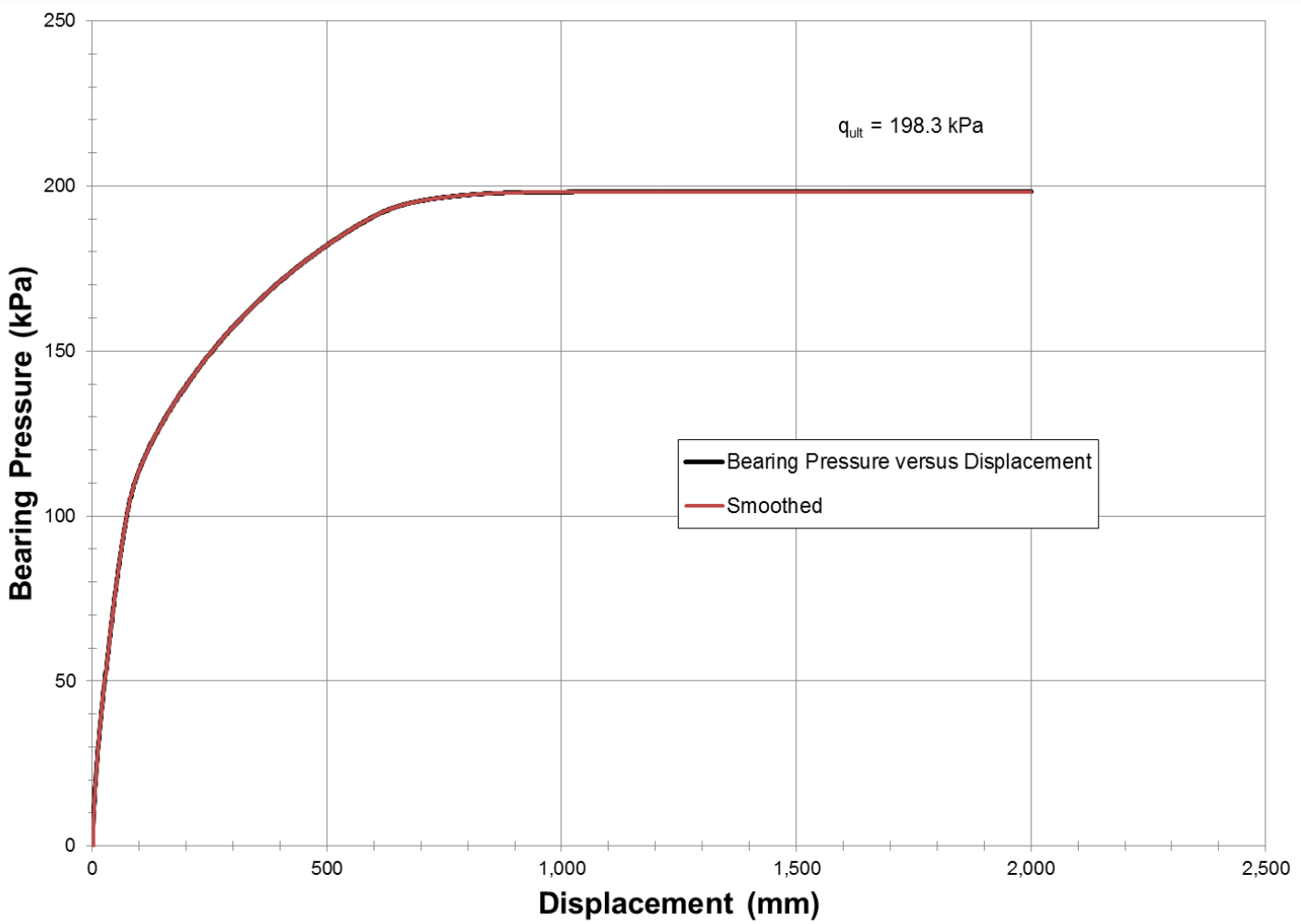


*Figure C-20: Bearing pressure versus displacement (single 6 m long, 0.9 m wide trench in 20 kPa native clay; 1.5 m embedment depth)*

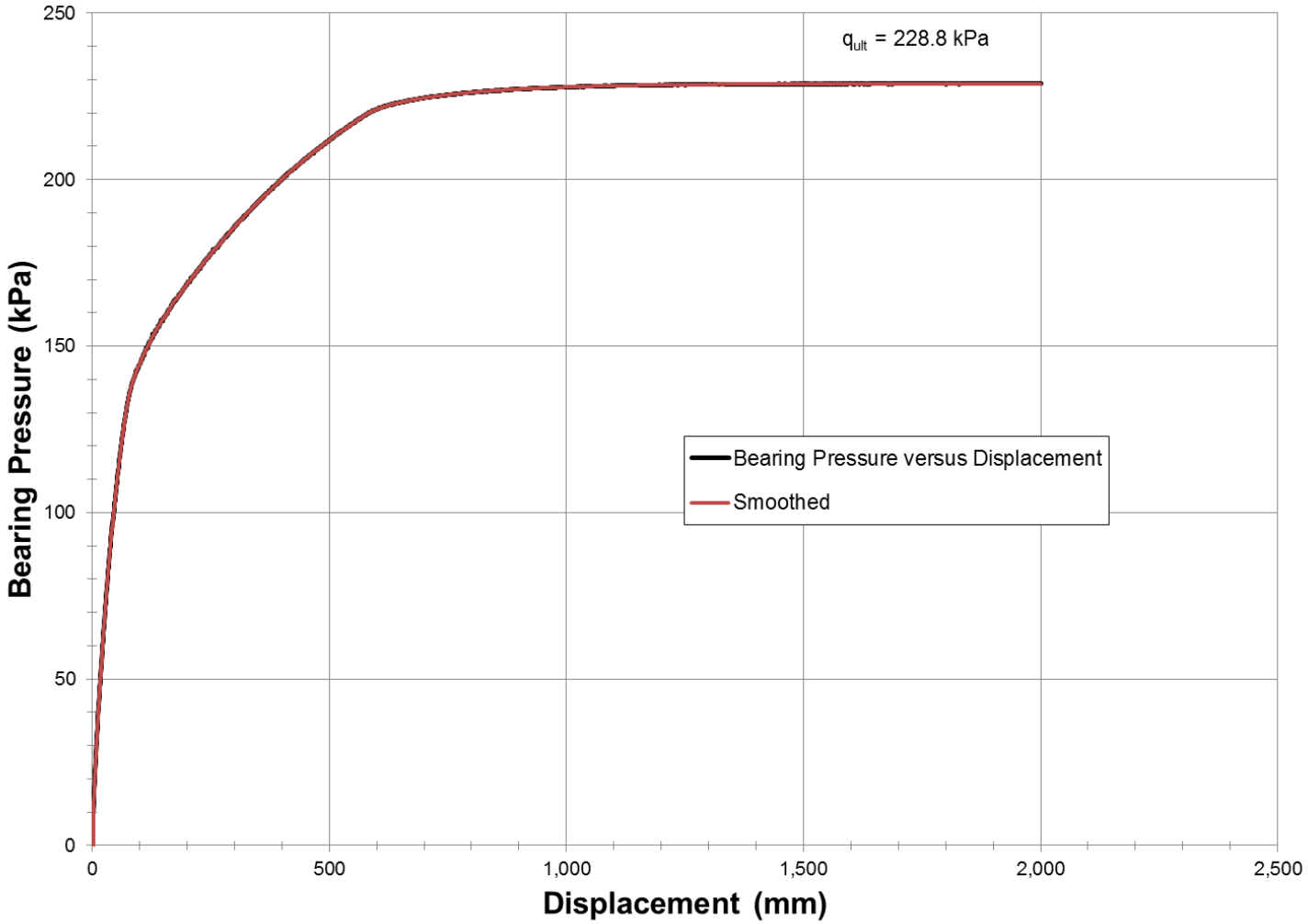


*Figure C-21: Bearing pressure versus displacement (single 6 m long, 0.9 m wide trench in 20 kPa native clay; 3 m embedment depth)*

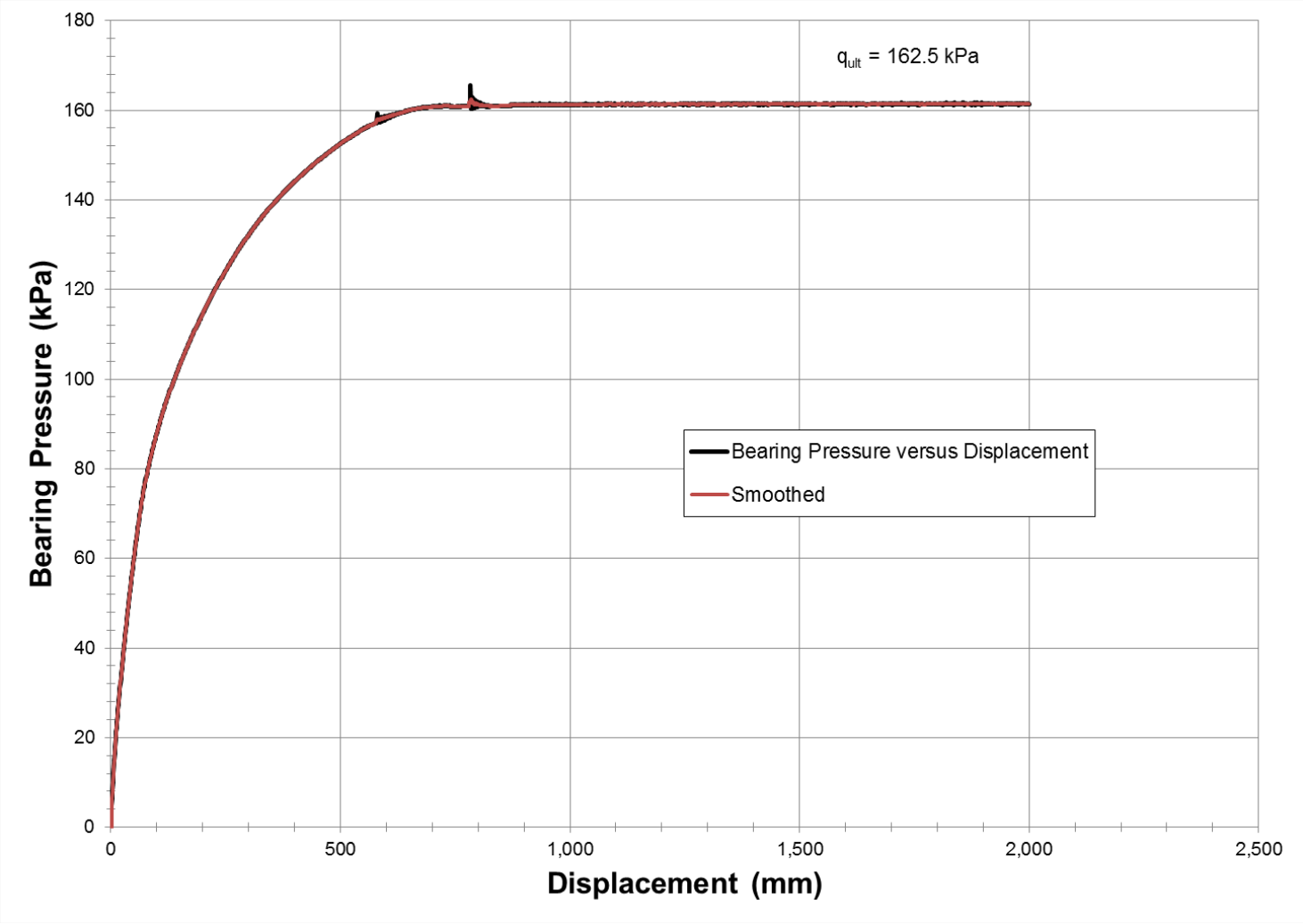


*Figure C-22: Bearing pressure versus displacement (single 6 m long, 0.6 m wide trench in 20 kPa native clay; no embedment depth)*

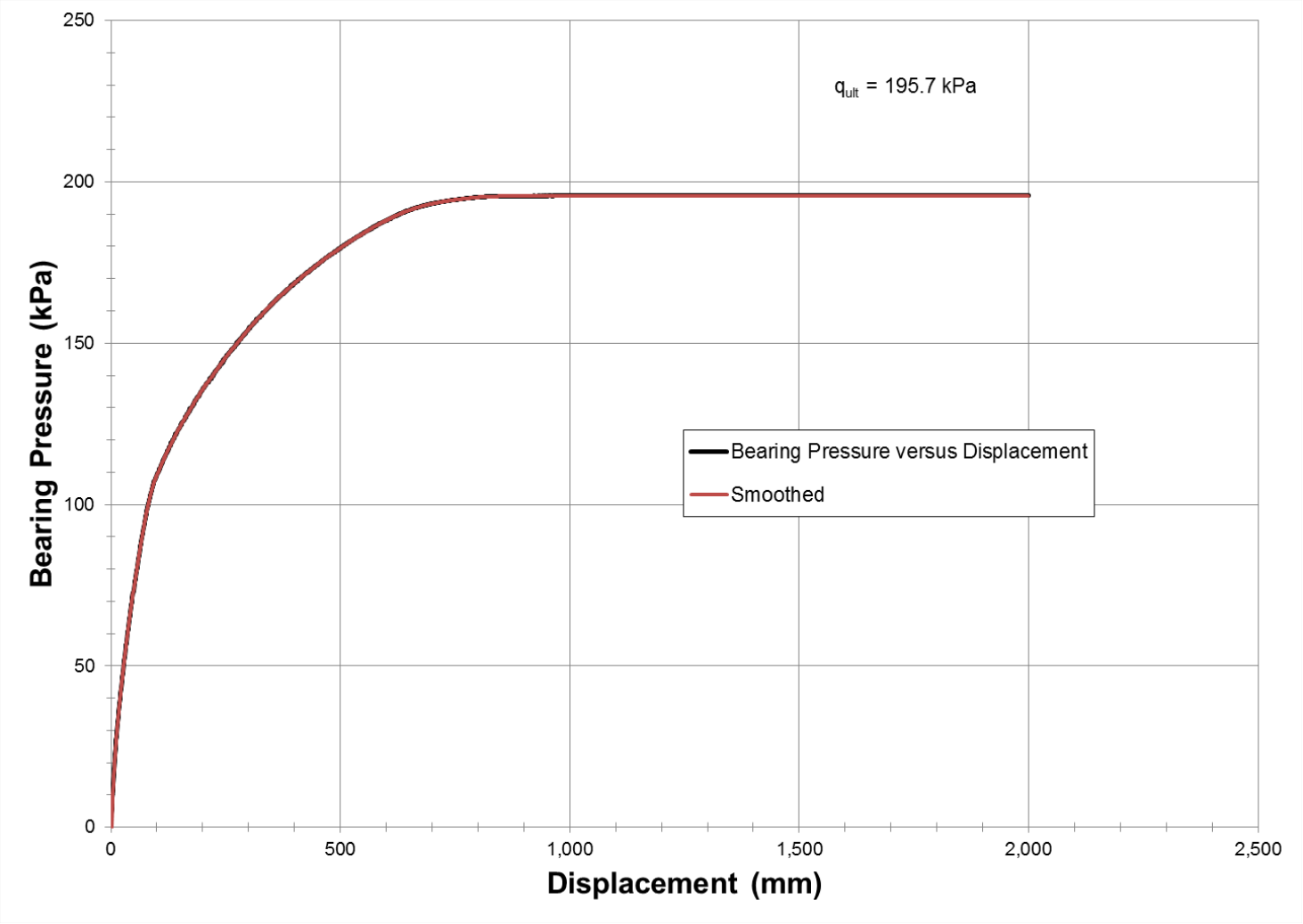


*Figure C-23: Bearing pressure versus displacement (single 6 m long, 0.6 m wide trench in 20 kPa native clay; 1.5 m embedment depth)*

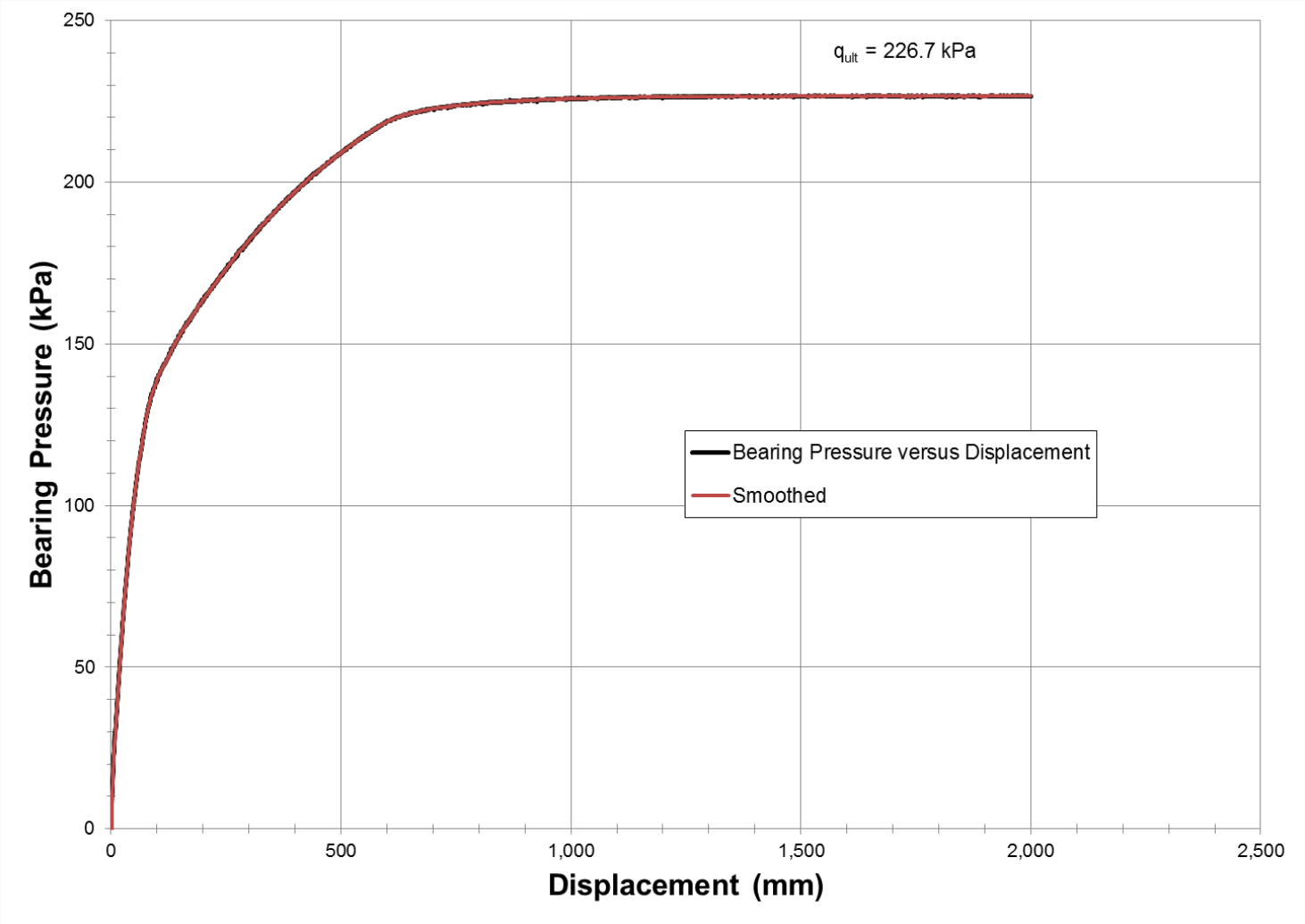


*Figure C-24: Bearing pressure versus displacement (single 6 m long, 0.6 m wide trench in 20 kPa native clay; 3 m embedment depth)*

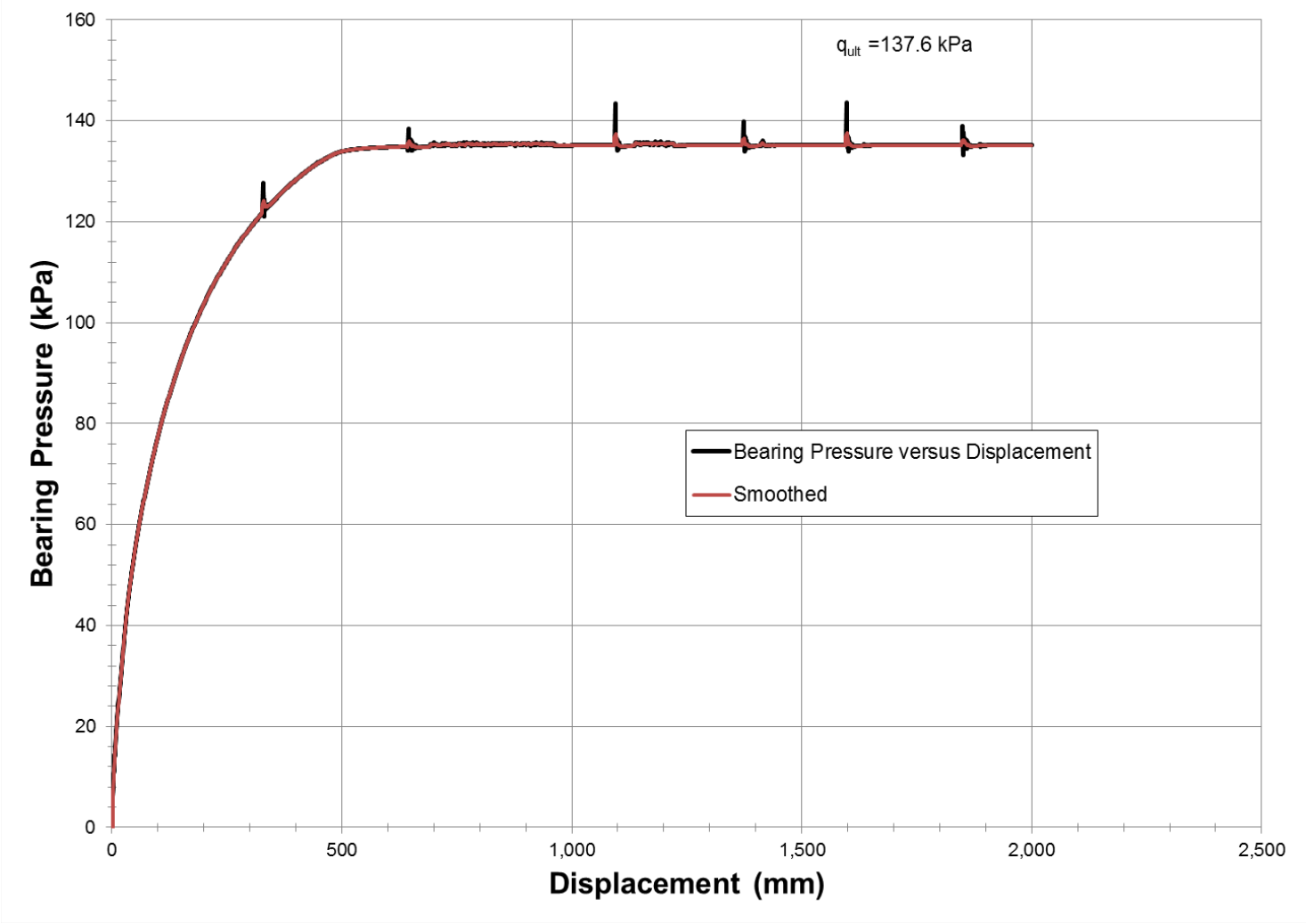


*Figure C-25: Bearing pressure versus displacement (single 3 m long, 1.5 m wide trench in 20 kPa native clay; no embedment depth)*

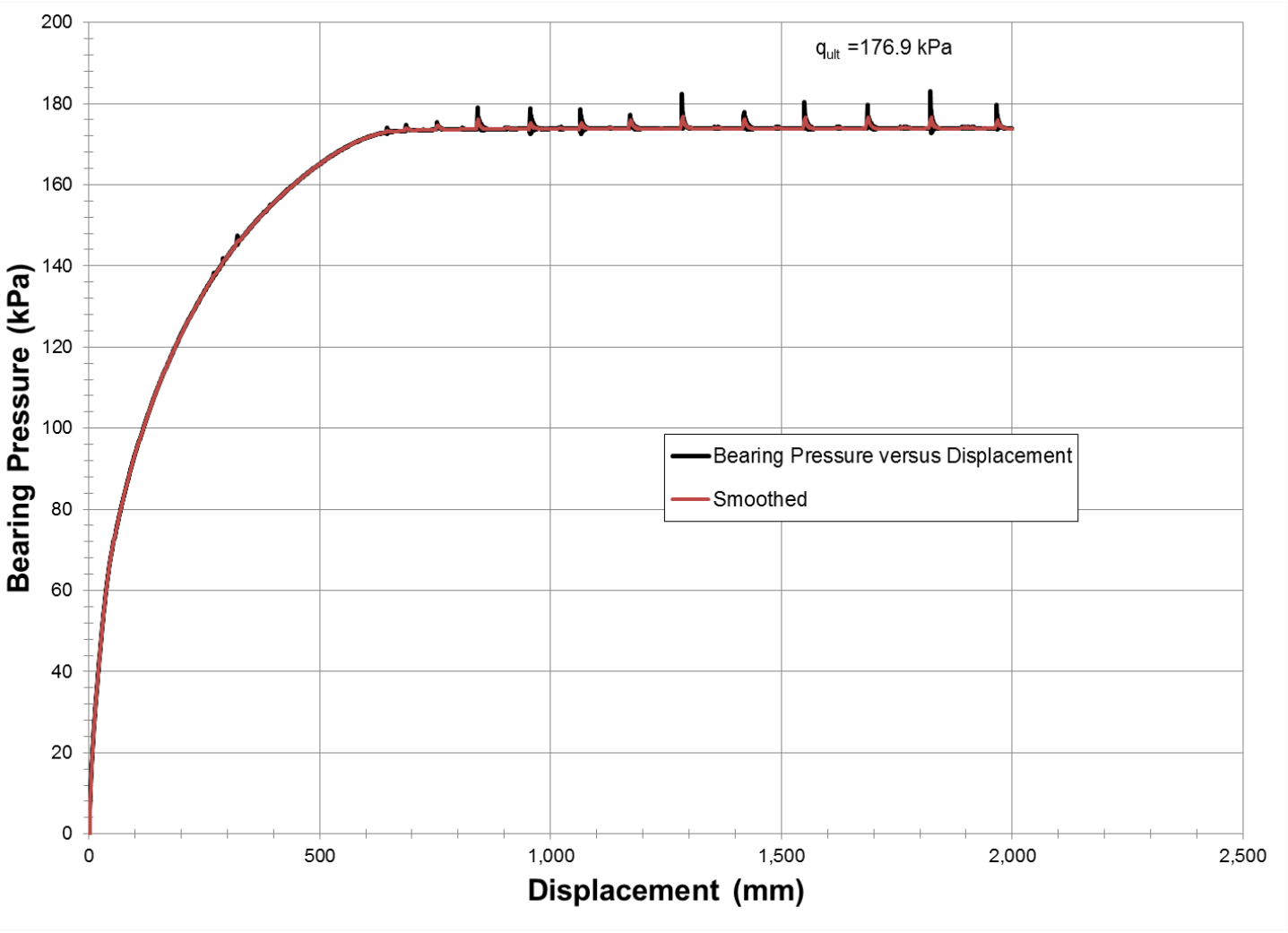


*Figure C-26: Bearing pressure versus displacement (single 3 m long, 1.5 m wide trench in 20 kPa native clay; 1.5 m embedment depth)*

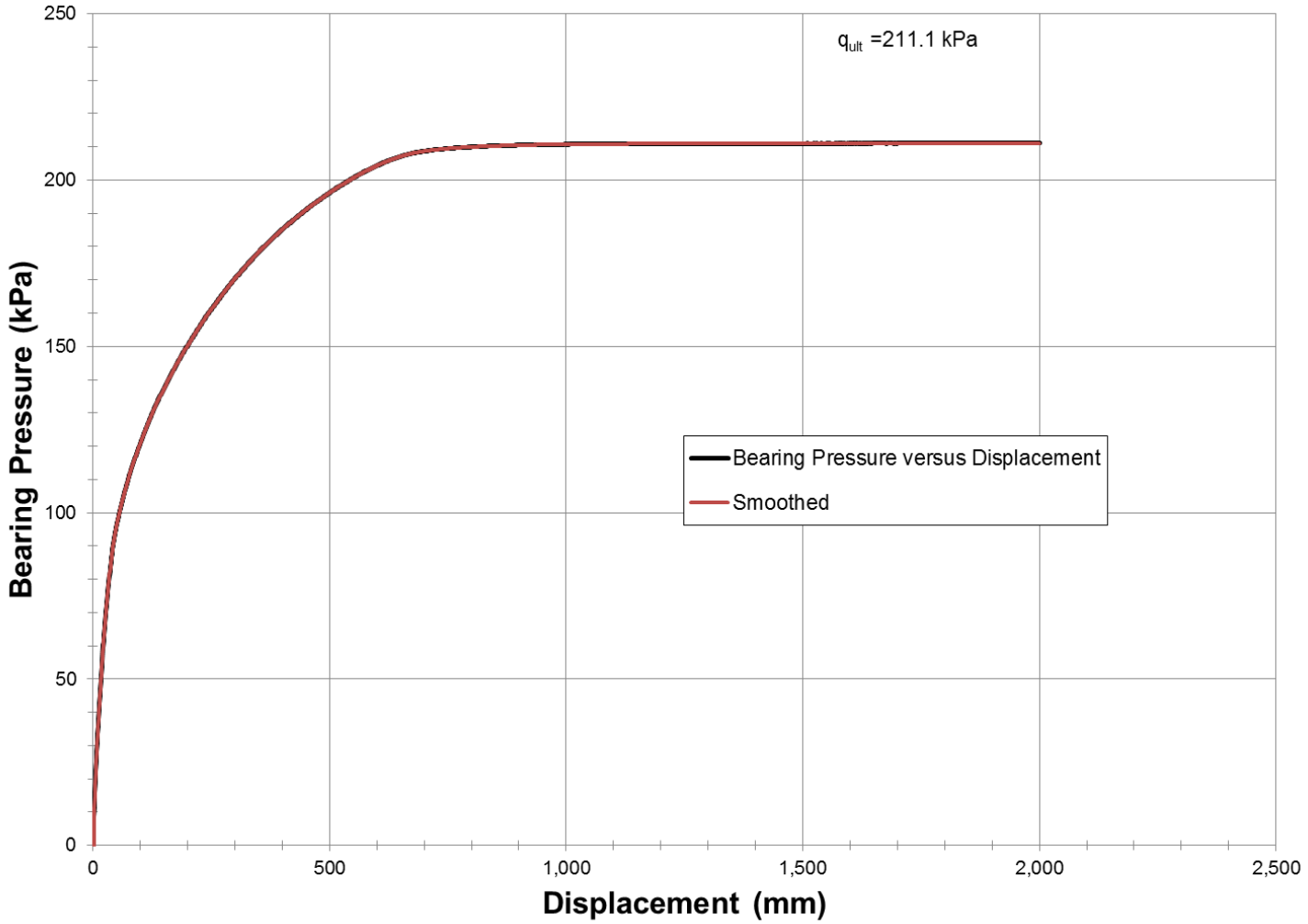


*Figure C-27: Bearing pressure versus displacement (single 3 m long, 1.5 m wide trench in 20 kPa native clay; 3 m embedment depth)*

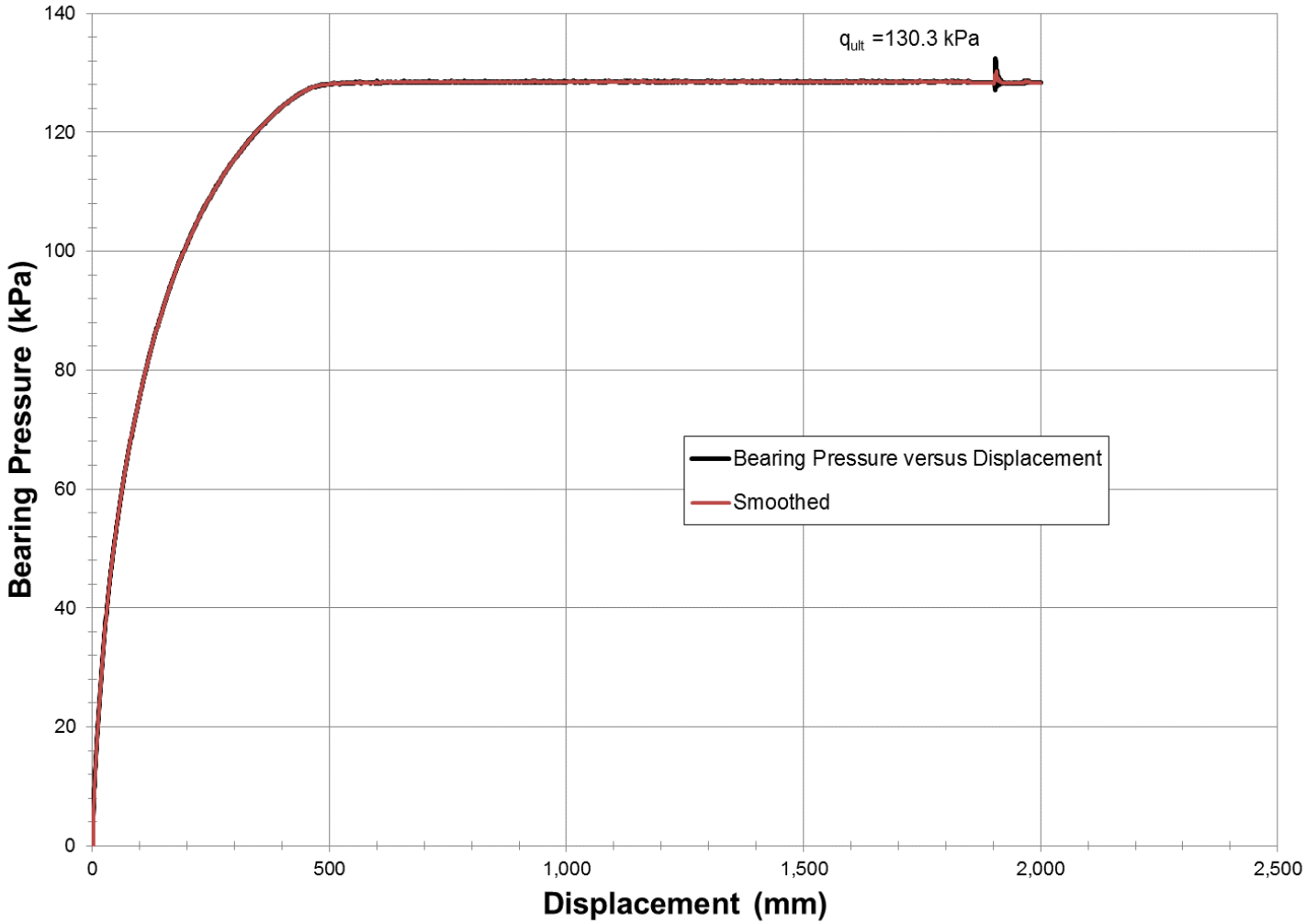


*Figure C-28: Bearing pressure versus displacement (single 3 m long, 0.9 m wide trench in 20 kPa native clay; no embedment depth)*

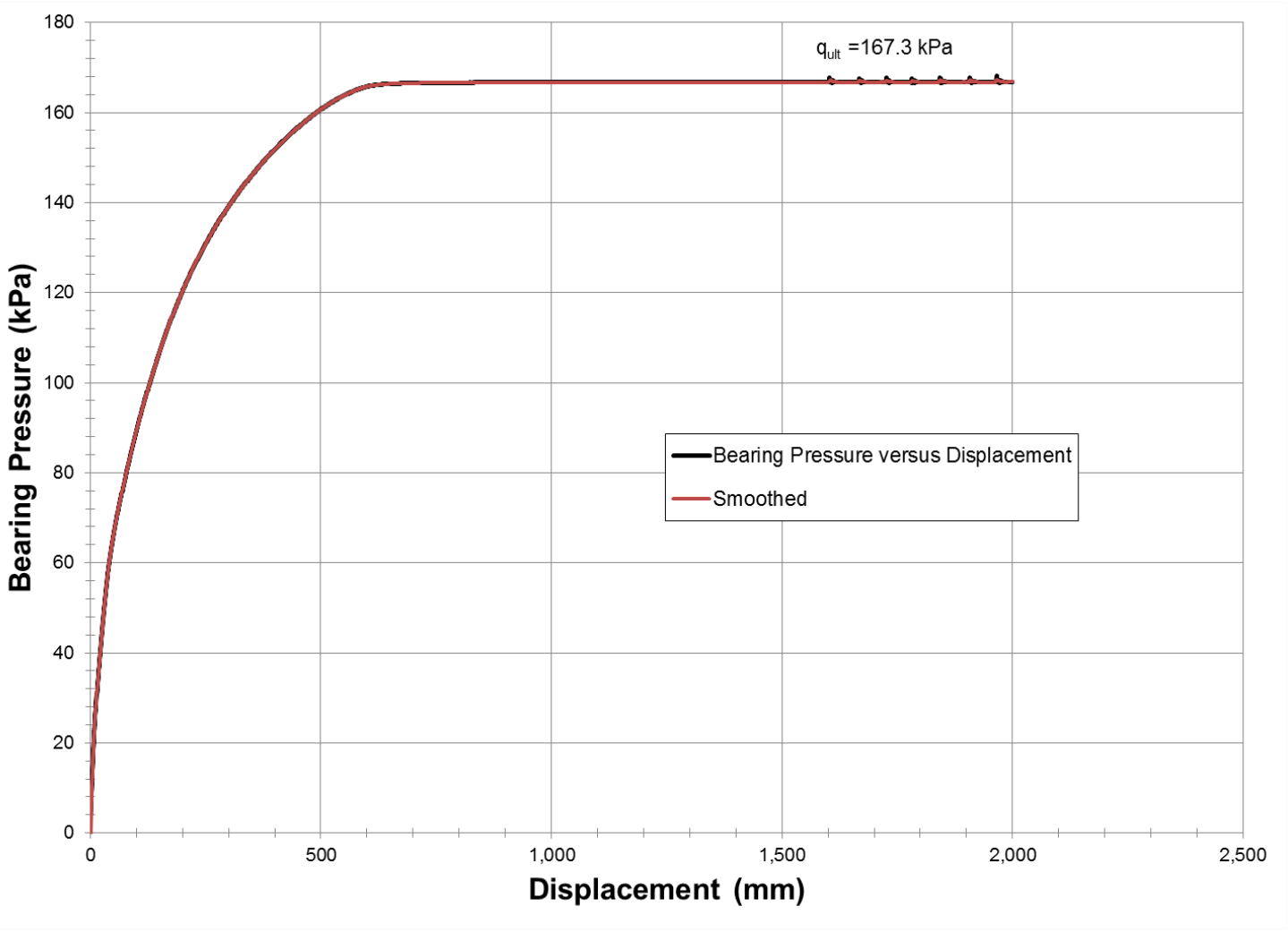


*Figure C-29: Bearing pressure versus displacement (single 3 m long, 0.9 m wide trench in 20 kPa native clay; 1.5 m embedment depth)*

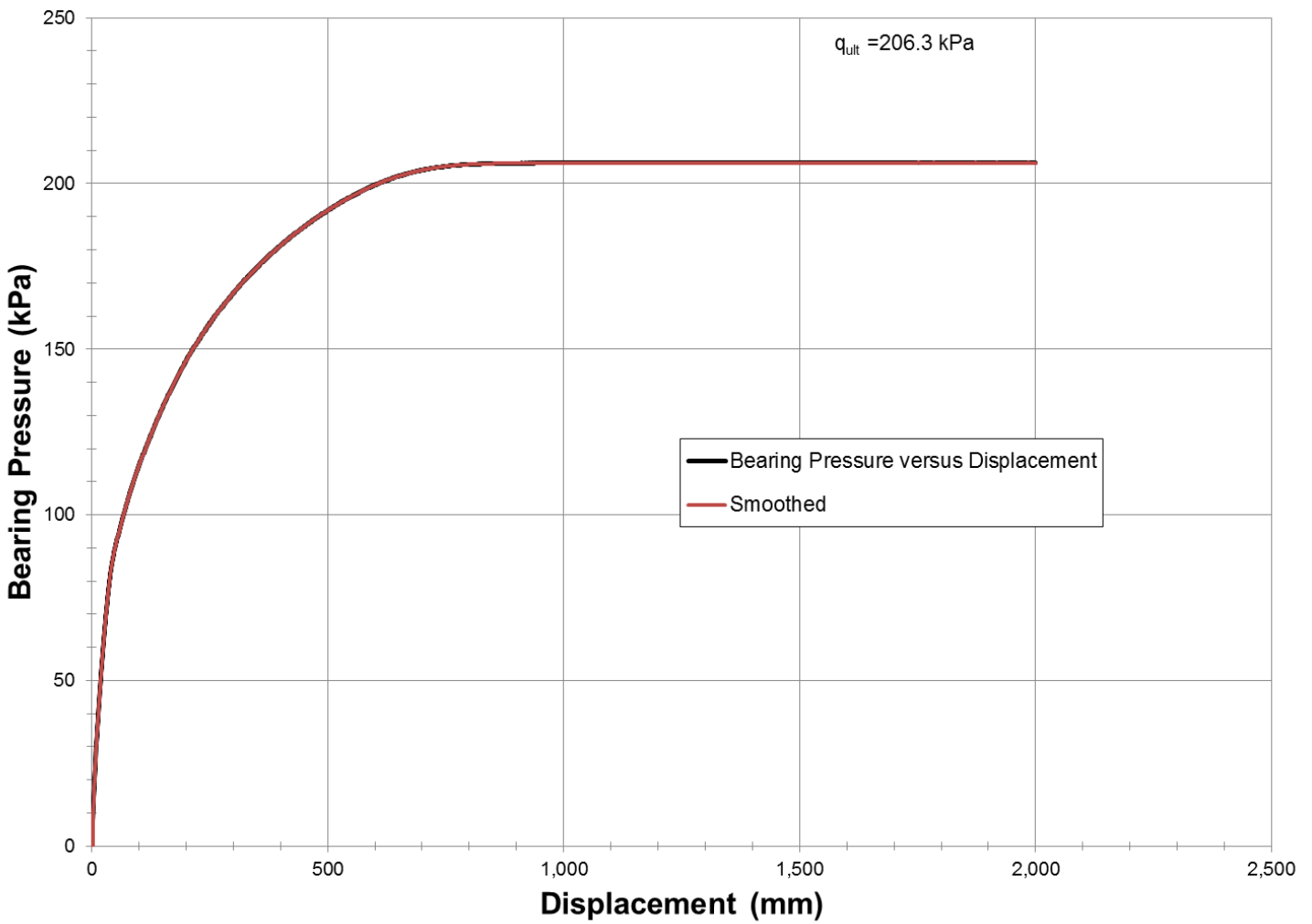


*Figure C-30: Bearing pressure versus displacement (single 3 m long, 0.9 m wide trench in 20 kPa native clay; 3 m embedment depth)*

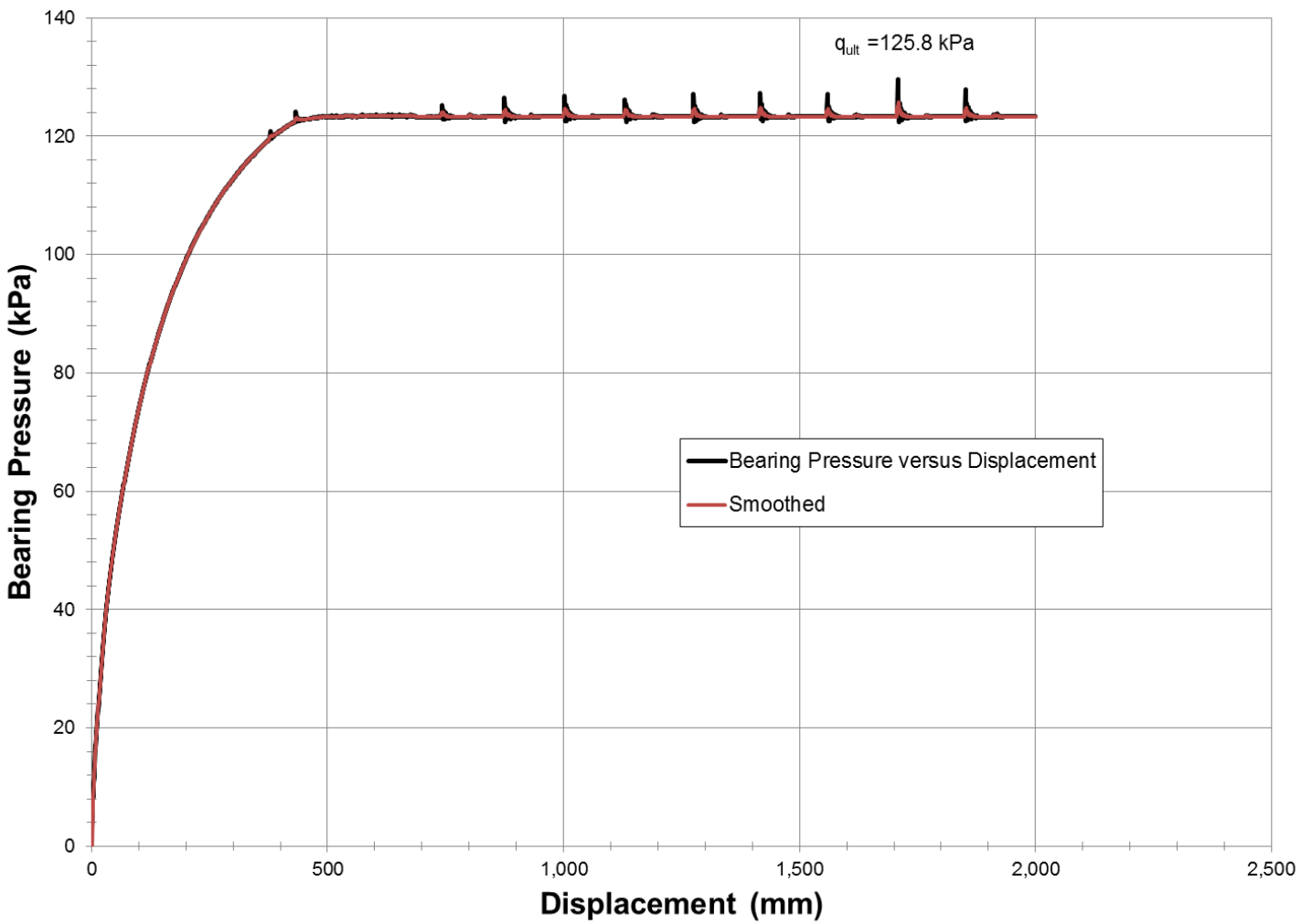


*Figure C-31: Bearing pressure versus displacement (single 3 m long, 0.6 m wide trench in 20 kPa native clay; no embedment depth)*

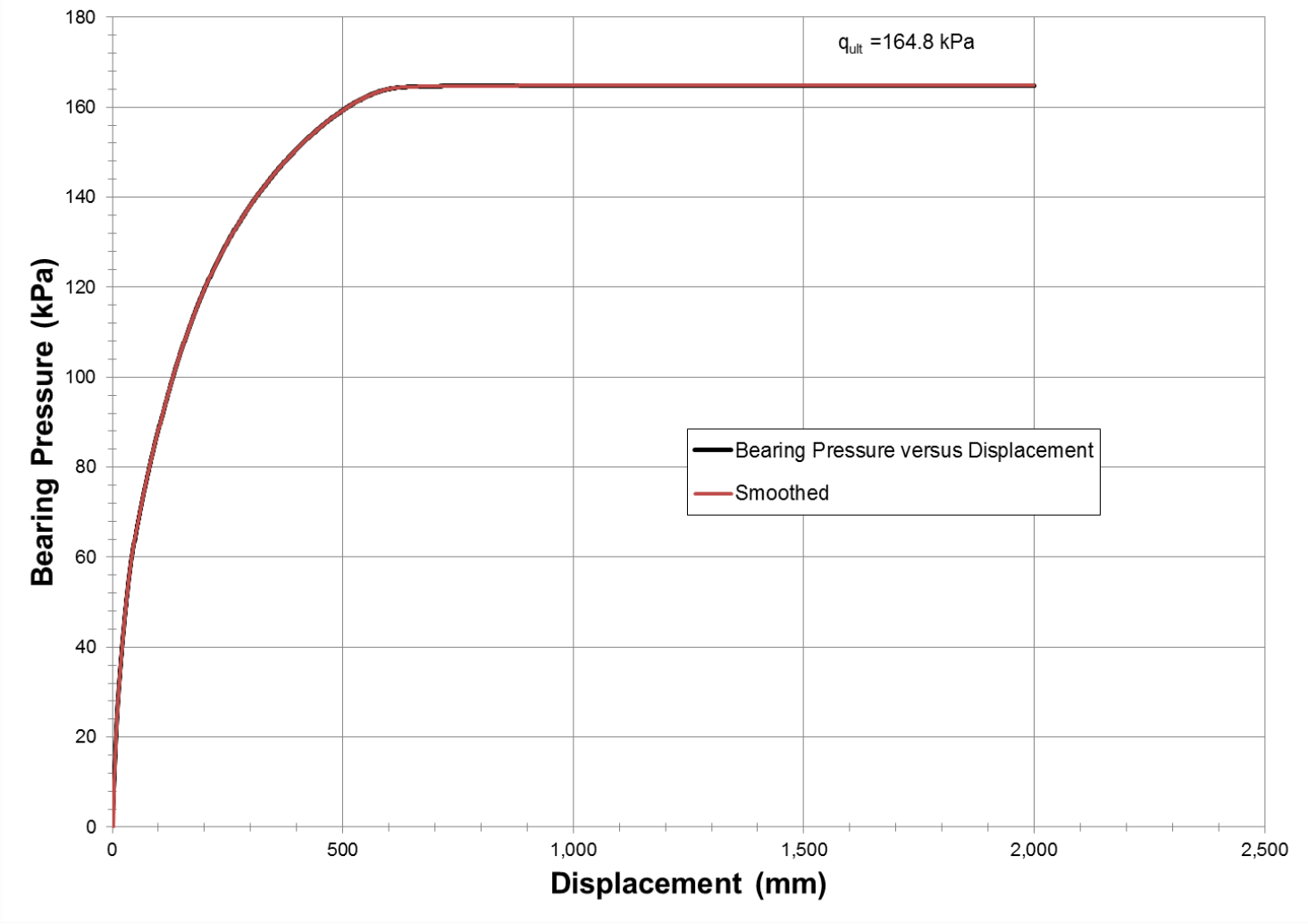


*Figure C-32: Bearing pressure versus displacement (single 3 m long, 0.6 m wide trench in 20 kPa native clay; 1.5 m embedment depth)*

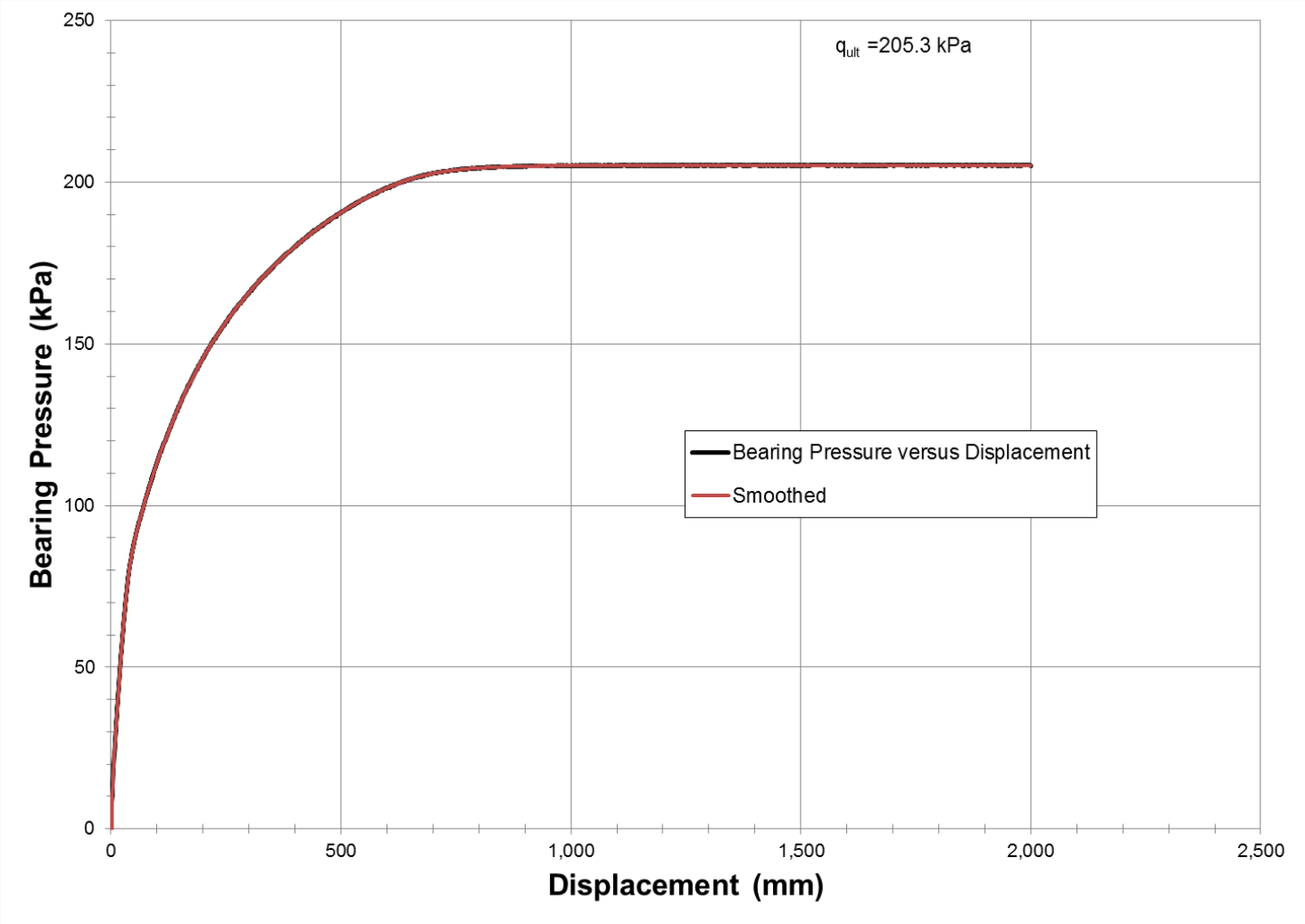


*Figure C-33: Bearing pressure versus displacement (single 3 m long, 0.6 m wide trench in 20 kPa native clay; 3 m embedment depth)*

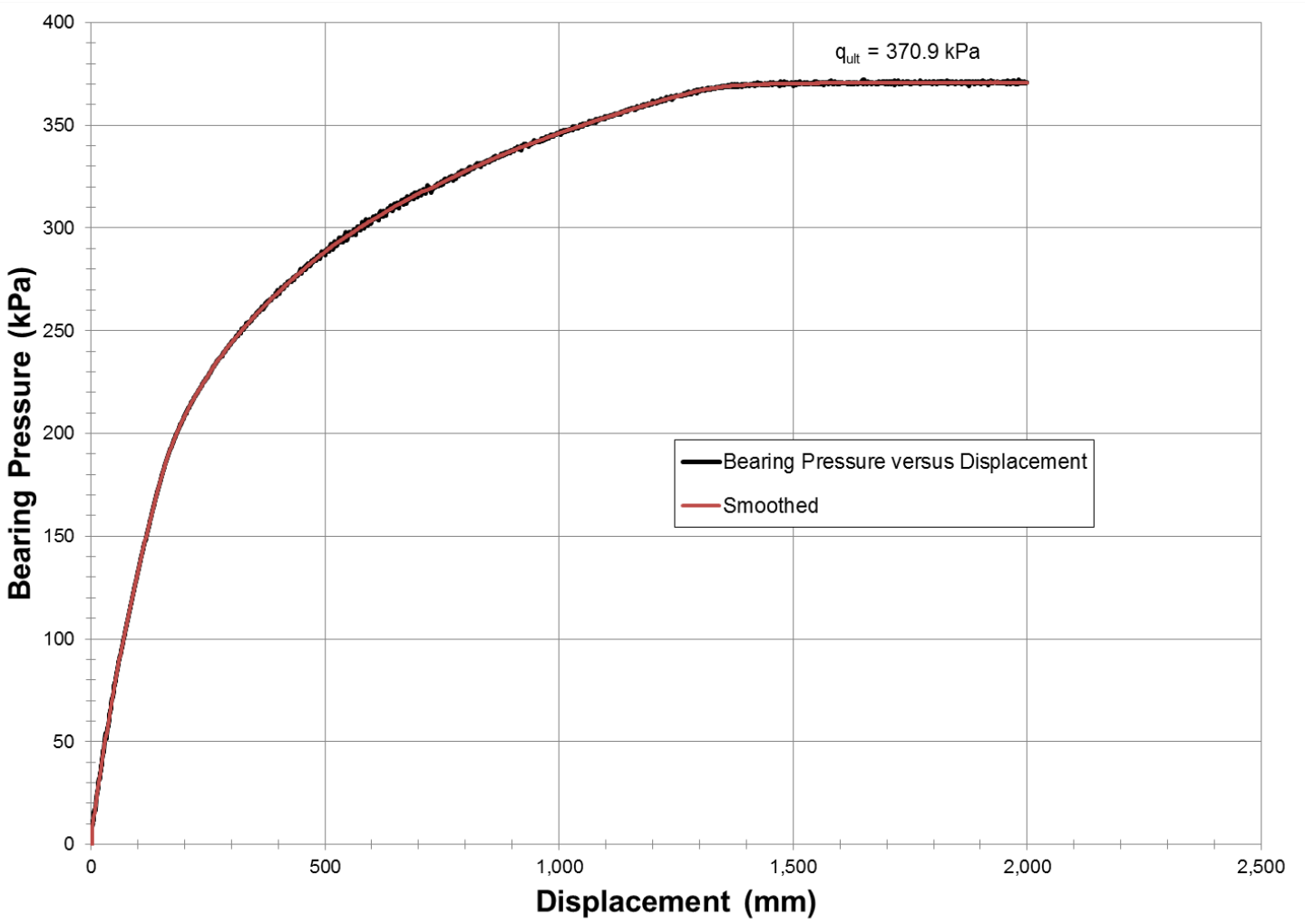


*Figure C-34: Bearing pressure versus displacement (single 7.2 m Long, 0.9 m wide trench in 40 kPa native clay; no embedment depth)*

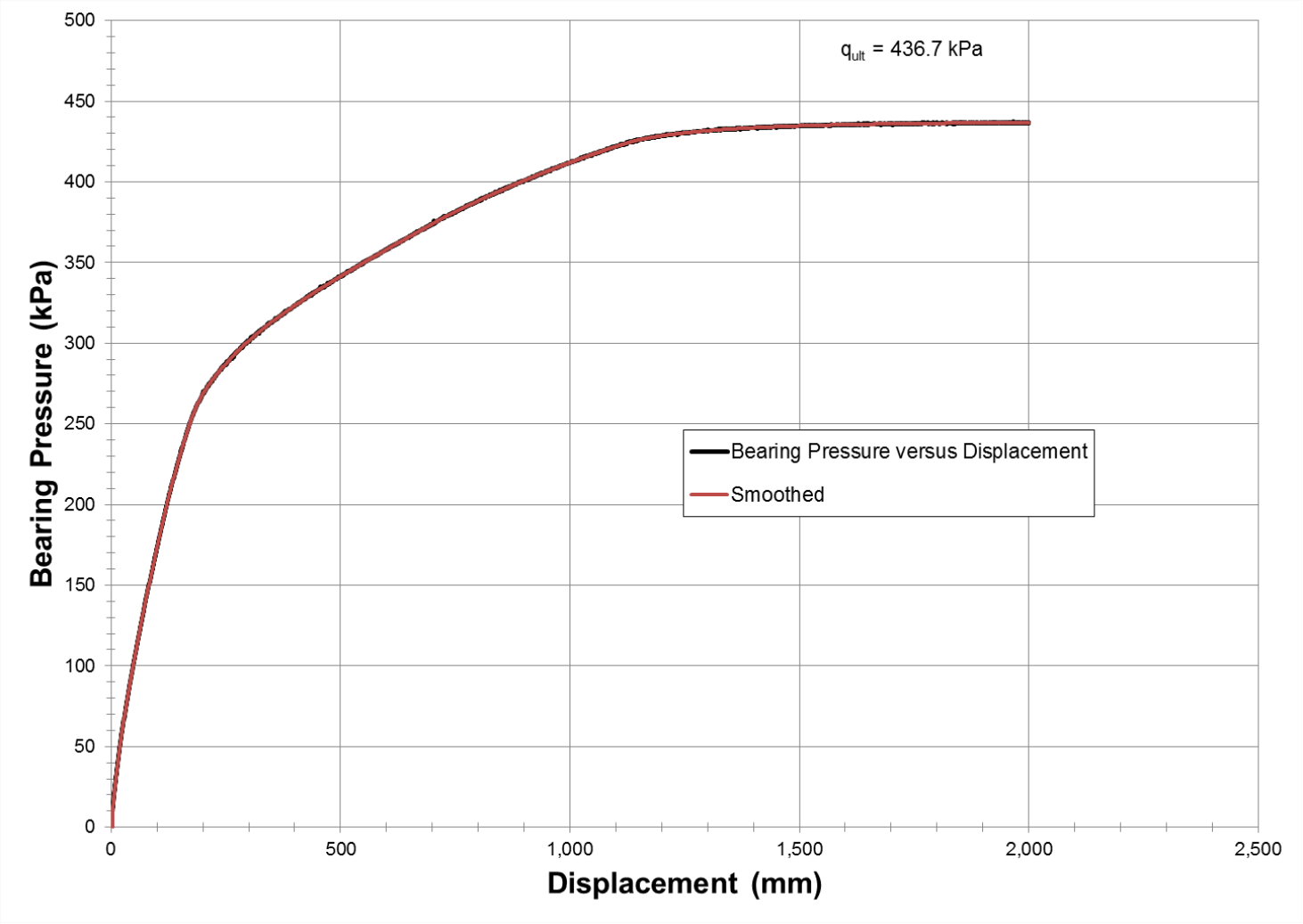


*Figure C-35: Bearing pressure versus displacement (single 7.2 m Long, 0.9 m wide trench in 40 kPa native clay; 3m embedment depth)*

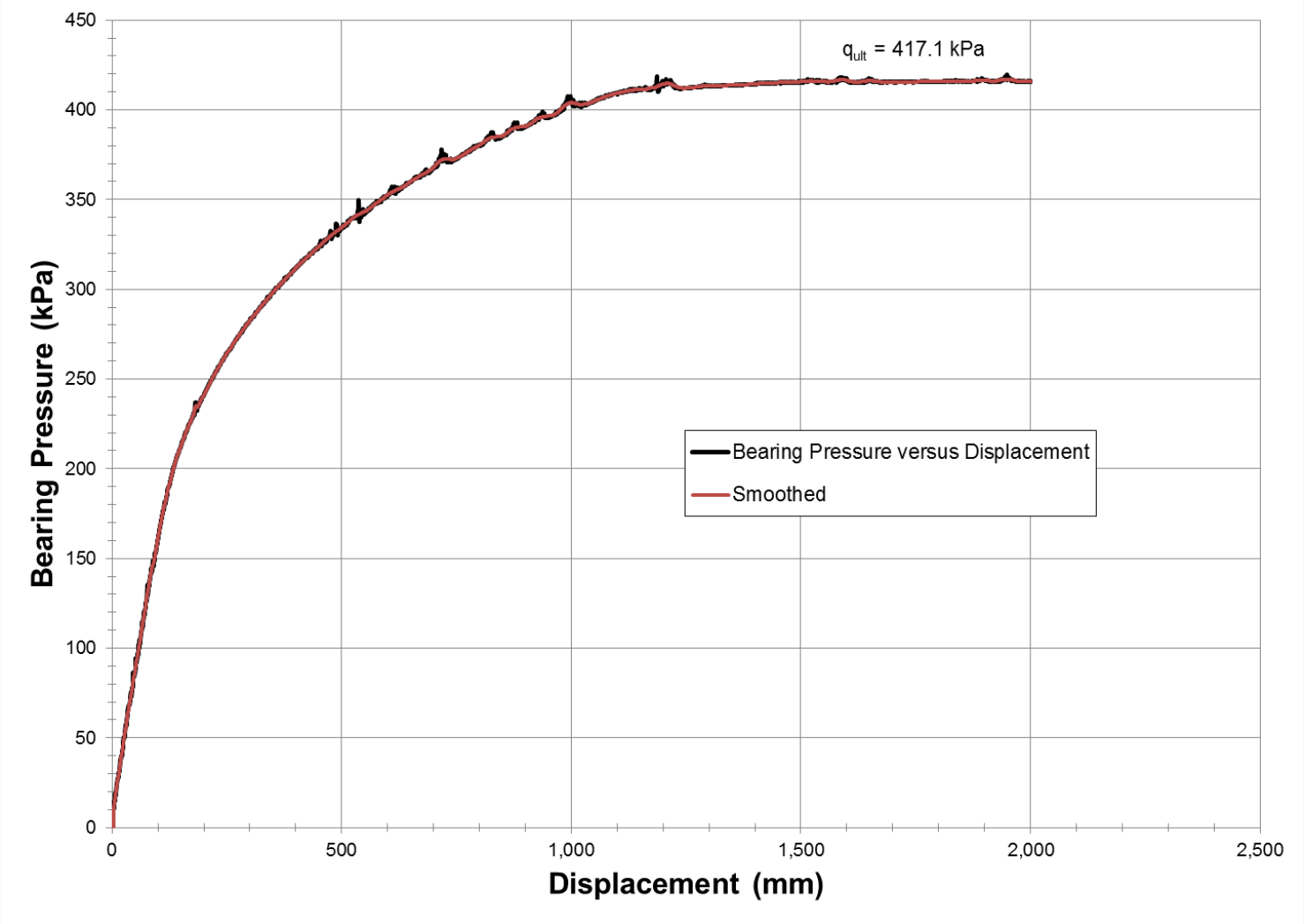


*Figure C-36: Bearing pressure versus displacement (single 6.8 m Long, 2.3 m wide trench in 40 kPa native clay; no embedment depth)*

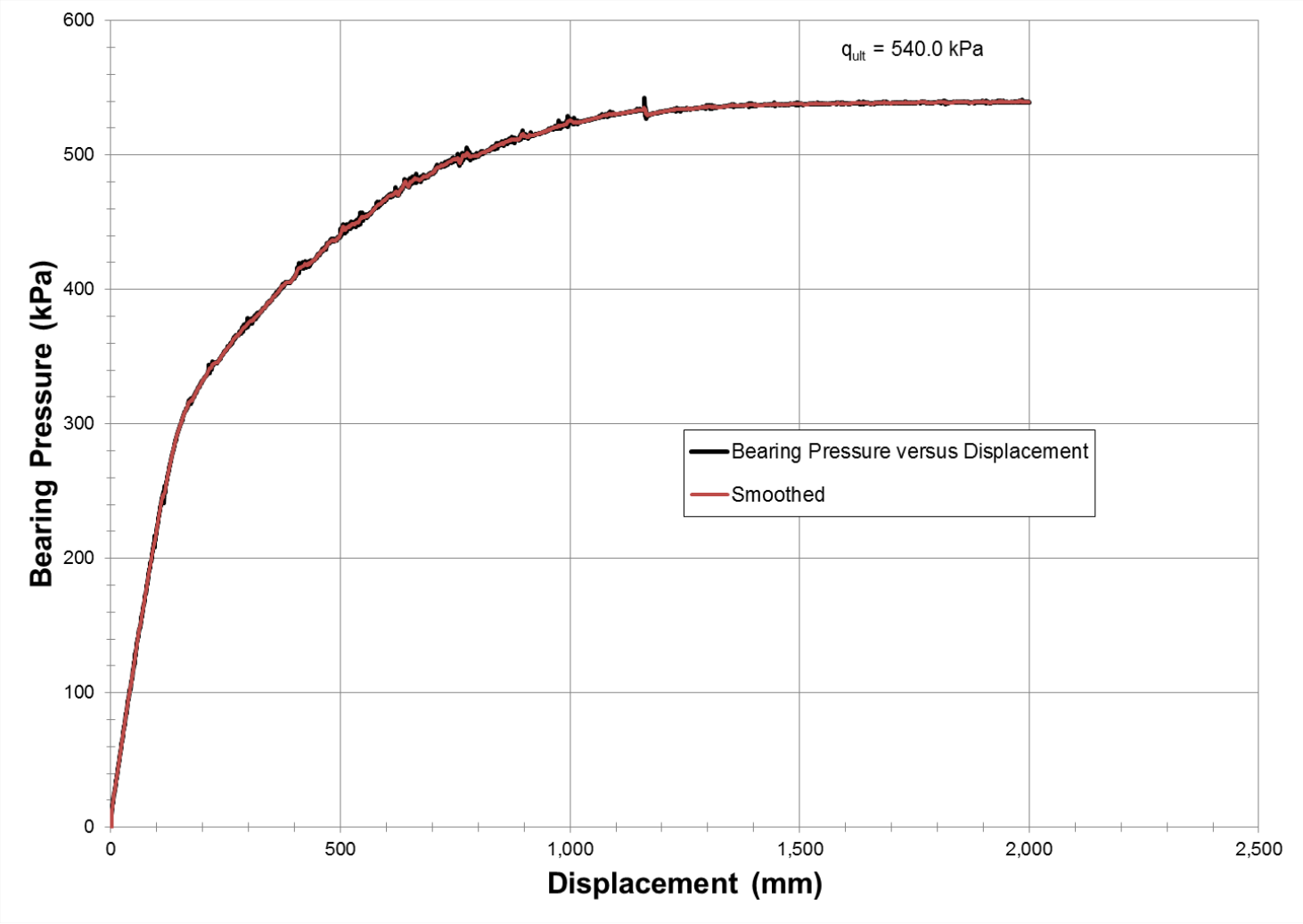


*Figure C-37: Bearing pressure versus displacement (single 6.8 m Long, 2.3 m wide trench in 40 kPa native clay; 3m embedment depth)*

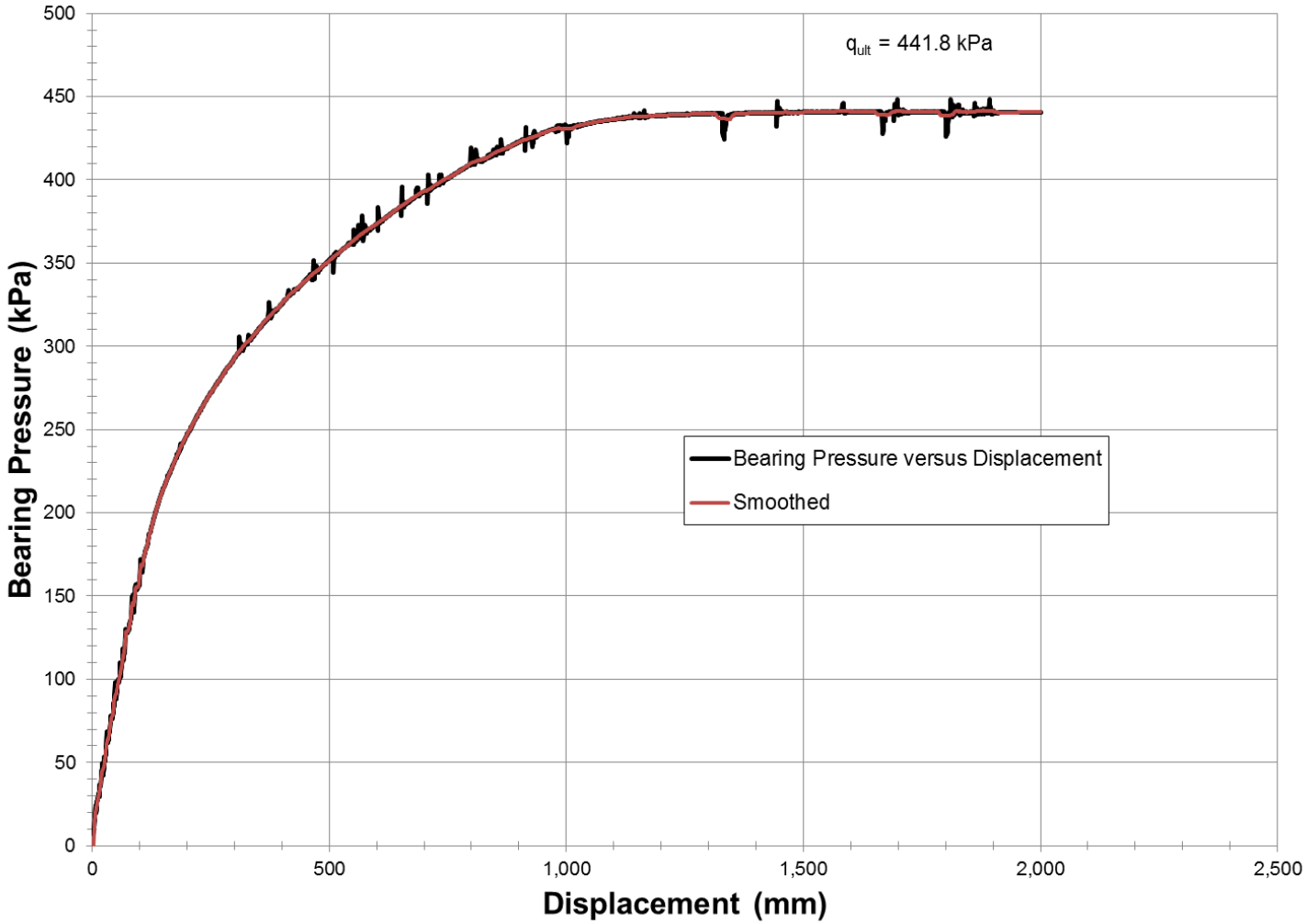


*Figure C-38: Bearing pressure versus displacement (single 6 m Long, 3 m wide trench in 40 kPa native clay; no embedment depth)*

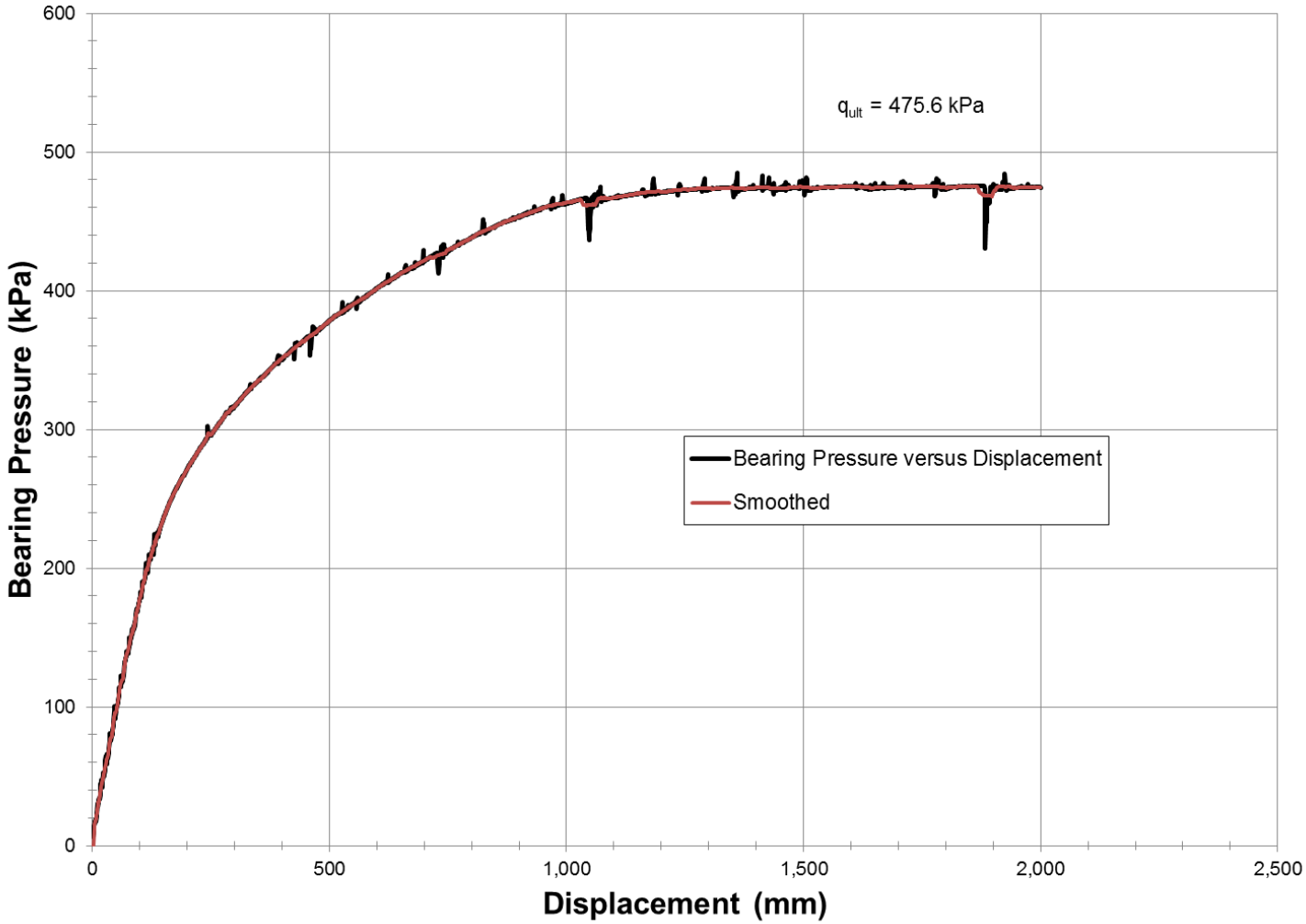


*Figure C-39: Bearing pressure versus displacement (single 6 m Long, 3 m wide trench in 40 kPa clay; 1 m embedment depth)*

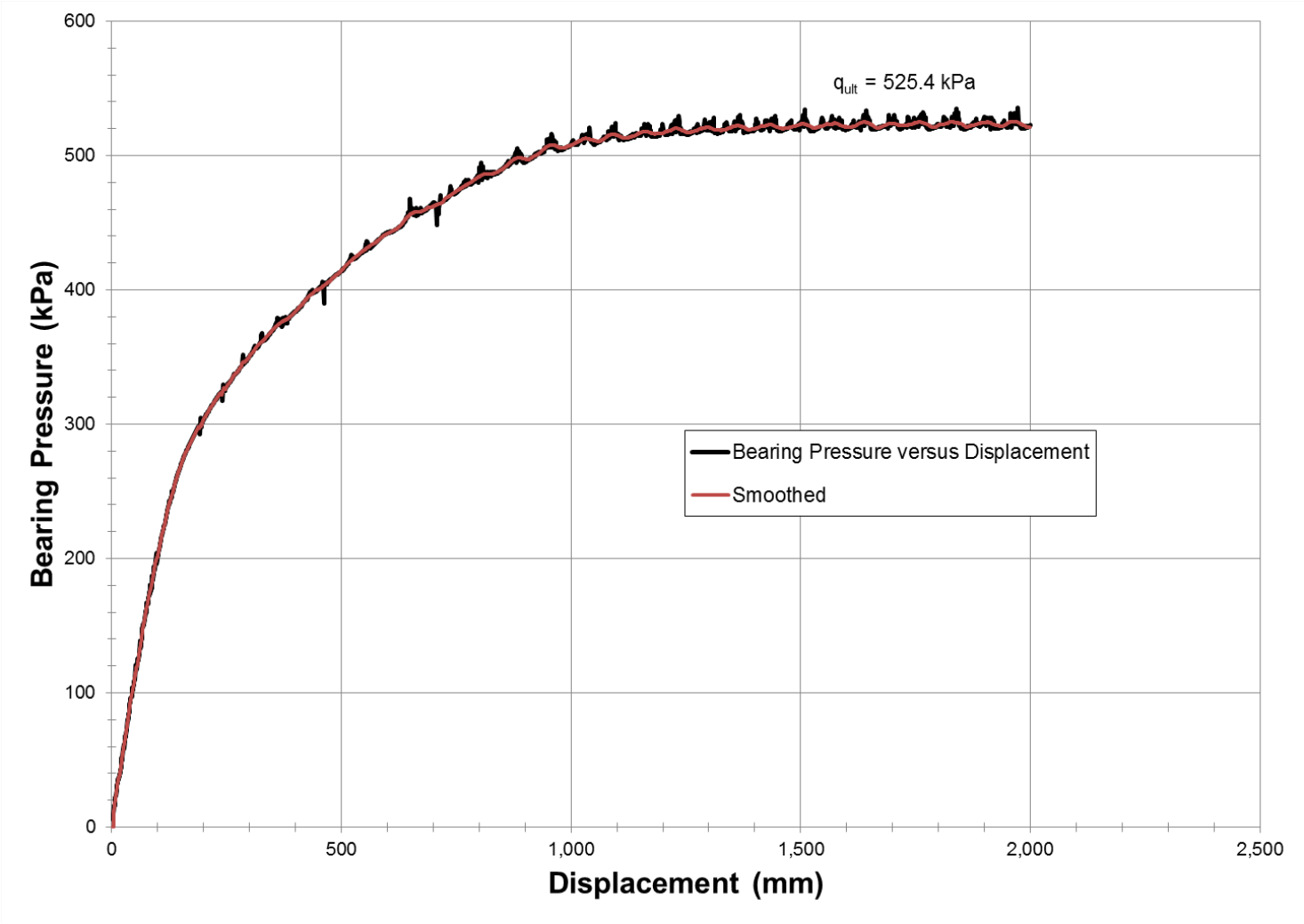


*Figure C-40: Bearing pressure versus displacement (single 6 m Long, 3 m wide trench in 40 kPa clay; 2 m embedment depth)*

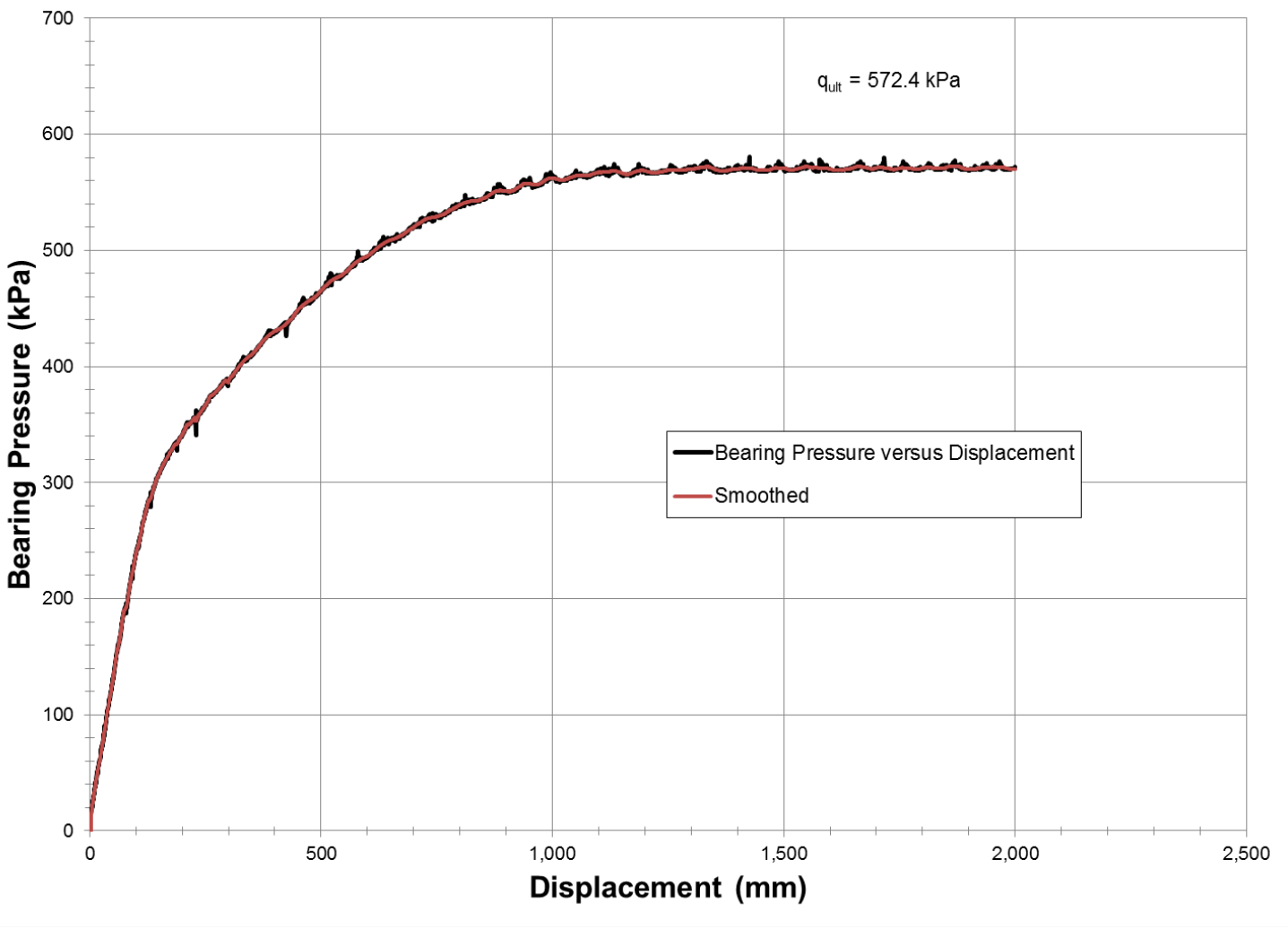


*Figure C-41: Bearing pressure versus displacement (single 6 m Long, 3 m wide trench in 40 kPa clay; 3 m embedment depth)*

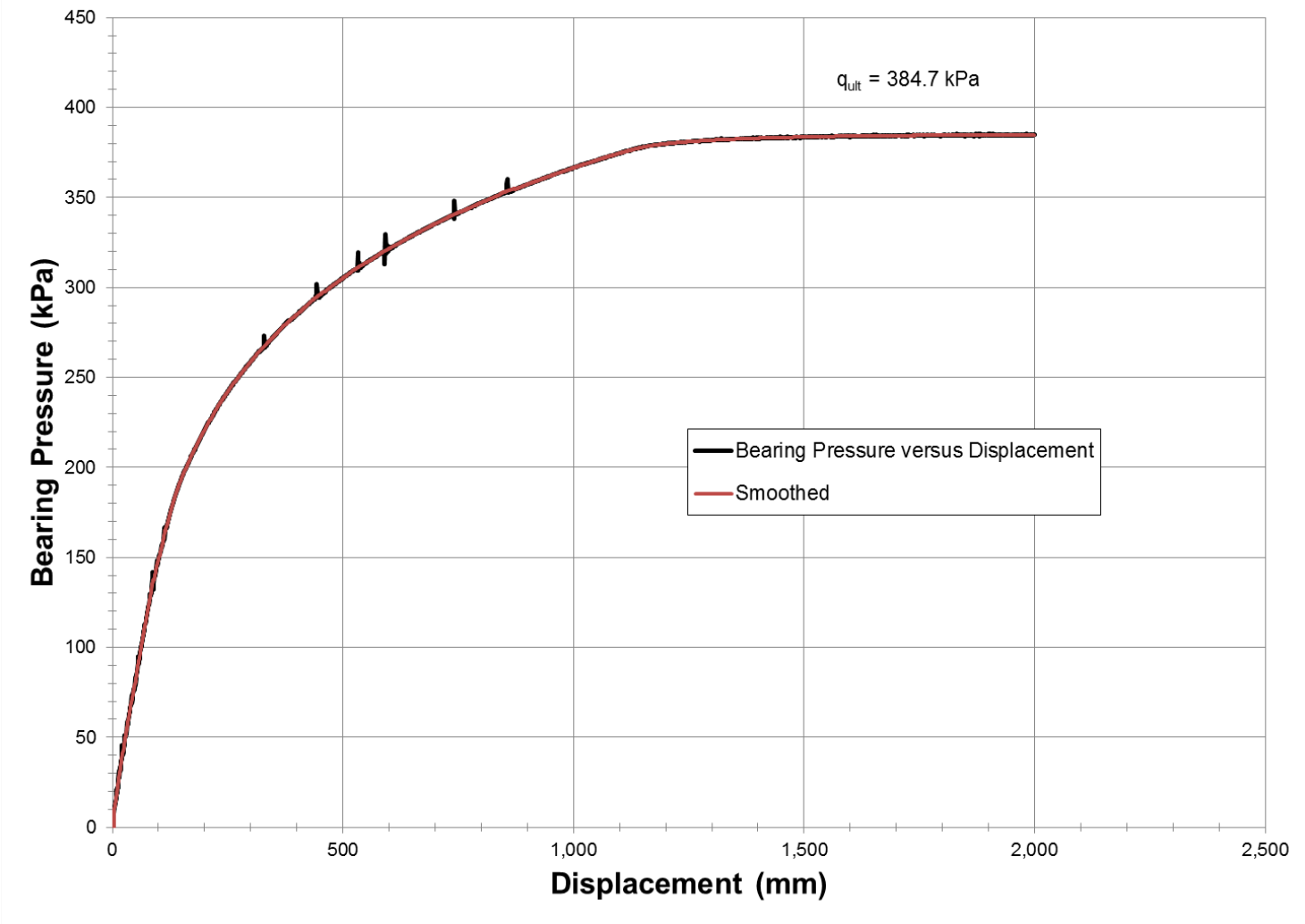


*Figure C-42: Bearing pressure versus displacement (single 6 m Long, 2 m wide trench in 40 kPa clay; no embedment depth)*

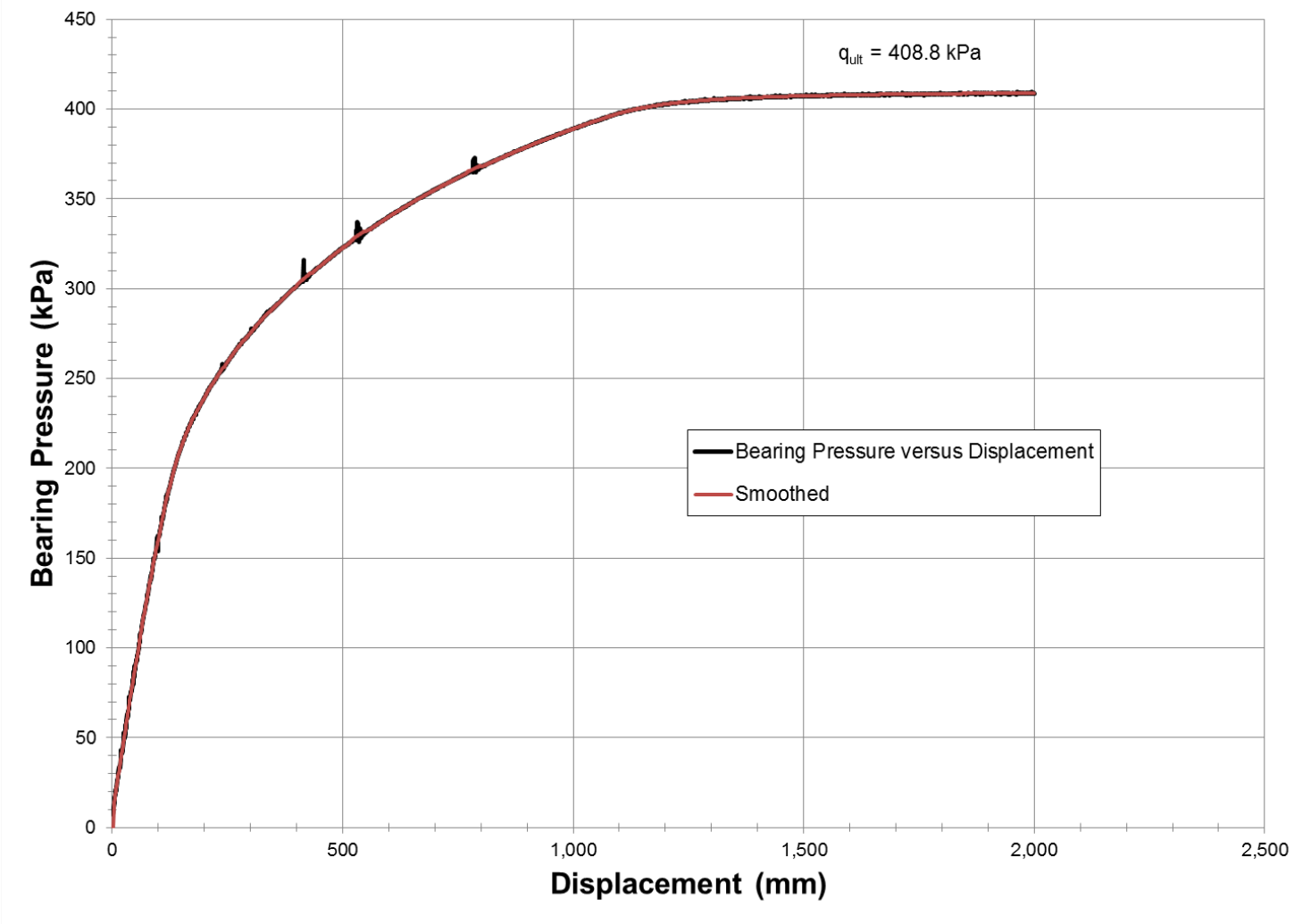


*Figure C-43: Bearing pressure versus displacement (single 6 m Long, 2 m wide trench in 40 kPa clay; 1 m embedment depth)*

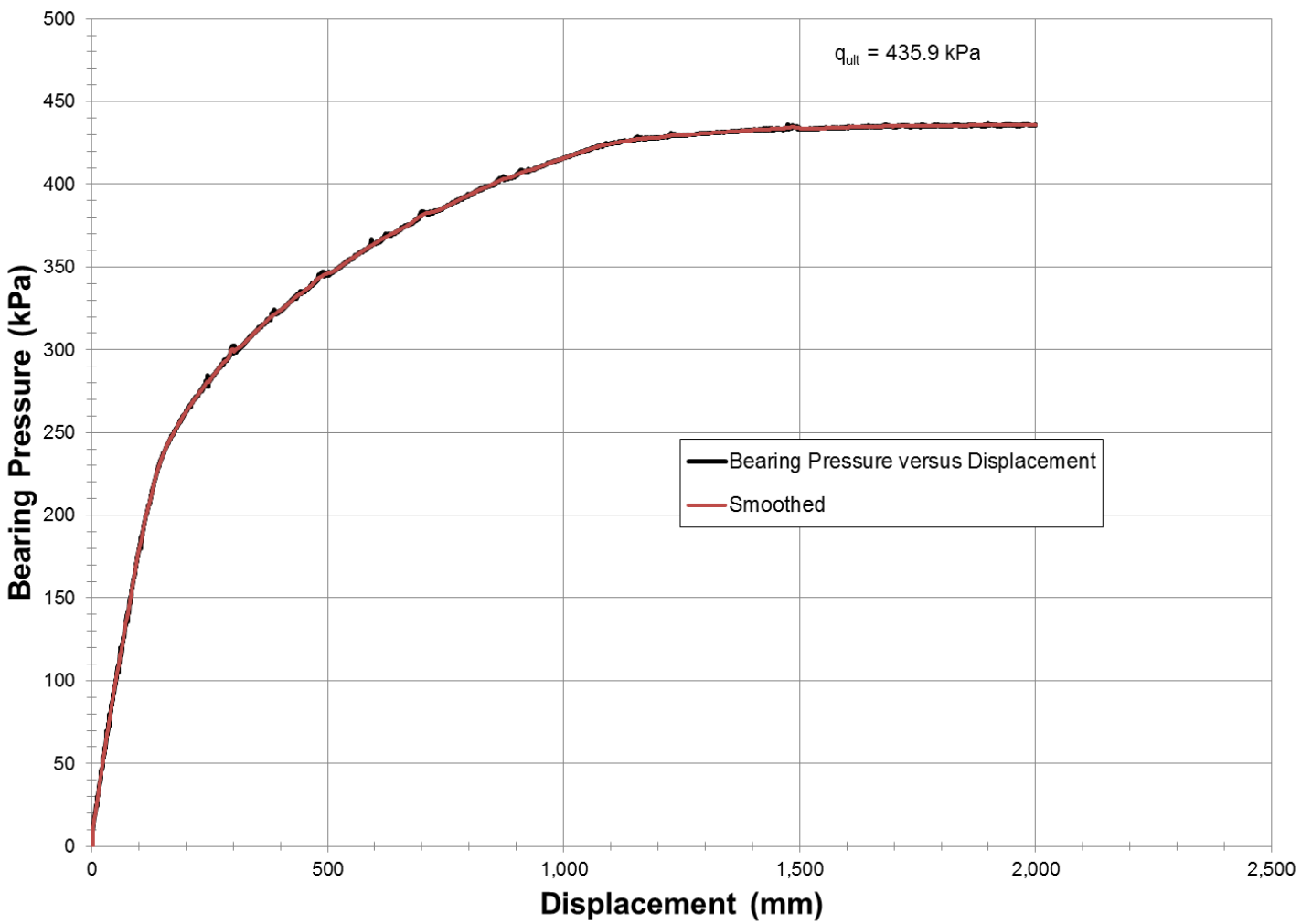


*Figure C-44: Bearing pressure versus displacement (single 6 m Long, 2 m wide trench in 40 kPa clay; 2 m embedment depth)*

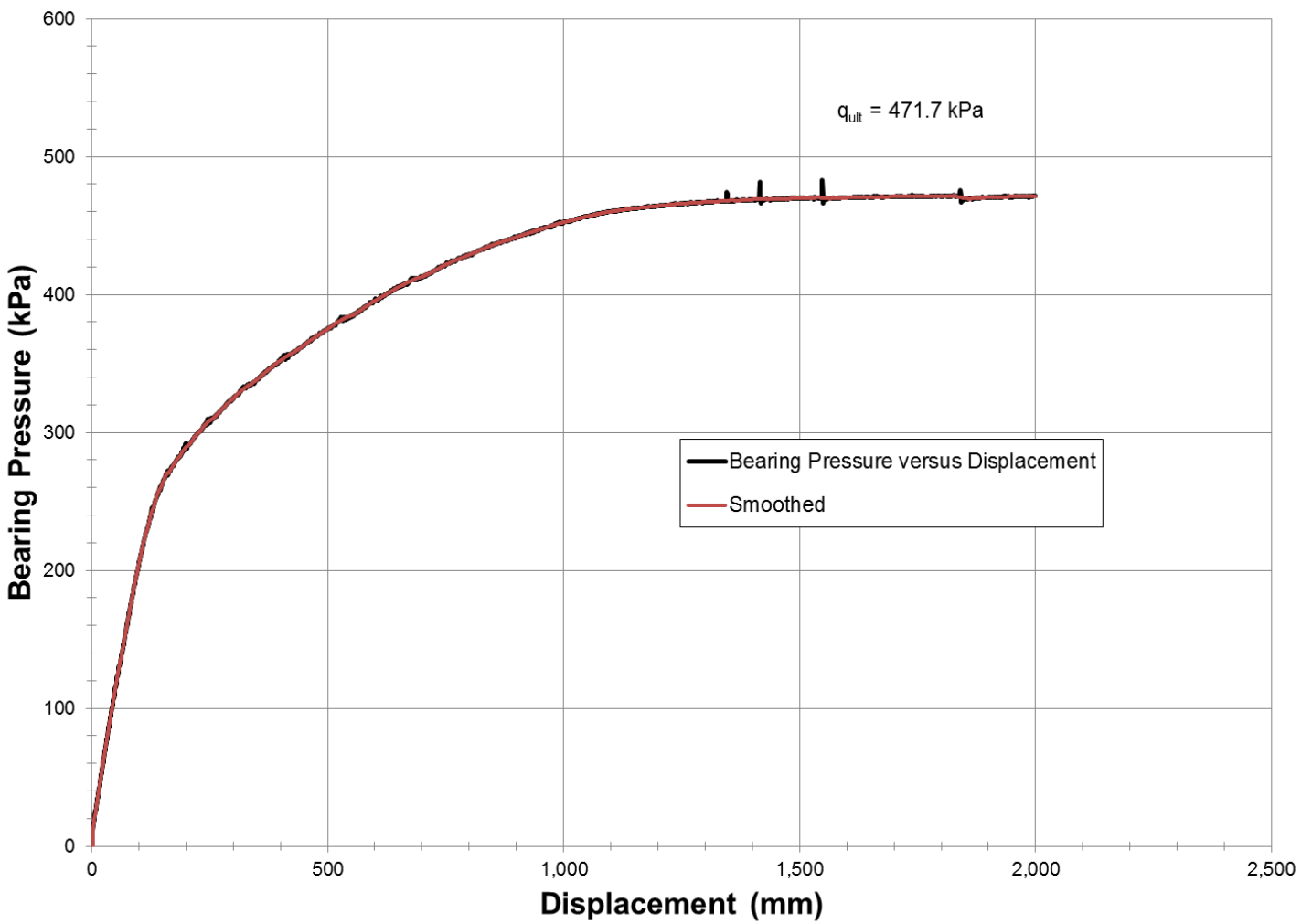


*Figure C-45: Bearing pressure versus displacement (single 6 m Long, 2 m wide trench in 40 kPa clay; 3 m embedment depth)*

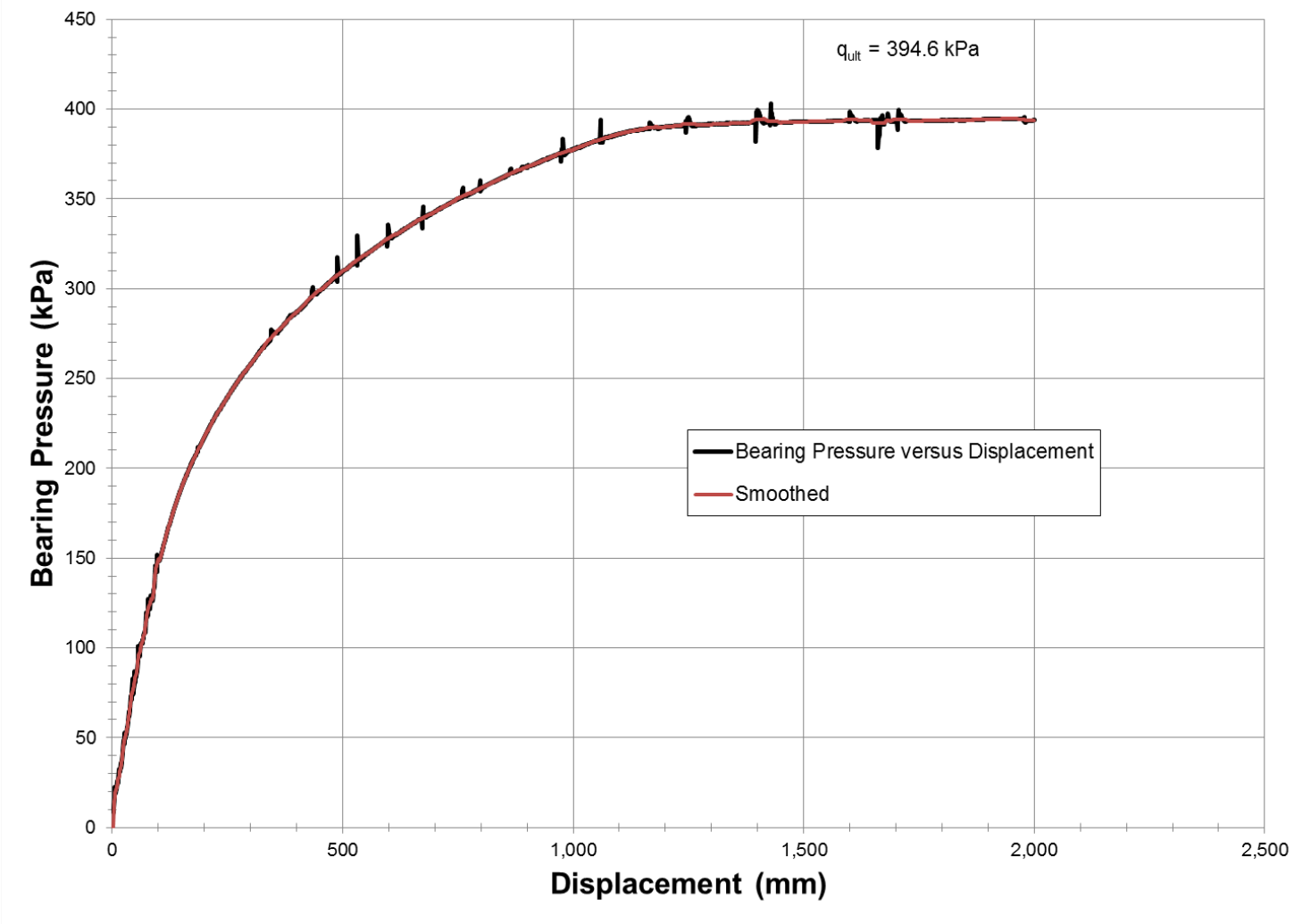


*Figure C-46: Bearing pressure versus displacement (single 5.22 m Long, 2.61 m wide trench in 40 kPa clay; no embedment depth)*

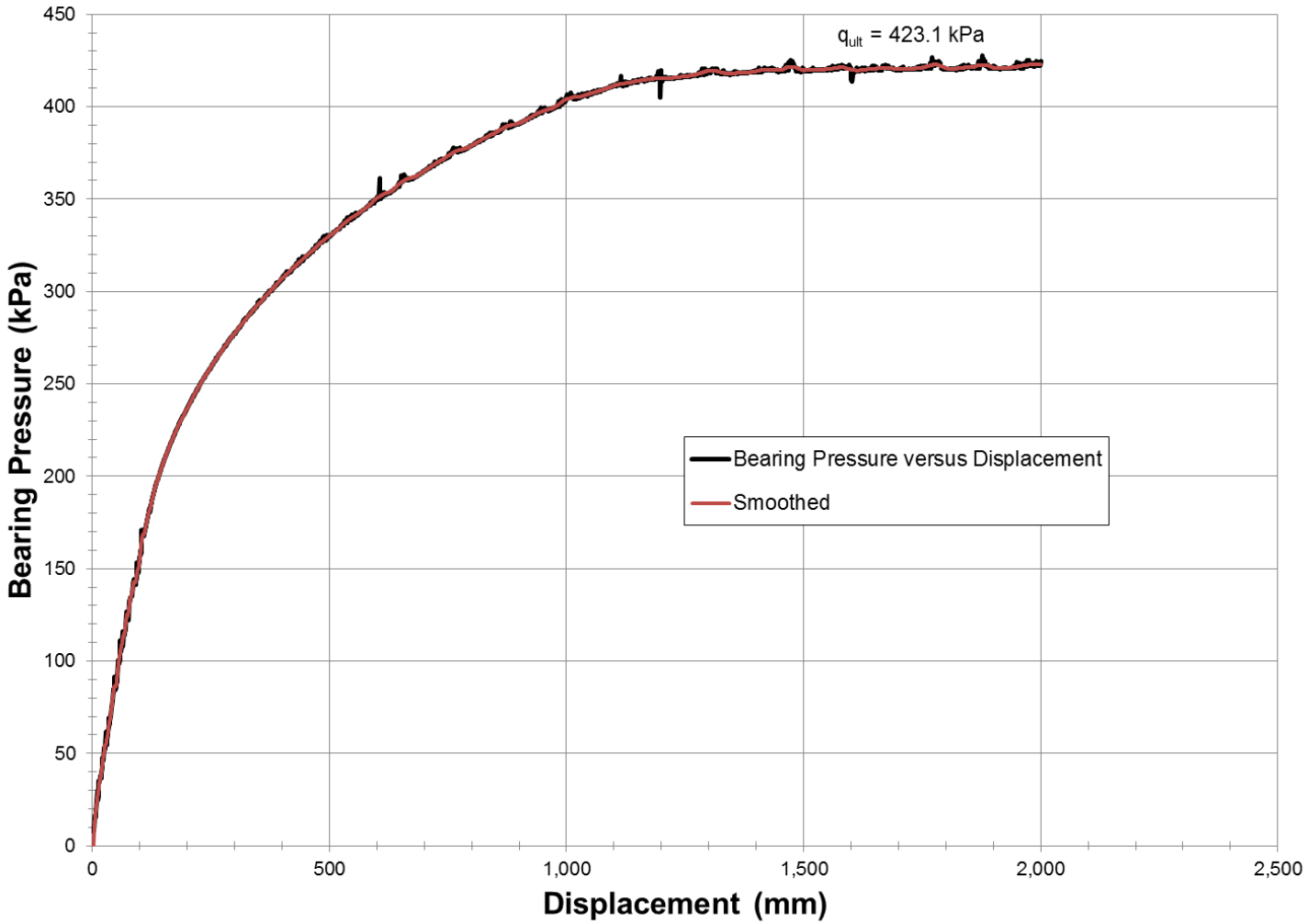


*Figure C-47: Bearing pressure versus displacement (single 5.22 m Long, 2.61 m wide trench in 40 kPa clay; 1 m embedment depth)*

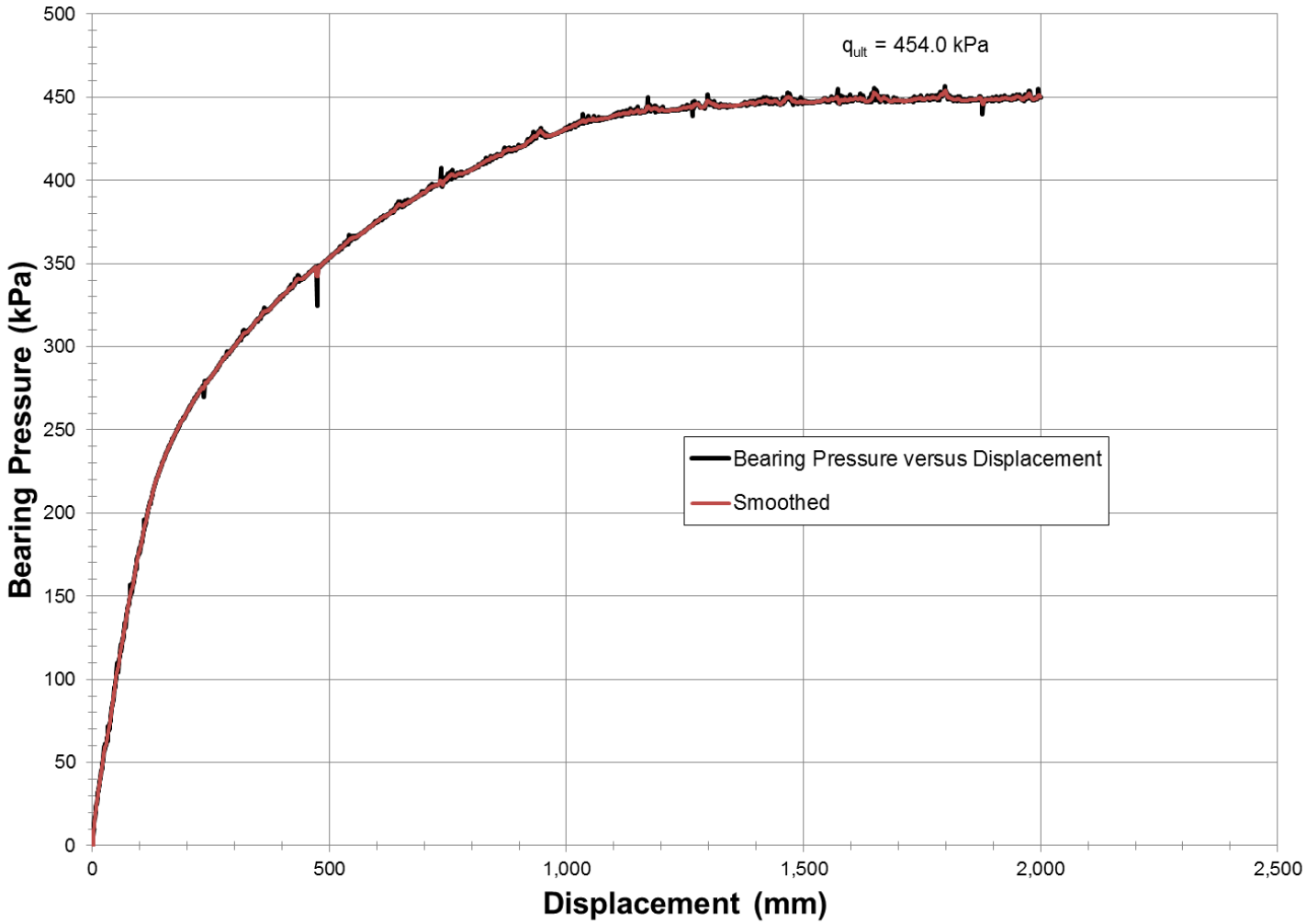


*Figure C-48: Bearing pressure versus displacement (single 5.22 m Long, 2.61 m wide trench in 40 kPa clay; 2 m embedment depth)*

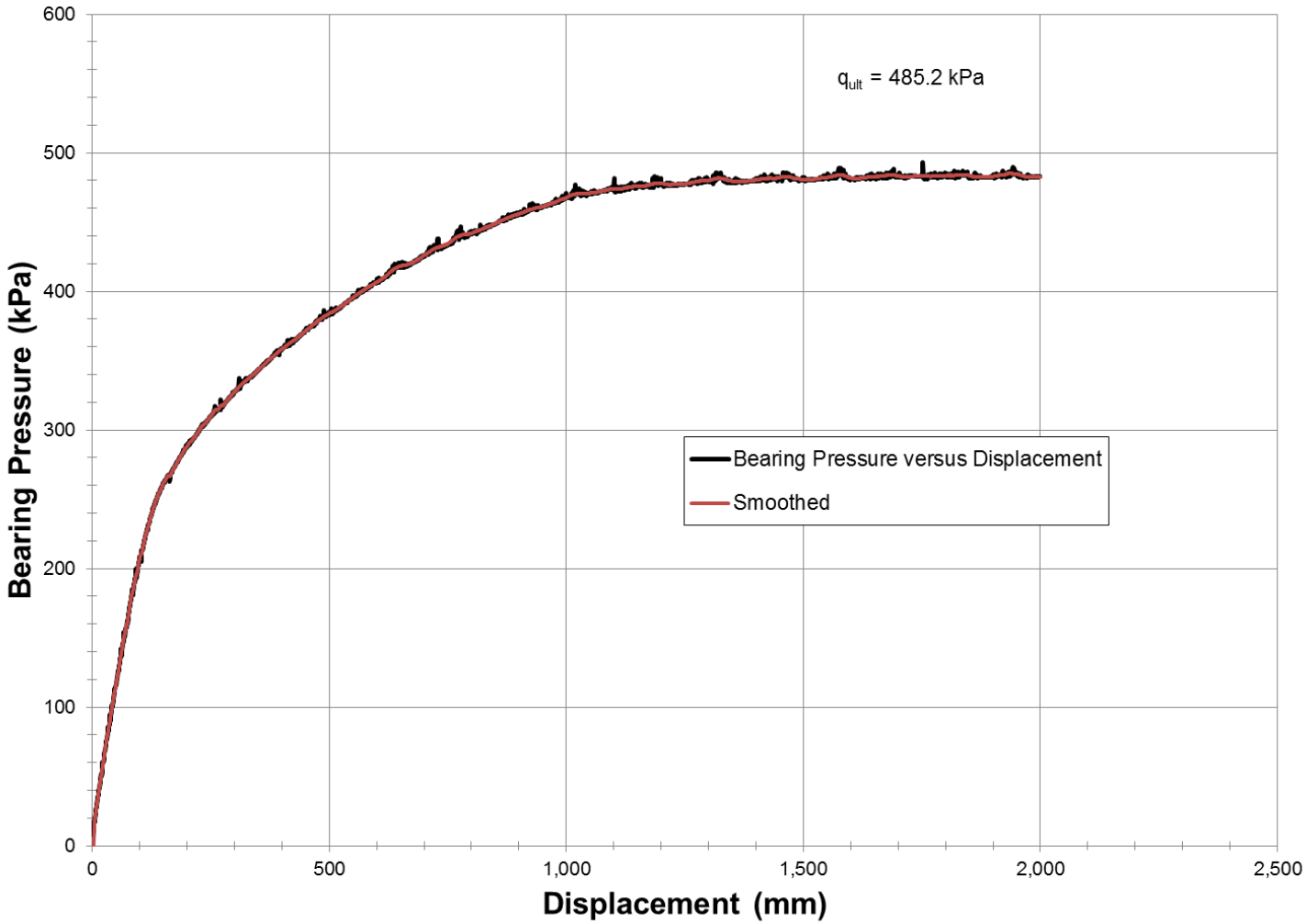


*Figure C-49: Bearing pressure versus displacement (single 5.22 m Long, 2.61 m wide trench in 40 kPa clay; 3 m embedment depth)*

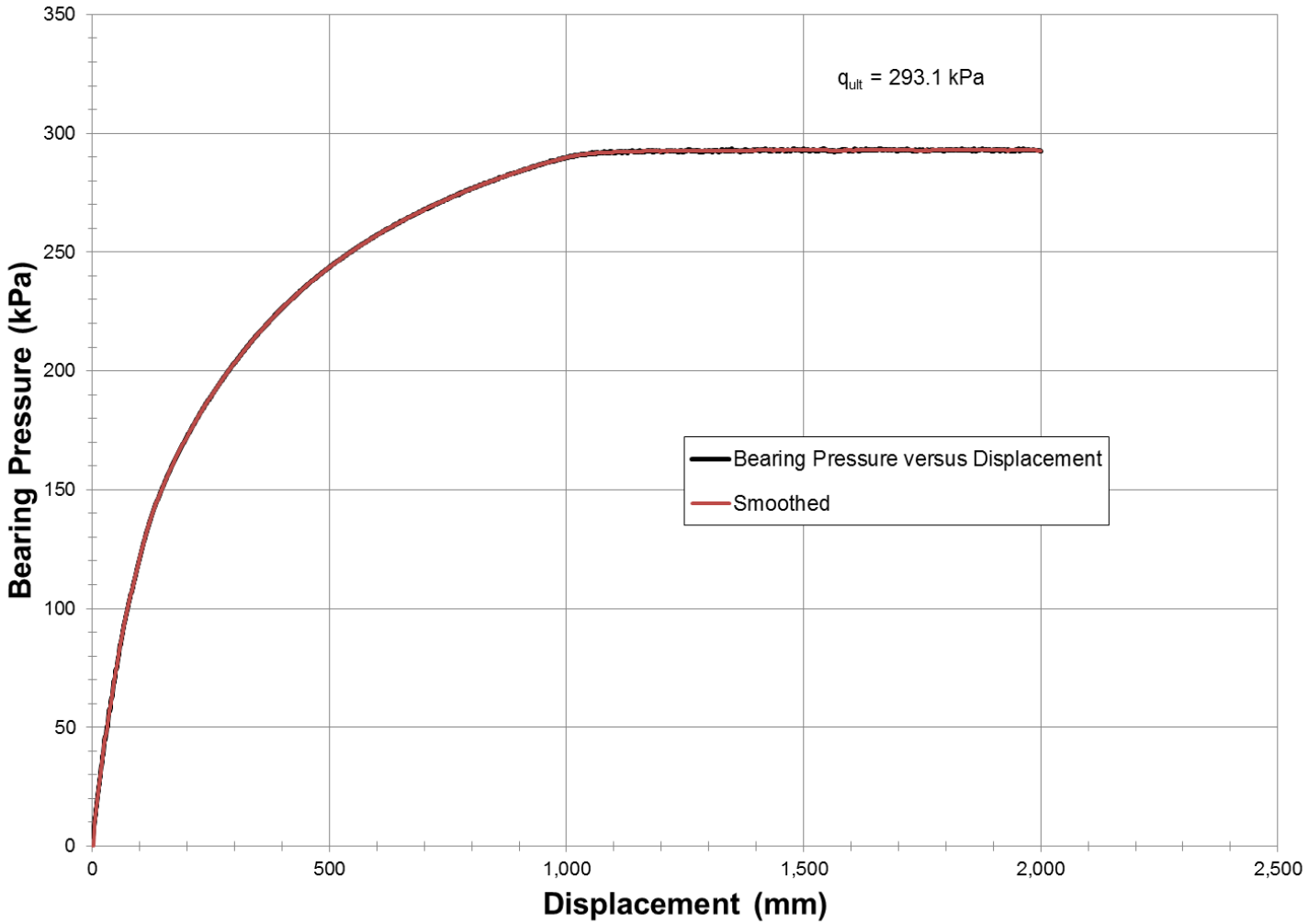


*Figure C-50: Bearing pressure versus displacement (single 4.8 m Long, 0.6 m wide trench in 40 kPa clay; no embedment depth)*

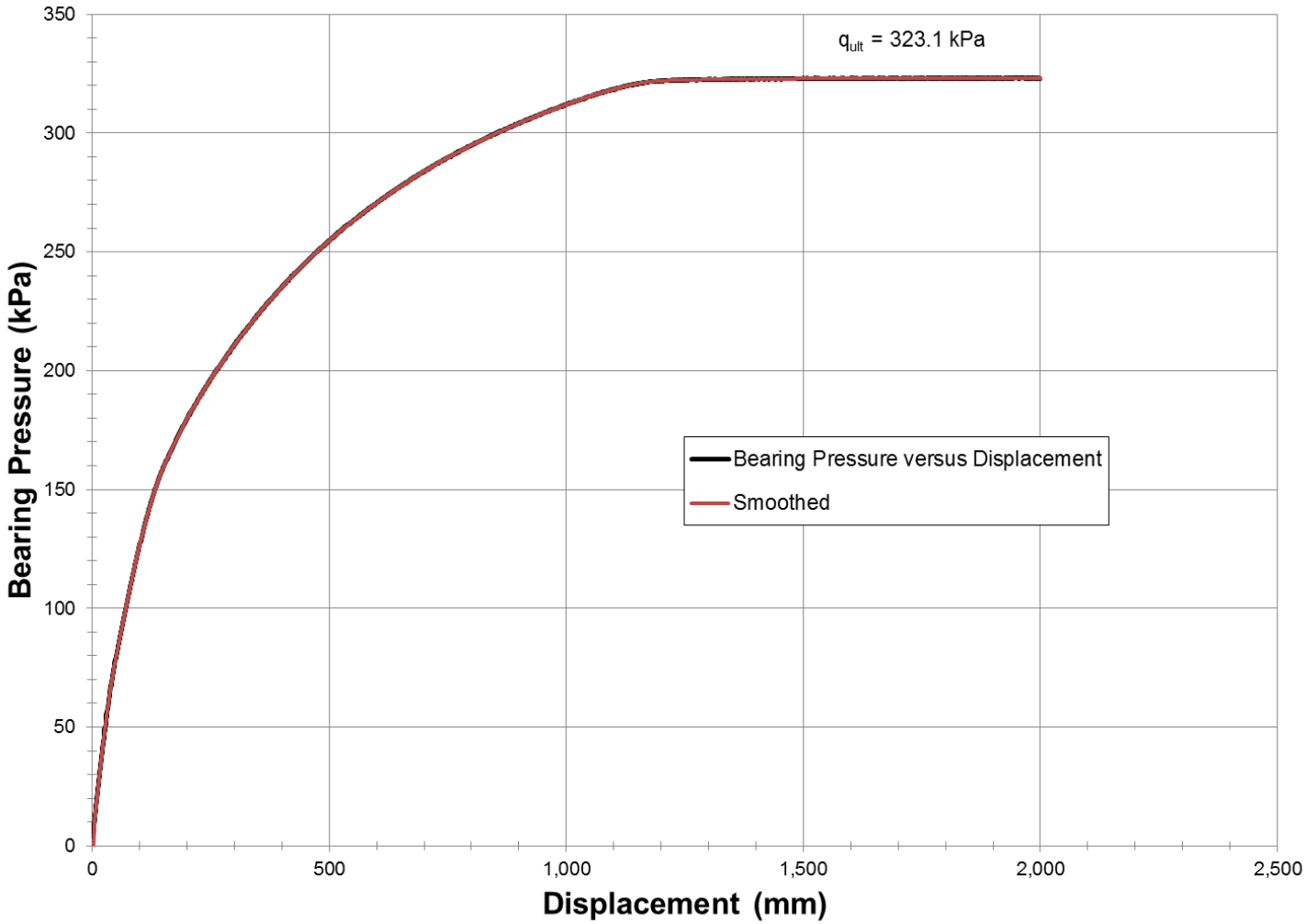


*Figure C-51: Bearing pressure versus displacement (single 4.8 m Long, 0.6 m wide trench in 40 kPa clay; 1 m embedment depth)*

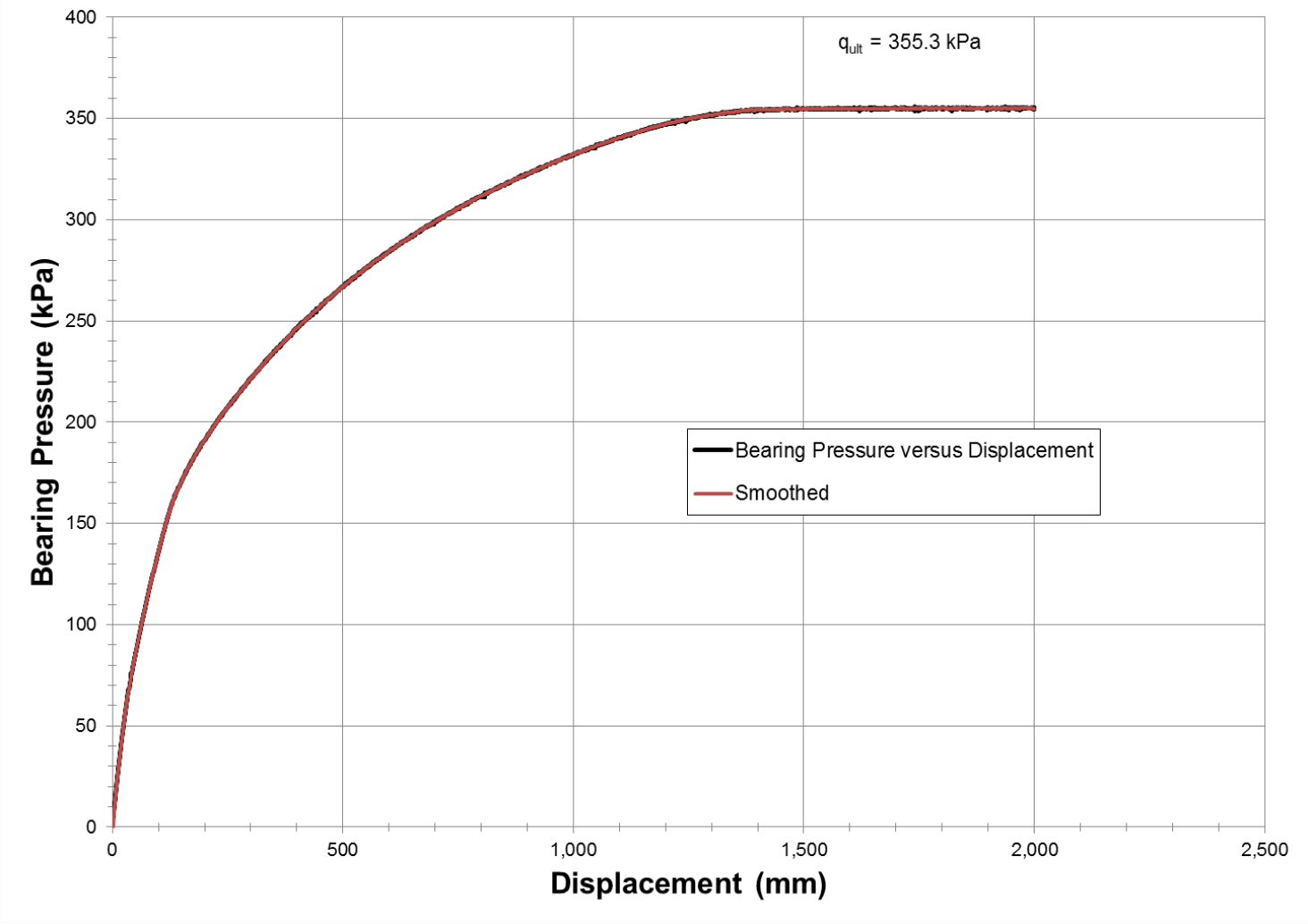


*Figure C-52: Bearing pressure versus displacement (single 4.8 m Long, 0.6 m wide trench in 40 kPa clay; 2 m embedment depth)*

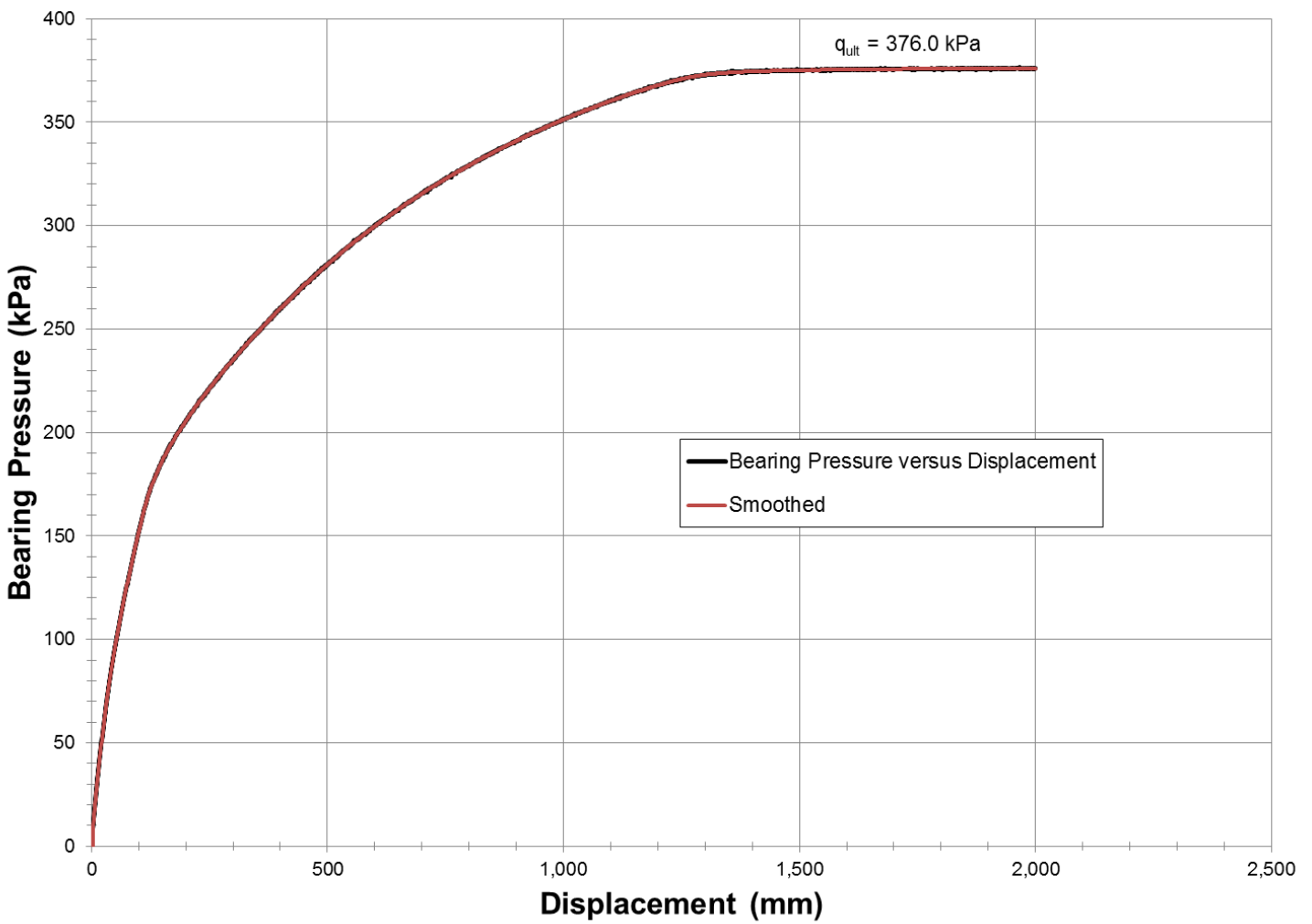


*Figure C-53: Bearing pressure versus displacement (single 4.8 m Long, 0.6 m wide trench in 40 kPa clay; 3 m embedment depth)*

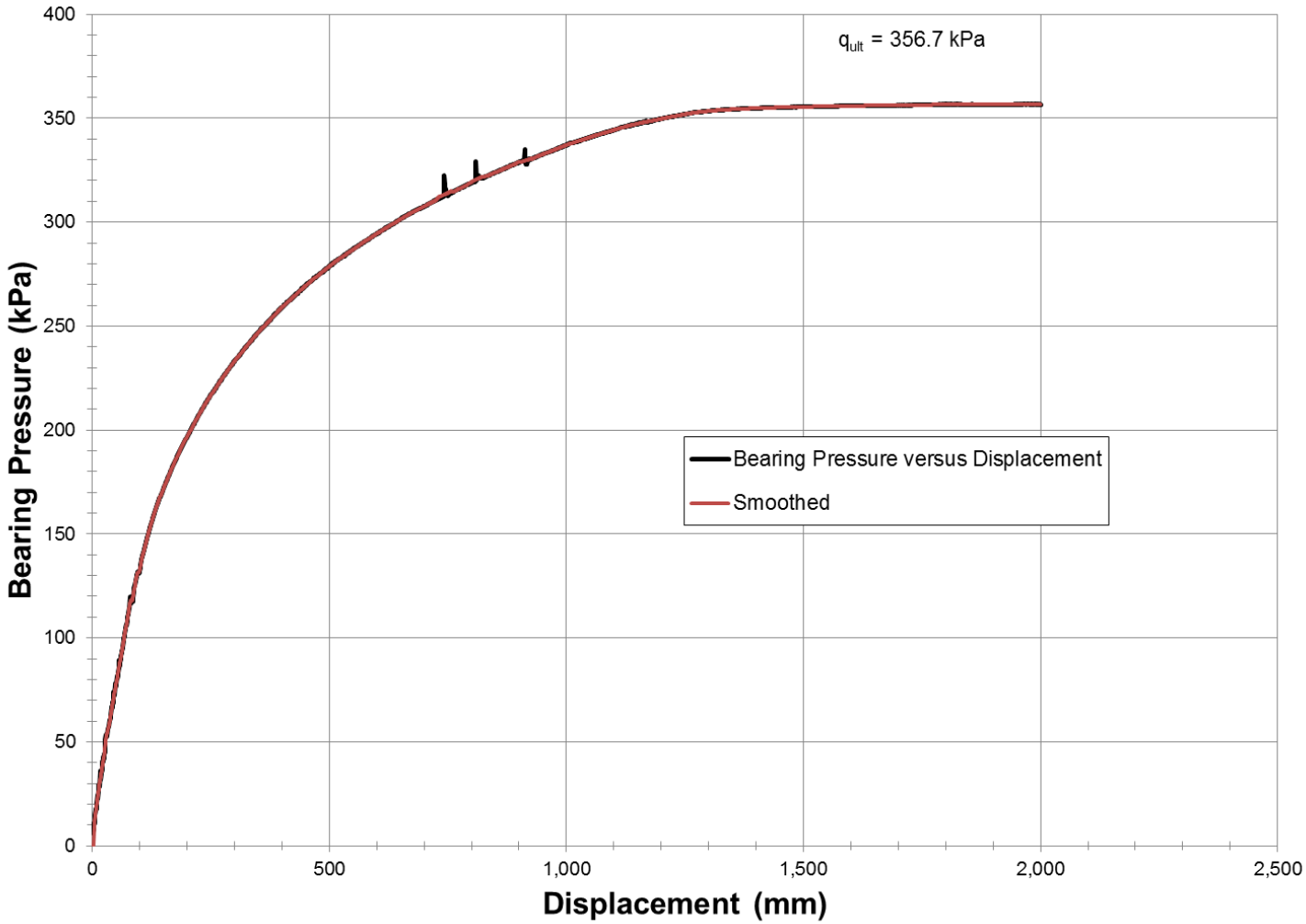


*Figure C-54: Bearing pressure versus displacement (single 4.51 m Long, 2.26 m wide trench in 40 kPa clay; no embedment depth)*

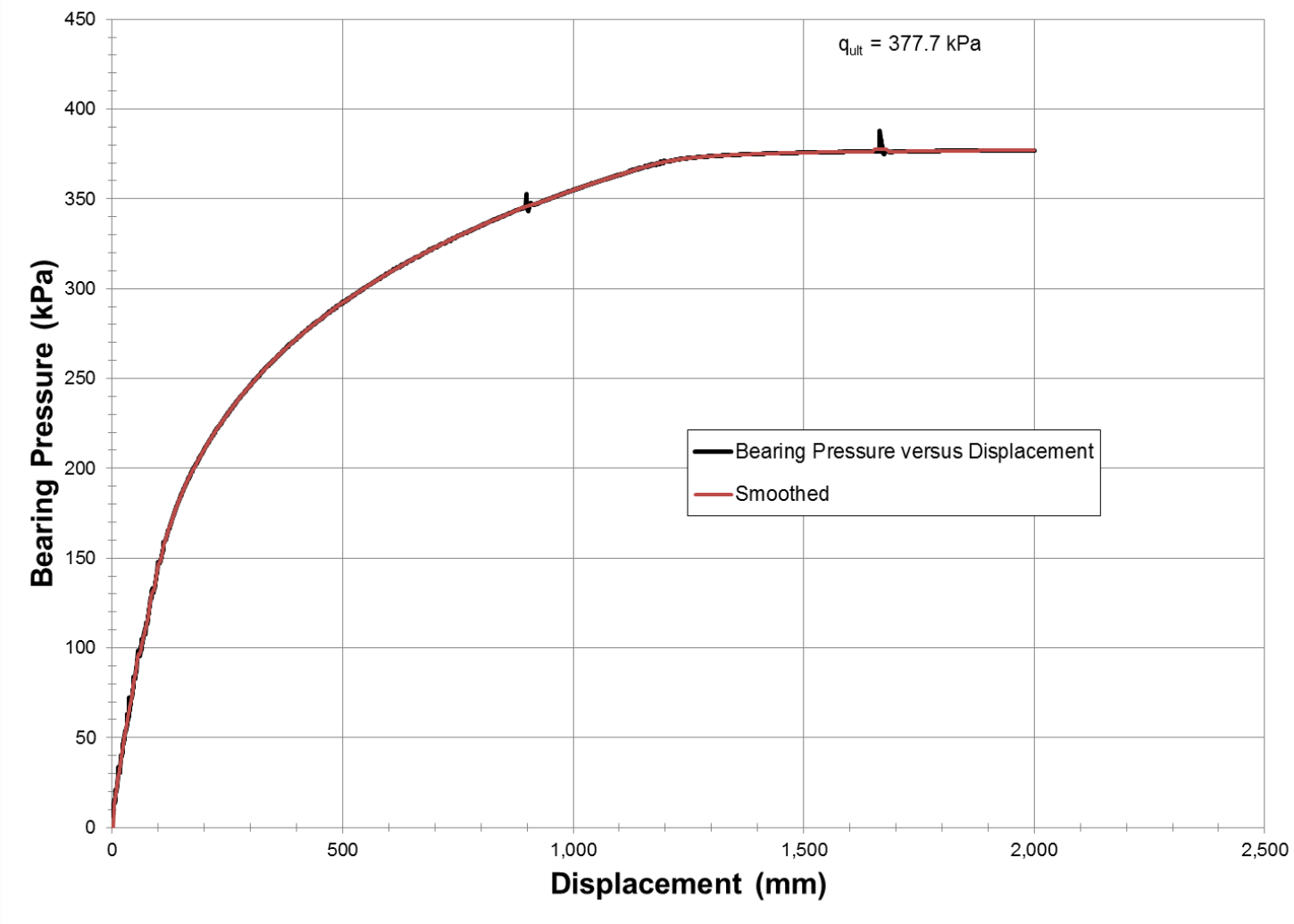


*Figure C-55: Bearing pressure versus displacement (single 4.51 m Long, 2.26 m wide trench in 40 kPa clay; 1 m embedment depth)*

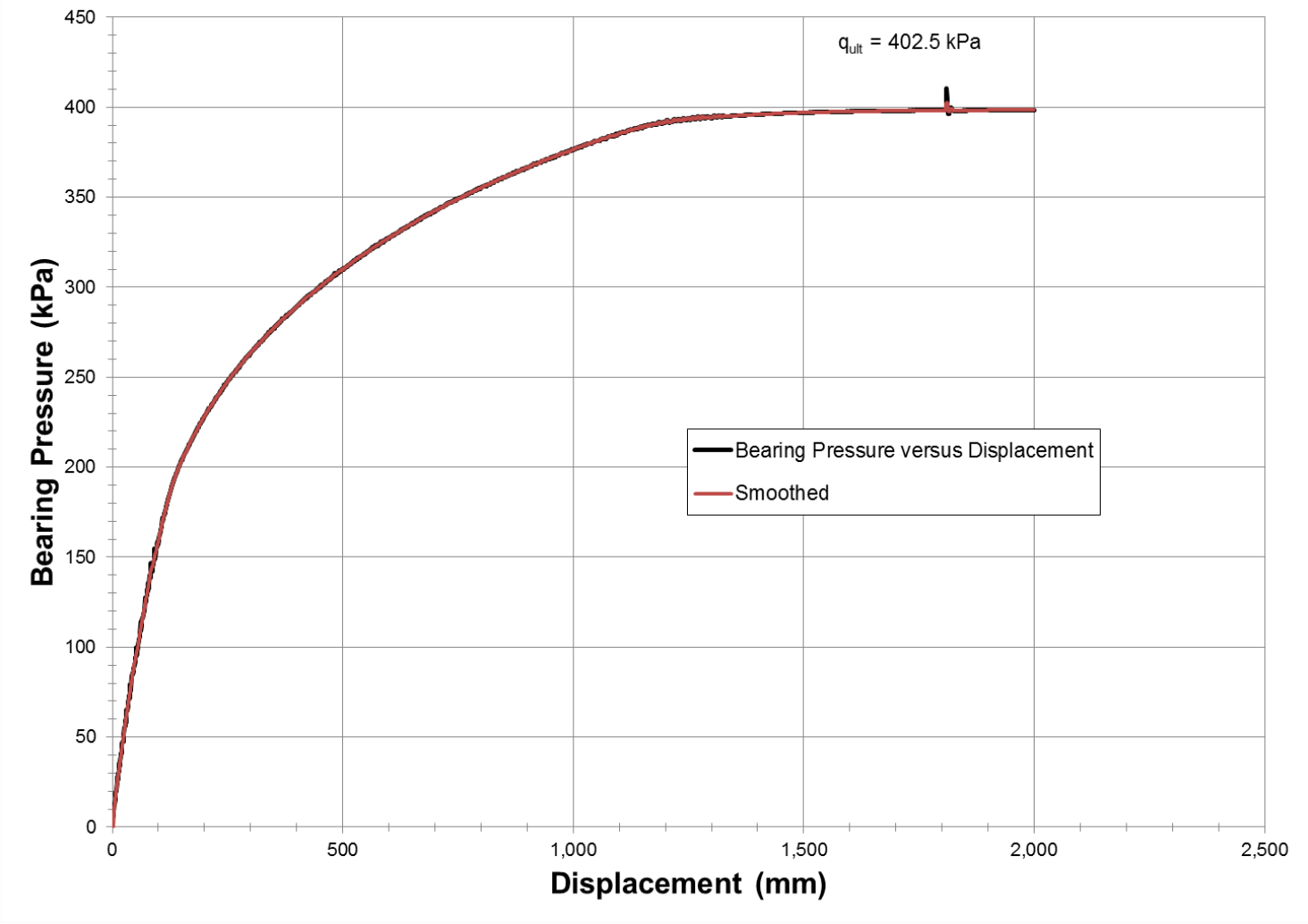


*Figure C-56: Bearing pressure versus displacement (single 4.51 m Long, 2.26 m wide trench in 40 kPa clay; 2 m embedment depth)*

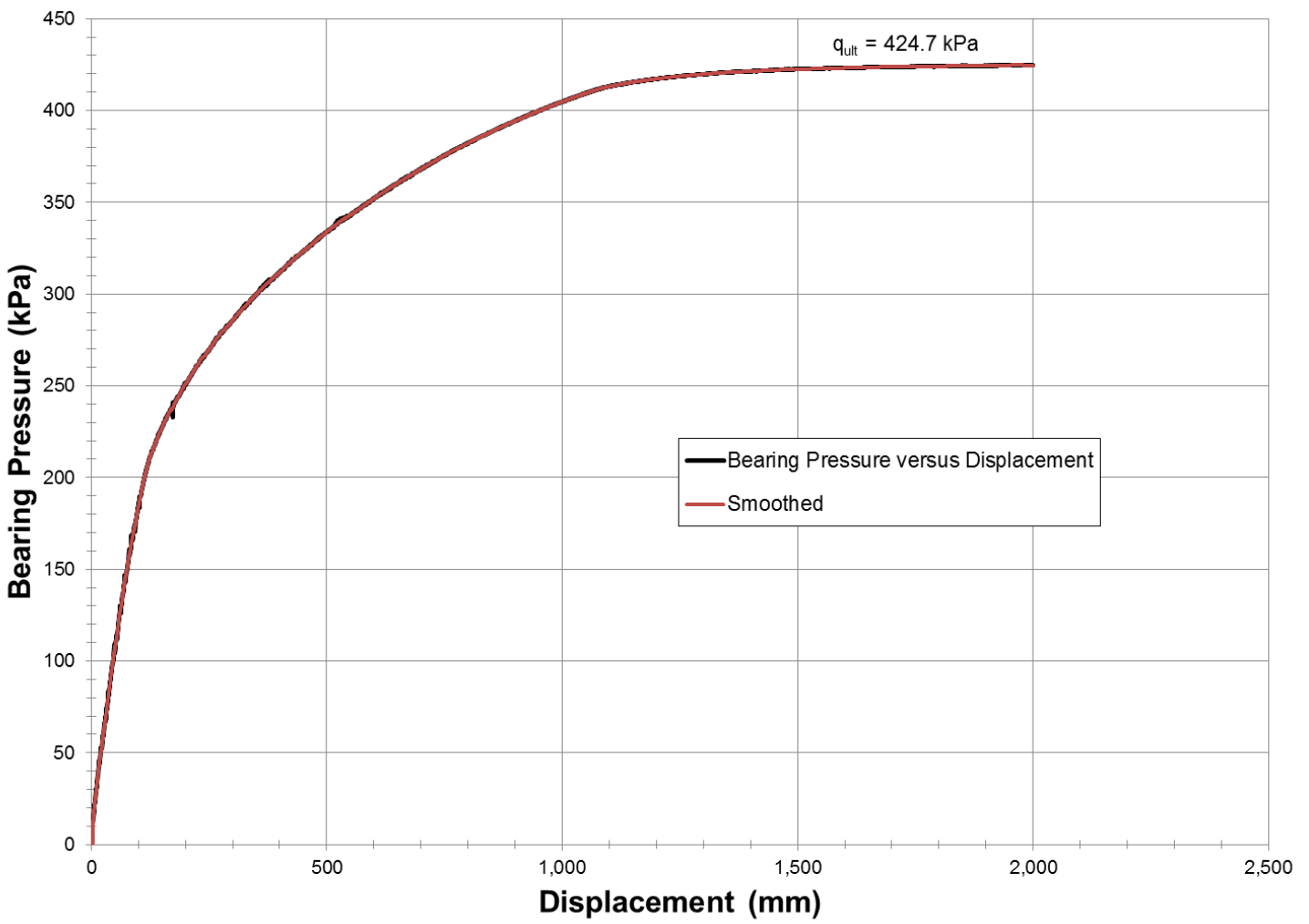


*Figure C-57: Bearing pressure versus displacement (single 4.51 m Long, 2.26 m wide trench in 40 kPa clay; 3 m embedment depth)*

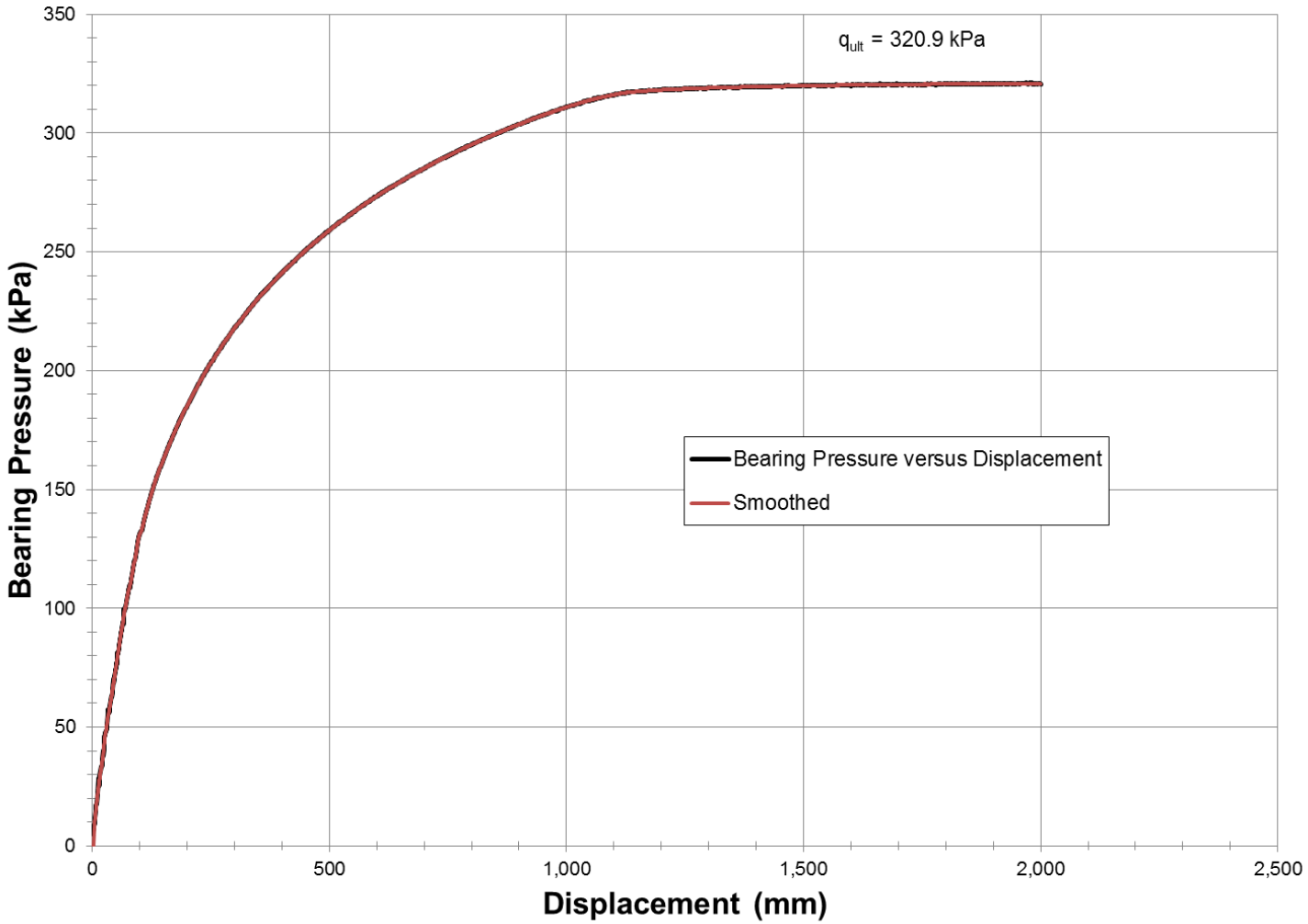


*Figure C-58: Bearing pressure versus displacement (single 4.5 m Long, 1.5 m wide trench in 40 kPa clay; no embedment depth)*

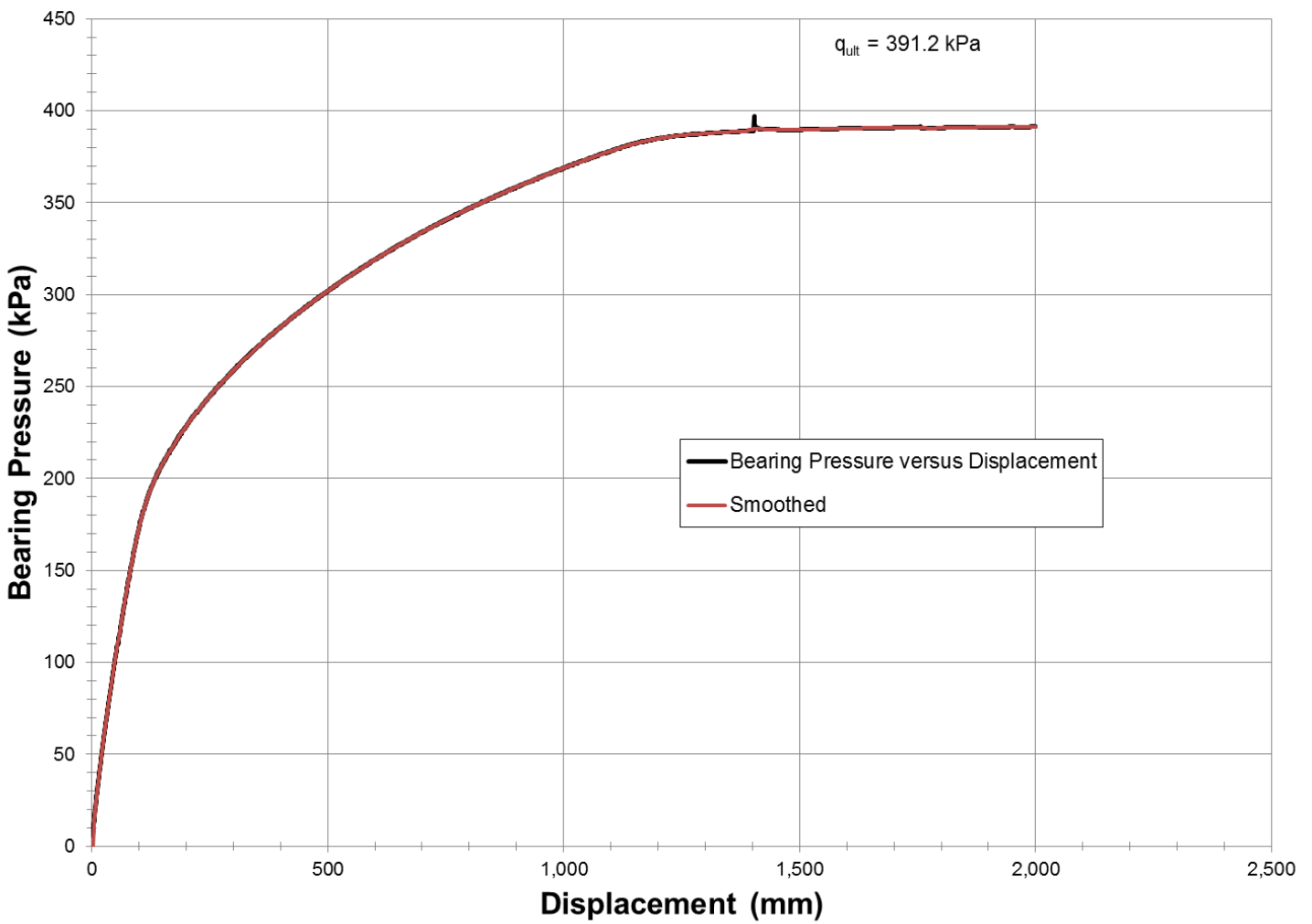


*Figure C-59: Bearing pressure versus displacement (single 4.5 m Long, 1.5 m wide trench in 40 kPa clay; 3 m embedment depth)*

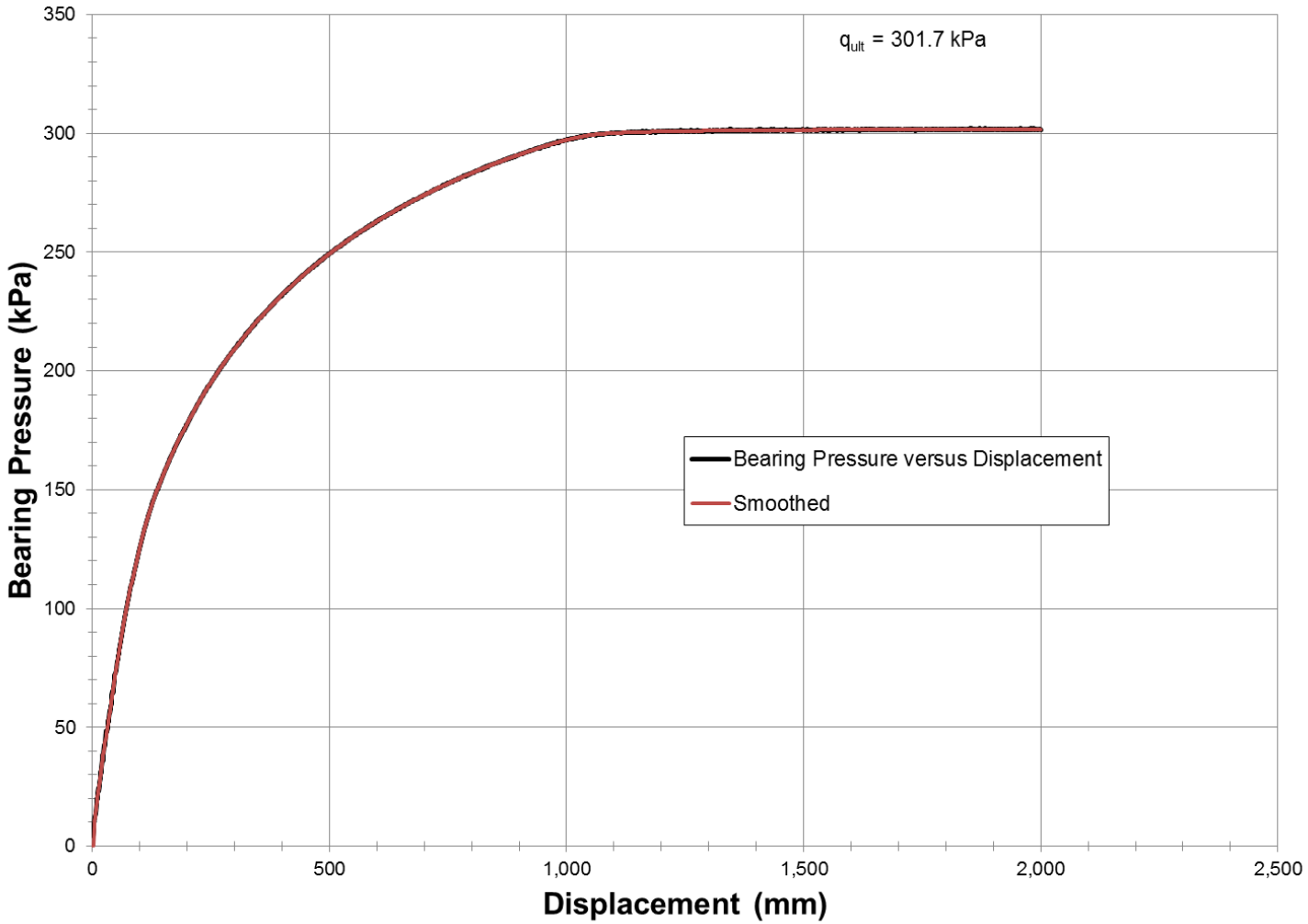


*Figure C-60: Bearing pressure versus displacement (single 4.5 m Long, .9 m wide trench in 40 kPa clay; no embedment depth)*

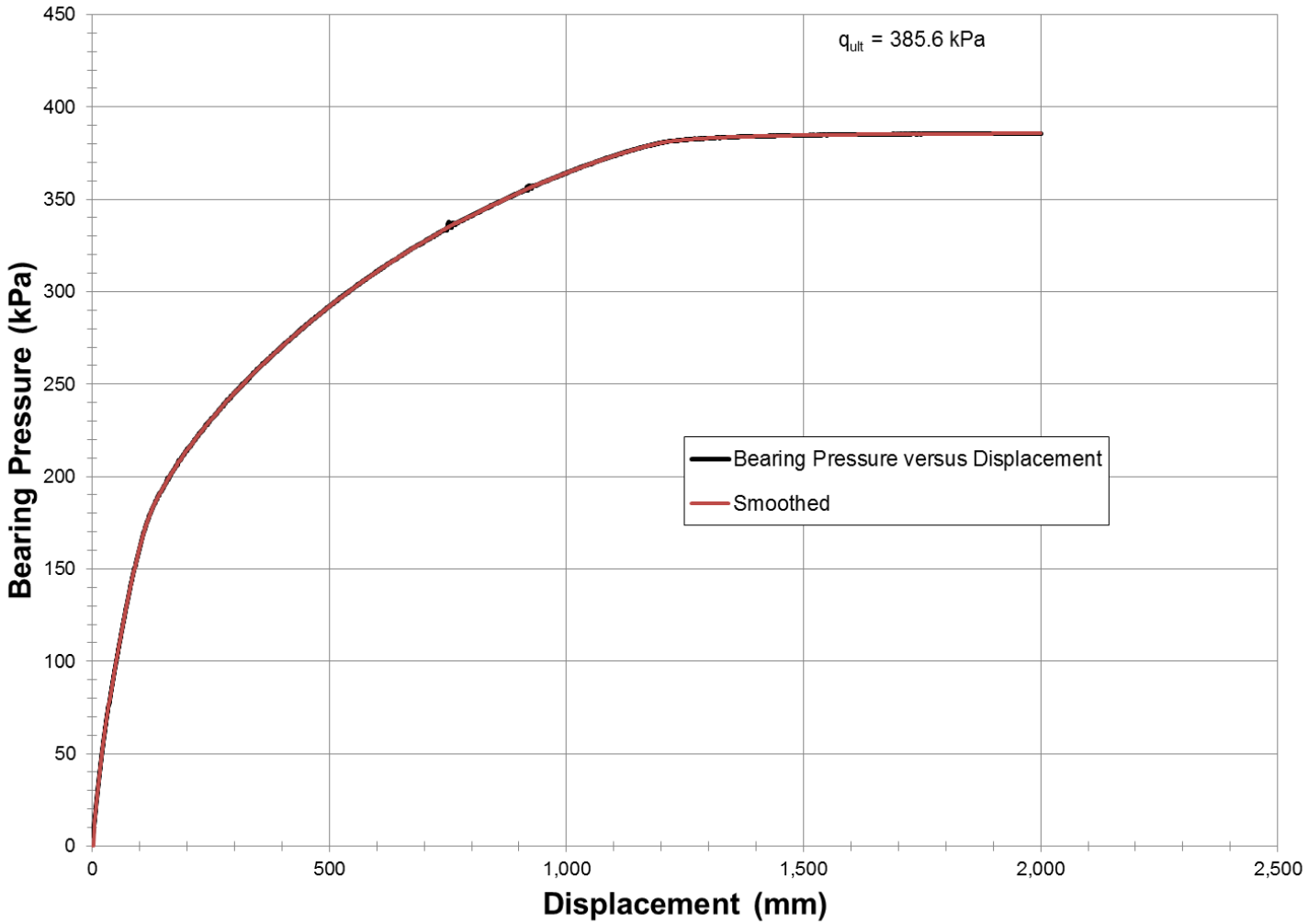


*Figure C-61: Bearing pressure versus displacement (single 4.5 m Long, .9 m wide trench in 40 kPa clay; 3 m embedment depth)*

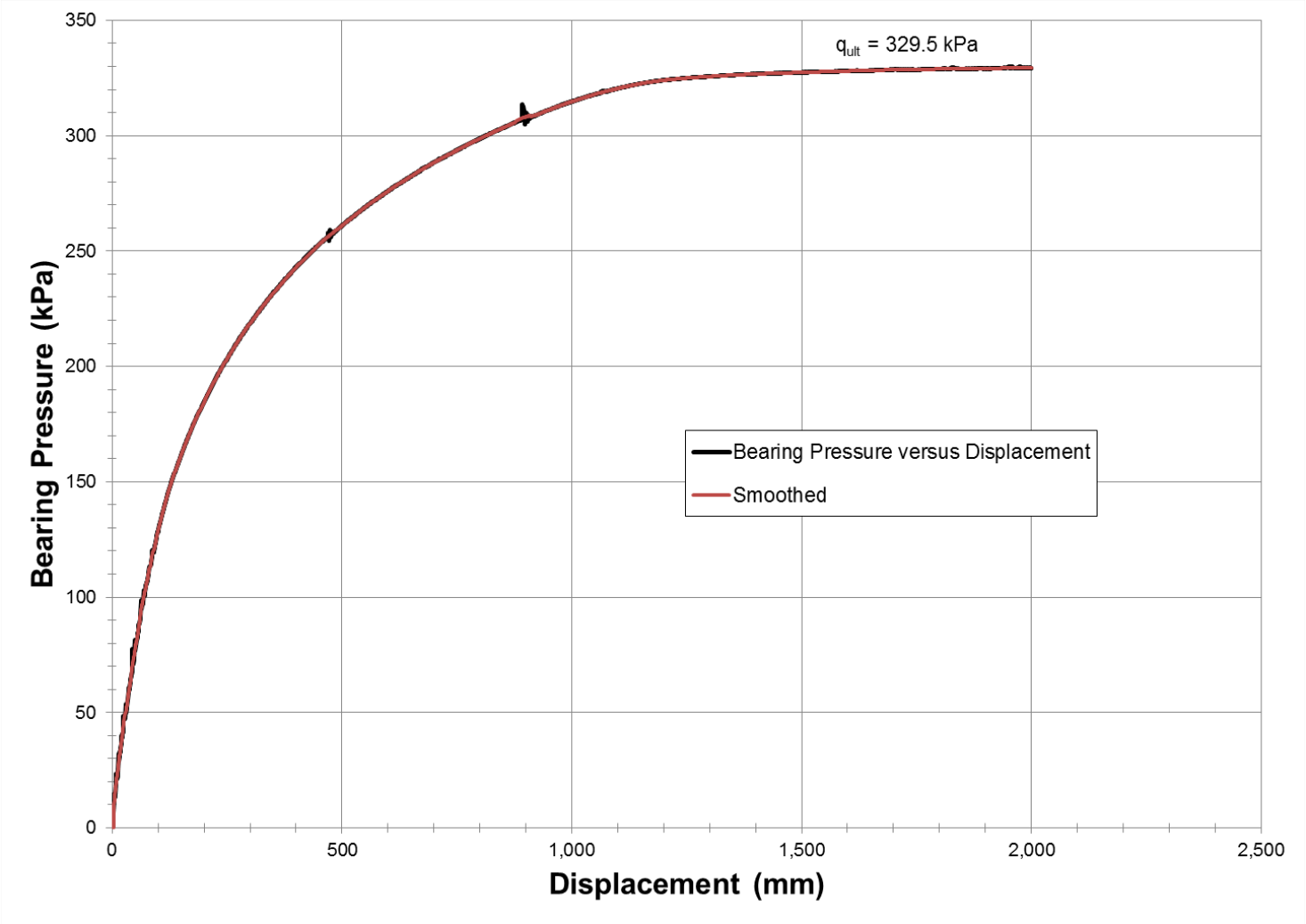


*Figure C-62: Bearing pressure versus displacement (single 4.5 m Long, 2 m wide trench in 40 kPa clay; no embedment depth)*

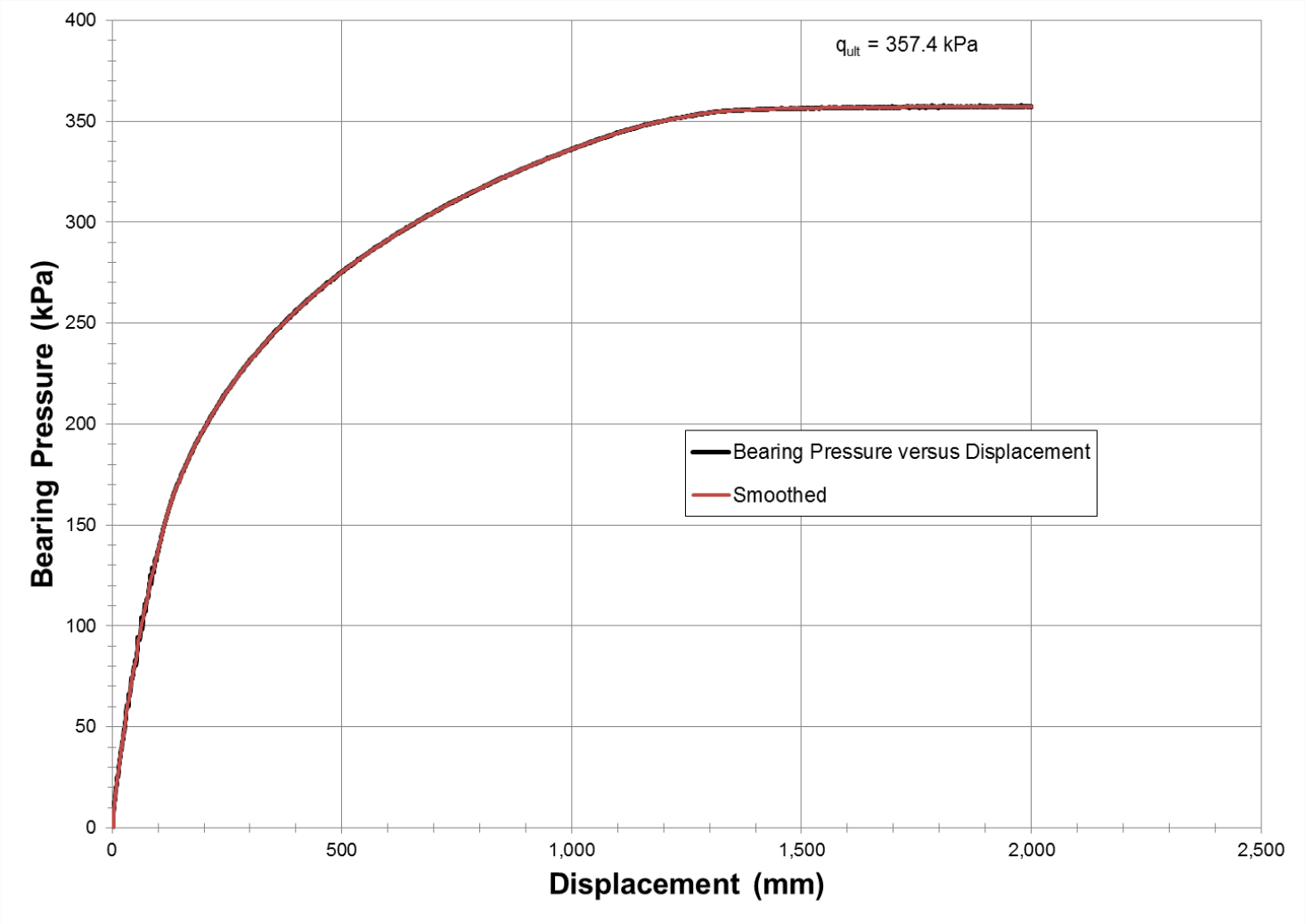


*Figure C-63: Bearing pressure versus displacement (single 4.5 m Long, 2 m wide trench in 40 kPa clay; 1 m embedment depth)*

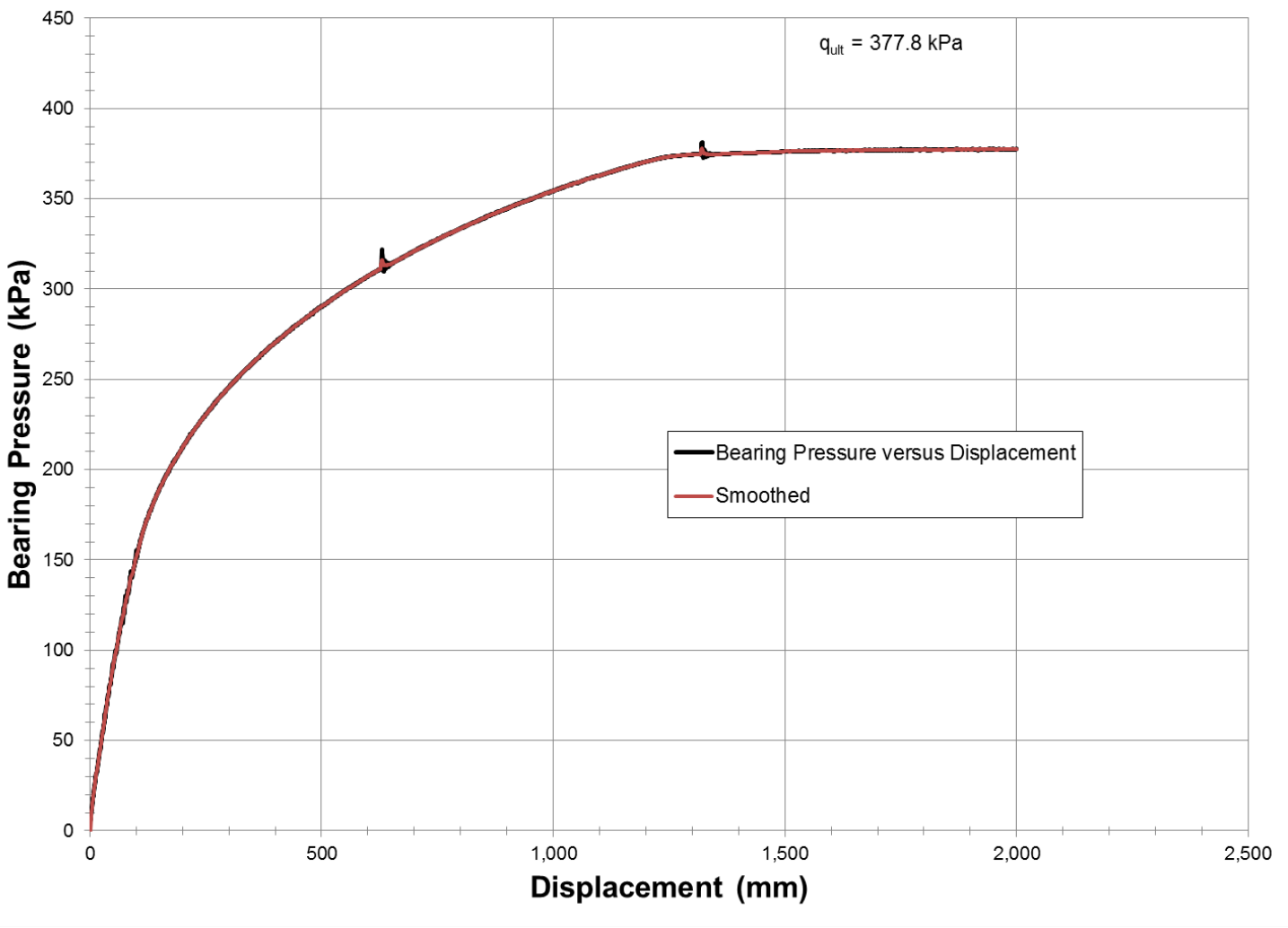


*Figure C-64: Bearing pressure versus displacement (single 4.5 m Long, 2 m wide trench in 40 kPa clay; 2 m embedment depth)*

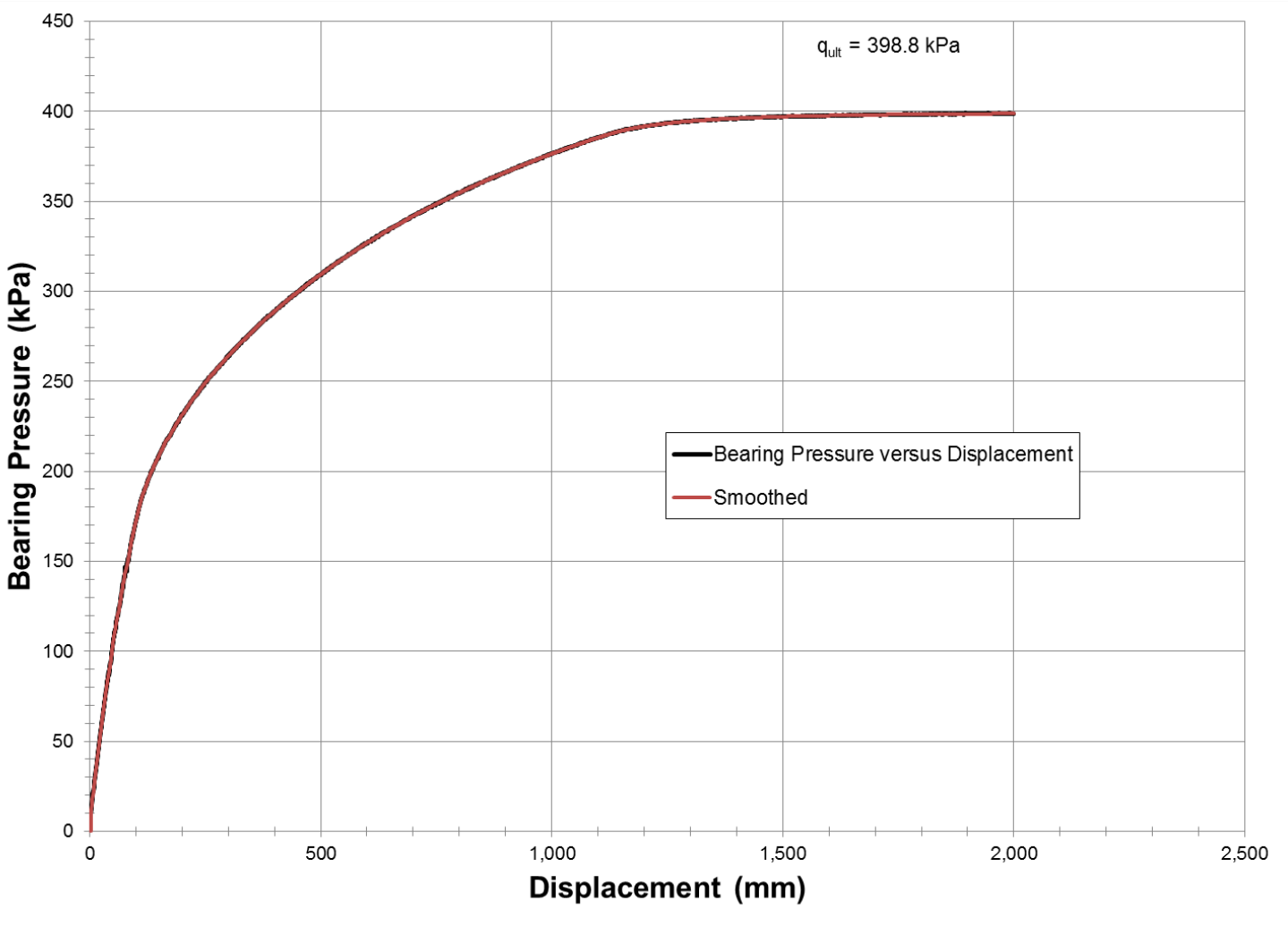


*Figure C-65: Bearing pressure versus displacement (single 4.5 m Long, 2 m wide trench in 40 kPa clay; 3 m embedment depth)*

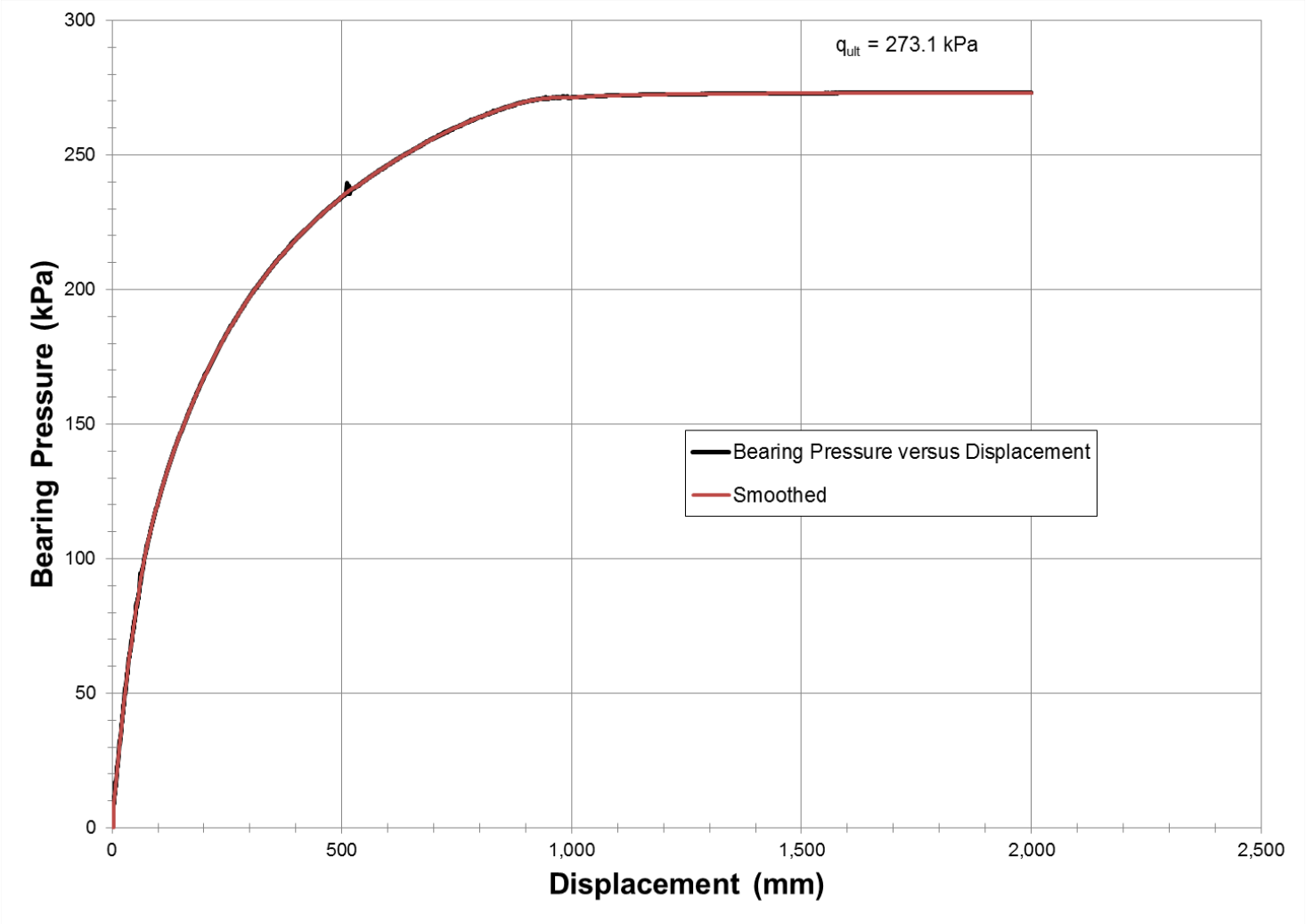


*Figure C-66: Bearing pressure versus displacement (single 3 m Long, 1.5 m wide trench in 40 kPa clay; no embedment depth)*

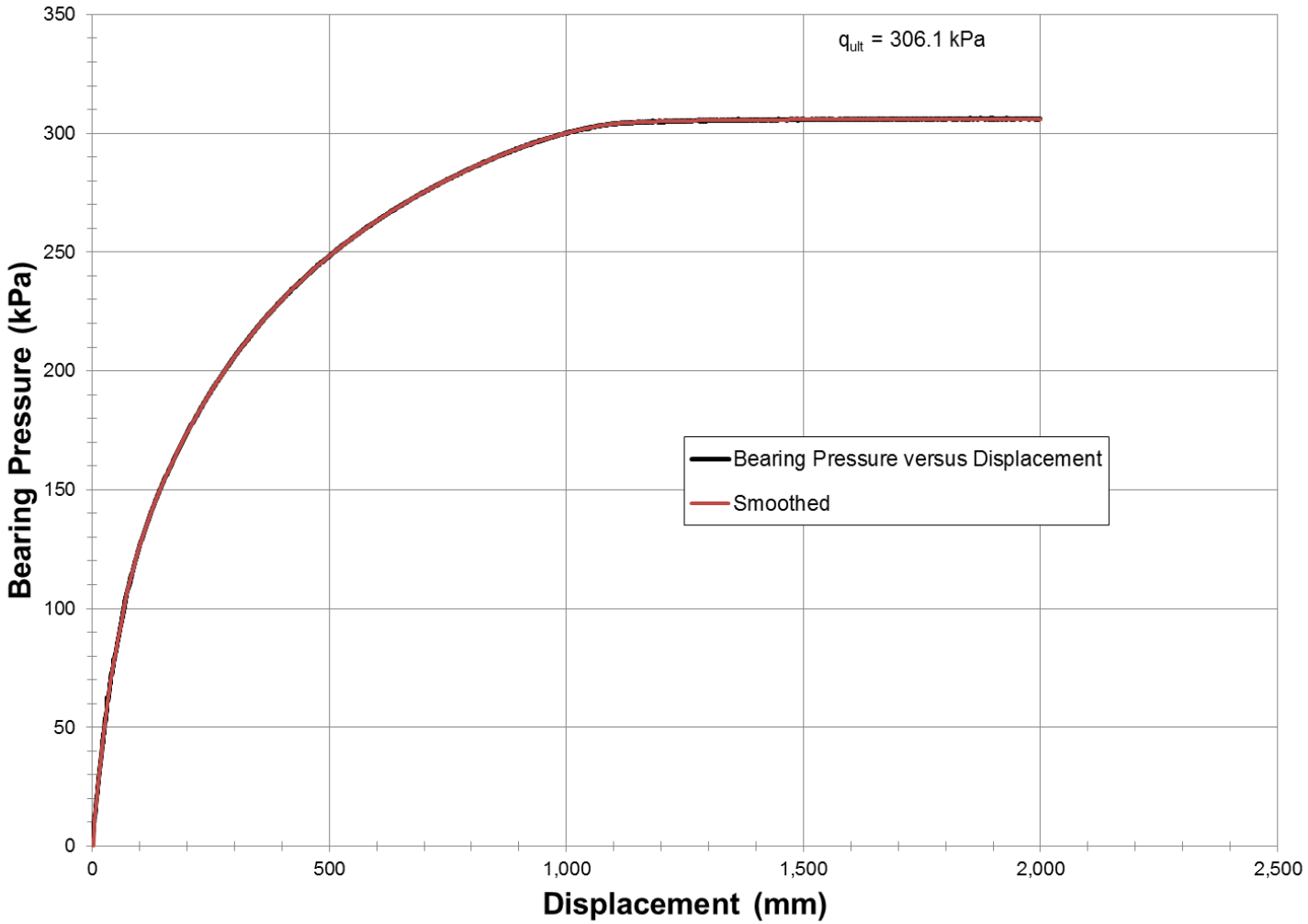


*Figure C-67: Bearing pressure versus displacement (single 3 m Long, 1.5 m wide trench in 40 kPa clay; 1 m embedment depth)*

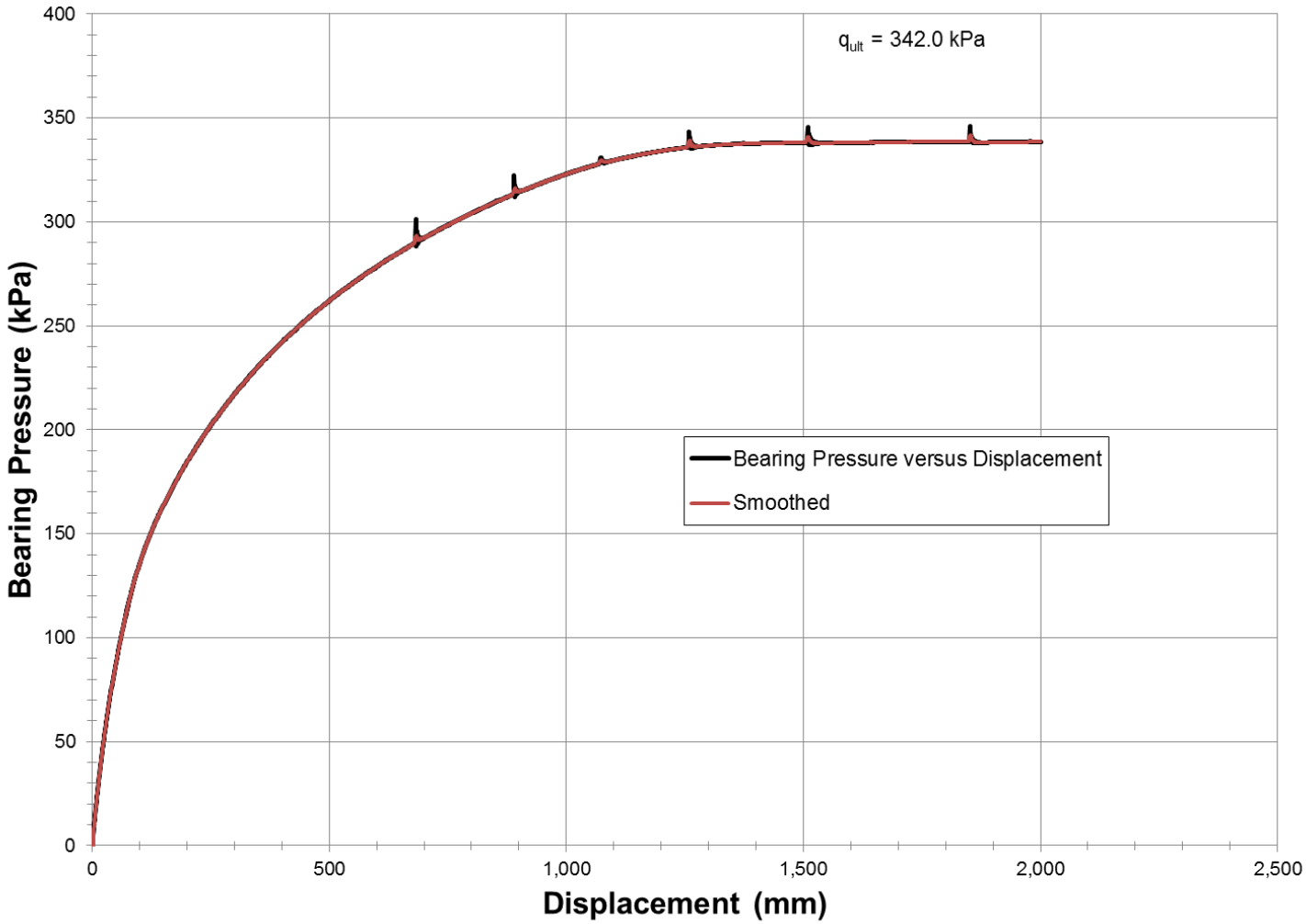


*Figure C-68: Bearing pressure versus displacement (single 3 m Long, 1.5 m wide trench in 40 kPa clay; 2 m embedment depth)*

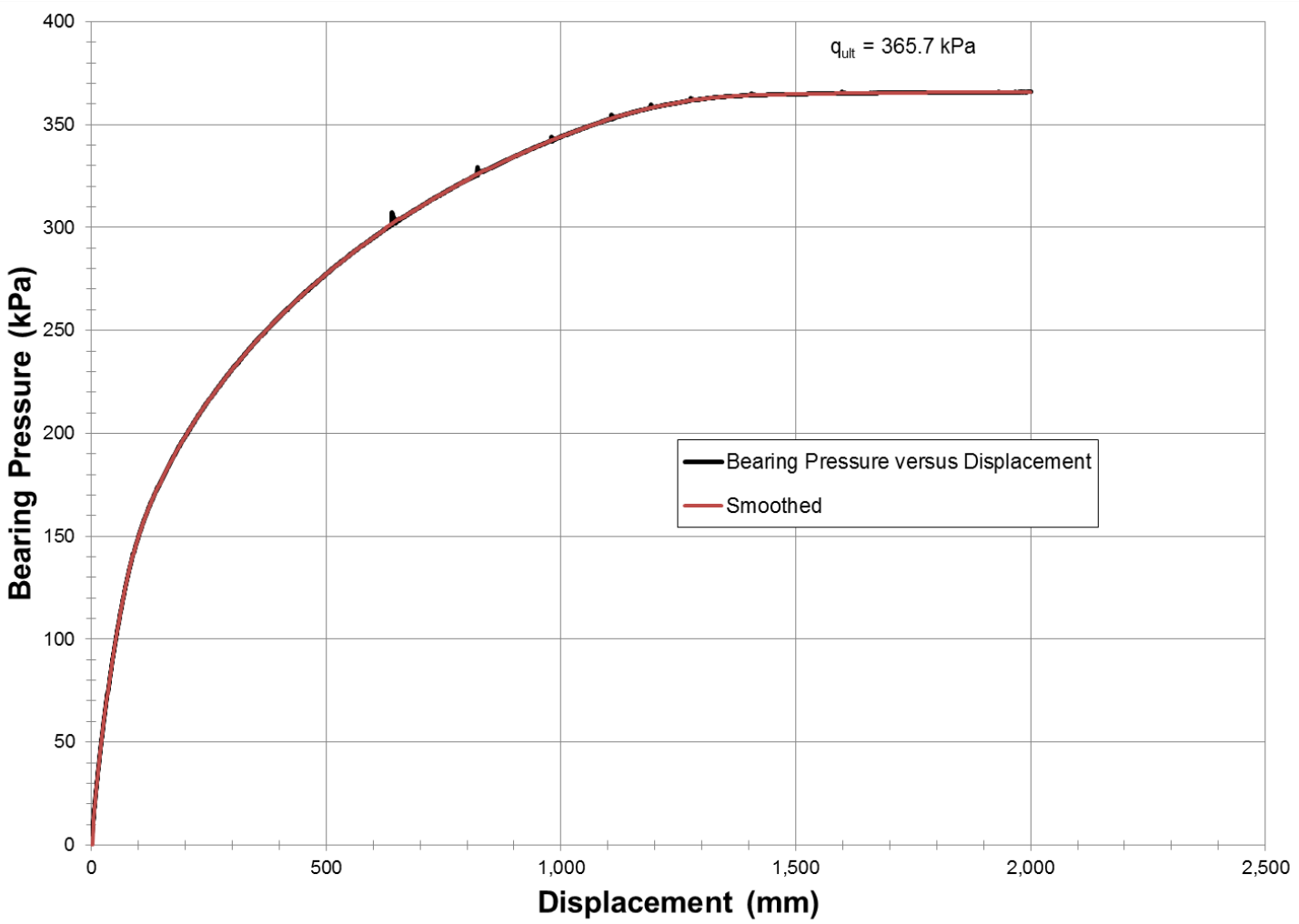


*Figure C-69: Bearing pressure versus displacement (single 3 m Long, 1.5 m wide trench in 40 kPa clay; 3 m embedment depth)*

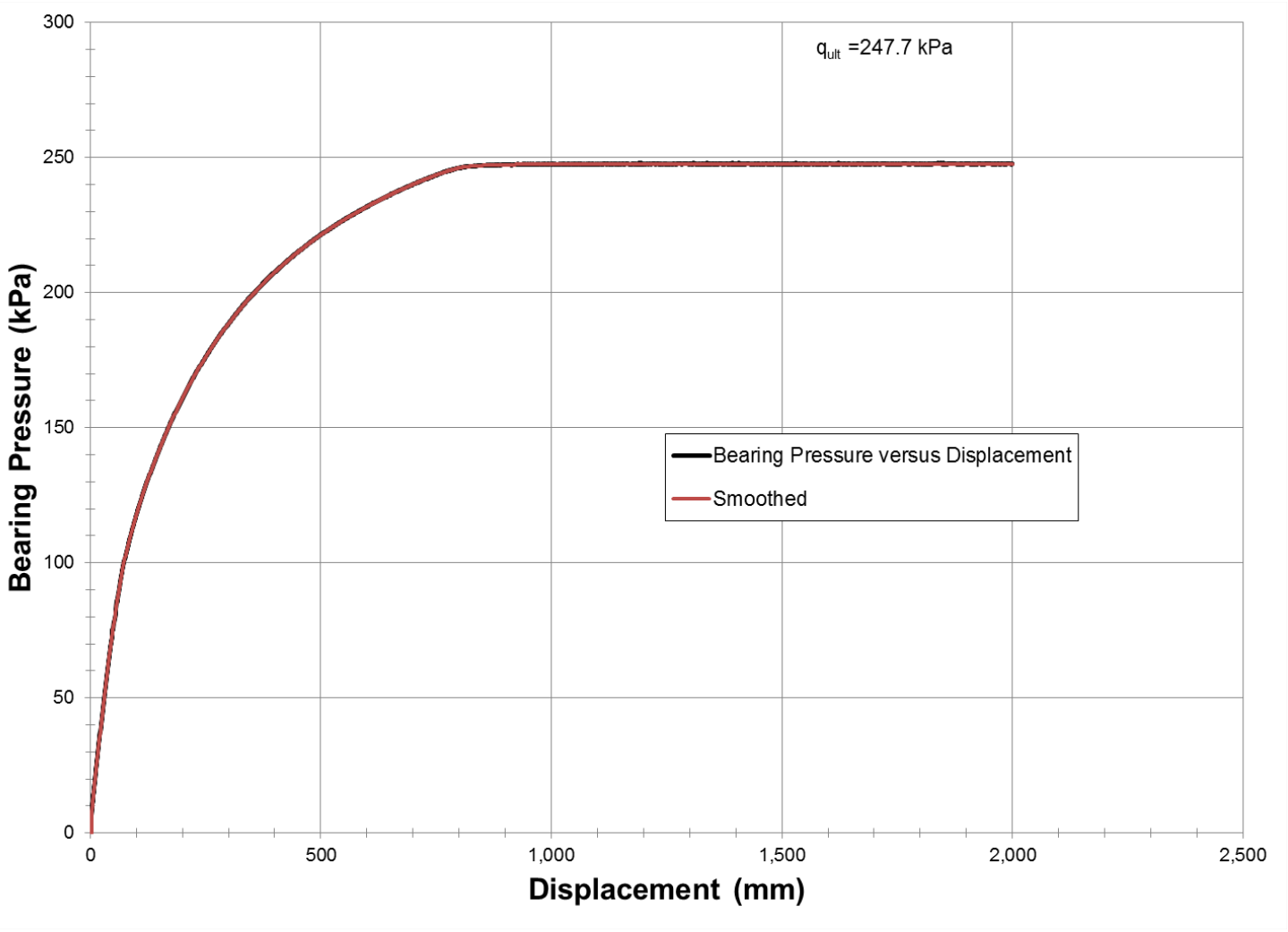


*Figure C-70: Bearing pressure versus displacement (single 3 m Long, 0.6 m wide trench in 40 kPa clay; no embedment depth)*

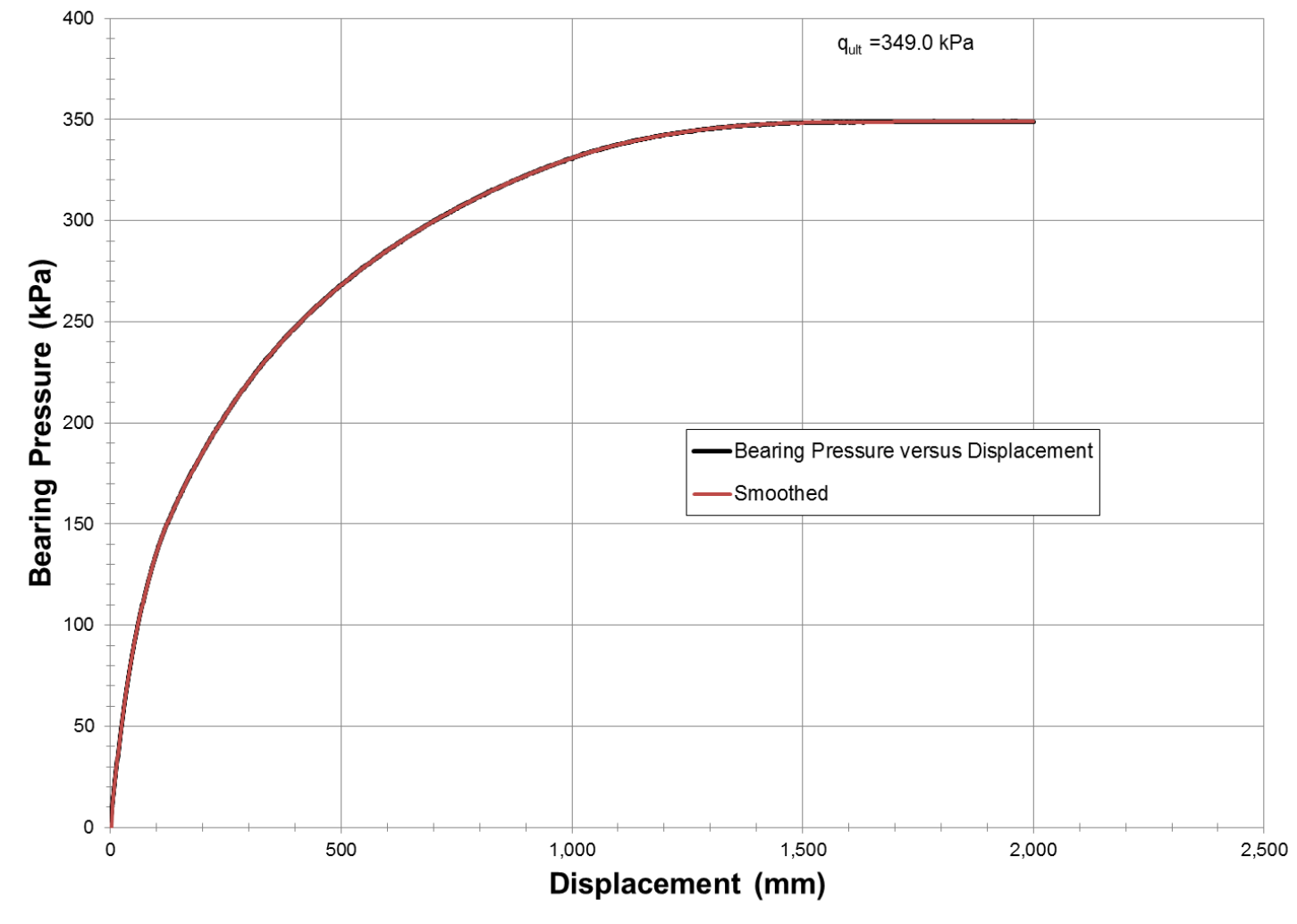


*Figure C-71: Bearing pressure versus displacement (single 3 m Long, 0.6 m wide trench in 40 kPa clay; 3 m embedment depth)*

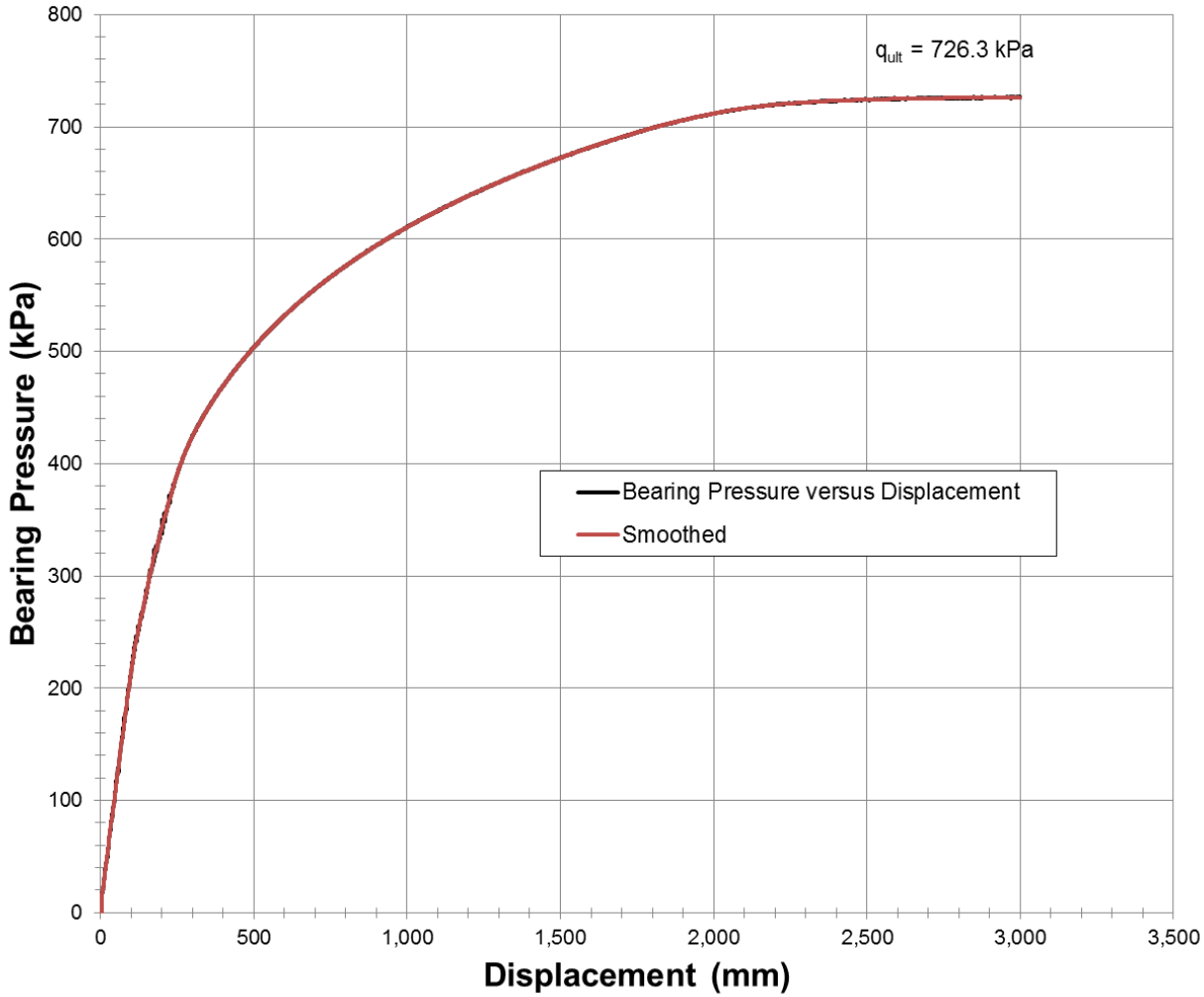


*Figure C-72: Bearing pressure versus displacement (single 6 m Long, 1.5 m wide trench in 80 kPa clay; no embedment depth)*

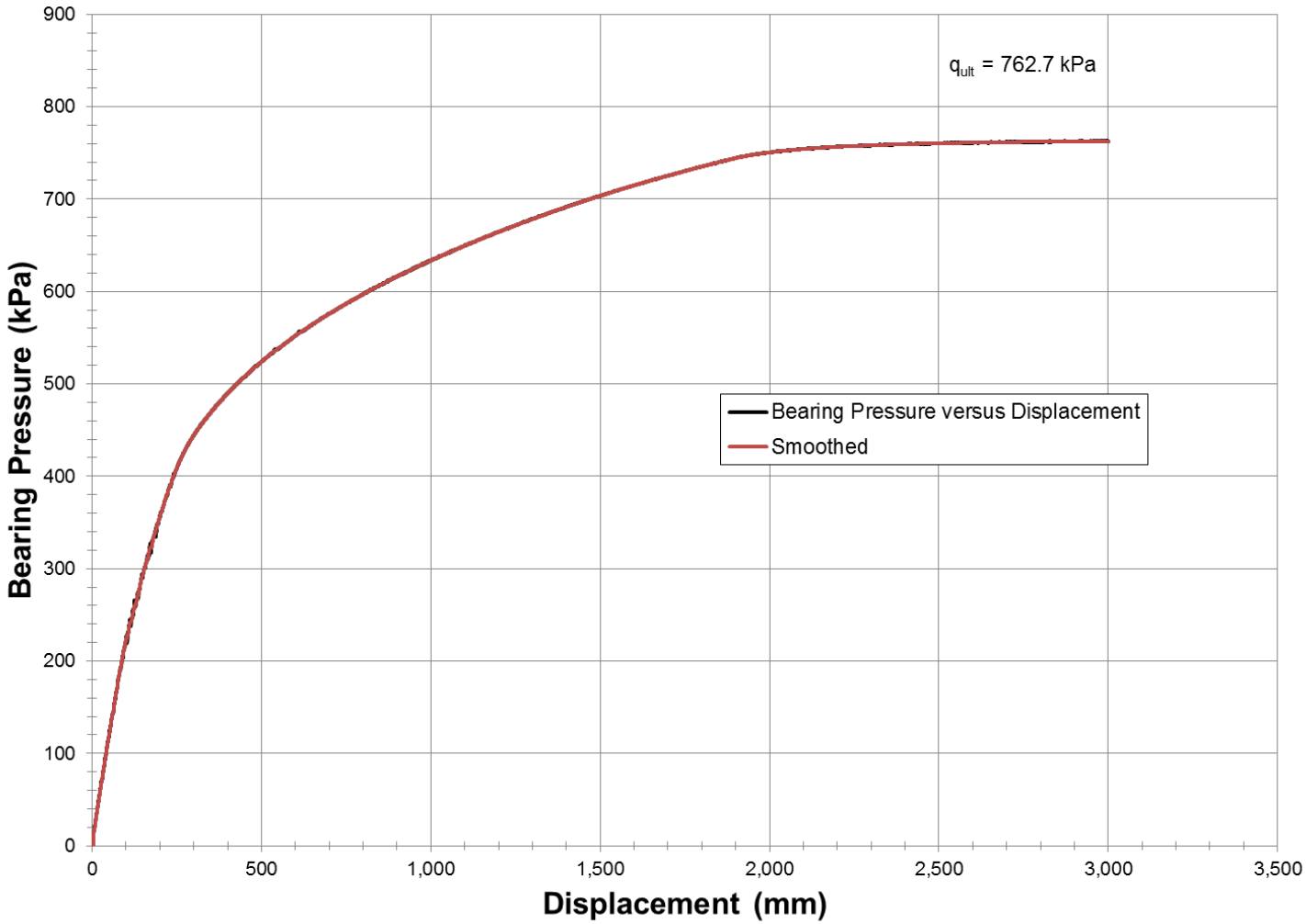


*Figure C-73: Bearing pressure versus displacement (single 6 m Long, 1.5 m wide trench in 80 kPa clay; 1.5 m embedment depth)*

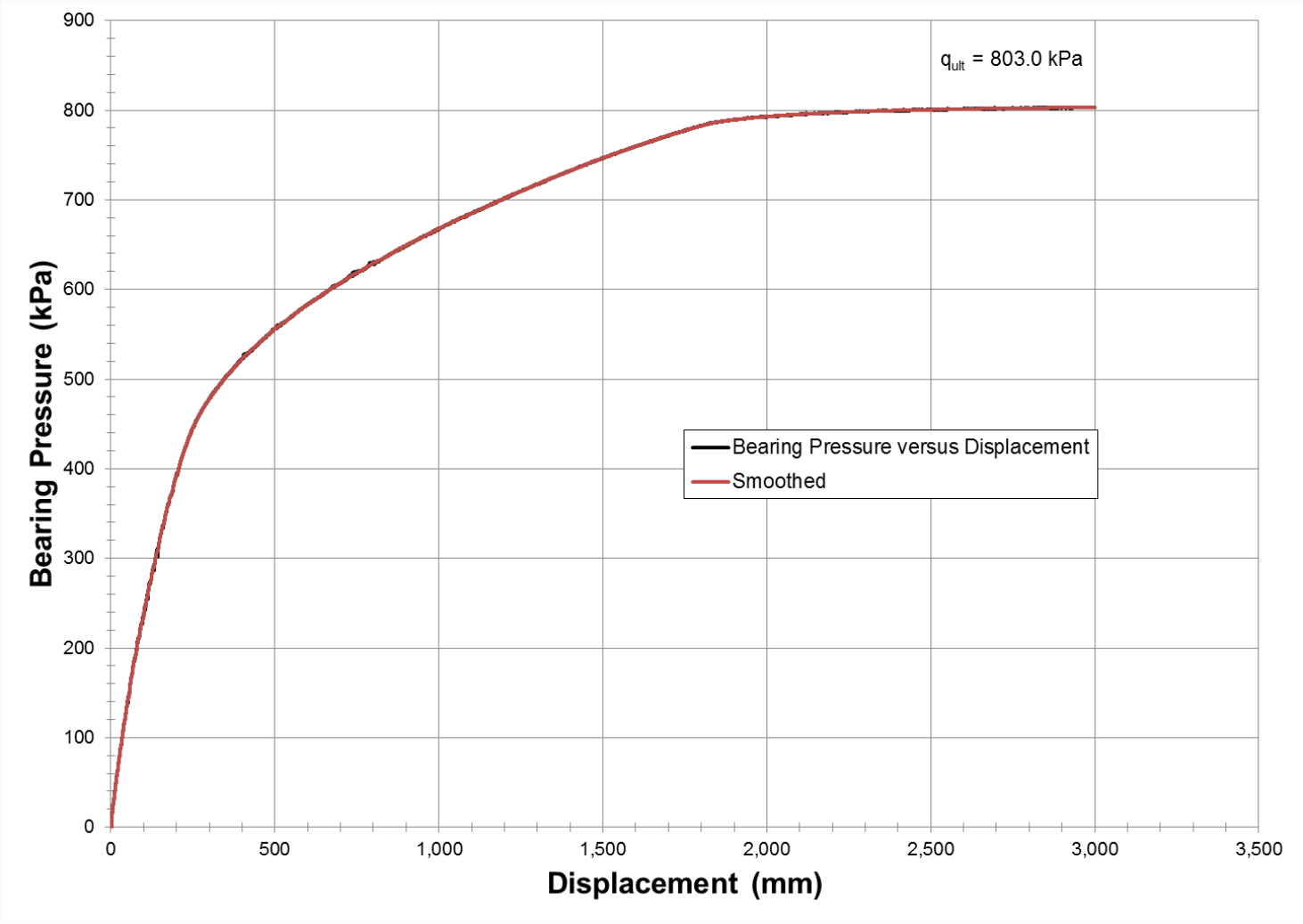


*Figure C-74: Bearing pressure versus displacement (single 6 m Long, 1.5 m wide trench in 80 kPa clay; 3 m embedment depth)*

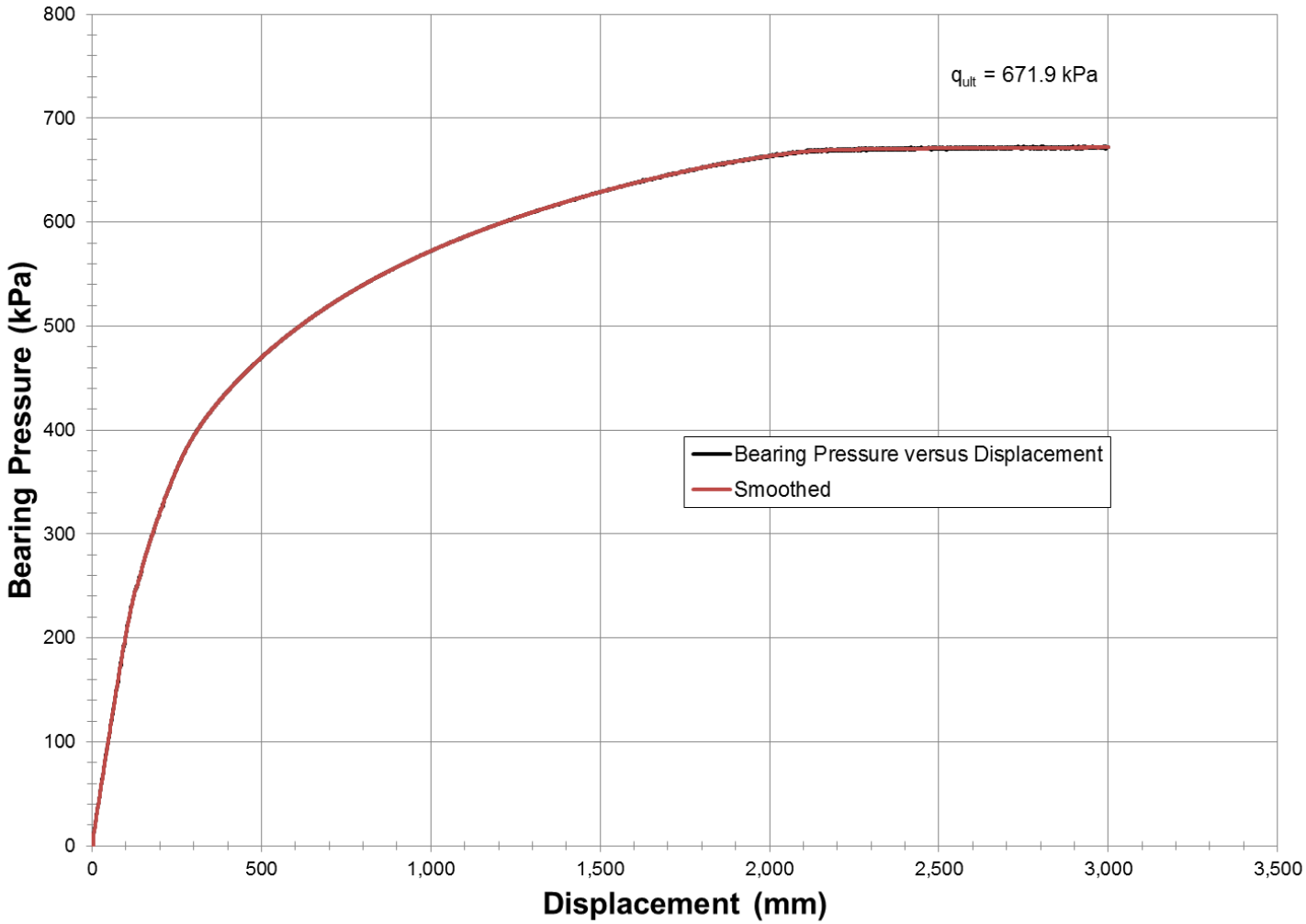


*Figure C-75: Bearing pressure versus displacement (single 6 m Long, 0.9 m wide trench in 80 kPa clay; no embedment depth)*

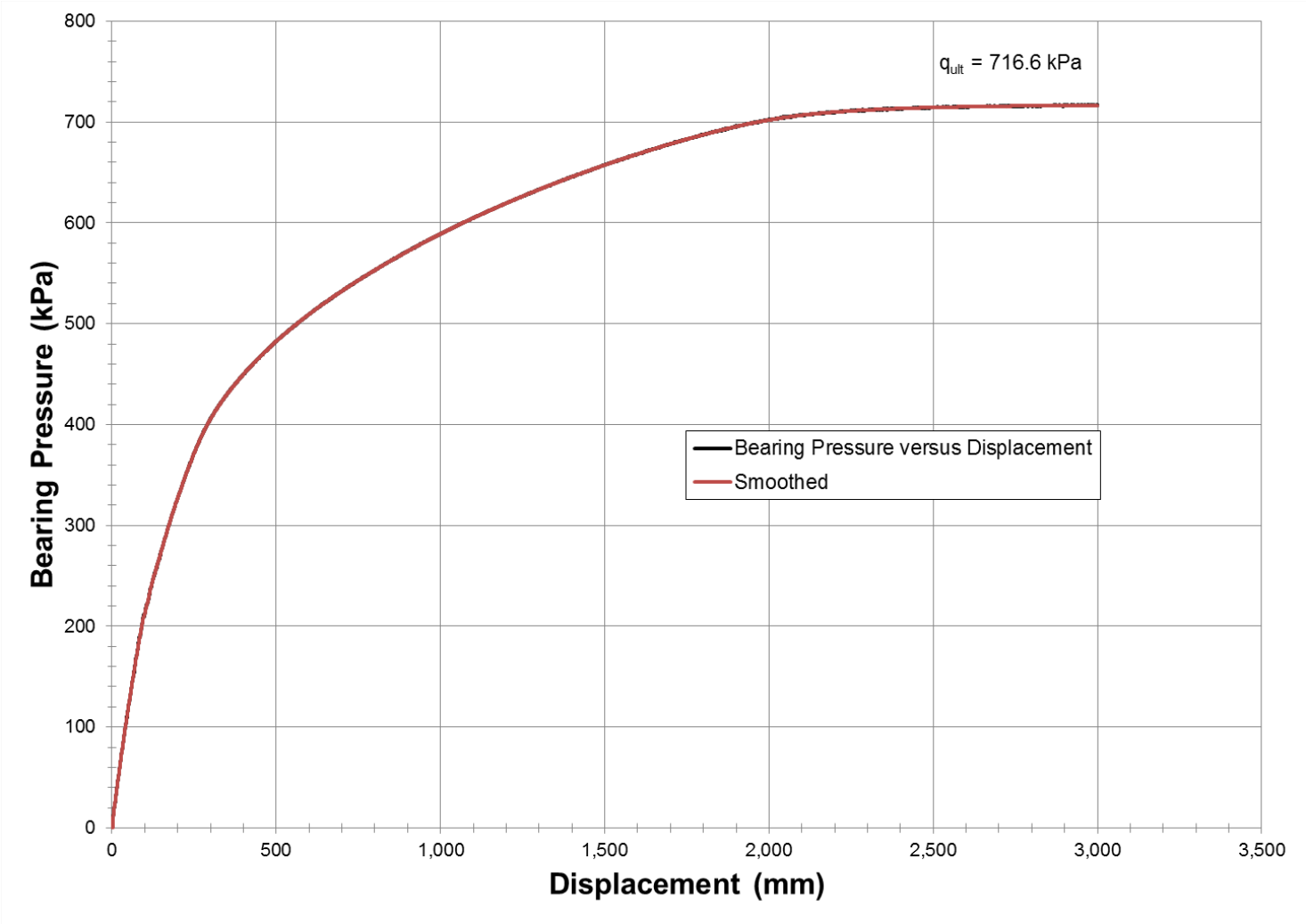


*Figure C-76: Bearing pressure versus displacement (single 6 m Long, 0.9 m wide trench in 80 kPa clay; 1.5 m embedment depth)*

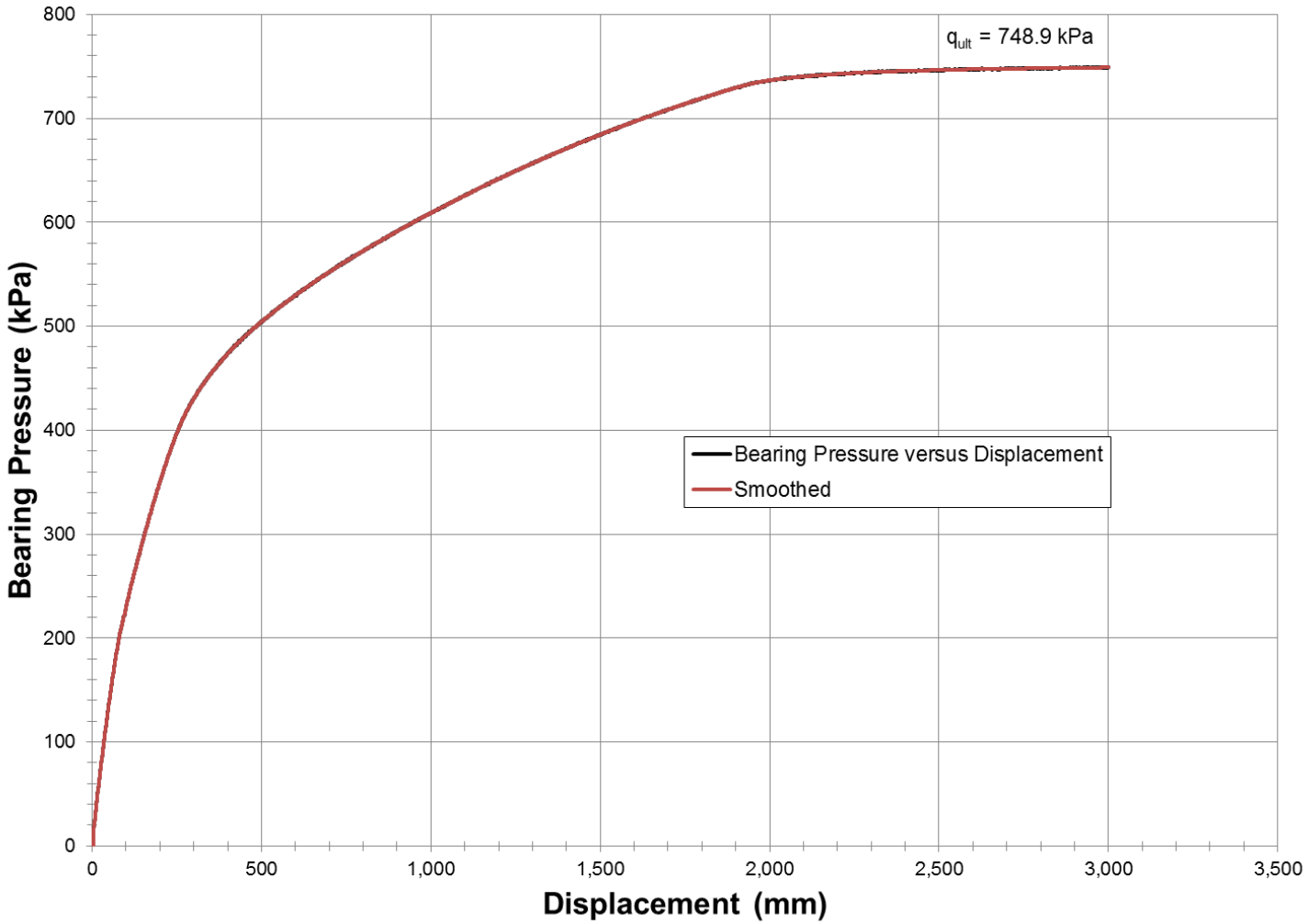


*Figure C-77: Bearing pressure versus displacement (single 6 m Long, 0.9 m wide trench in 80 kPa clay; 3 m embedment depth)*

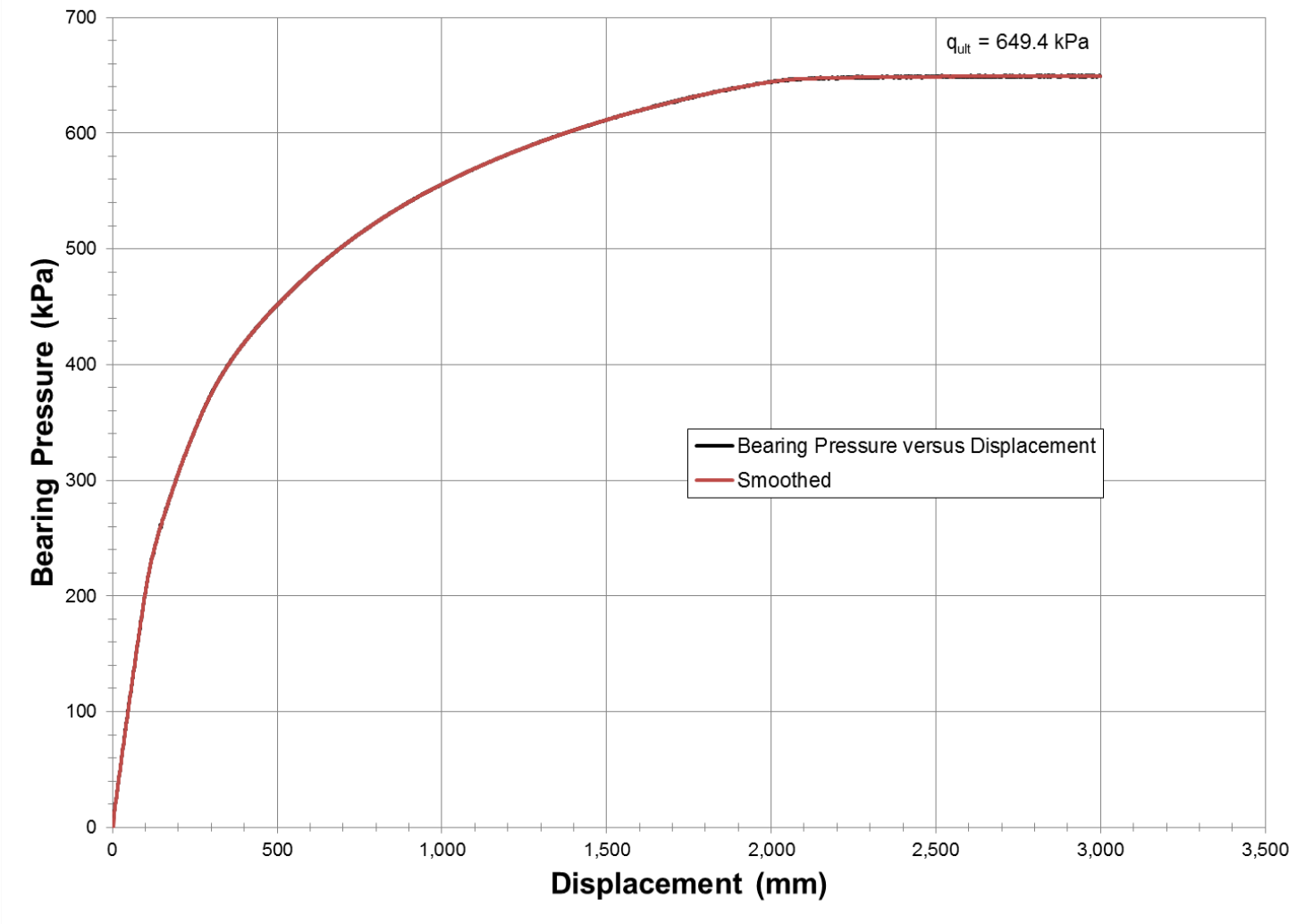


*Figure C-78: Bearing pressure versus displacement (single 6 m Long, 0.6 m wide trench in 80 kPa clay; no embedment depth)*

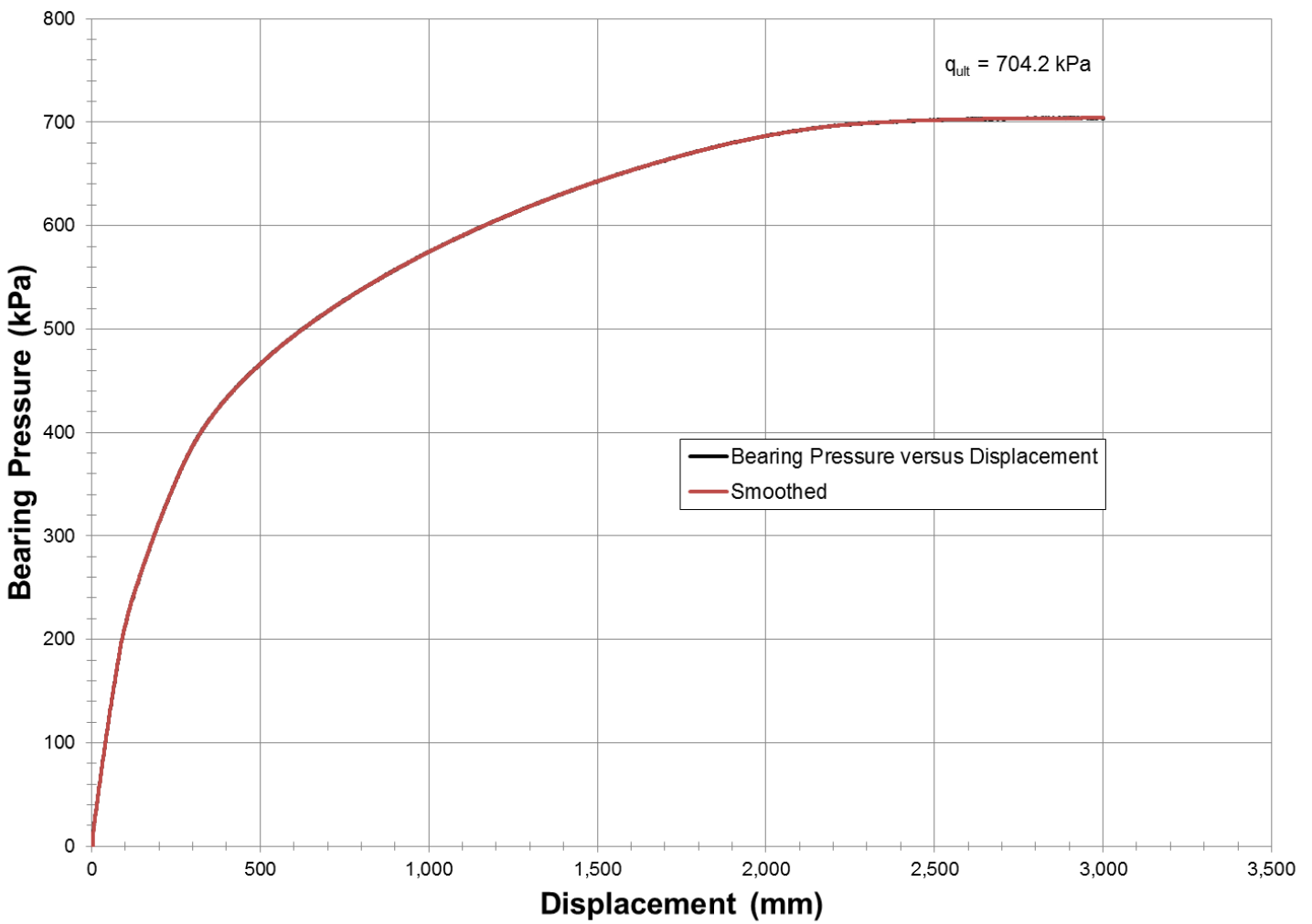


*Figure C-79: Bearing pressure versus displacement (single 6 m Long, 0.6 m wide trench in 80 kPa clay; 1.5 m embedment depth)*

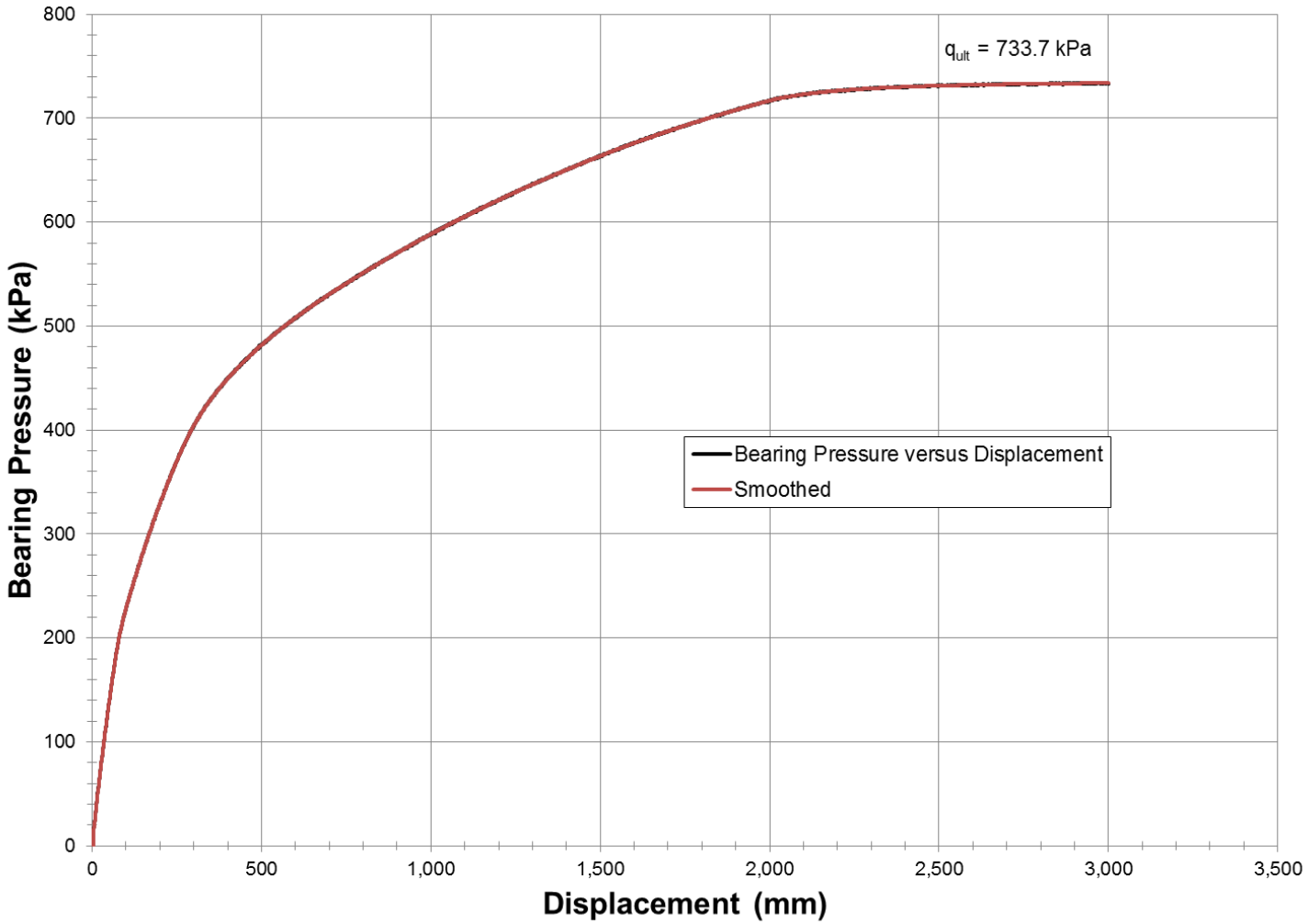


*Figure C-80: Bearing pressure versus displacement (single 6 m Long, 0.6 m wide trench in 80 kPa clay; 3 m embedment depth)*

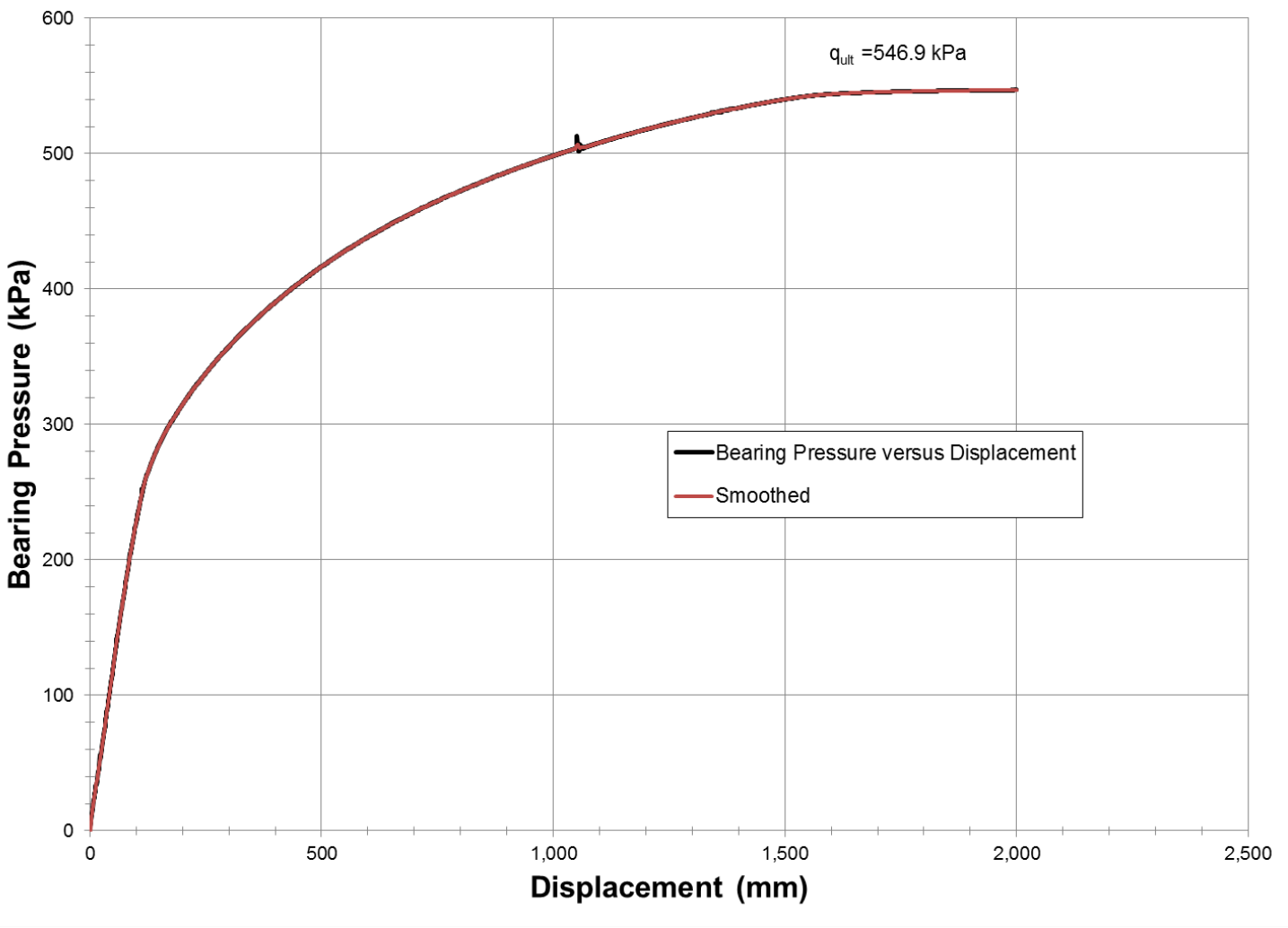


*Figure C-81: Bearing pressure versus displacement (single 3 m Long, 1.5 m wide trench in 80 kPa clay; no embedment depth)*

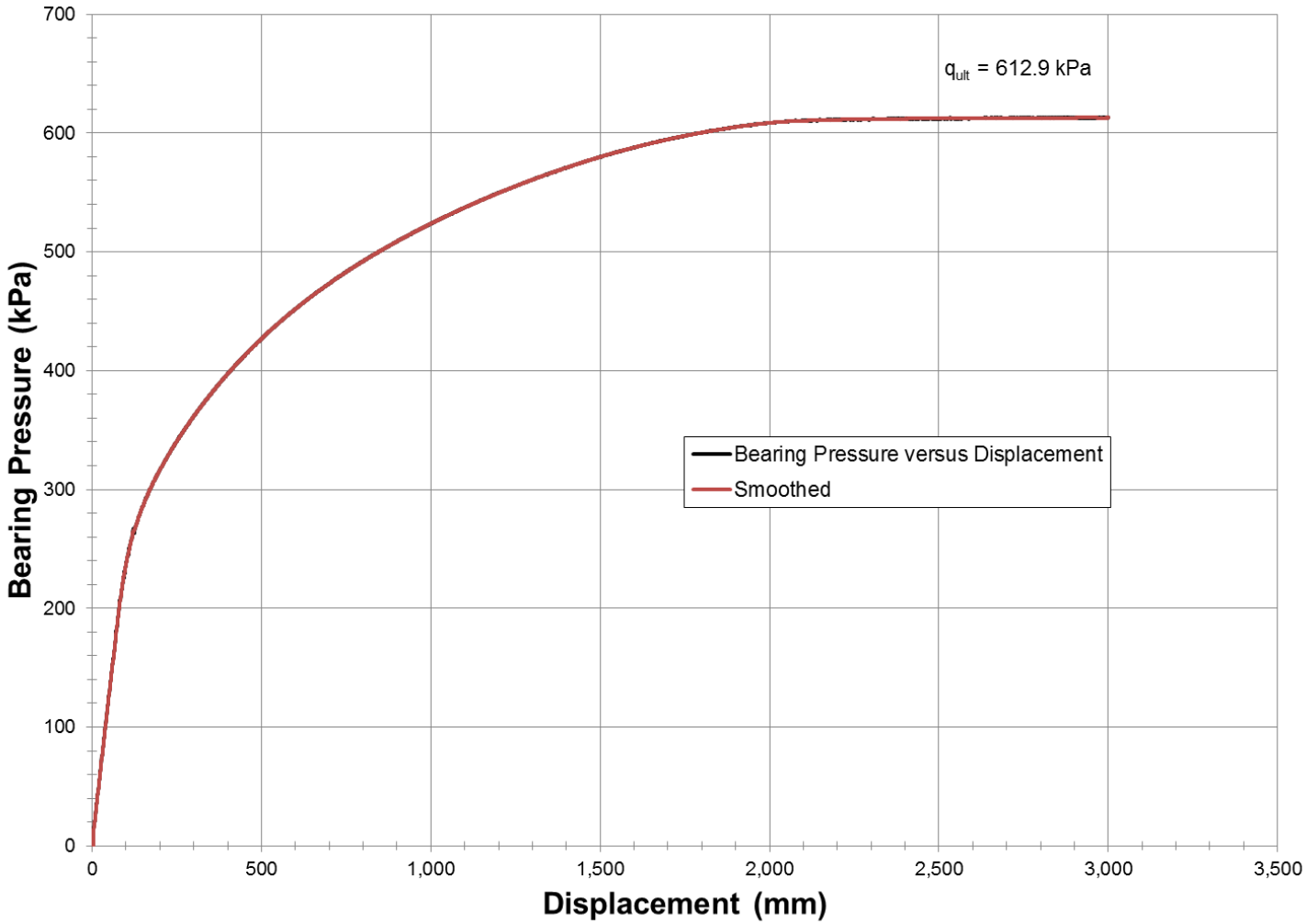


*Figure C-82: Bearing pressure versus displacement (single 3 m Long, 1.5 m wide trench in 80 kPa clay; 1.5 m embedment depth)*

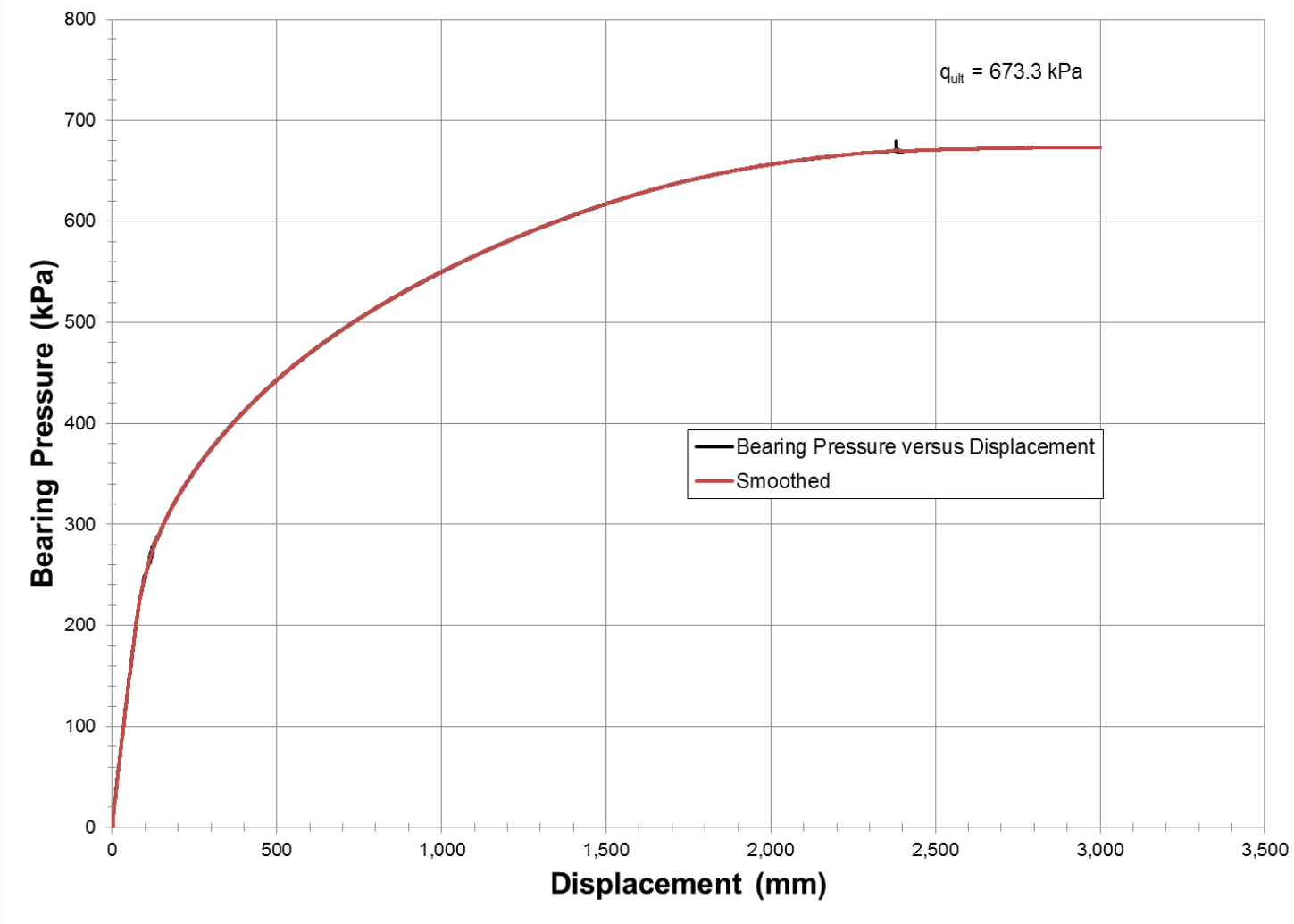


*Figure C-83: Bearing pressure versus displacement (single 3 m Long, 1.5 m wide trench in 80 kPa clay; 3 m embedment depth)*

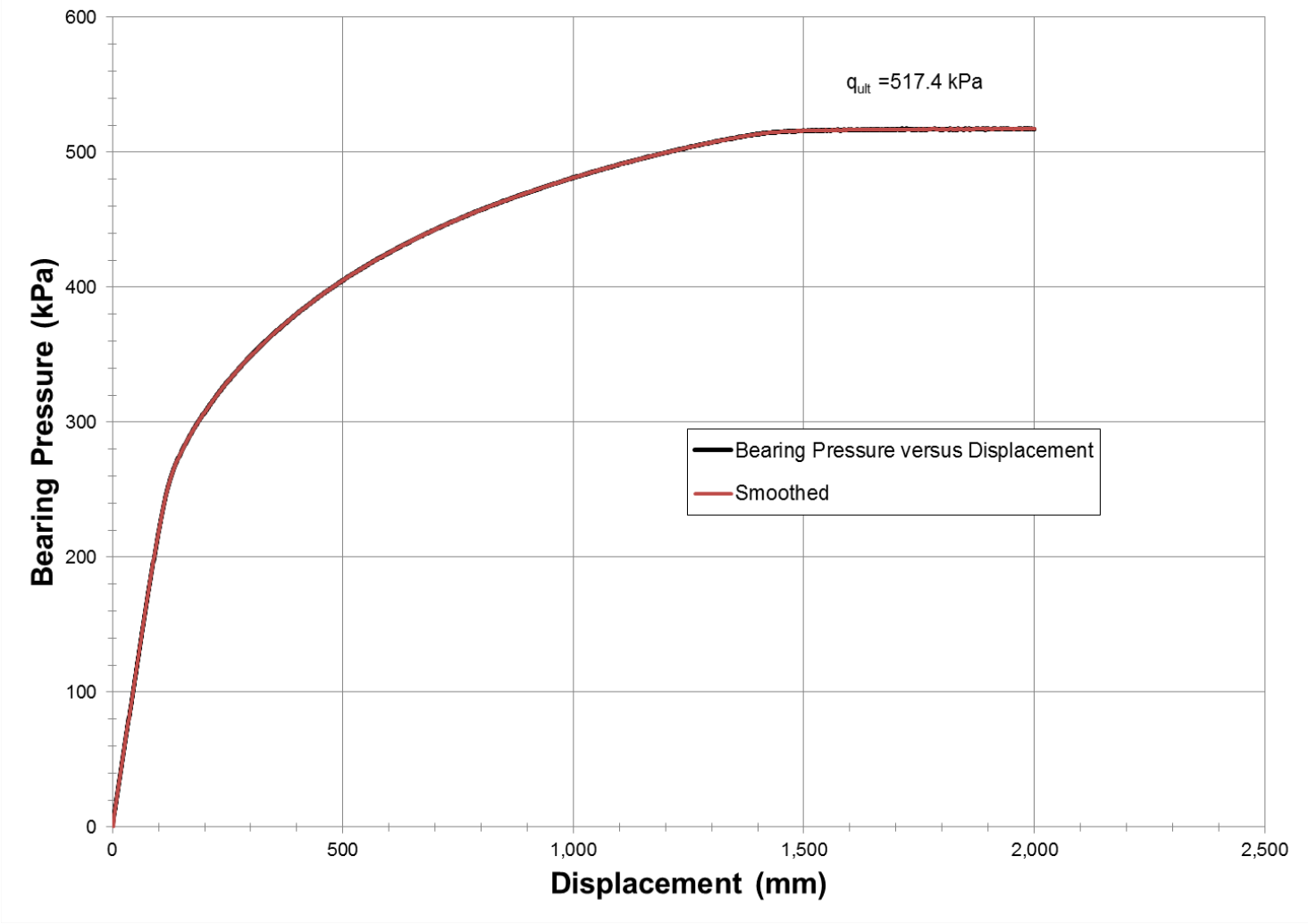


*Figure C-84: Bearing pressure versus displacement (single 3 m Long, 0.9 m wide trench in 80 kPa clay; no embedment depth)*

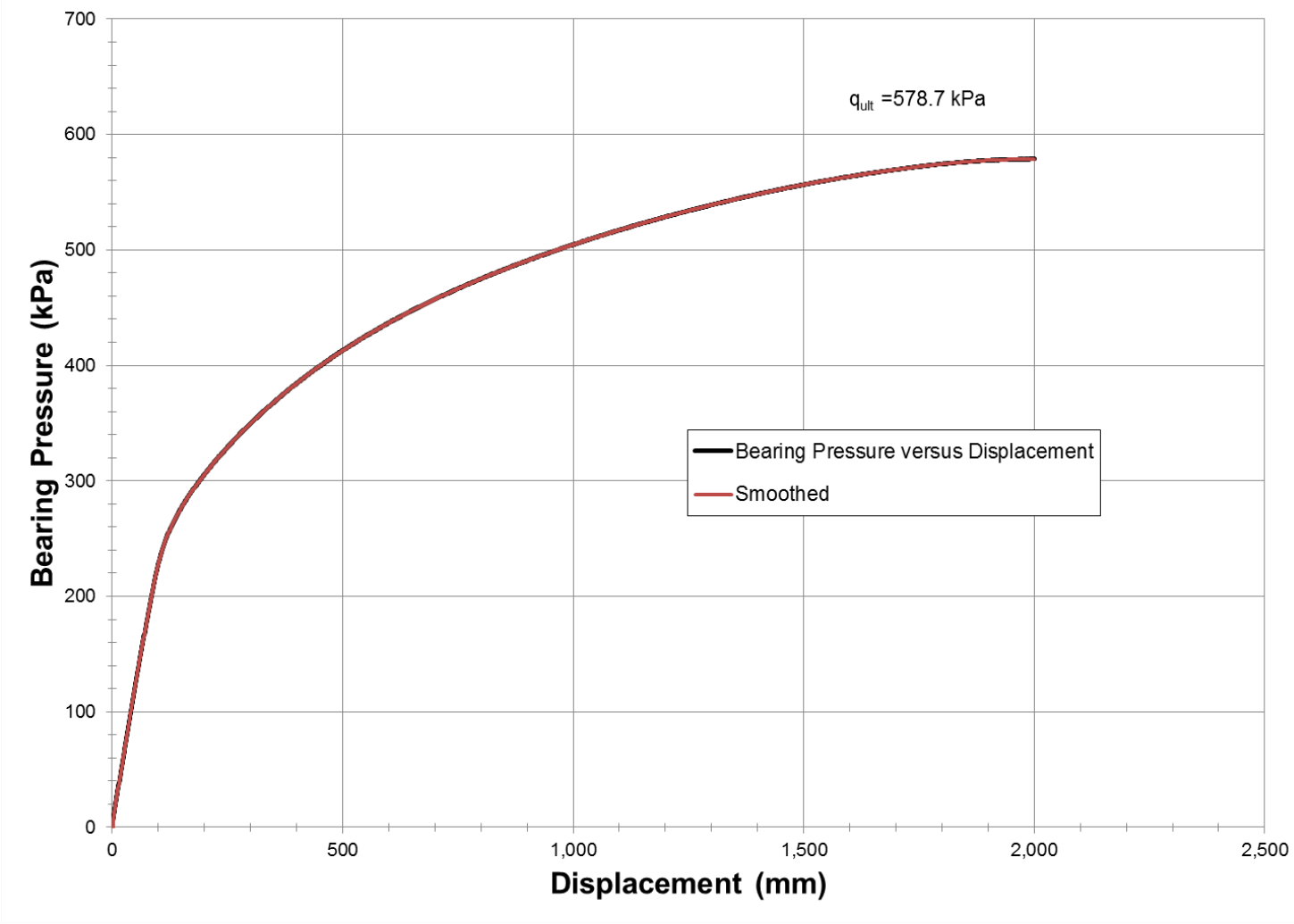


*Figure C-85: Bearing pressure versus displacement (single 3 m Long, 0.9 m wide trench in 80 kPa clay; 1.5 m embedment depth)*

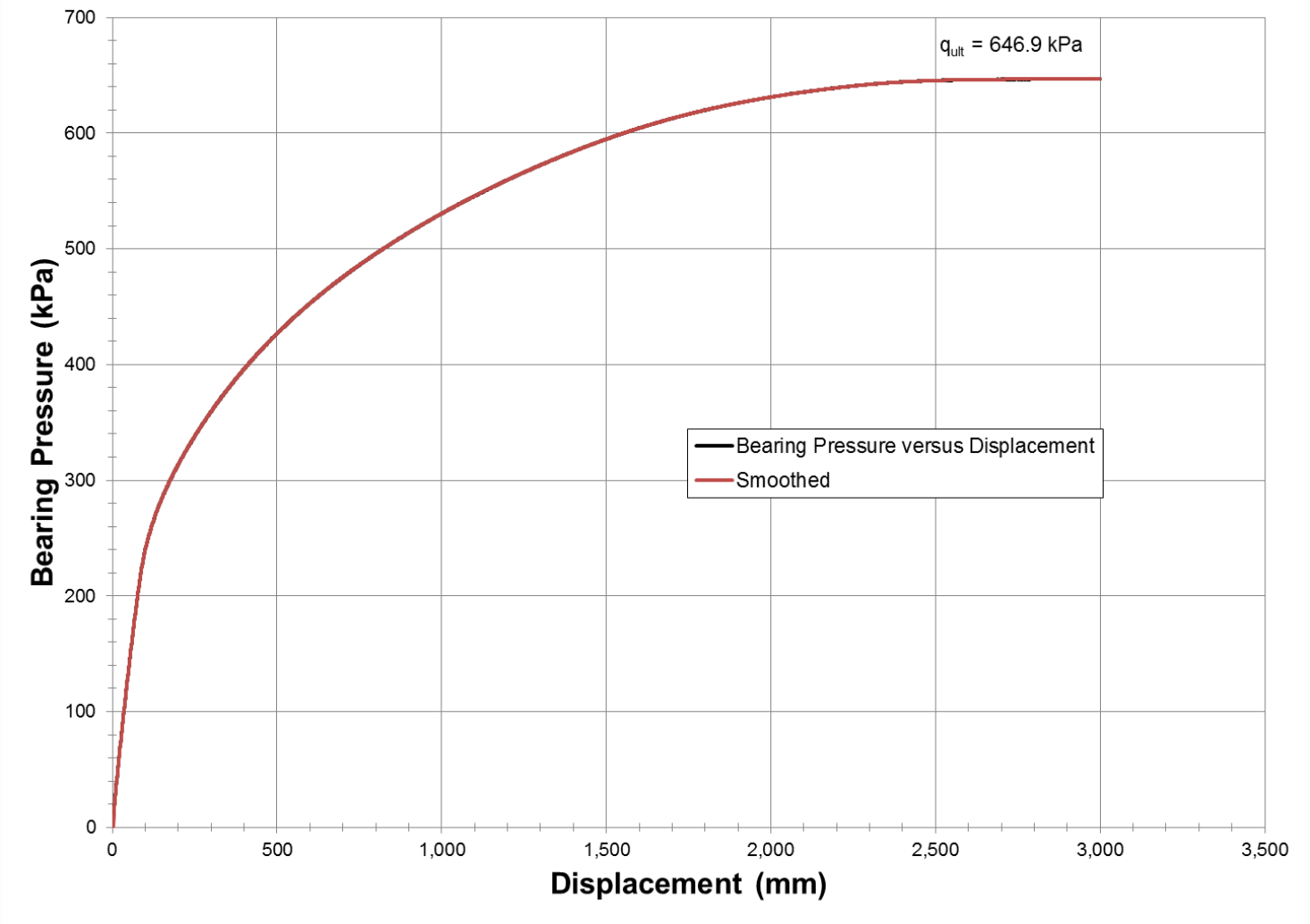


*Figure C-86: Bearing pressure versus displacement (single 3 m Long, 0.9 m wide trench in 80 kPa clay; 3 m embedment depth)*

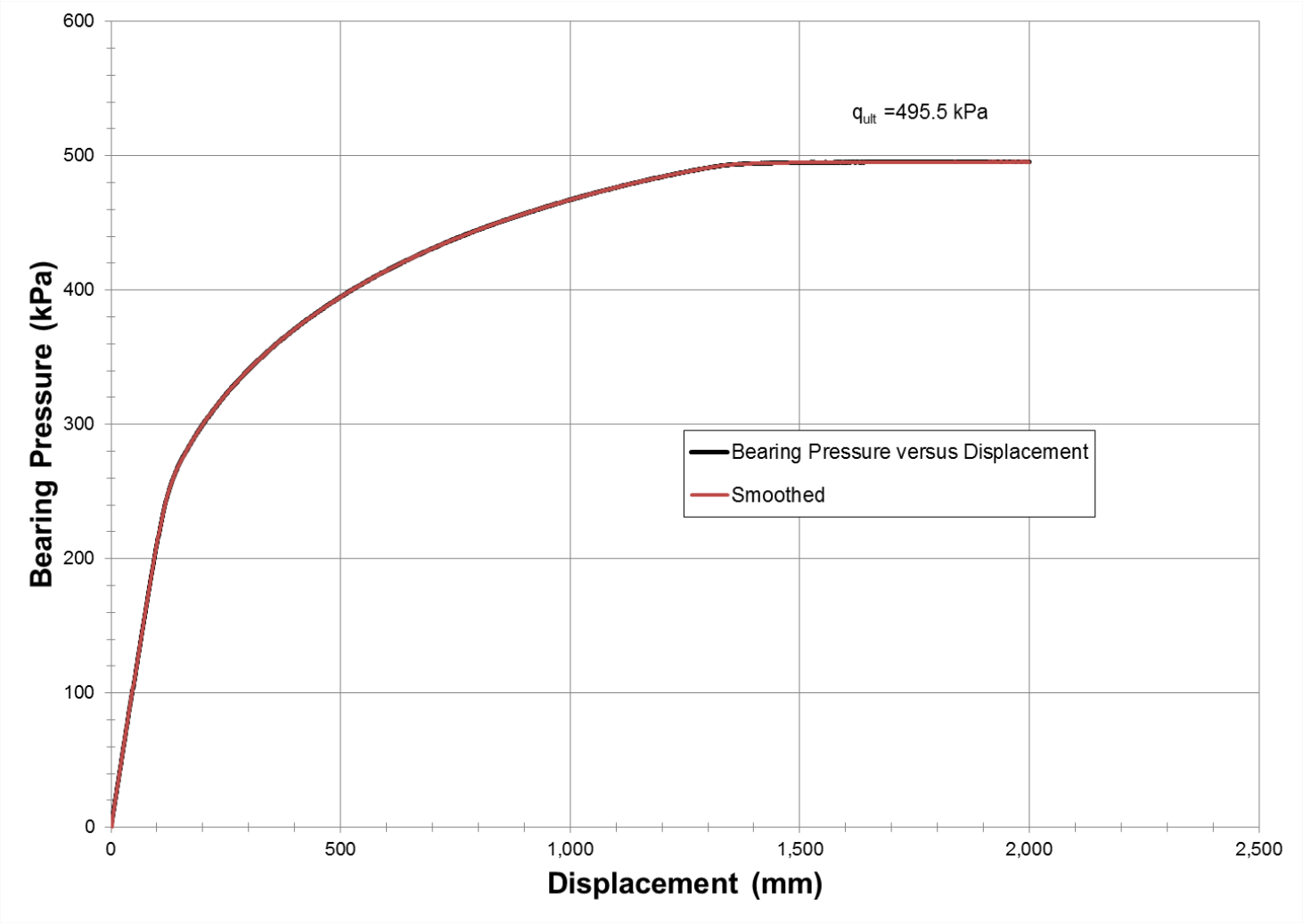


*Figure C-87: Bearing pressure versus displacement (single 3 m Long, 0.6 m wide trench in 80 kPa clay; no embedment depth)*

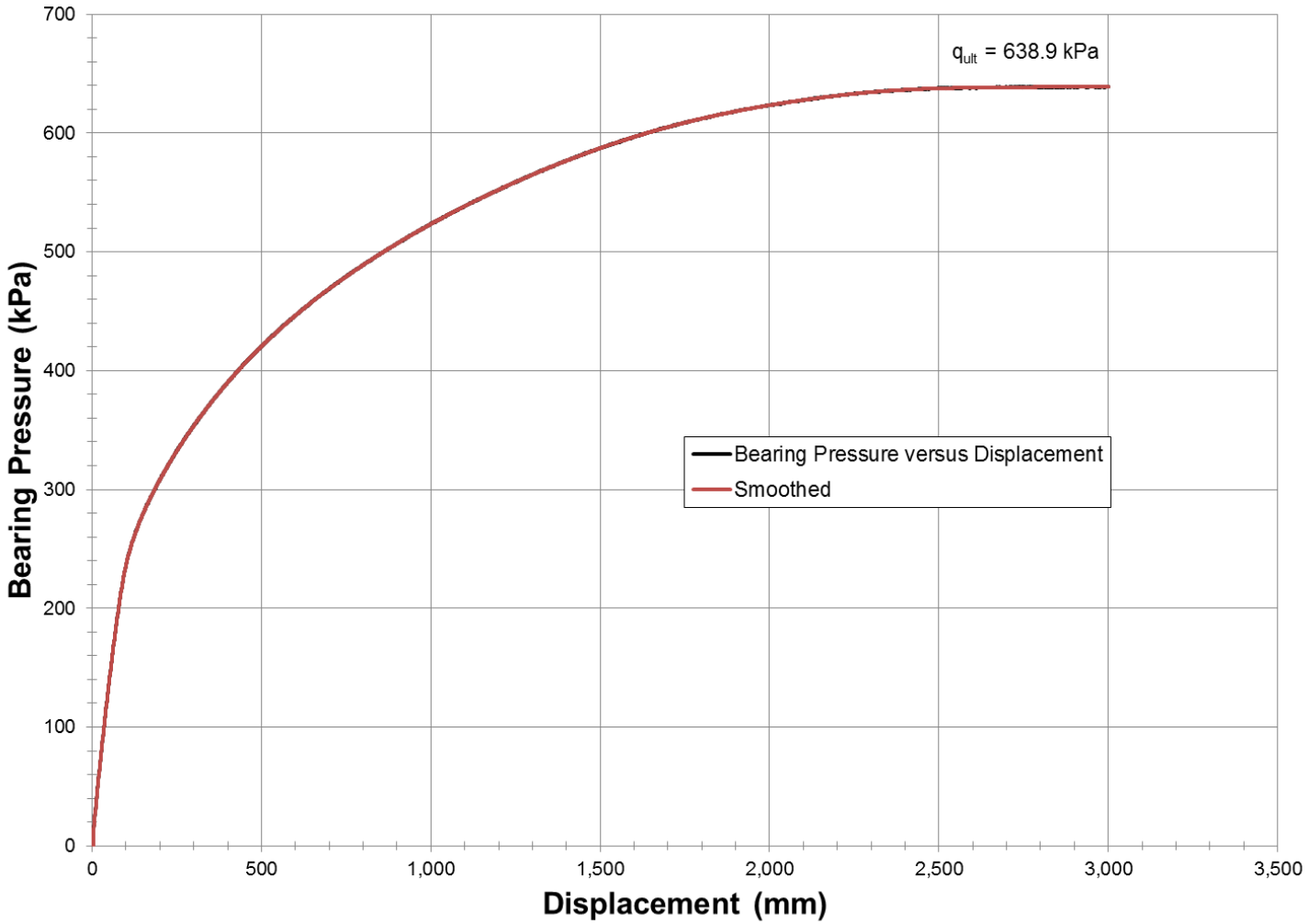


*Figure C-88: Bearing pressure versus displacement (single 3 m Long, 0.6 m wide trench in 80 kPa clay; 3 m embedment depth)*

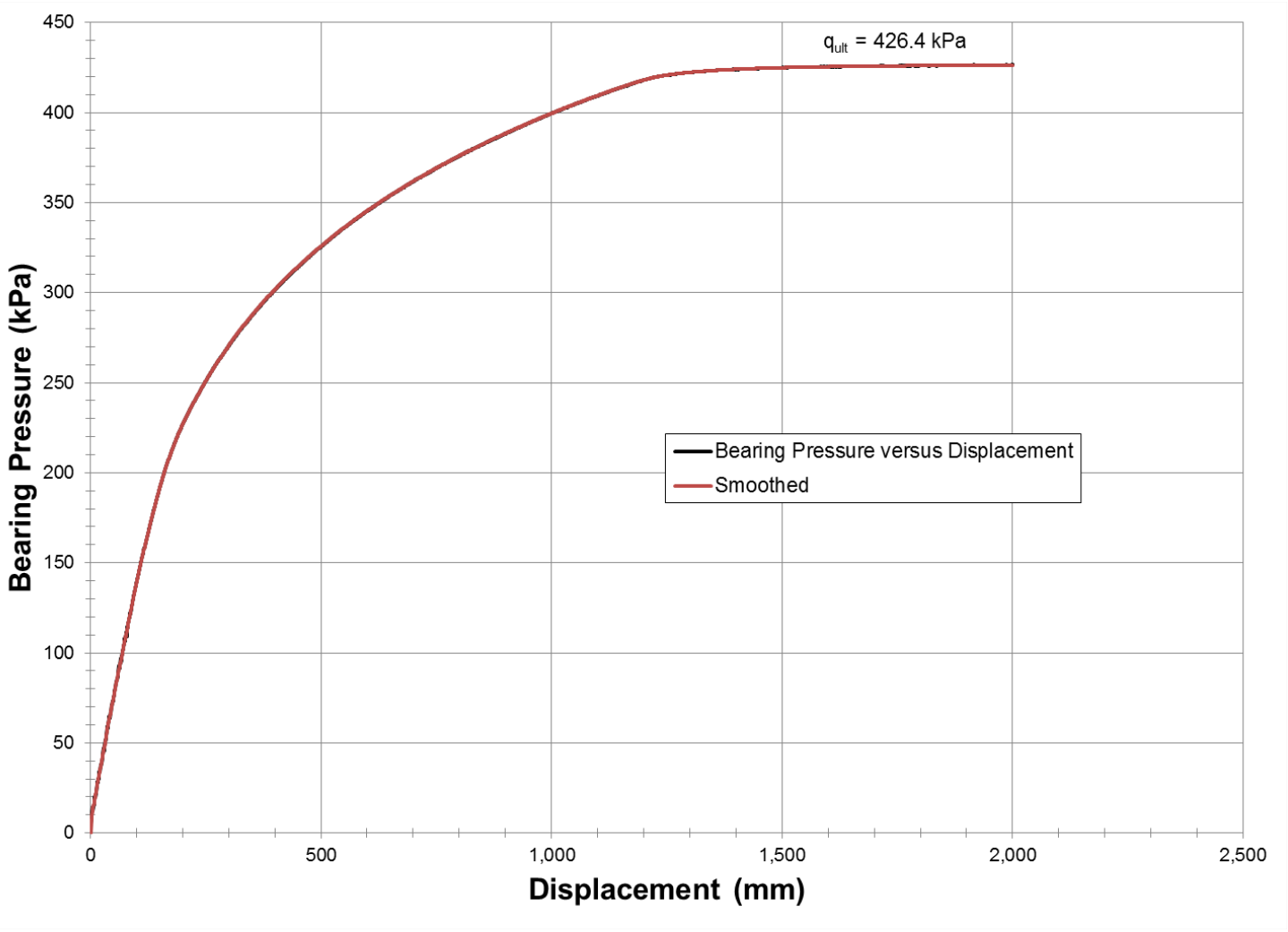


*Figure C-89: Bearing pressure versus displacement (two 6 m Long, 0.75 m wide trenches in 40 kPa clay; no embedment depth)*

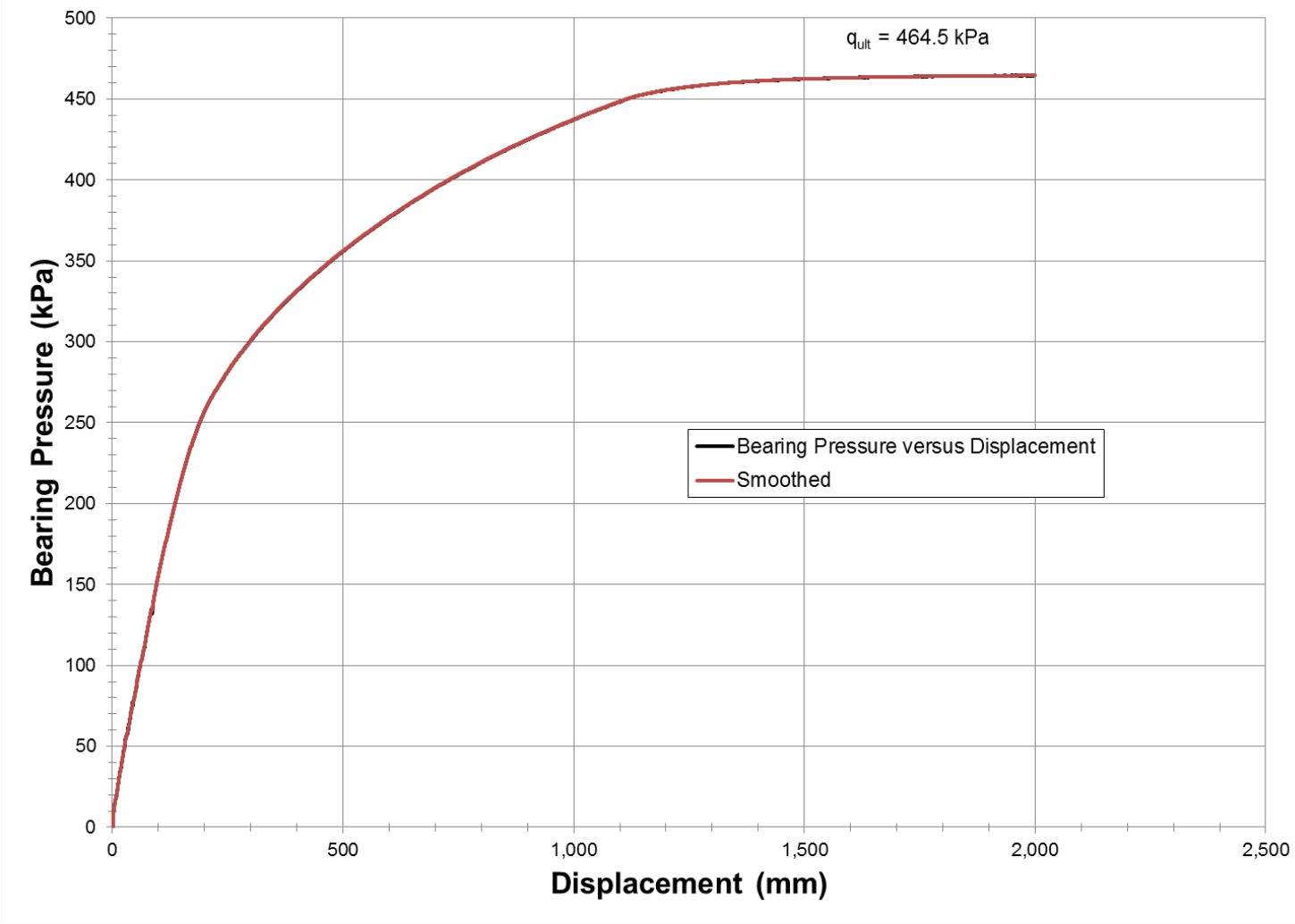


*Figure C-90: Bearing pressure versus displacement (two 6 m Long, 0.75 m wide trenches in 40 kPa clay; 1.5 m embedment depth)*

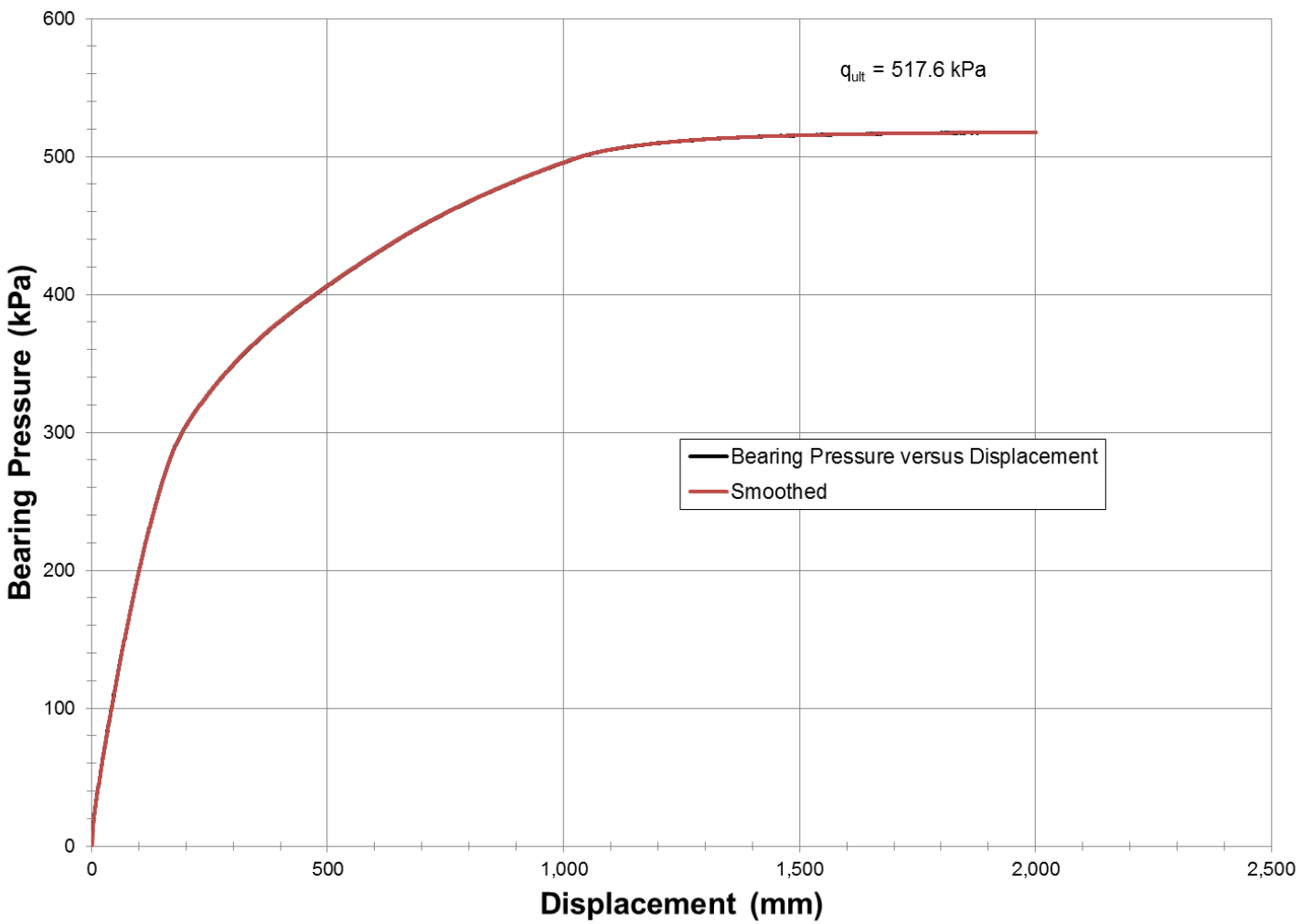


*Figure C-91: Bearing pressure versus displacement (two 6 m Long, 0.75 m wide trenches in 40 kPa clay; 3 m embedment depth)*

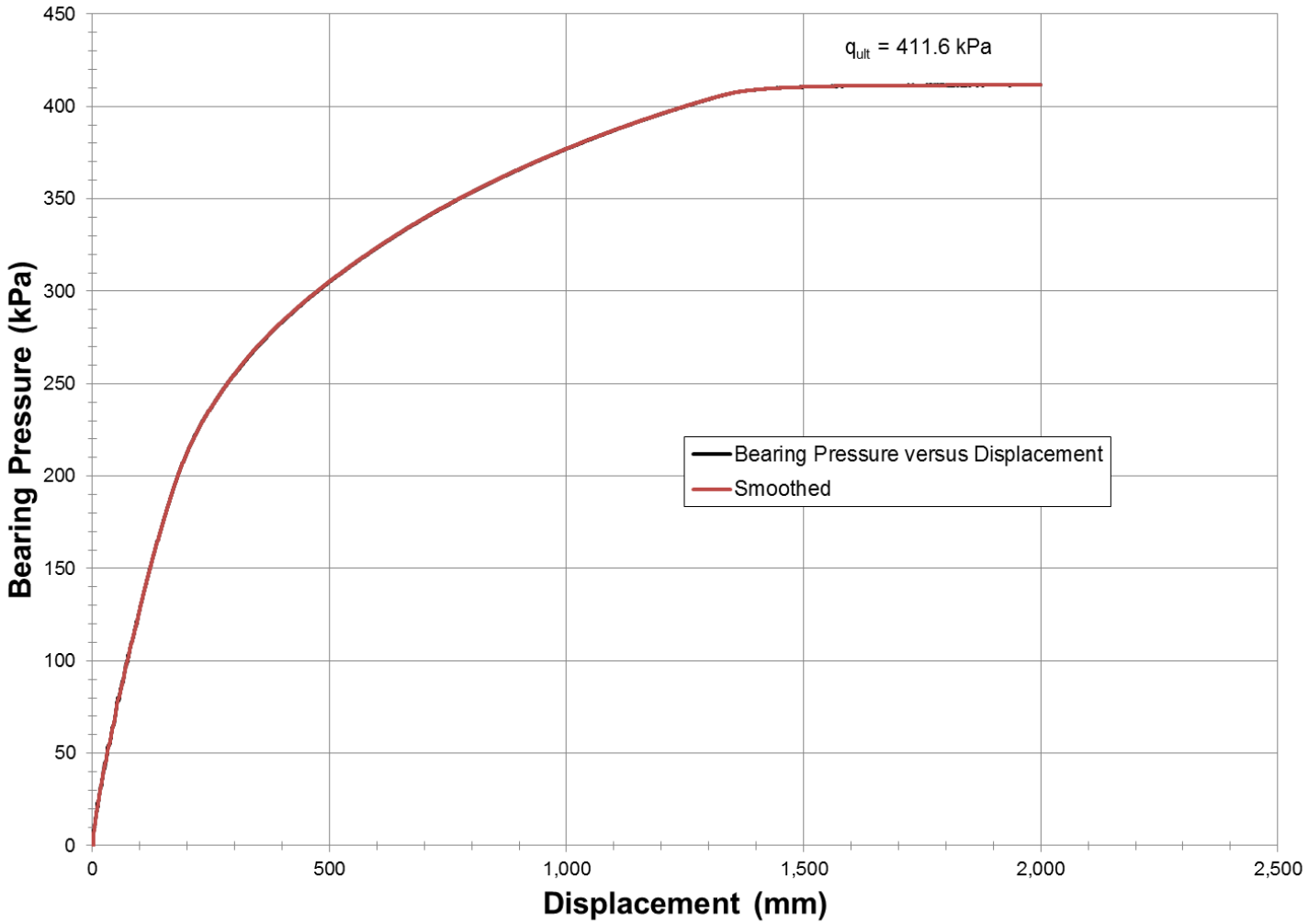


*Figure C-92: Bearing pressure versus displacement (two 6 m Long, 0.45 m wide trenches in 40 kPa clay; no embedment depth)*

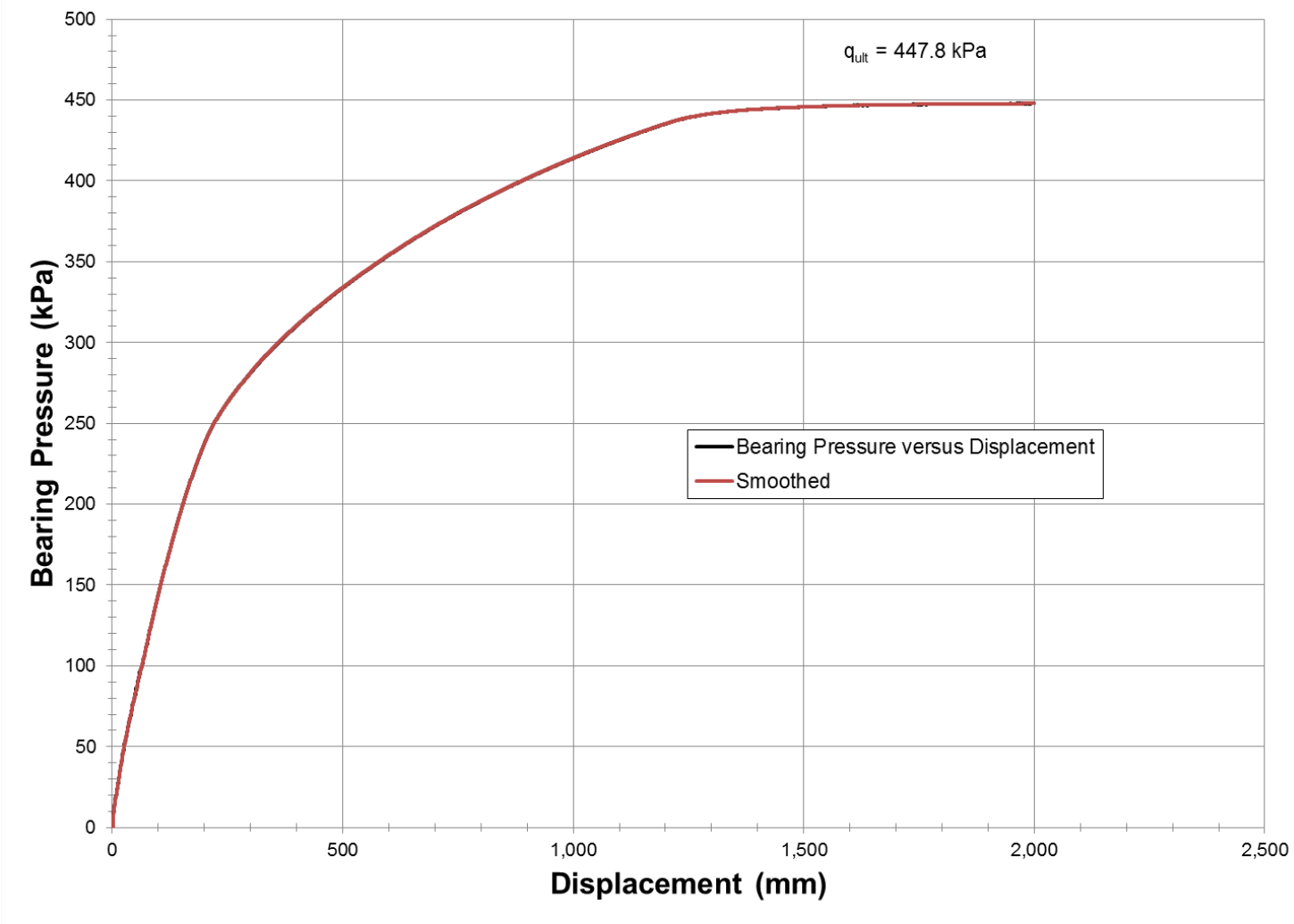


*Figure C-93: Bearing pressure versus displacement (two 6 m Long, 0.45 m wide trenches in 40 kPa clay; 1.5 m embedment depth)*

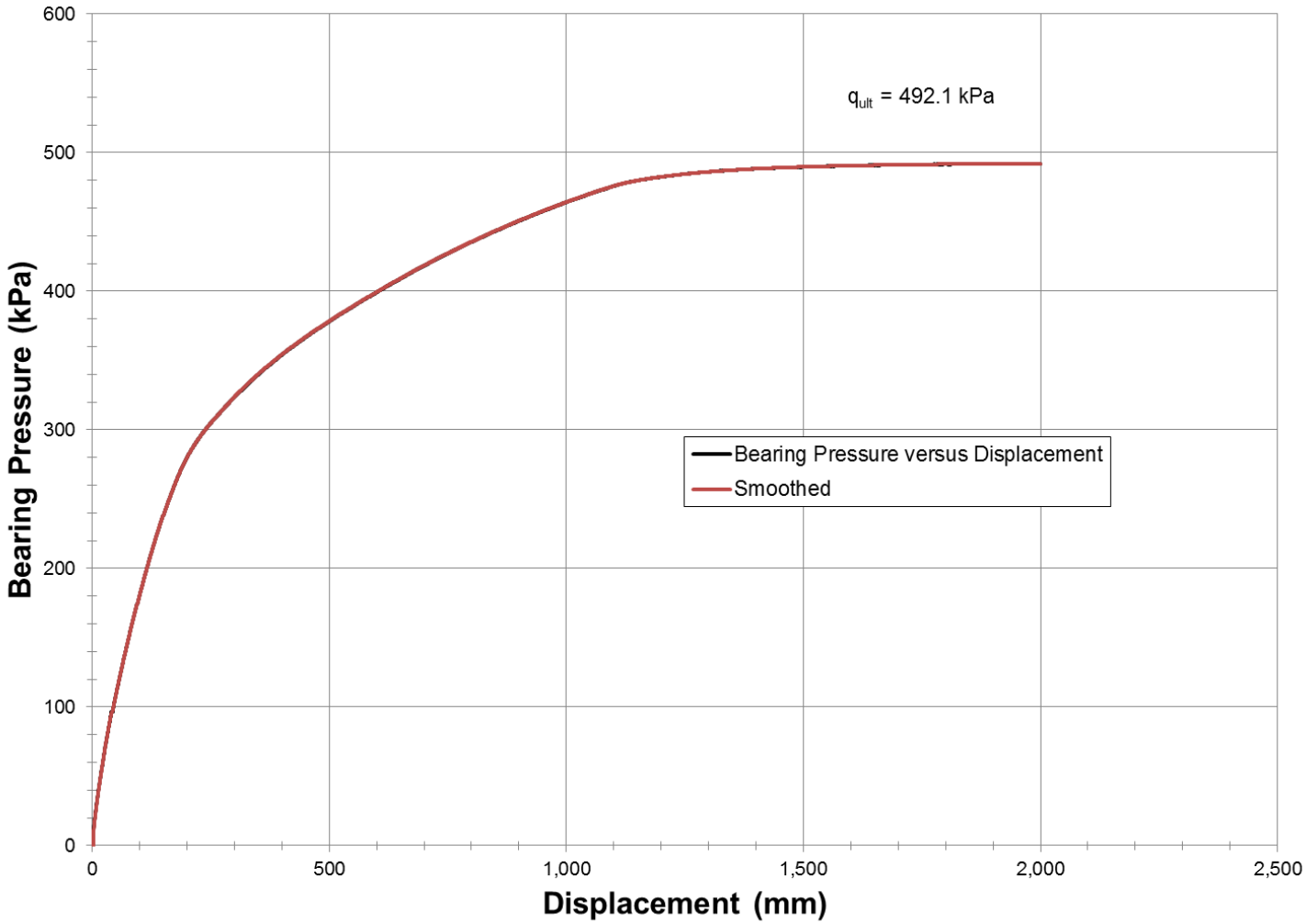


*Figure C-94: Bearing pressure versus displacement (two 6 m Long, 0.45 m wide trenches in 40 kPa clay; 3 m embedment depth)*

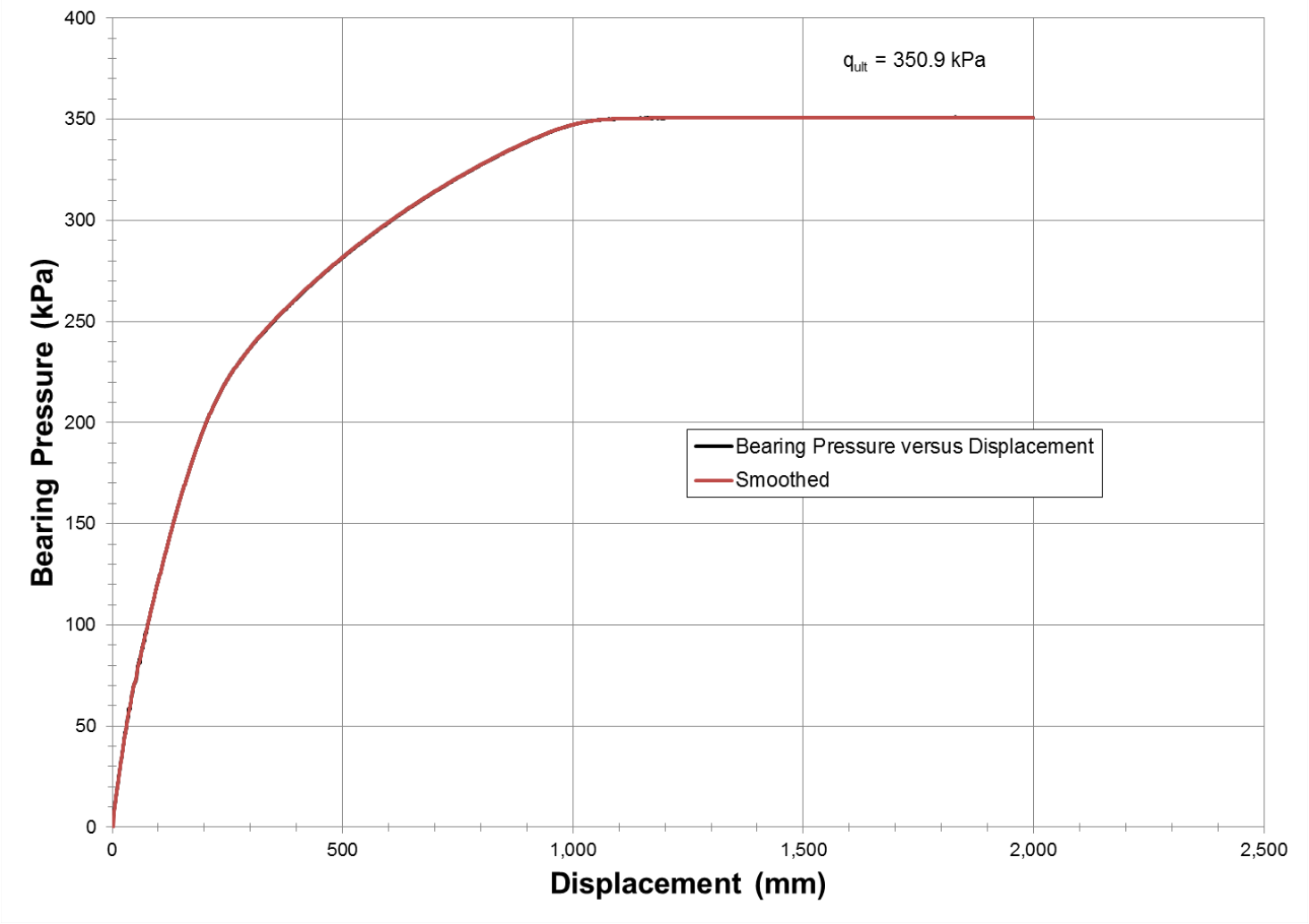


*Figure C-95: Bearing pressure versus displacement (two 6 m Long, 0.3 m wide trenches in 40 kPa clay; no embedment depth)*

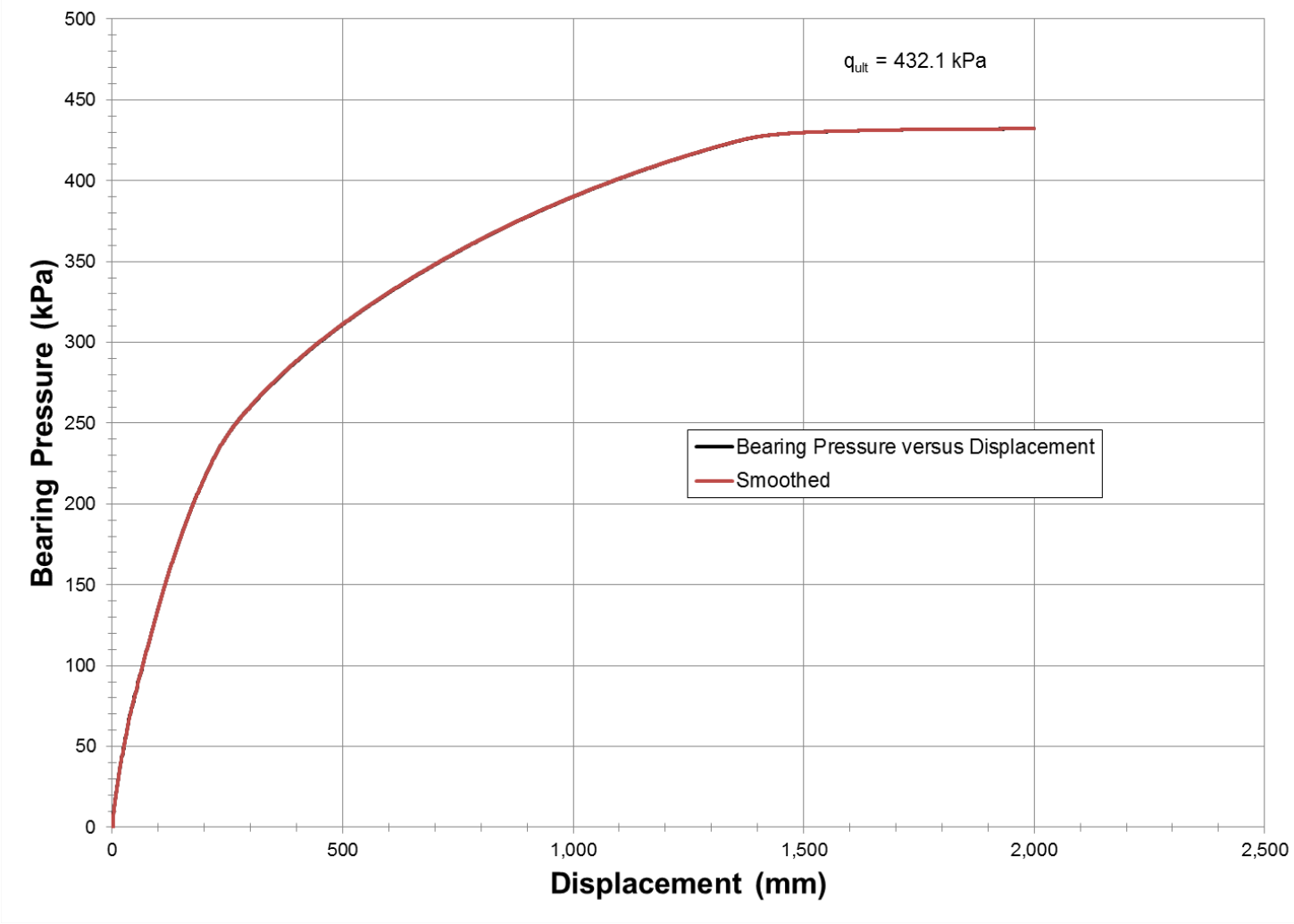


*Figure C-96: Bearing pressure versus displacement (two 6 m Long, 0.3 m wide trenches in 40 kPa clay; 1.5 m embedment depth)*

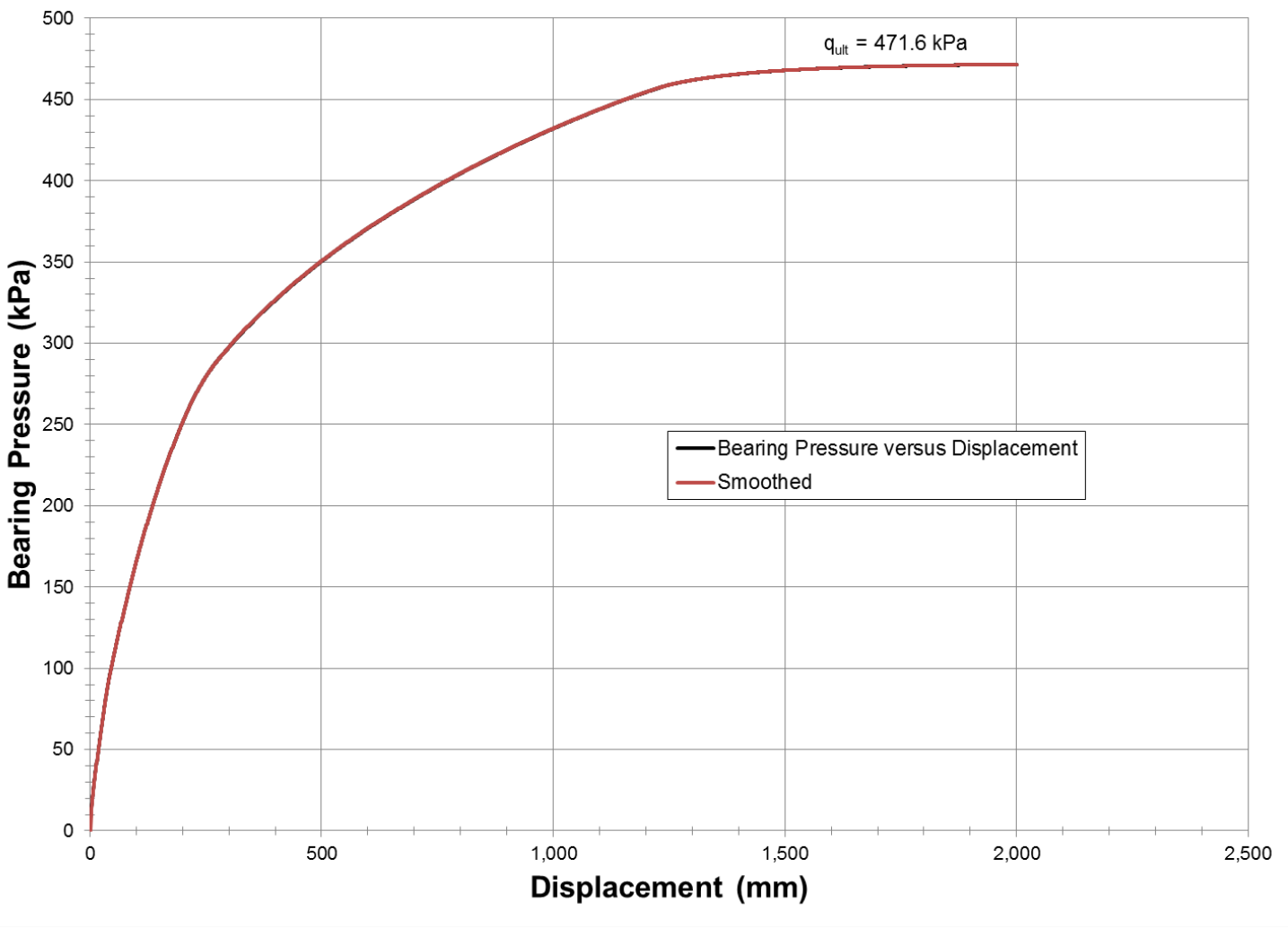


*Figure C-97: Bearing pressure versus displacement (two 6 m Long, 0.3 m wide trenches in 40 kPa clay; 3 m embedment depth)*

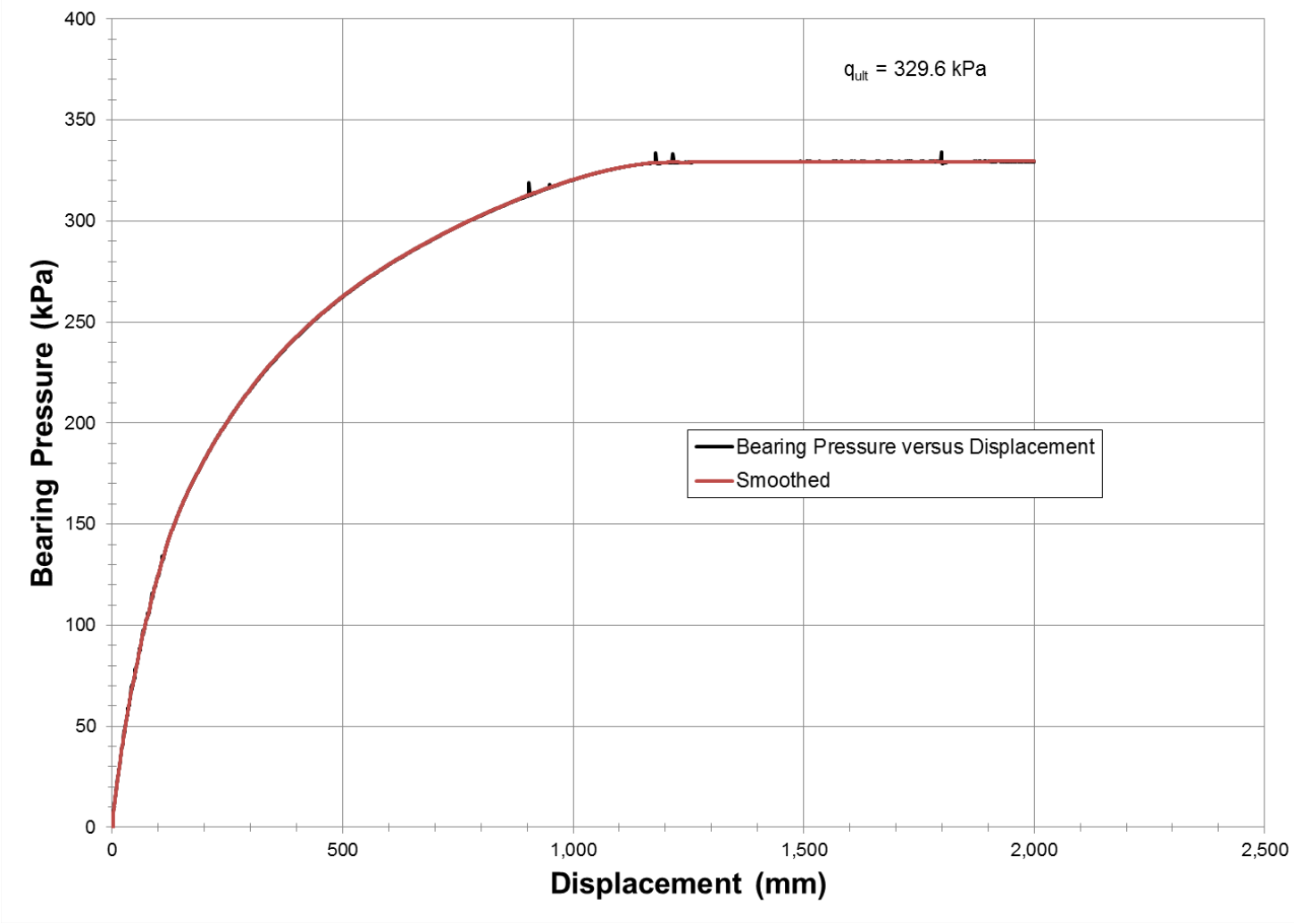


*Figure C-98: Bearing pressure versus displacement (two 3 m Long, 0.75 m wide trenches in 40 kPa clay; no embedment depth)*

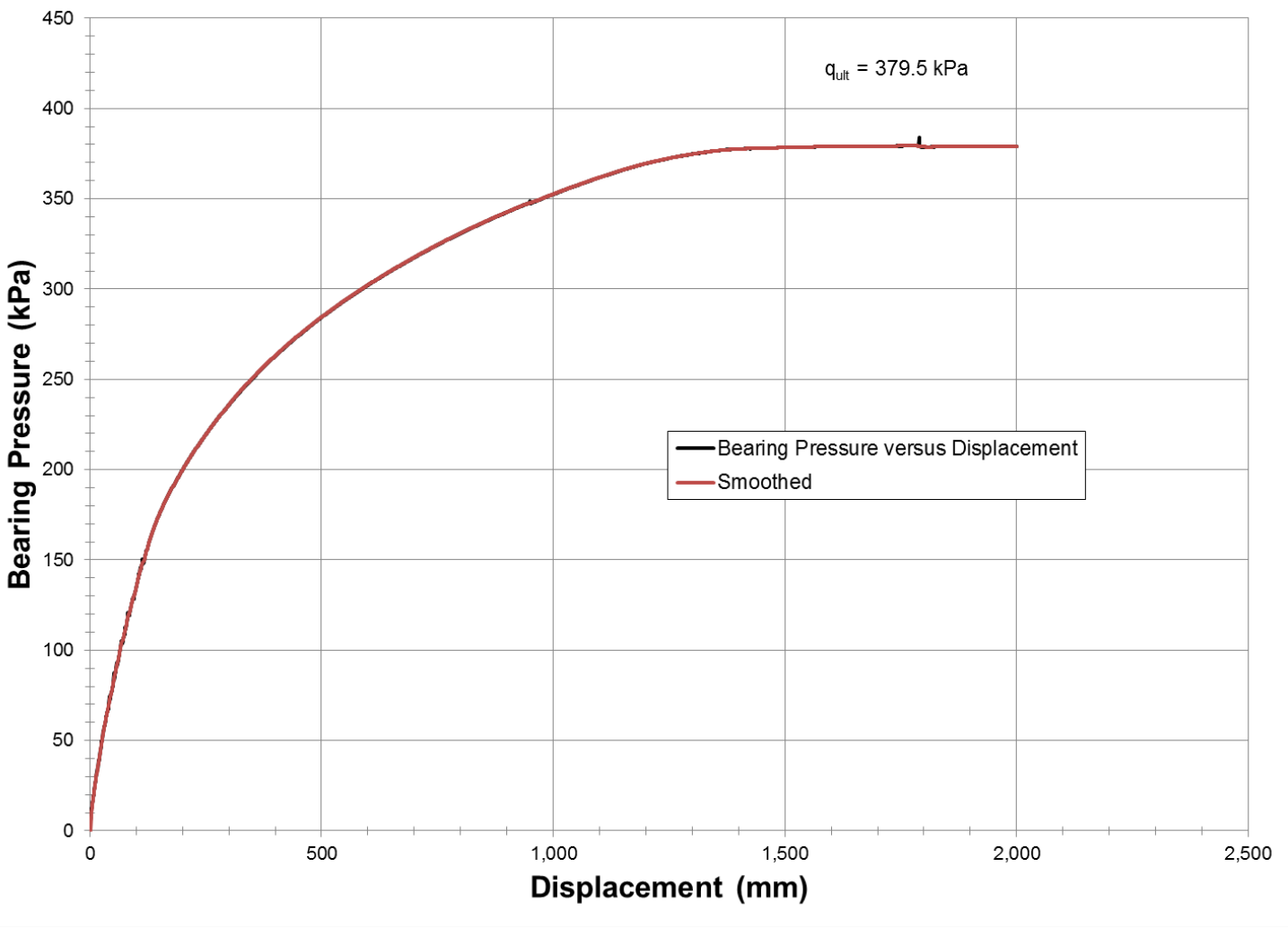


*Figure C-99: Bearing pressure versus displacement (two 3 m Long, 0.75 m wide trenches in 40 kPa clay; 1.5 m embedment depth)*

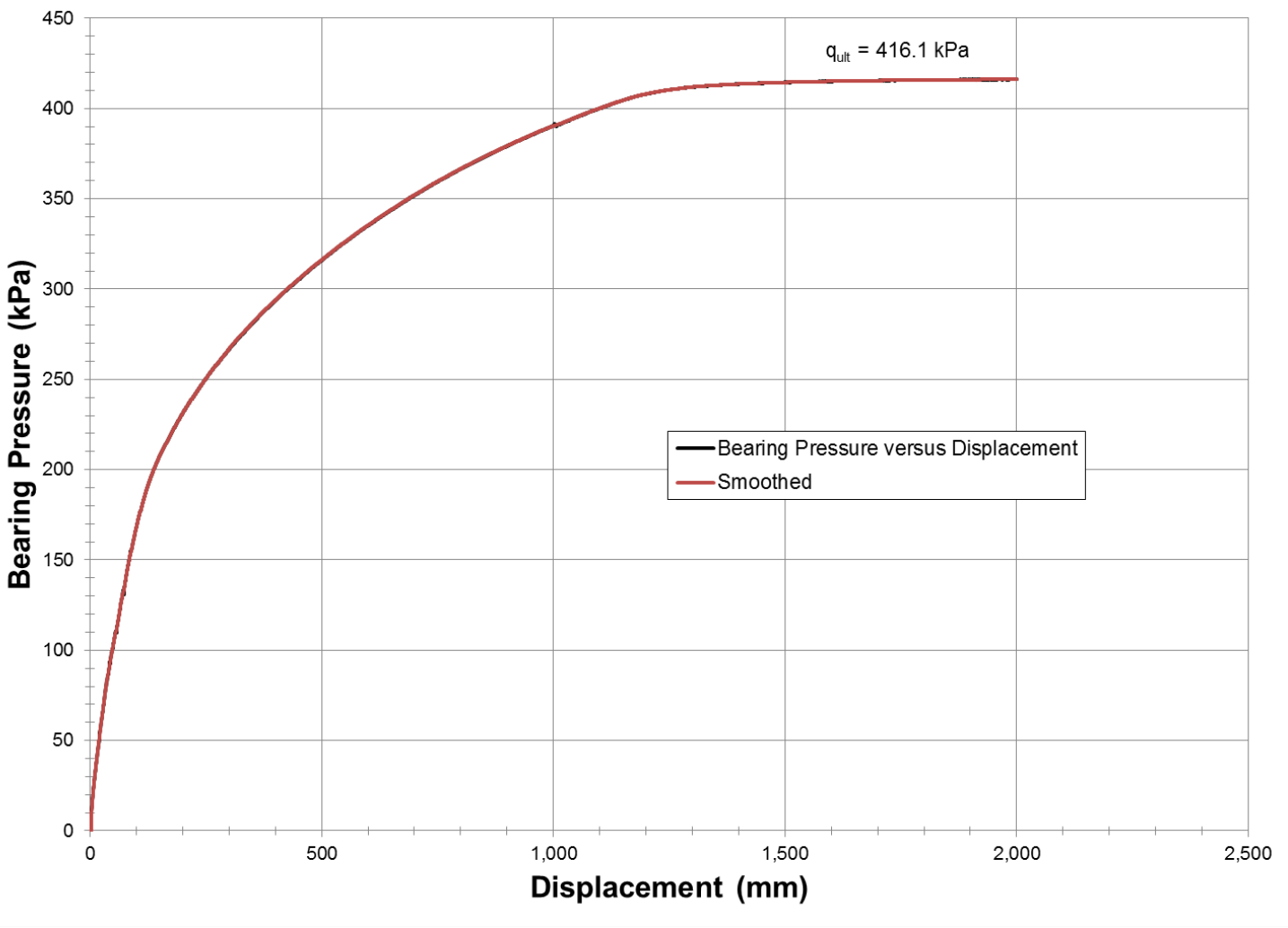


*Figure C-100: Bearing pressure versus displacement (two 3 m Long, 0.75 m wide trenches in 40 kPa clay; 3 m embedment depth)*

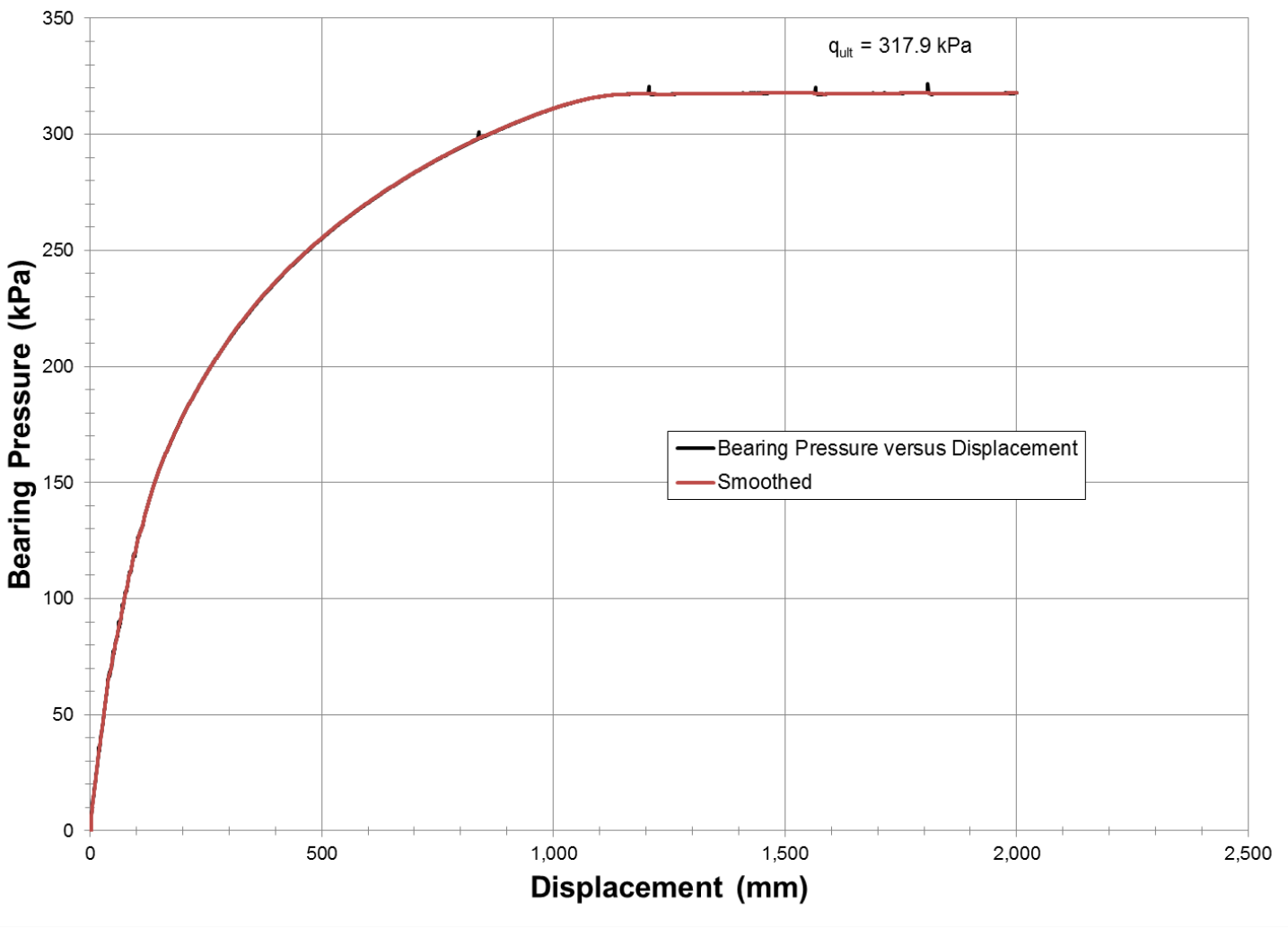


*Figure C-101: Bearing pressure versus displacement (two 3 m Long, 0.45 m wide trenches in 40 kPa clay; no embedment depth)*

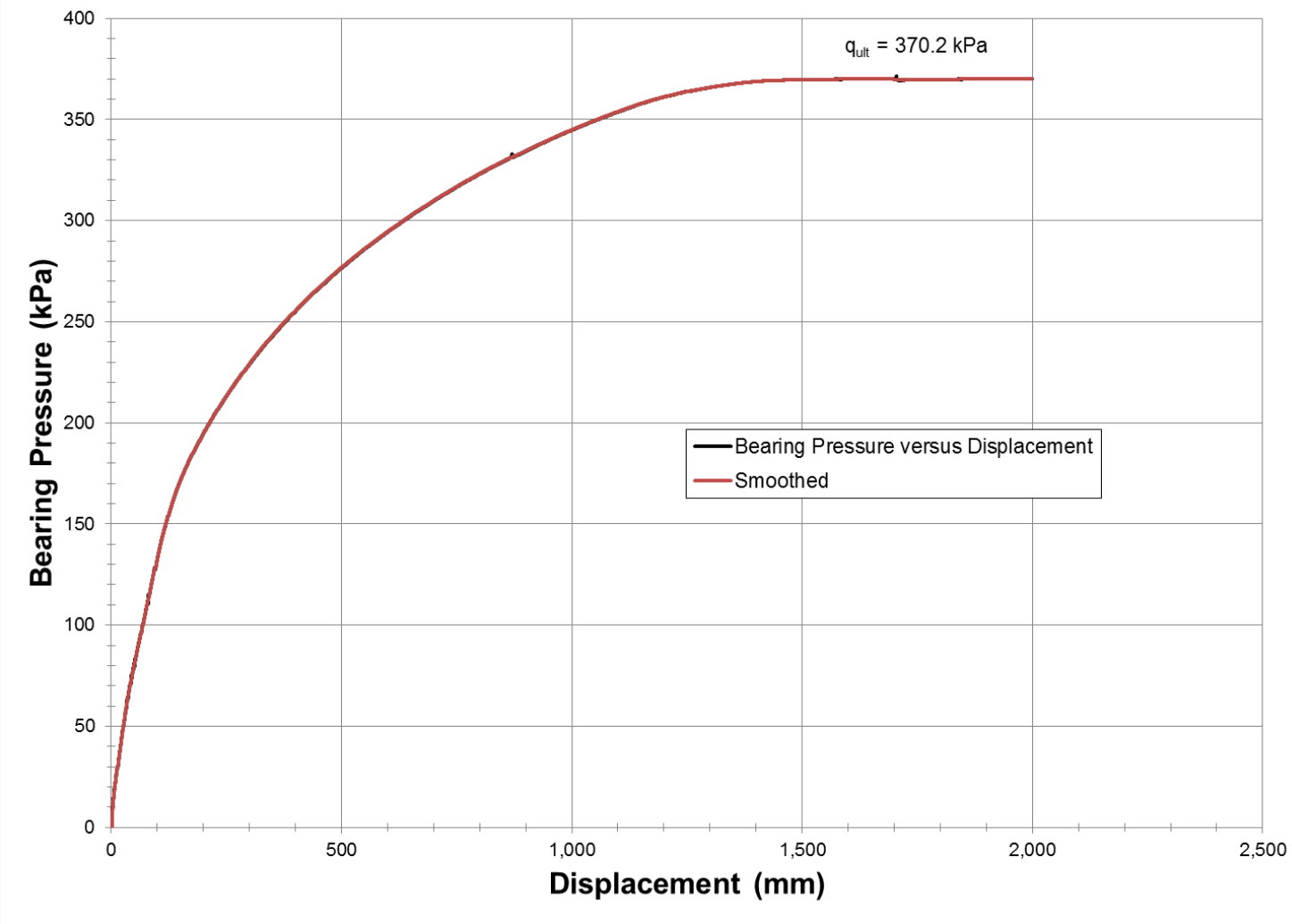


*Figure C-102: Bearing pressure versus displacement (two 3 m Long, 0.45 m wide trenches in 40 kPa clay; 1.5 m embedment depth)*

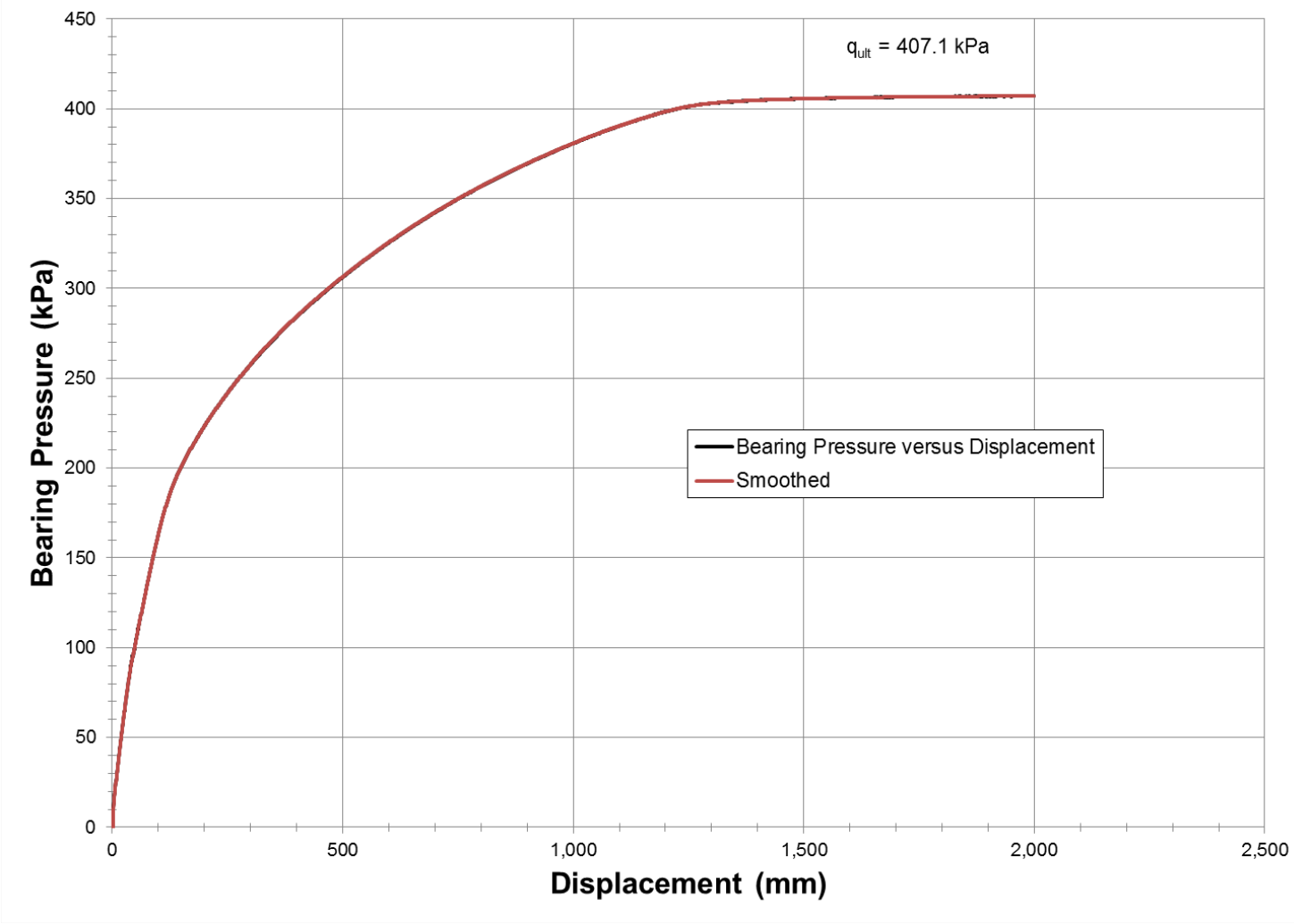


*Figure C-103: Bearing pressure versus displacement (two 3 m Long, 0.45 m wide trenches in 40 kPa clay; 3 m embedment depth)*

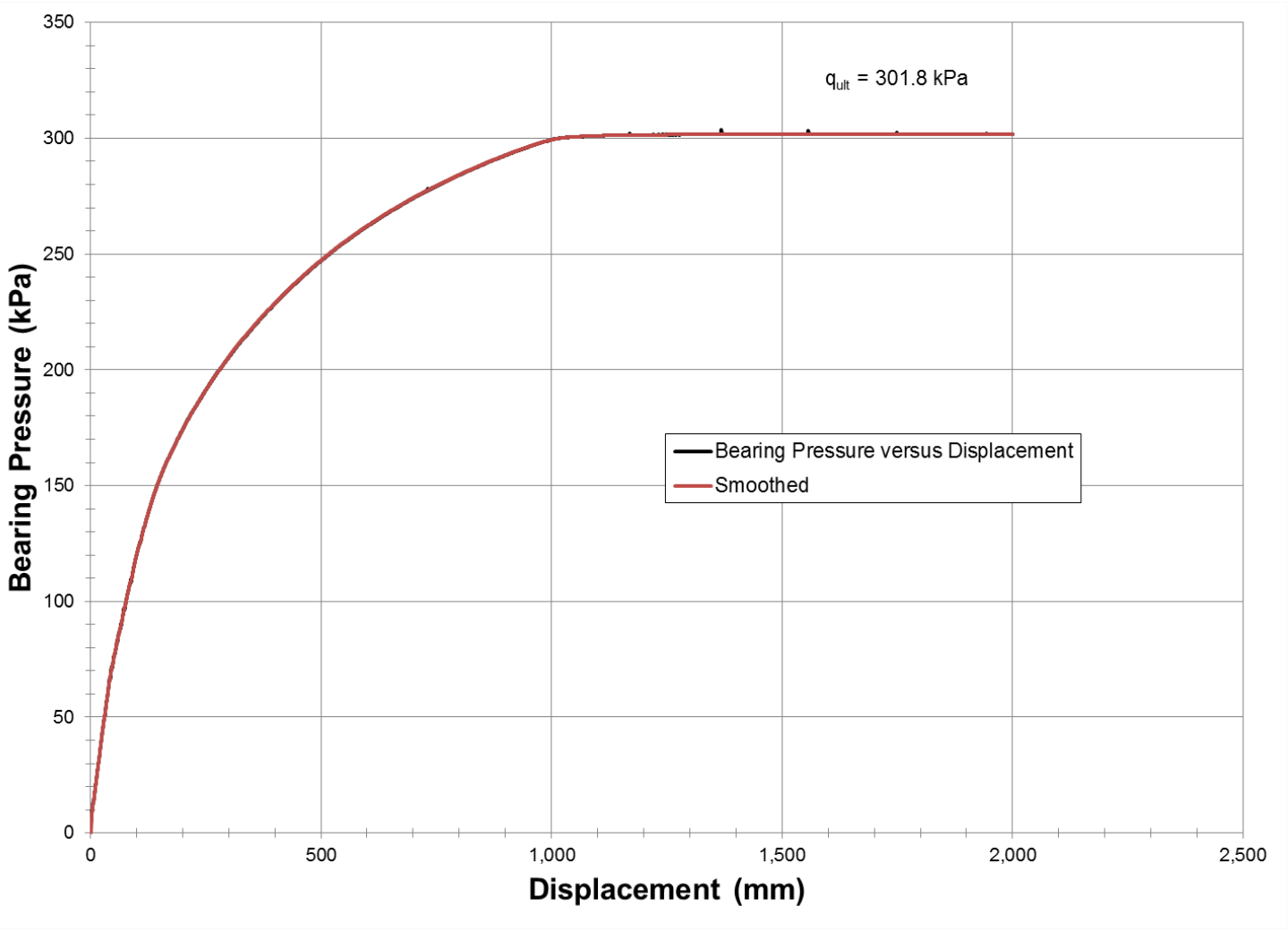


*Figure C-104: Bearing pressure versus displacement (two 3 m Long, 0.3 m wide trenches in 40 kPa clay; no embedment depth)*

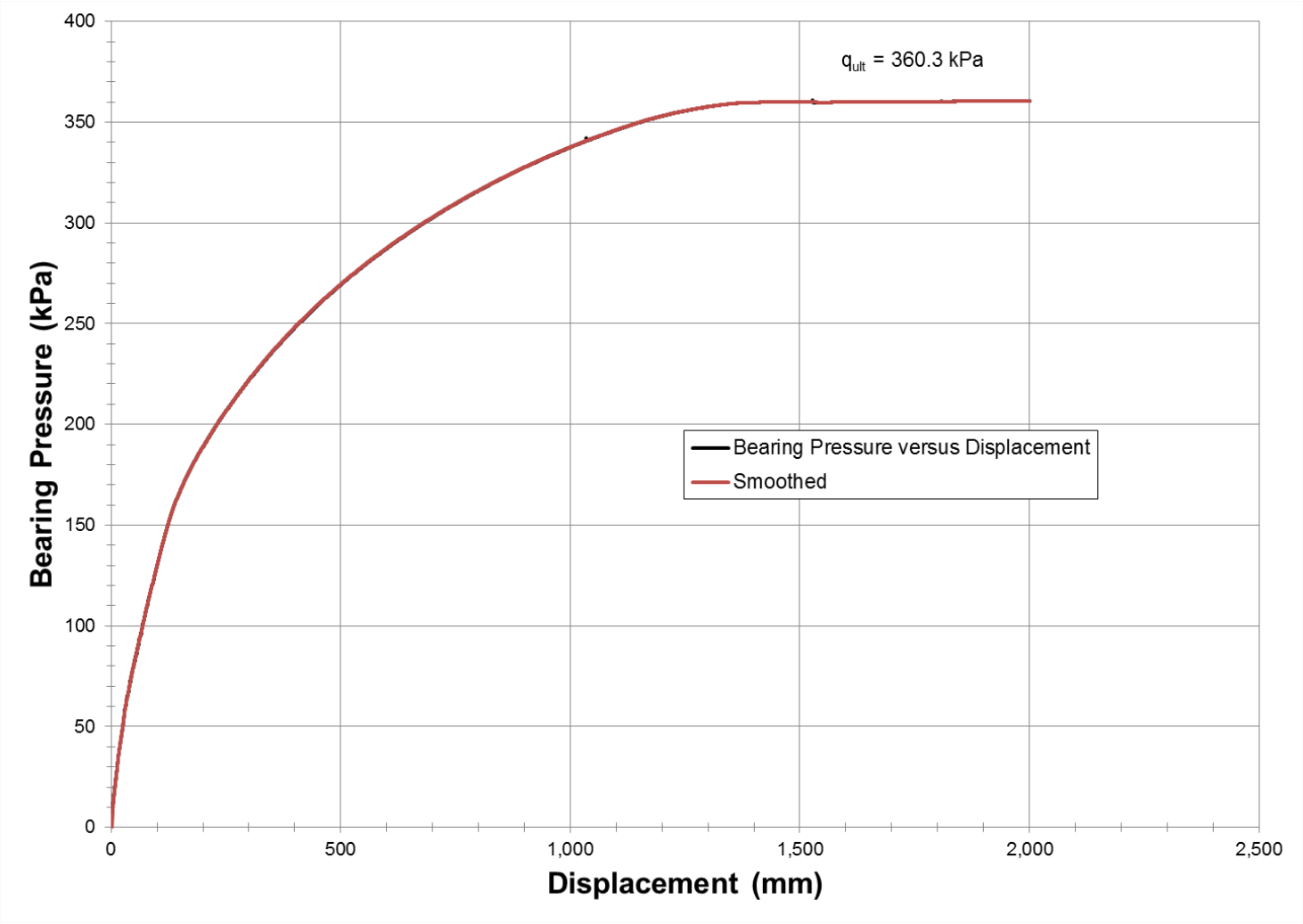


*Figure C-105: Bearing pressure versus displacement (two 3 m Long, 0.3 m wide trenches in 40 kPa clay; 1.5 m embedment depth)*

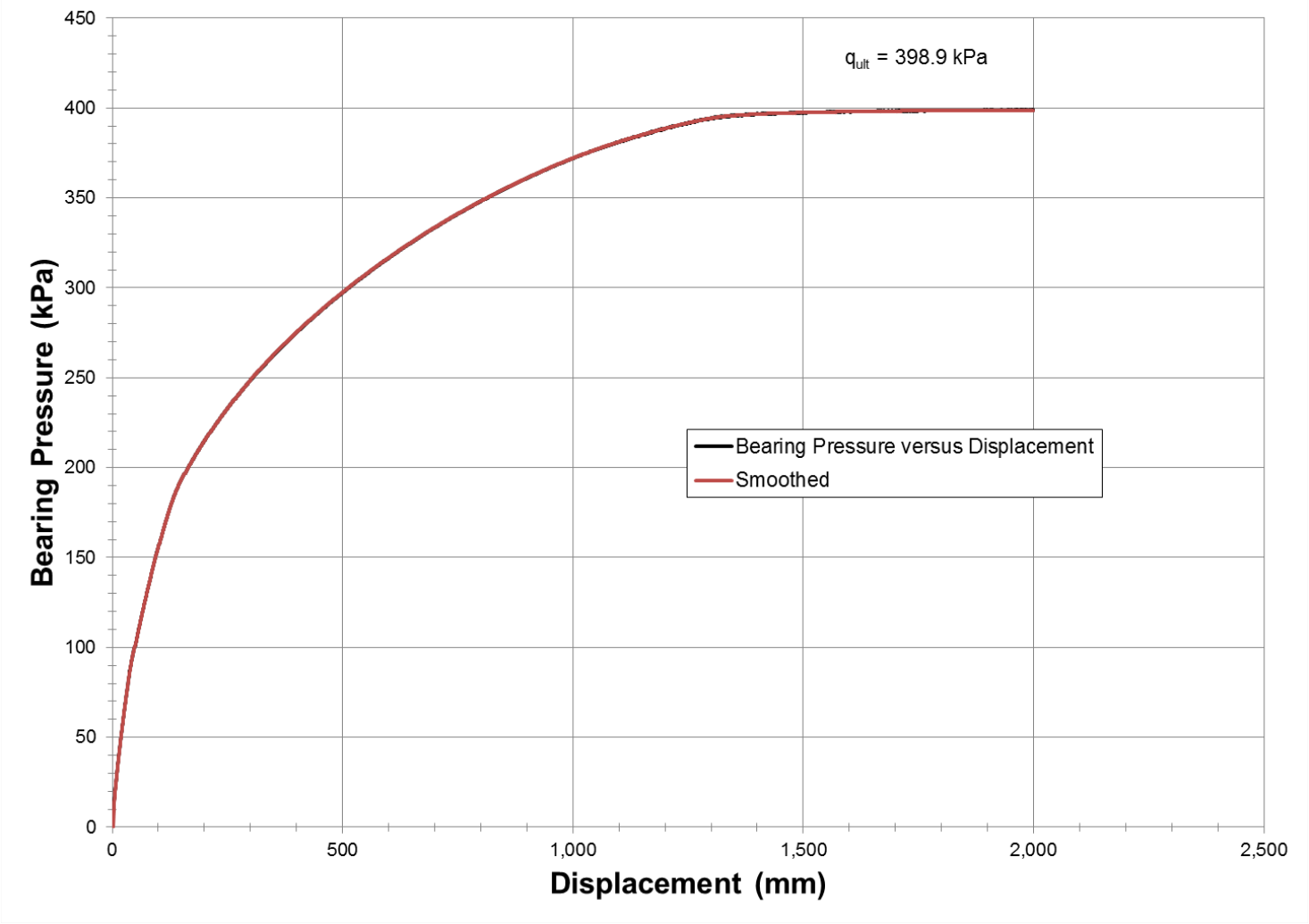


*Figure C-106: Bearing pressure versus displacement (two 3 m Long, 0.3 m wide trenches in 40 kPa clay; 3 m embedment depth)*

## D. Appendix: MATLAB Script for the Extrapolation of Relevant Contact Pressure Data

```
%file that imports geotech data from .fis or other file types to pull
%specific values

%2/2/2016 19:16

clear
clc

[ ~ , pathname]=uigetfile('.fis', 'Select a file in the appropriate folder');  %Specifies the folder path
files = dir(fullfile(pathname,'*.fis'));    %finds all files in approrpriate folder with suffix ".fis"
files= {files.name};    %specifies the "name" from the file info matrix

for k=1:length(files);  %repeat for all files in folder

    %list of requested rows
    rowlist=[
        104             504             1504
        2108            2508            3508
        4112            4512            5512
        6116            6516            7516
        8120            8520            9520
        10124           10524           11524
        12128           12528           13528
        14132           14532           15532
        16136           16536           17536
        18140           18540           19540
        20144           20544           21544
        22148           22548           23548
        24152           24552           25552
        26156           26556           27556
        28160           28560           29560
        30164           30564           31564
        32168           32568           33568
        34172           34572           35572
        36176           36576           37576
        38180           38580           39580
        40184           40584           41584];

    [height,width]=size(rowlist);

    for i=1:height;
        for j=1:width;
            row=rowlist(i,j)-1; %find appropriate offset for import from list of desired rows
            M=dlmread(fullfile(pathname,files{k}),' ',[row 21 row 21]); %read the row
            matrix(j,i)=M;  %place called value in results matrix (as a transpose)
        end
    end

    filename=strsplit(files{k},'.');    %remove ".fis" from filename
    xlswrite(filename{1,1},matrix);     %write to excel and save as 'filename'

end
```

## E. Appendix: Contact Pressure Distribution – All Trench Improved Cases

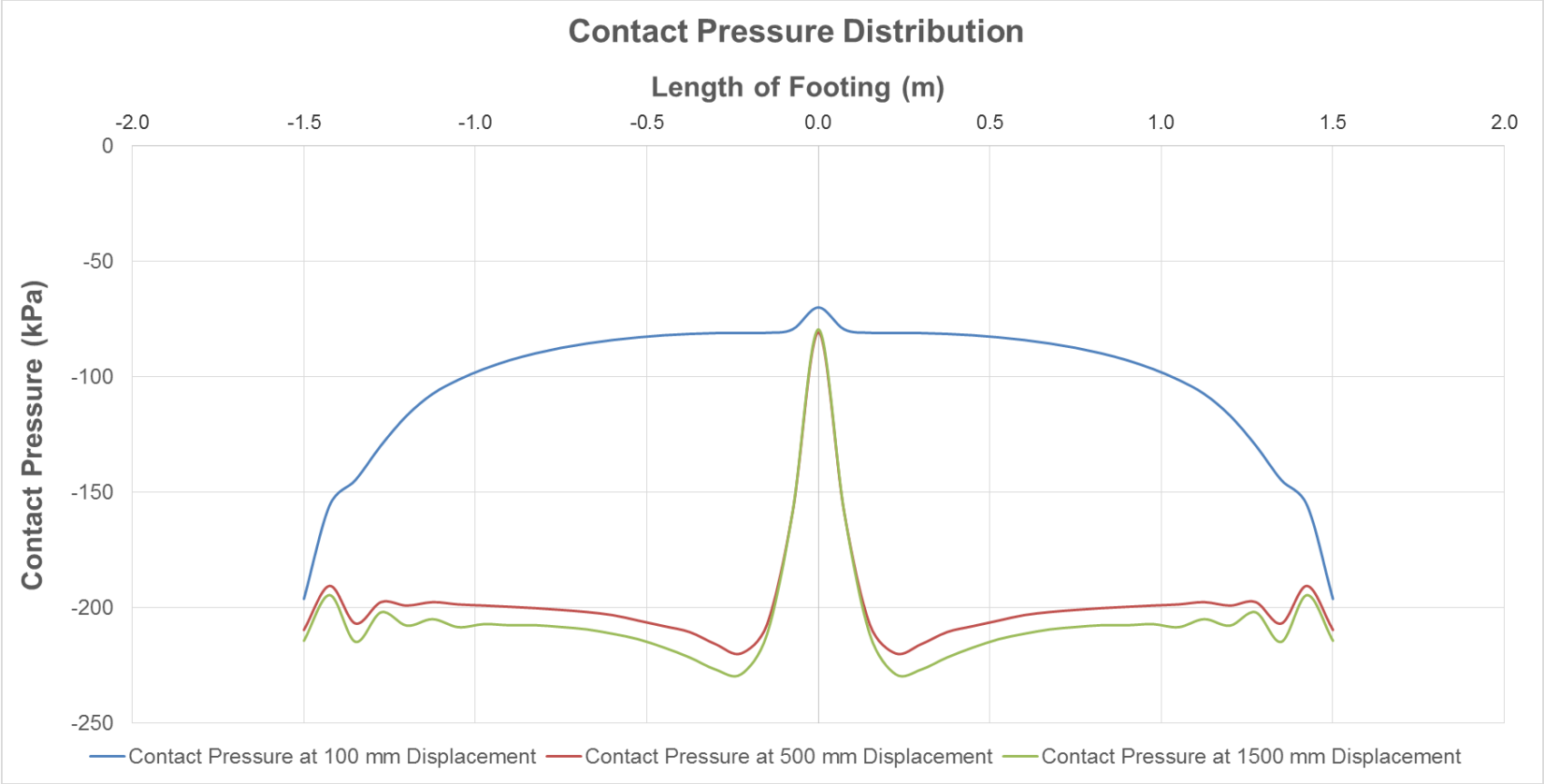


*Figure E-1: Contact pressure distribution (40 kPa native clay; no embedment depth)*

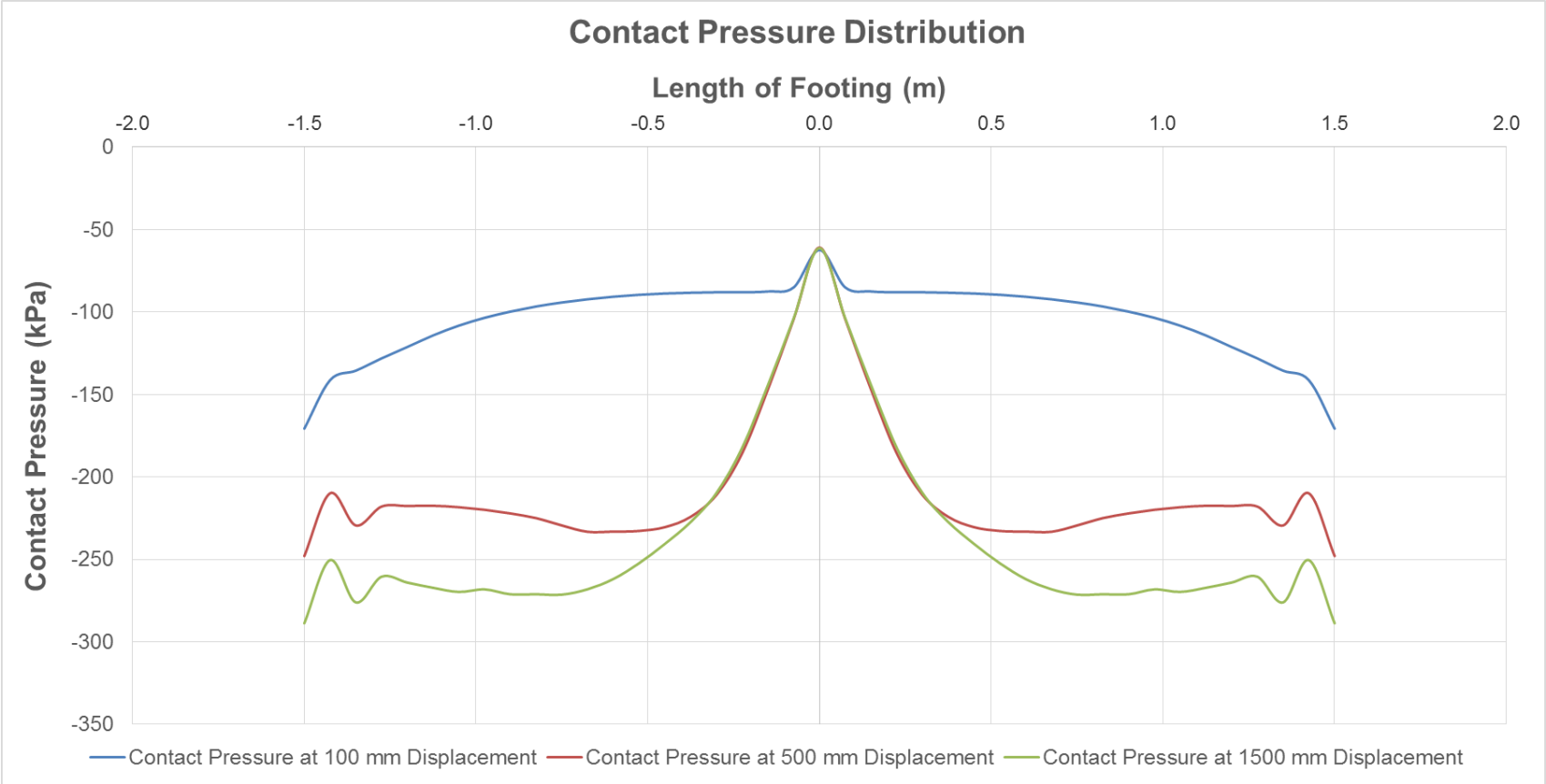


*Figure E-2: Contact pressure distribution (40 kPa native clay; 1 m embedment depth)*

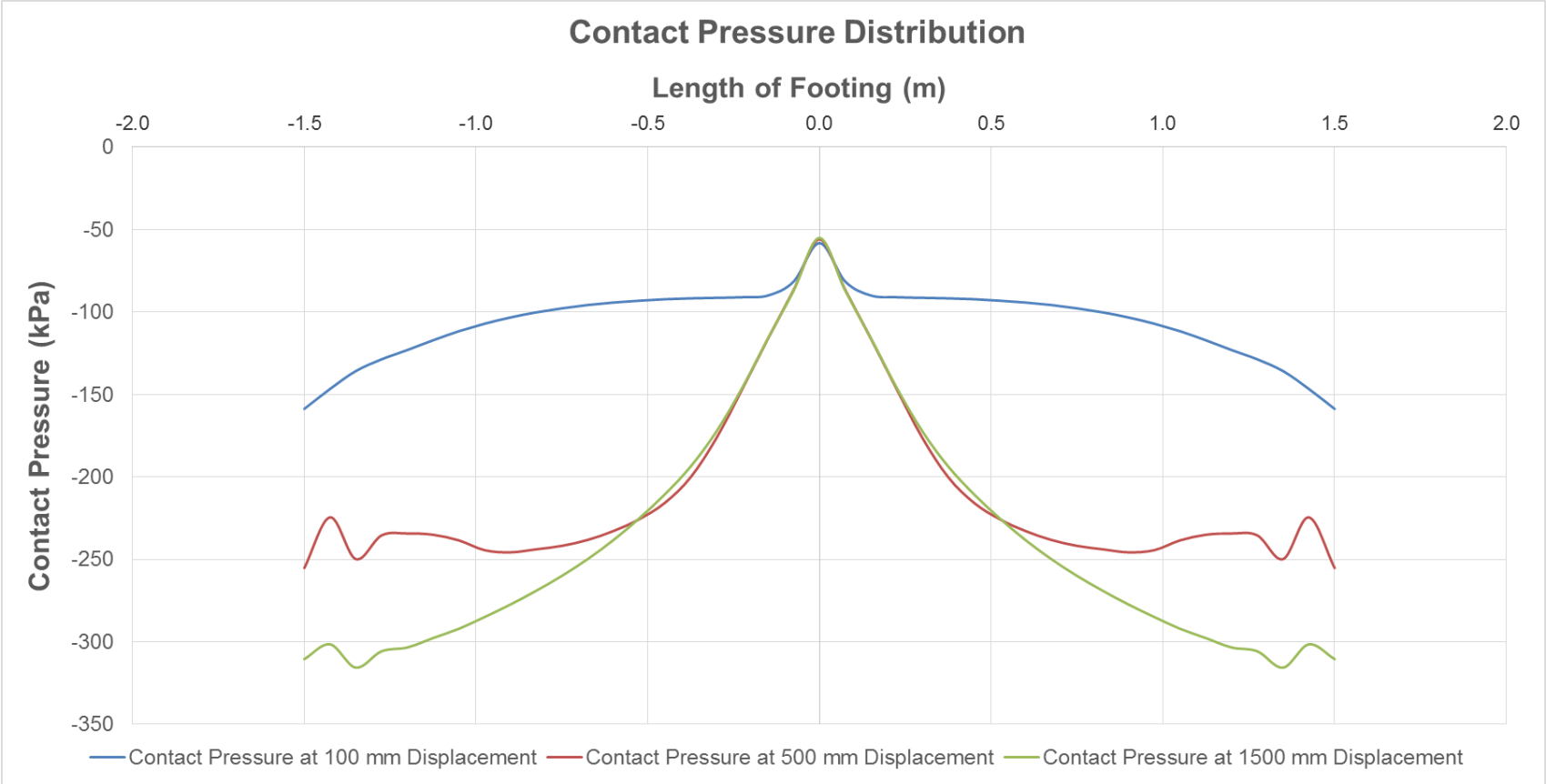


*Figure E-3: Contact pressure distribution (40 kPa native clay; 1.5 m embedment depth)*

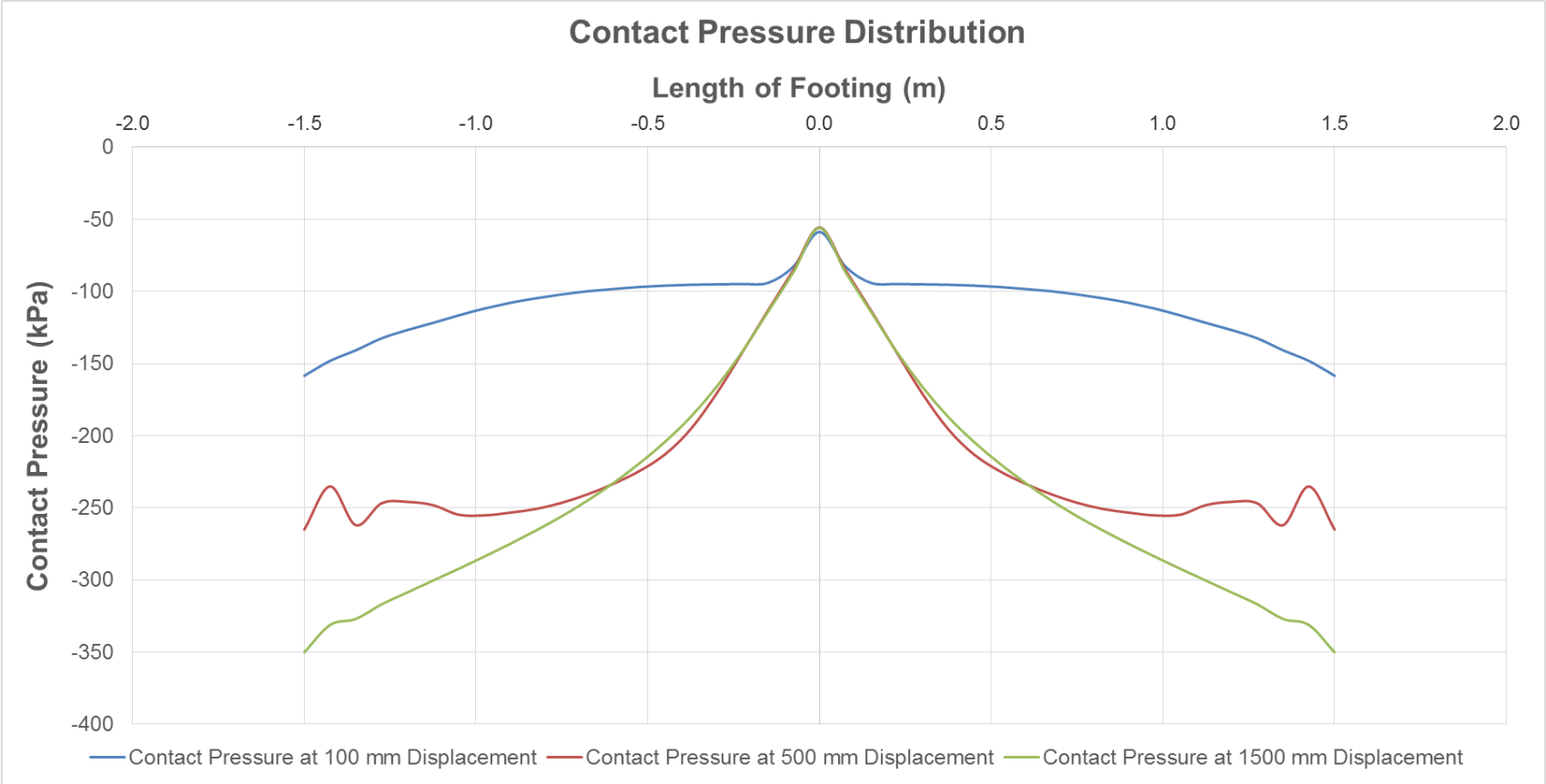


*Figure E-4: Contact pressure distribution (40 kPa native clay; 2 m embedment depth)*

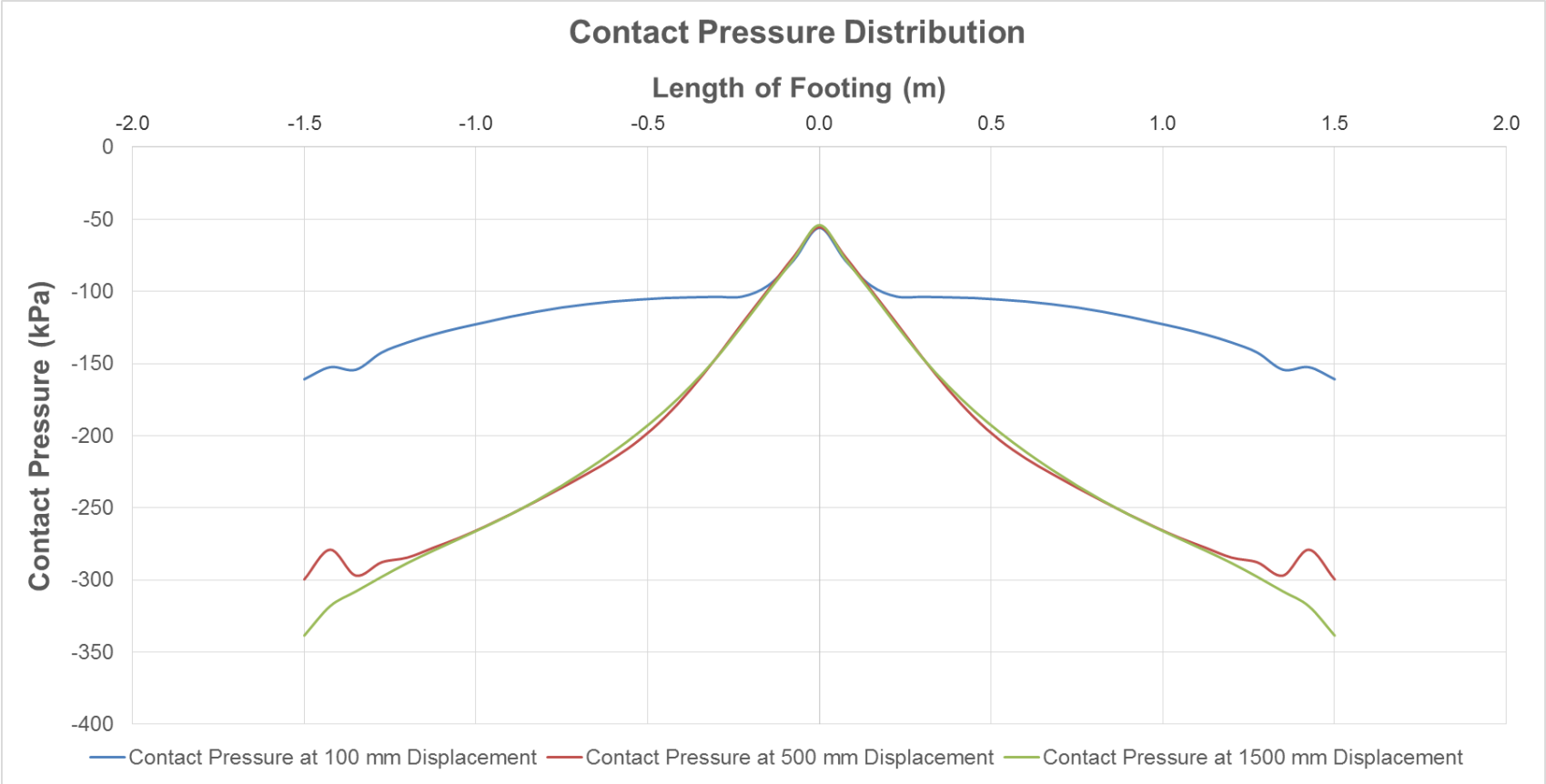


*Figure E-5: Contact pressure distribution (40 kPa native clay; 3 m embedment depth)*

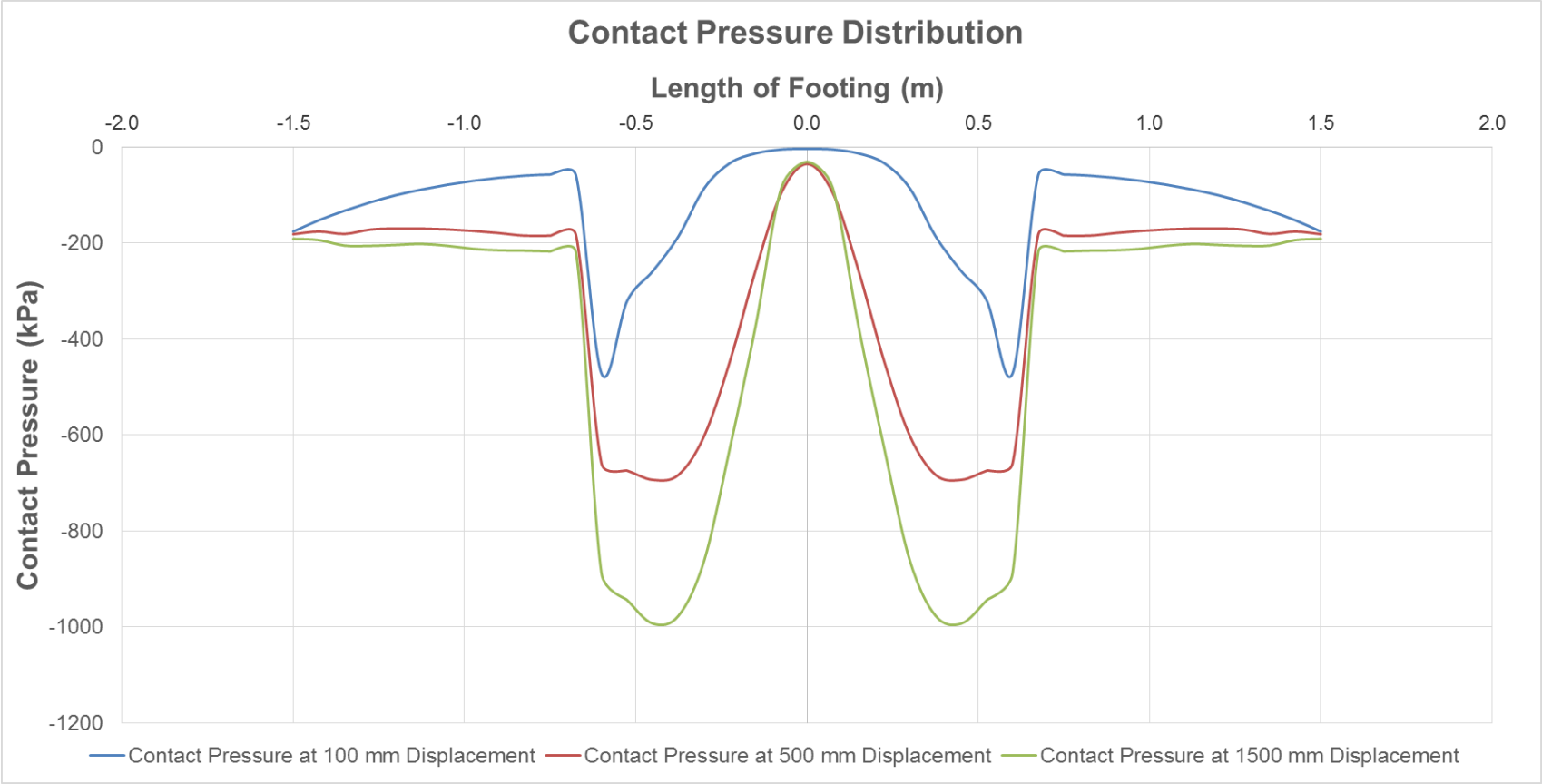


*Figure E-6: Contact pressure distribution (single 7.21 m long, 0.9 m wide trench in 40 kPa native clay; no embedment depth)*

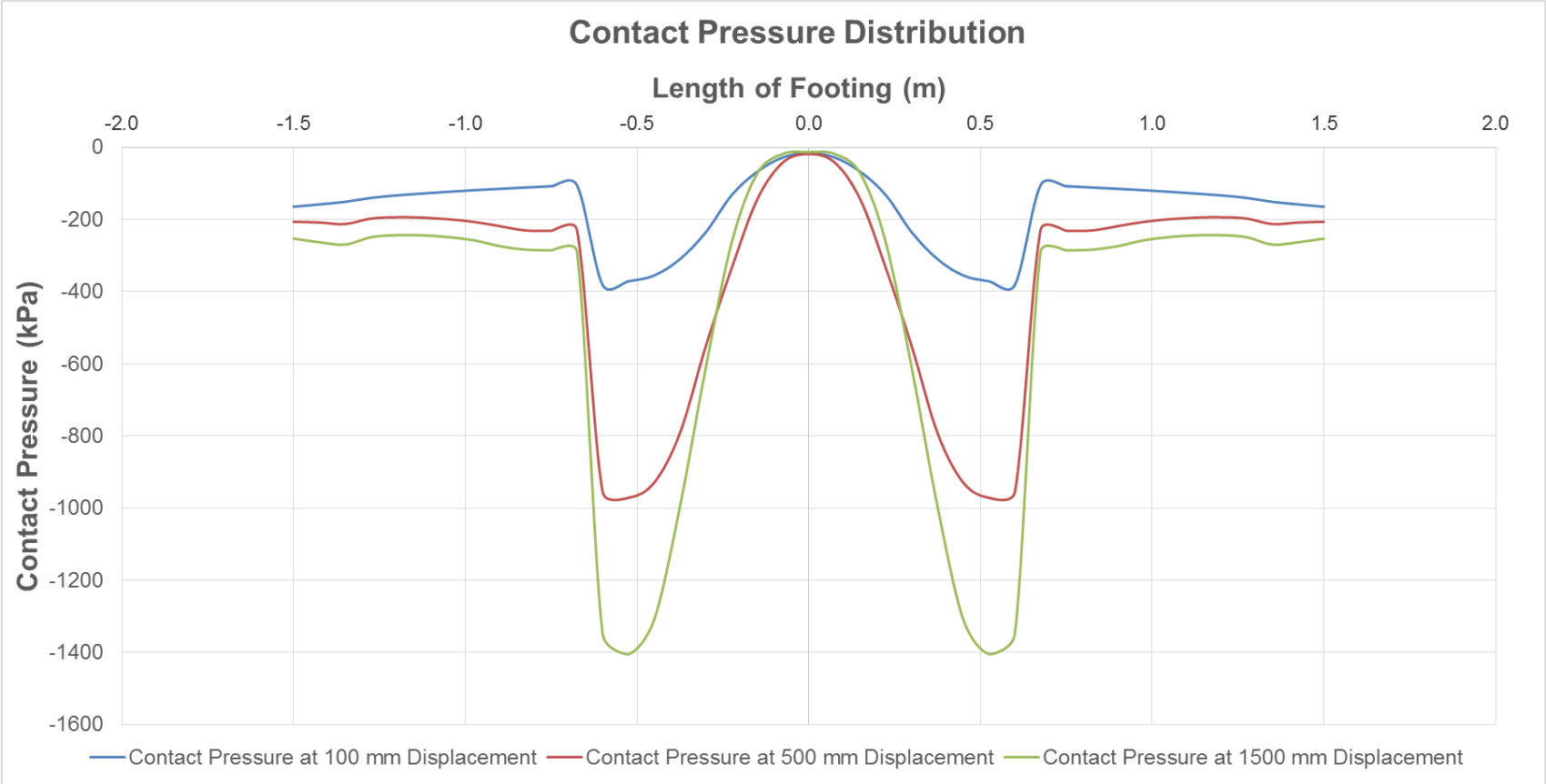


*Figure E-7: Contact pressure distribution (single 7.21 m long, 0.9 m wide trench in 40 kPa native clay; 3 m embedment depth)*

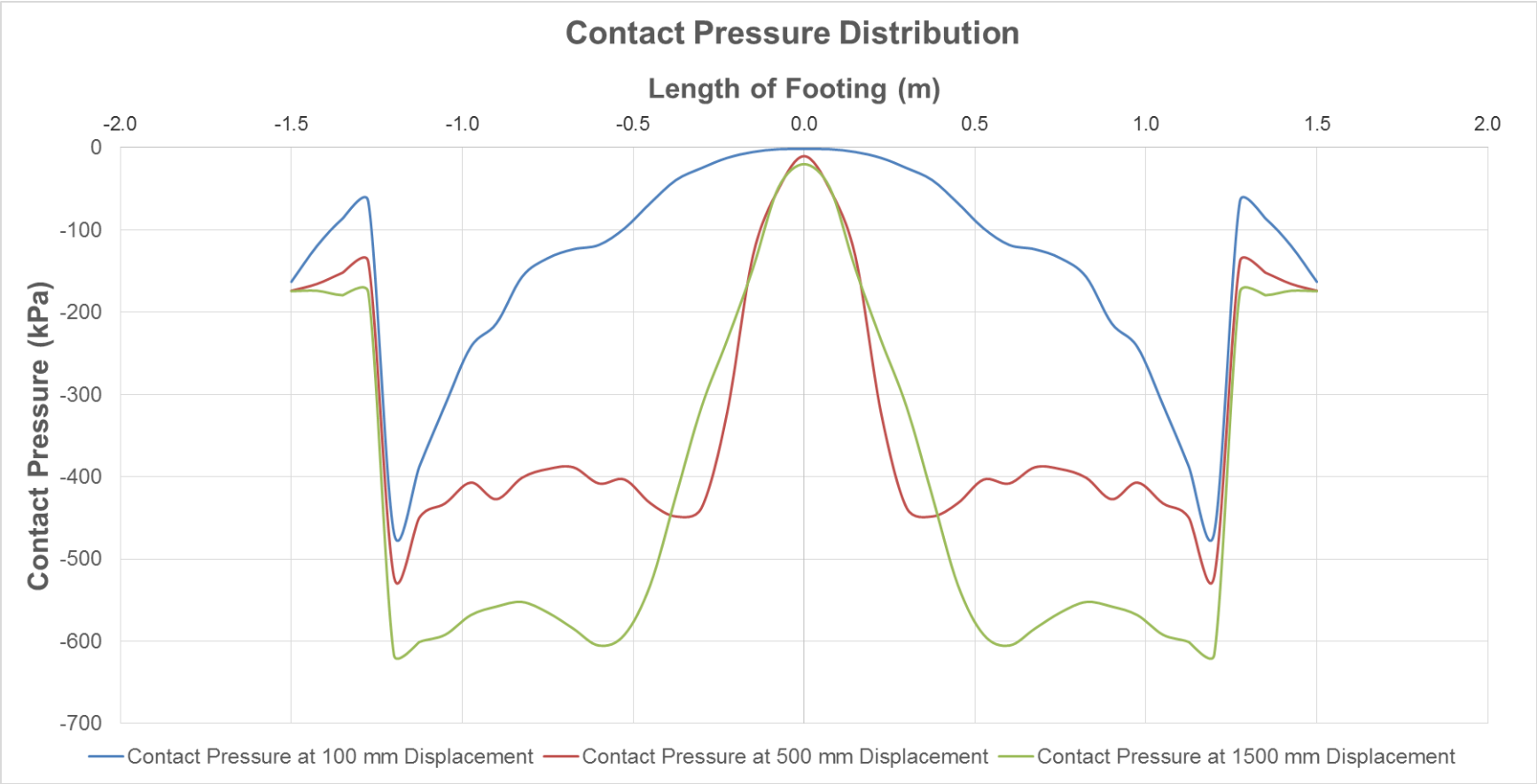


*Figure E-8: Contact pressure distribution (single 6.77 m long, 2.26 m wide trench in 40 kPa native clay; no embedment depth)*

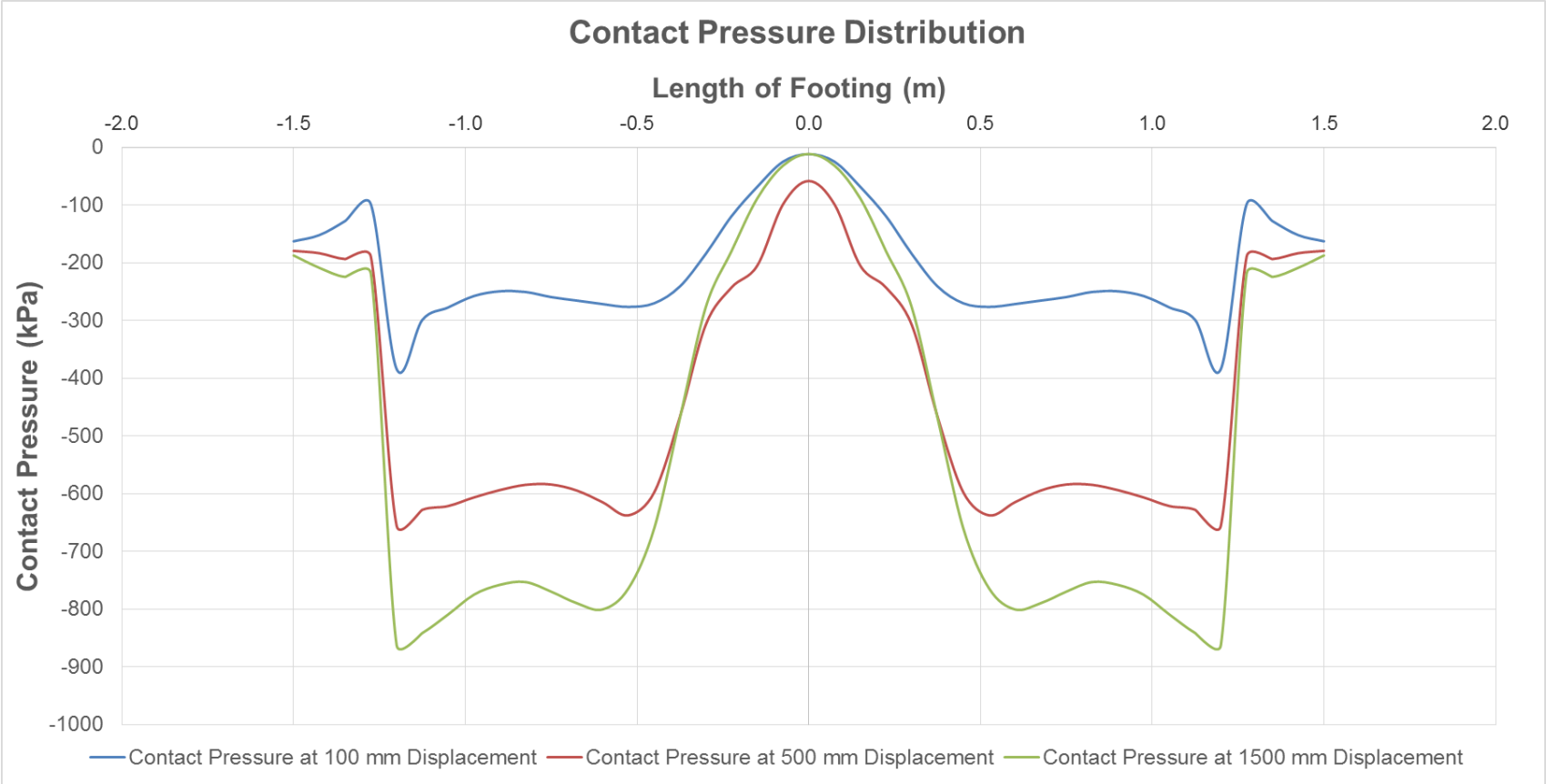


*Figure E-9: Contact pressure distribution (single 6.77 m long, 2.26 m wide trench in 40 kPa native clay; 3 m embedment depth)*

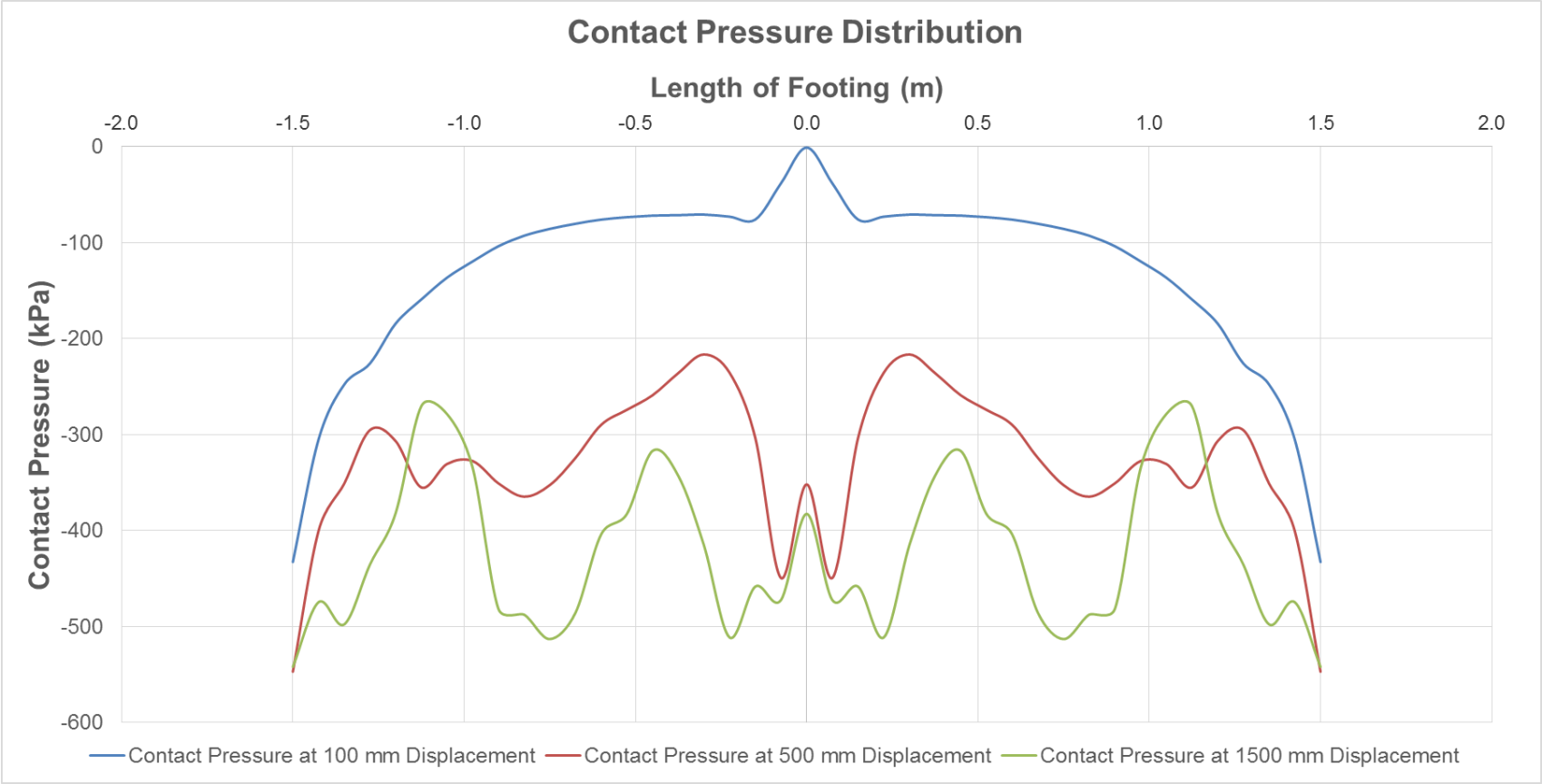


*Figure E-10: Contact pressure distribution (single 6 m long, 3 m wide trench in 40 kPa native clay; no embedment depth)*

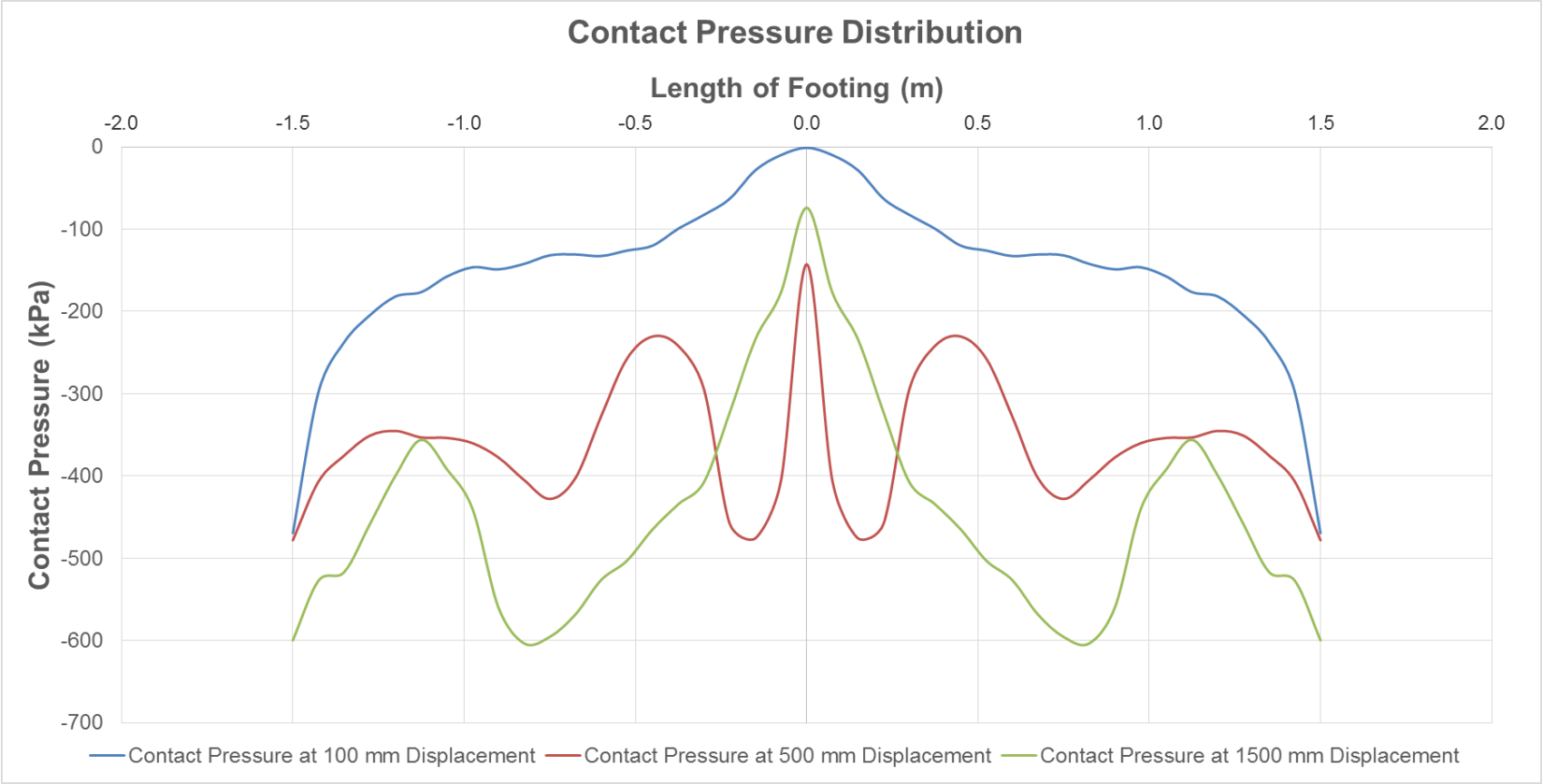


*Figure E-11: Contact pressure distribution (single 6 m long, 3 m wide trench in 40 kPa native clay; 1 m embedment depth)*

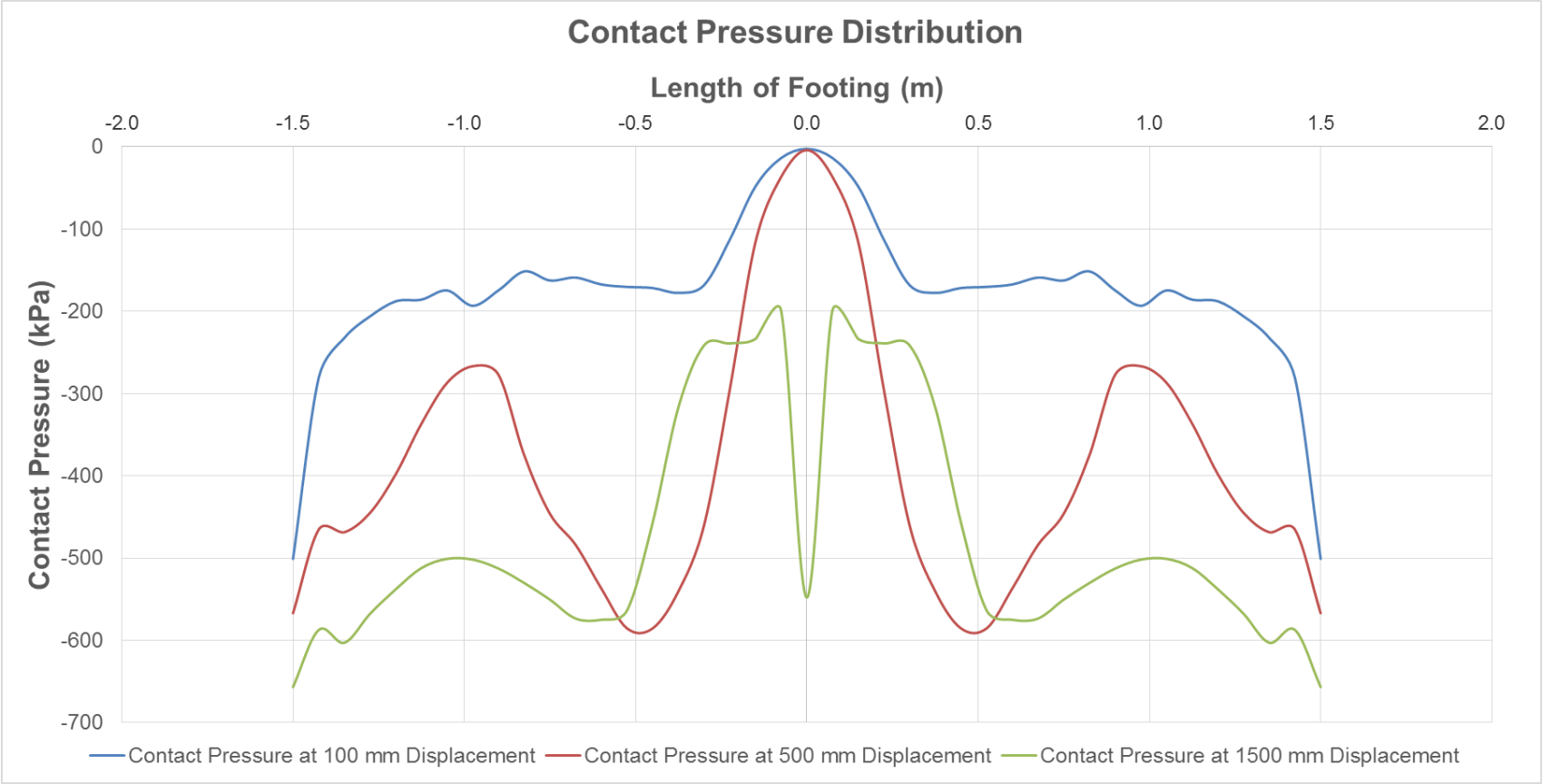


*Figure E-12: Contact pressure distribution (single 6 m long, 3 m wide trench in 40 kPa native clay; 2 m embedment depth)*

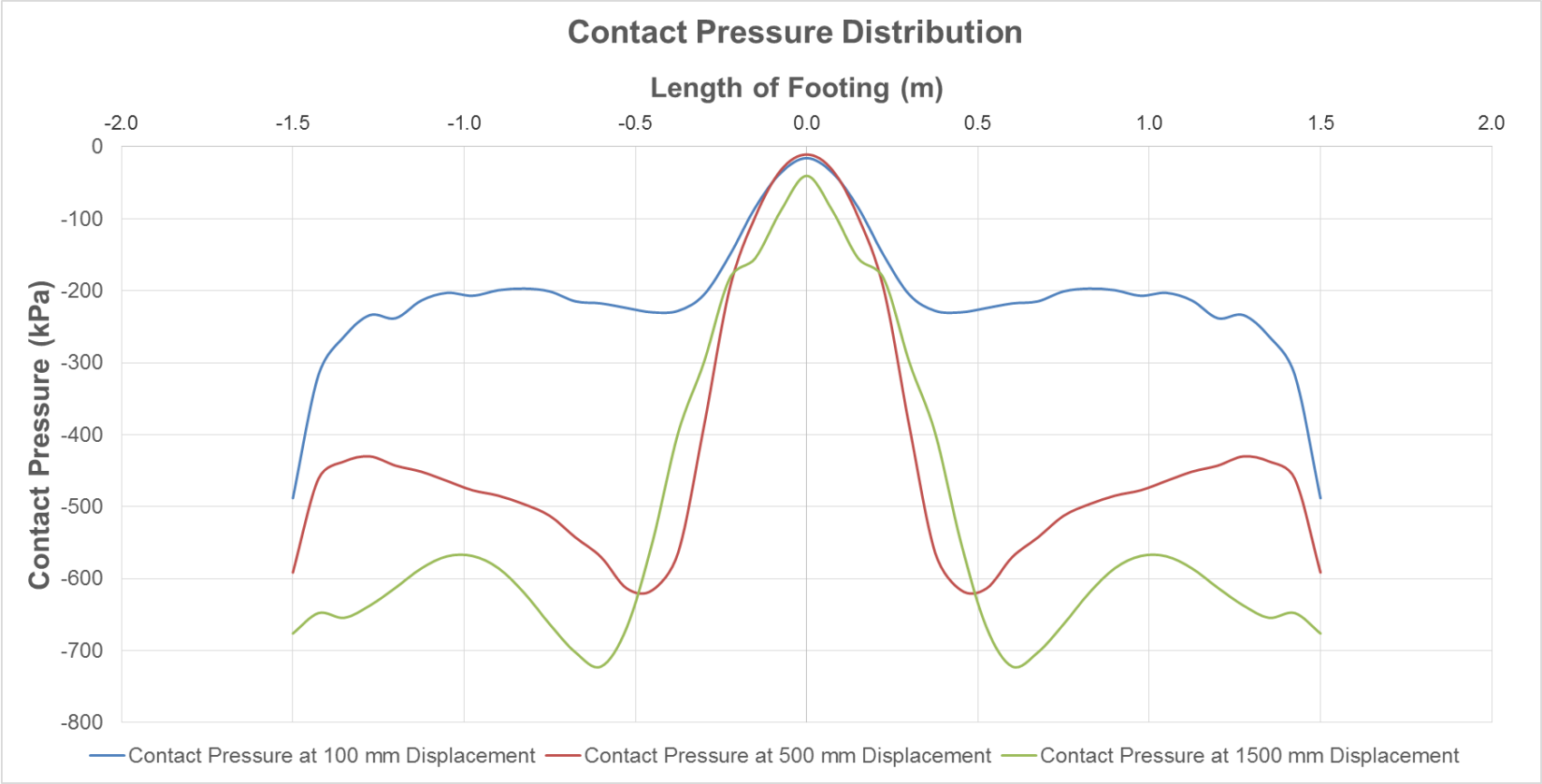


*Figure E-13: Contact pressure distribution (single 6 m long, 3 m wide trench in 40 kPa native clay; 3 m embedment depth)*

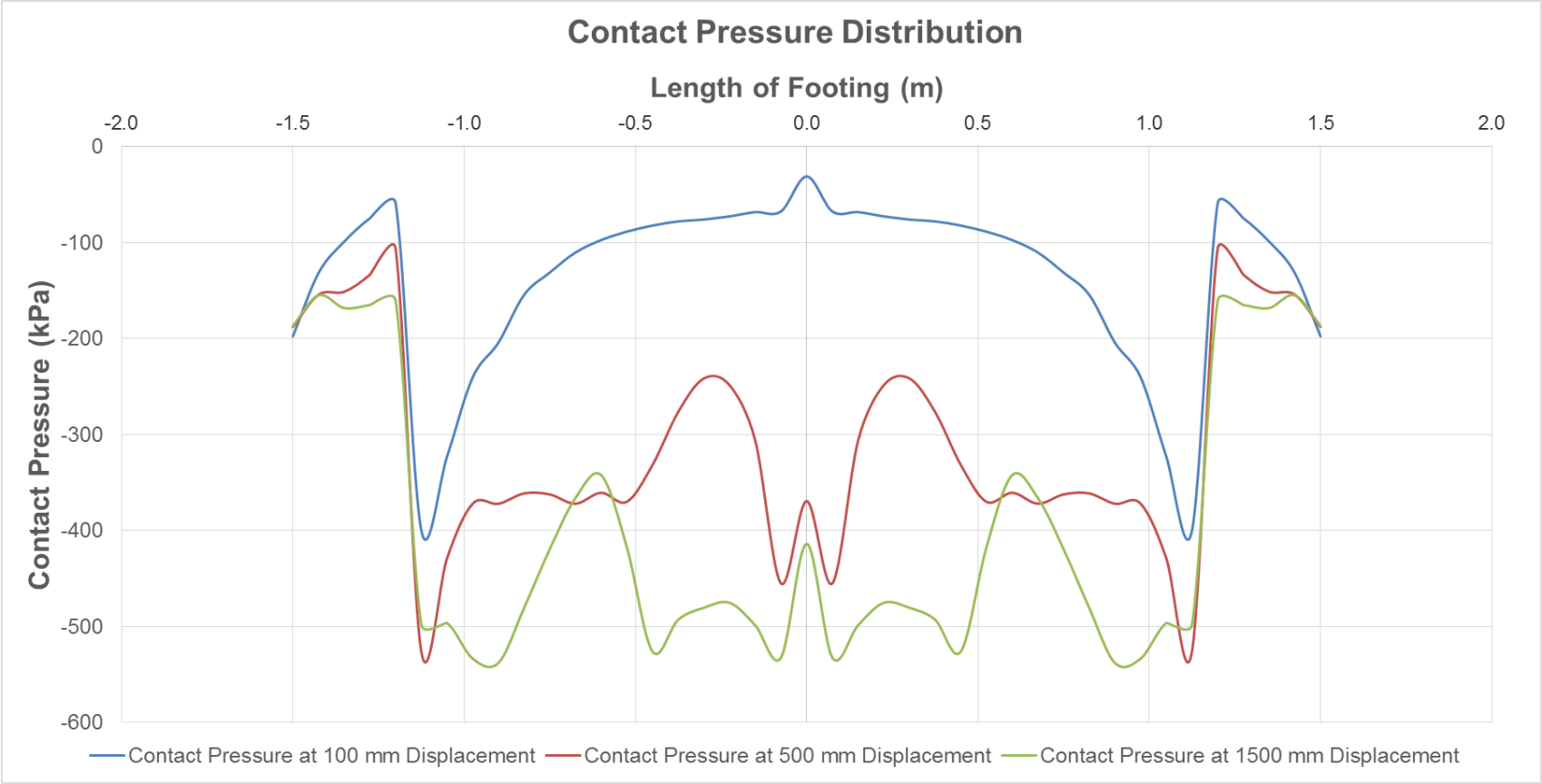


*Figure E-14: Contact pressure distribution (single 6 m long, 2 m wide trench in 40 kPa native clay; no embedment depth)*

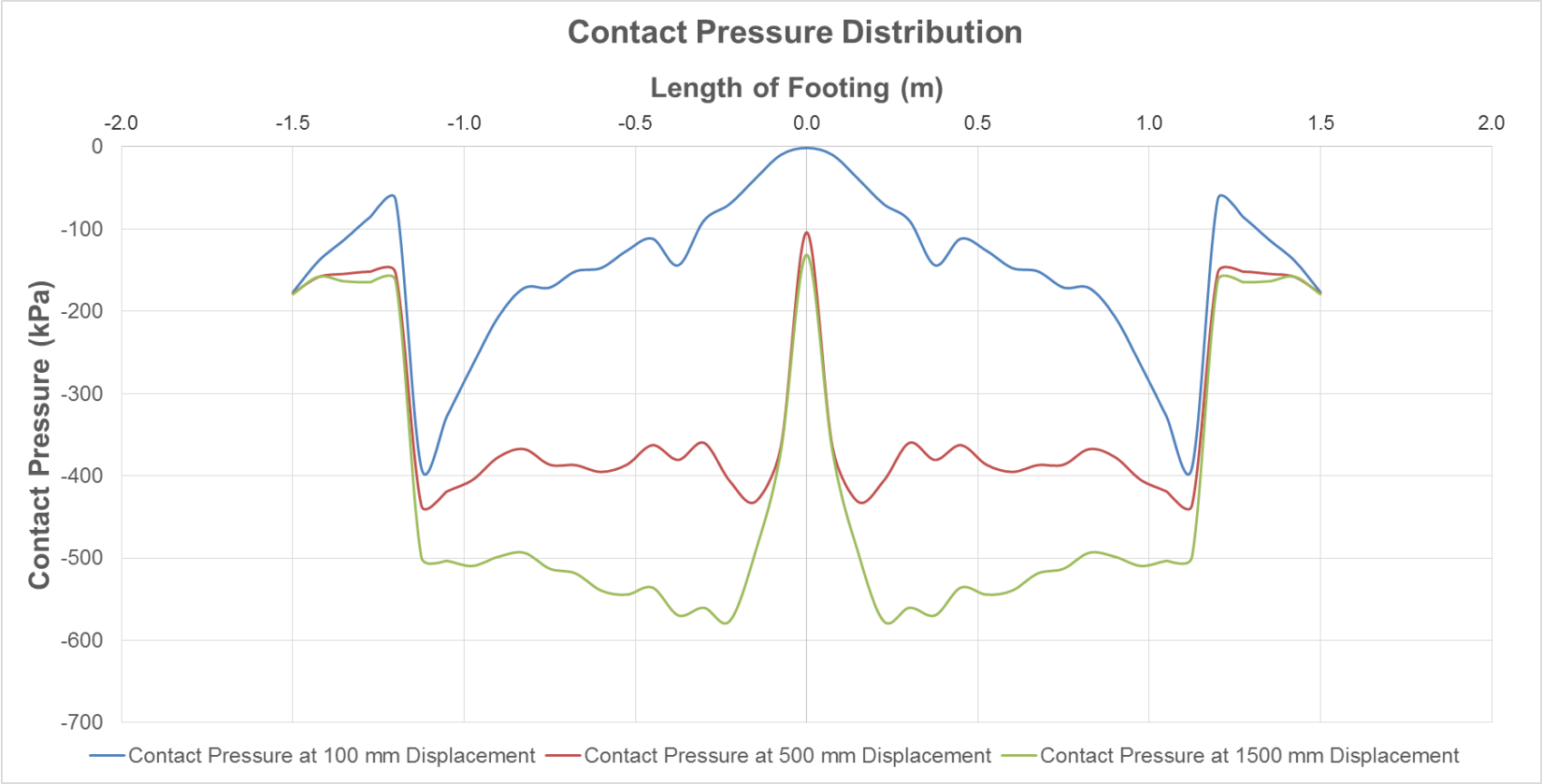


*Figure E-15: Contact pressure distribution (single 6 m long, 2 m wide trench in 40 kPa native clay; 1 m embedment depth)*

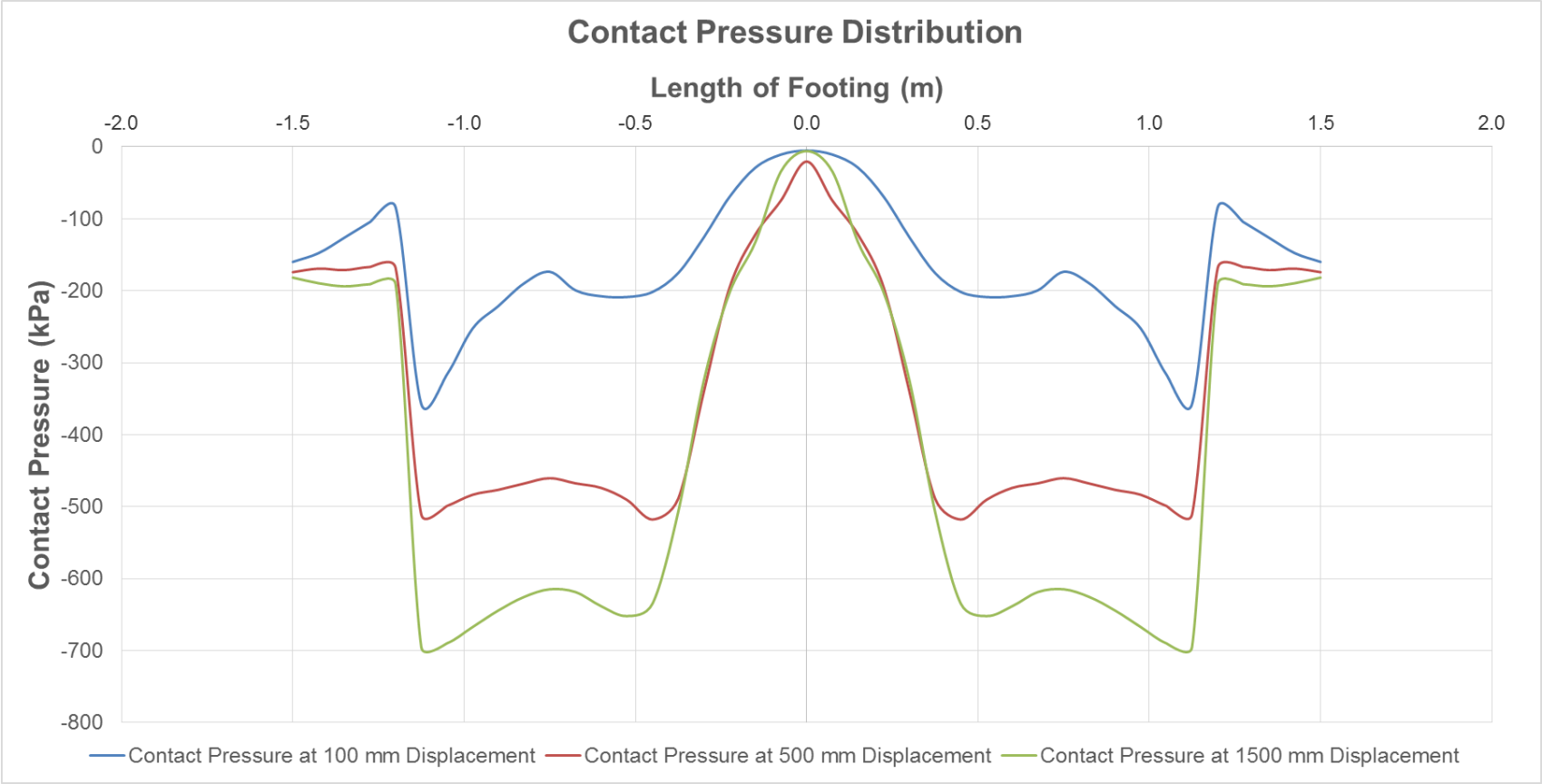


*Figure E-16: Contact pressure distribution (single 6 m long, 2 m wide trench in 40 kPa native clay; 2 m embedment depth)*

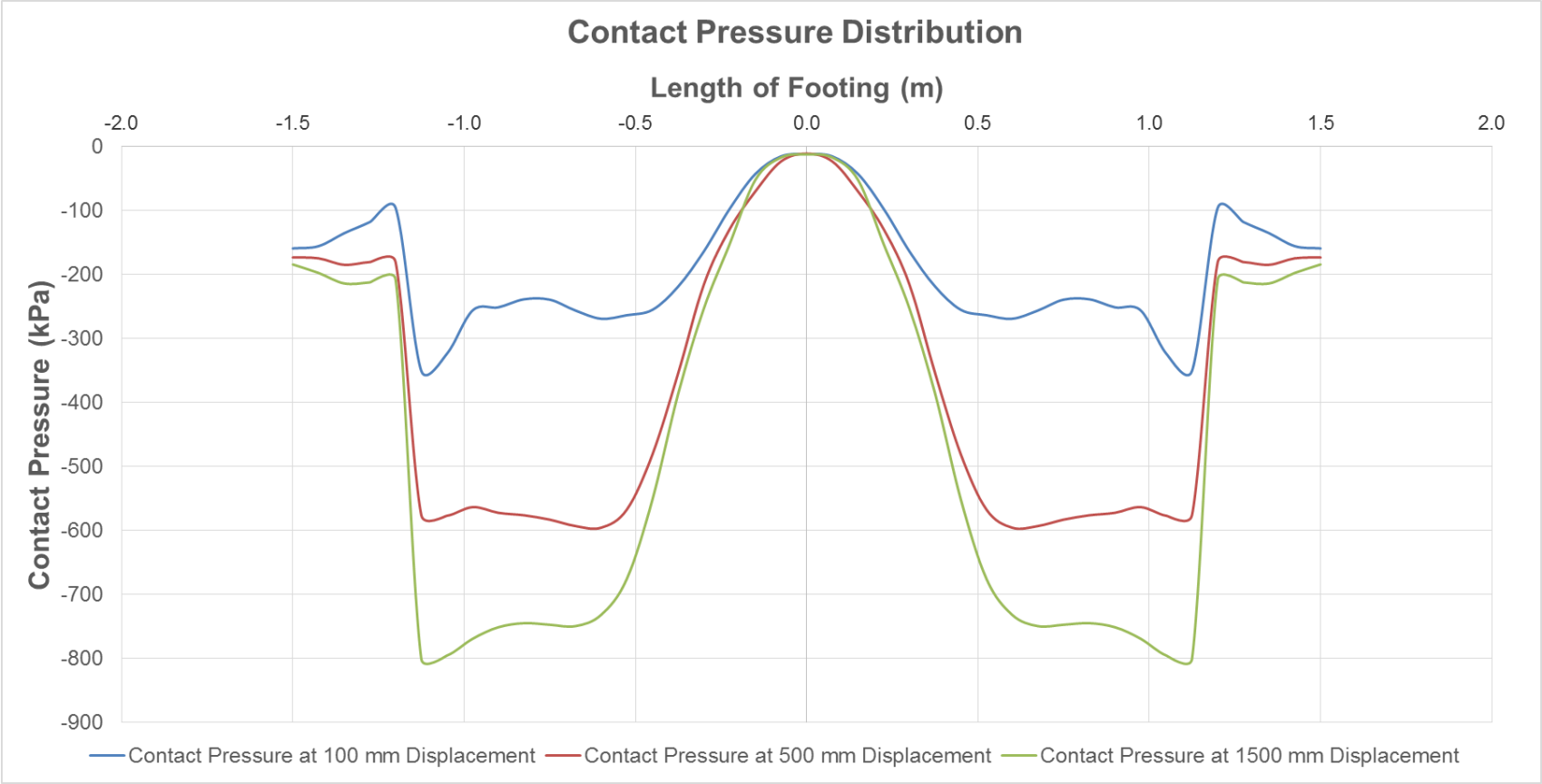


*Figure E-17: Contact pressure distribution (single 6 m long, 2 m wide trench in 40 kPa native clay; 3 m embedment depth)*

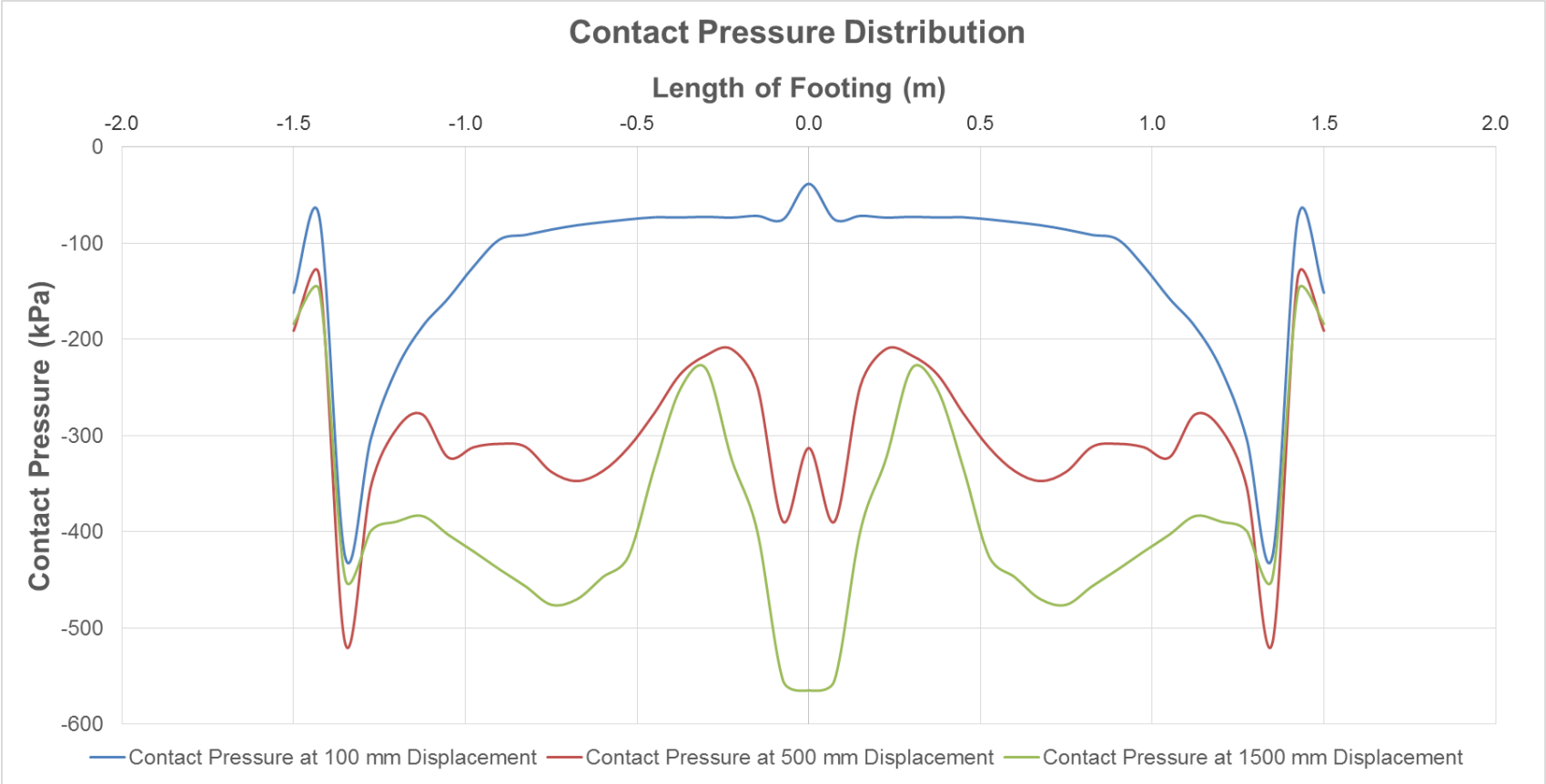


*Figure E-18: Contact pressure distribution (single 5.22 m long, 2.61 m wide trench in 40 kPa native clay; no embedment depth)*

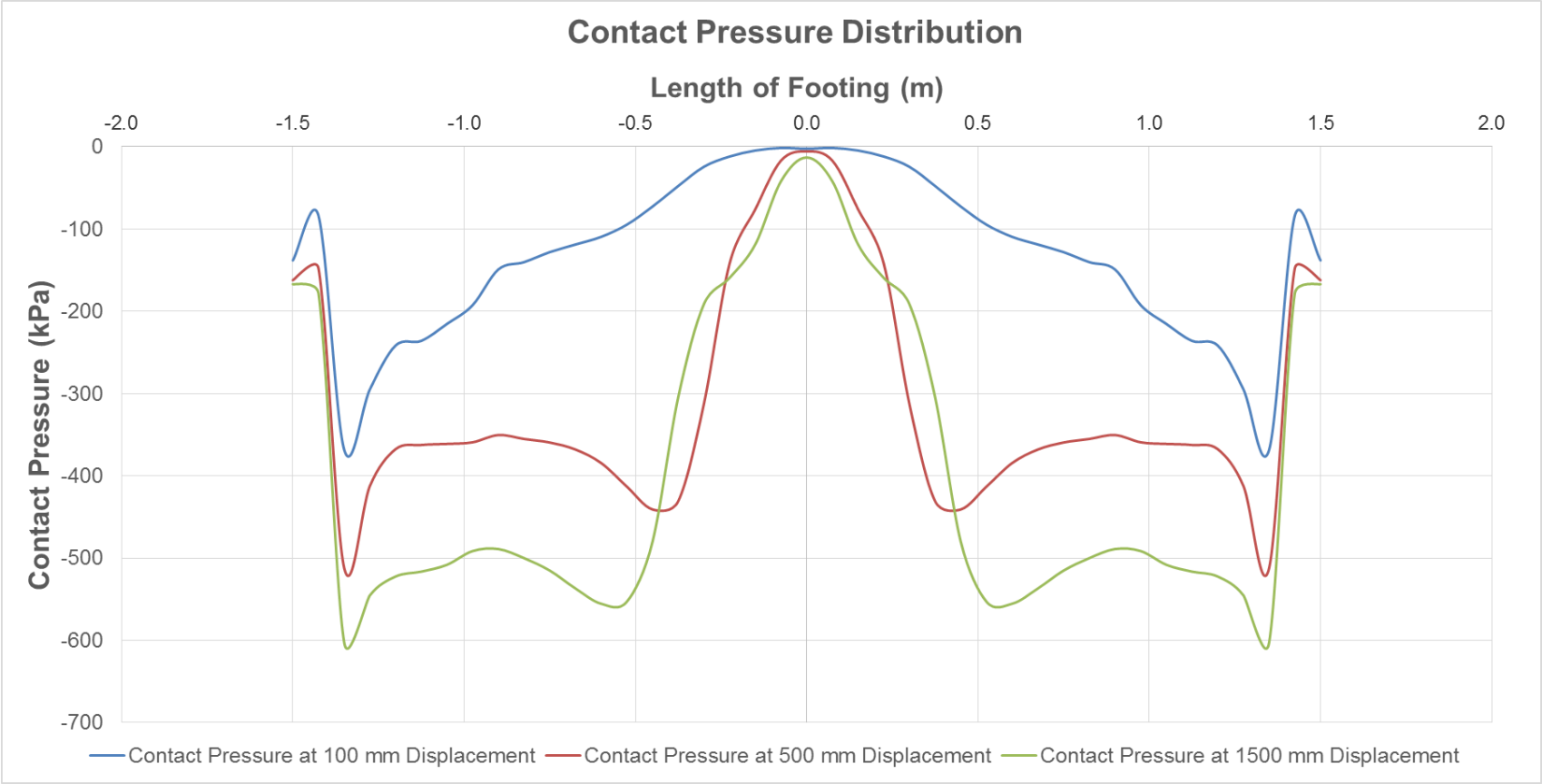


*Figure E-19: Contact pressure distribution (single 5.22 m long, 2.61 m wide trench in 40 kPa native clay; 1 m embedment depth)*

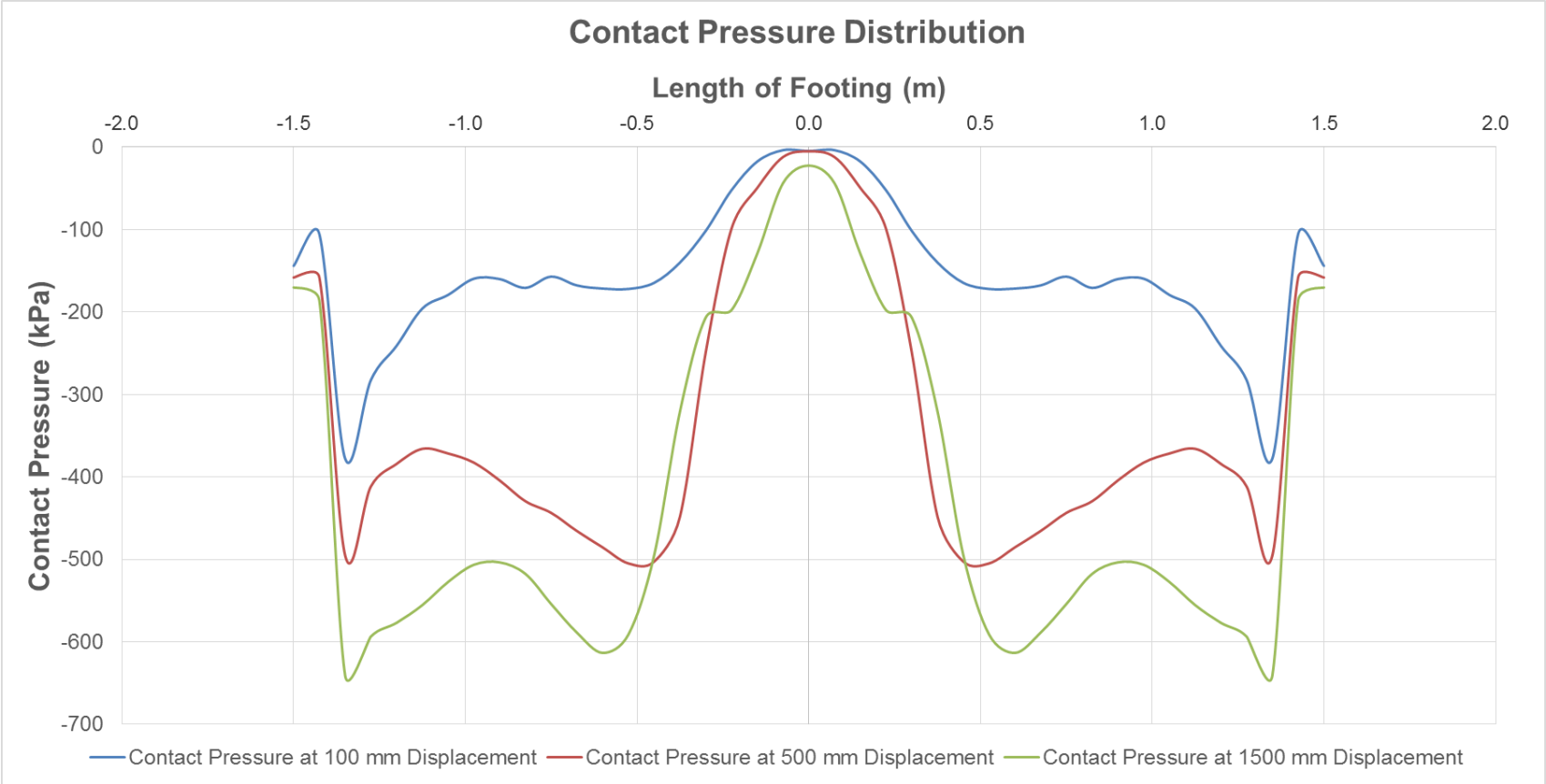


*Figure E-20: Contact pressure distribution (single 5.22 m long, 2.61 m wide trench in 40 kPa native clay; 2 m embedment depth)*

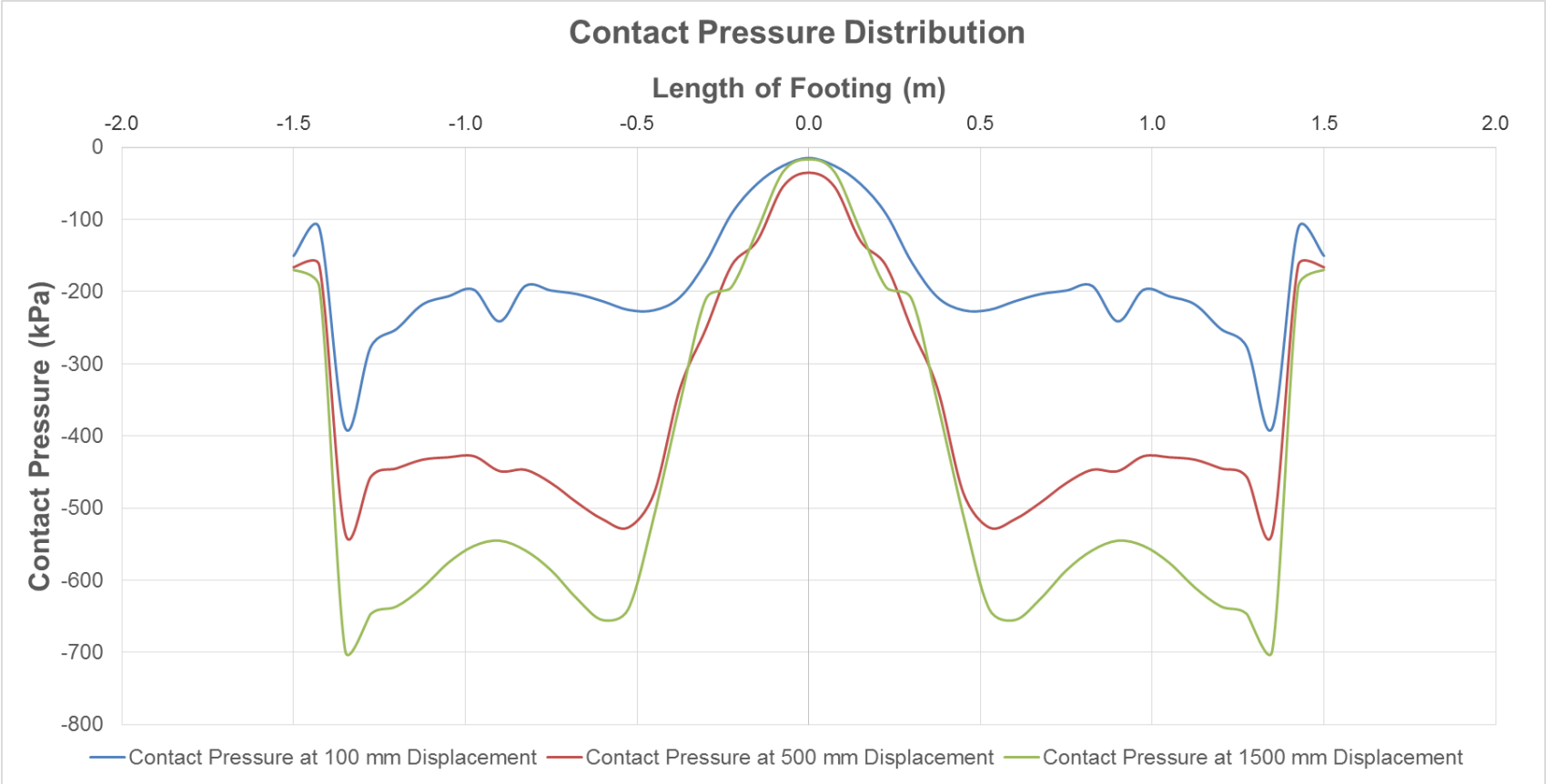


*Figure E-21: Contact pressure distribution (single 5.22 m long, 2.61 m wide trench in 40 kPa native clay; 3 m embedment depth)*

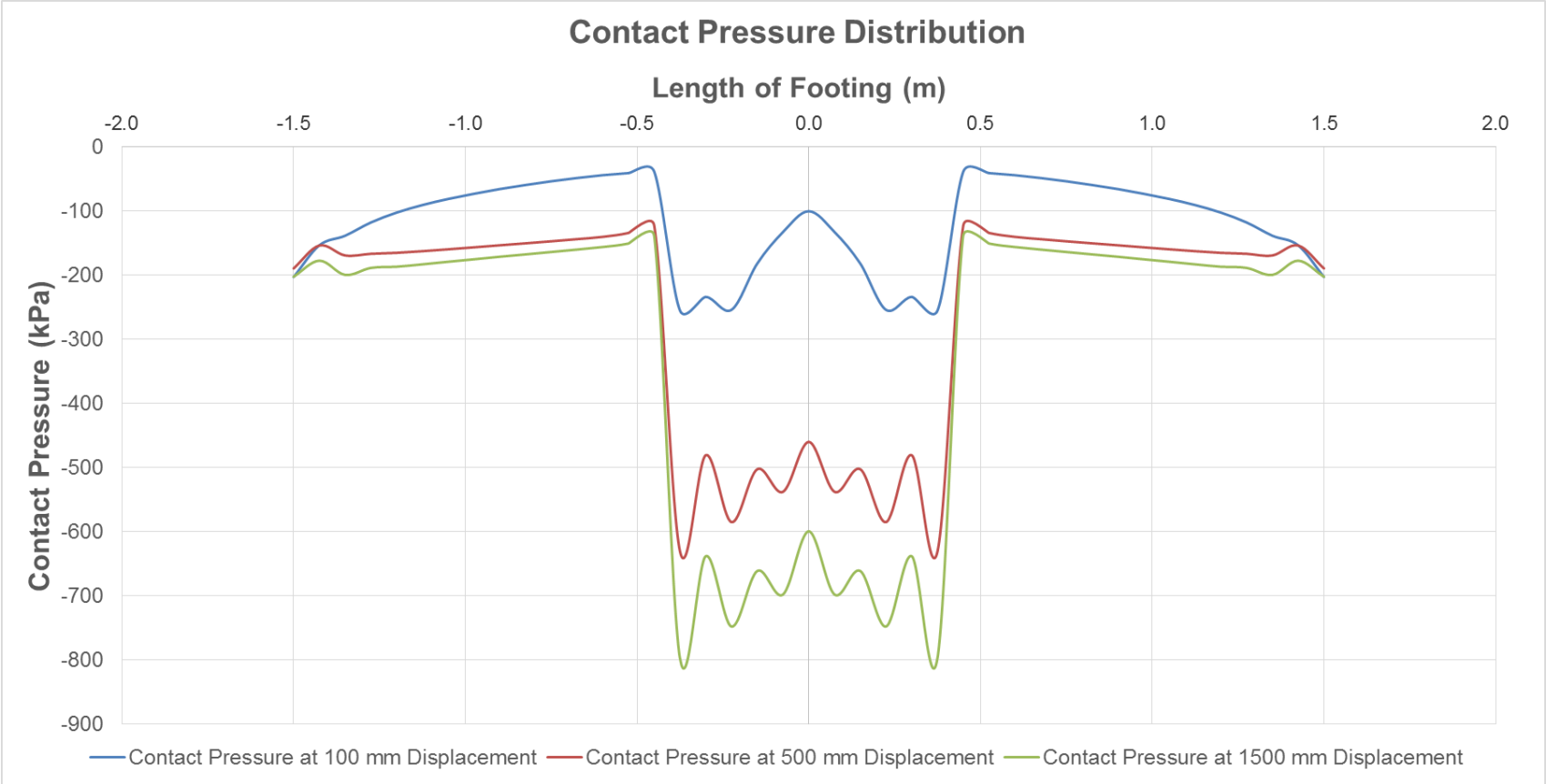


*Figure E-22: Contact pressure distribution (single 4.8 m long, 0.6 m wide trench in 40 kPa native clay; no embedment depth)*

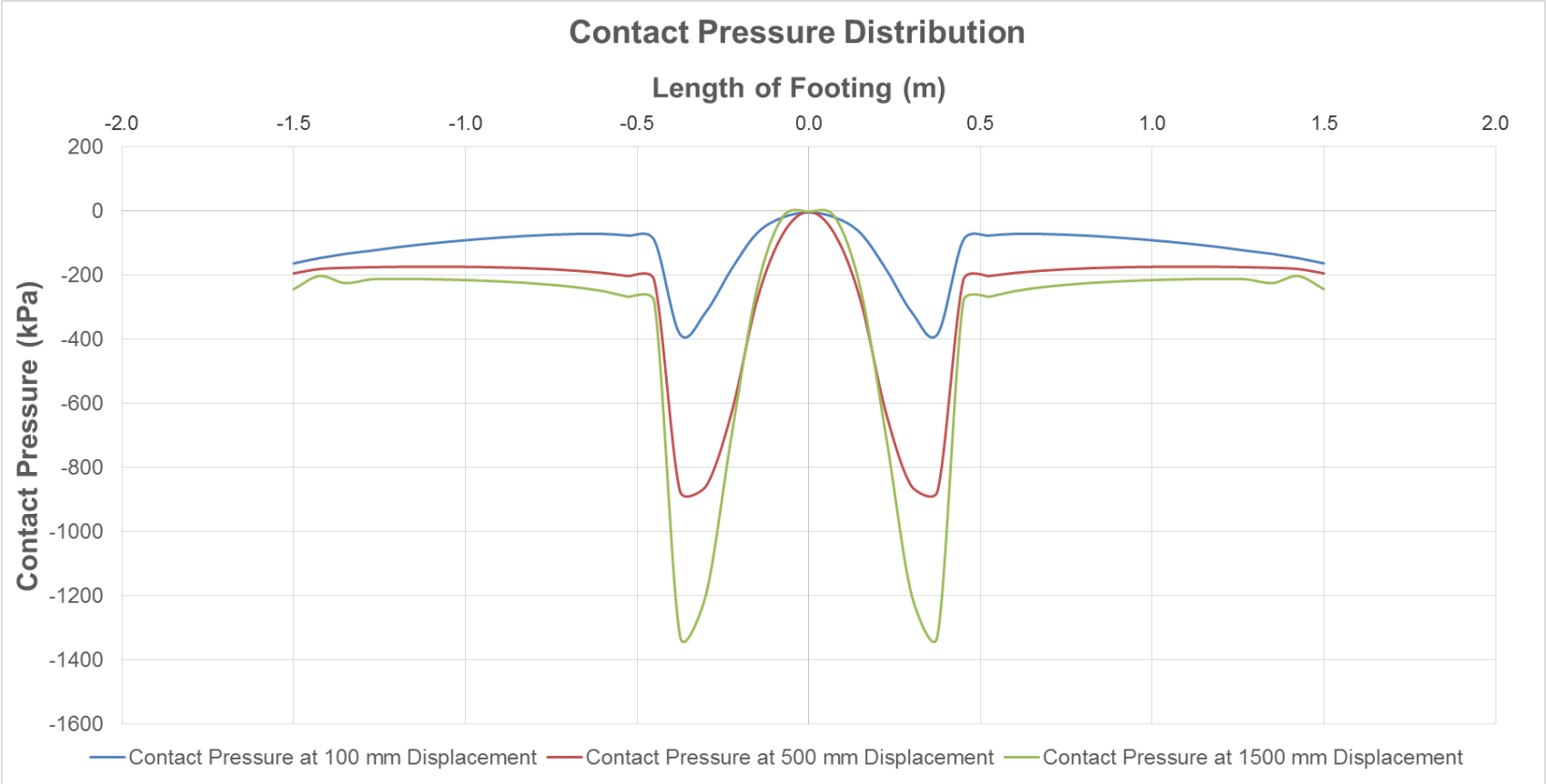


*Figure E-23: Contact pressure distribution (single 4.8 m long, 0.6 m wide trench in 40 kPa native clay; 1 m embedment depth)*

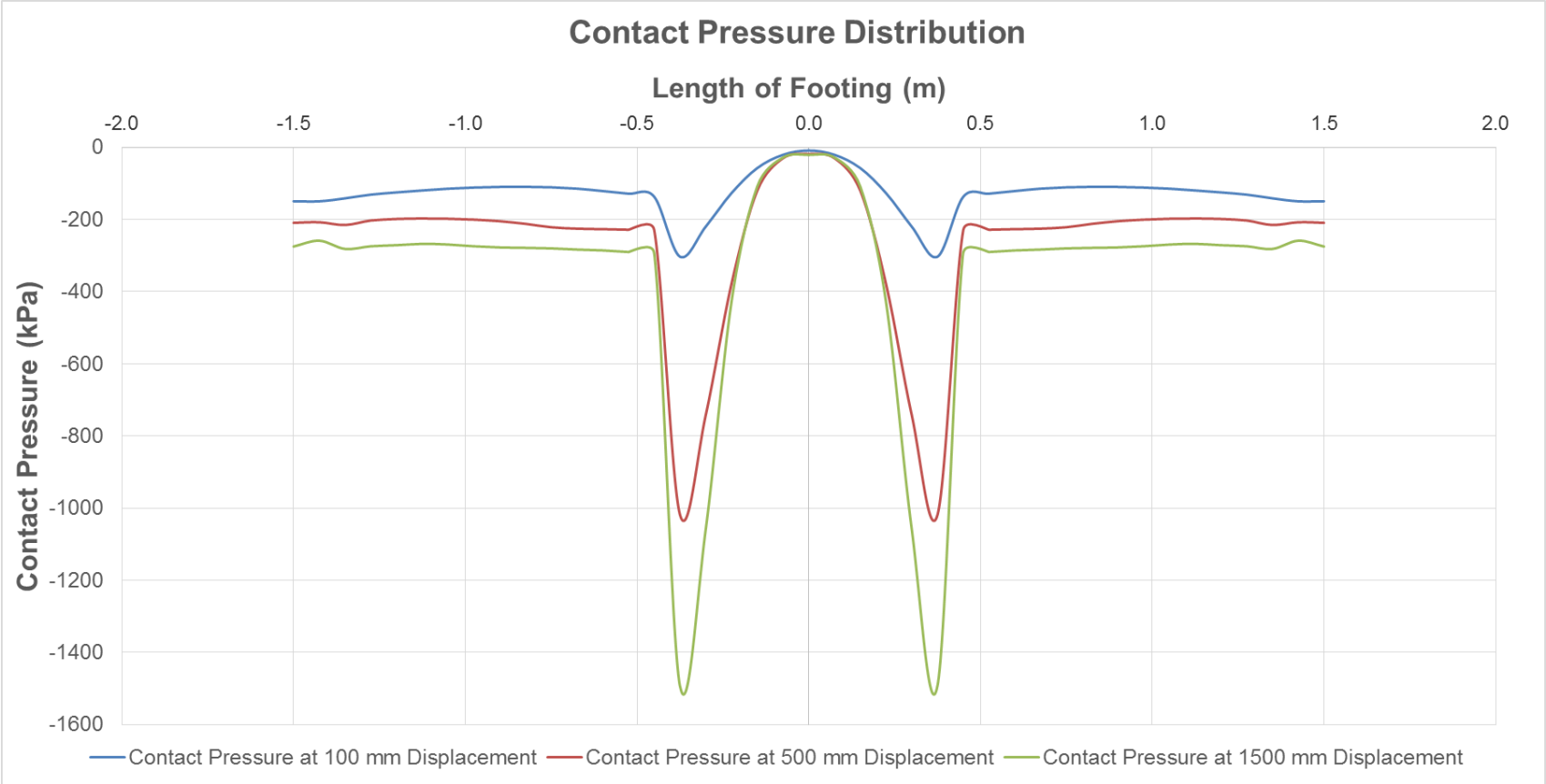


*Figure E-24: Contact pressure distribution (single 4.8 m long, 0.6 m wide trench in 40 kPa native clay; 2 m embedment depth)*

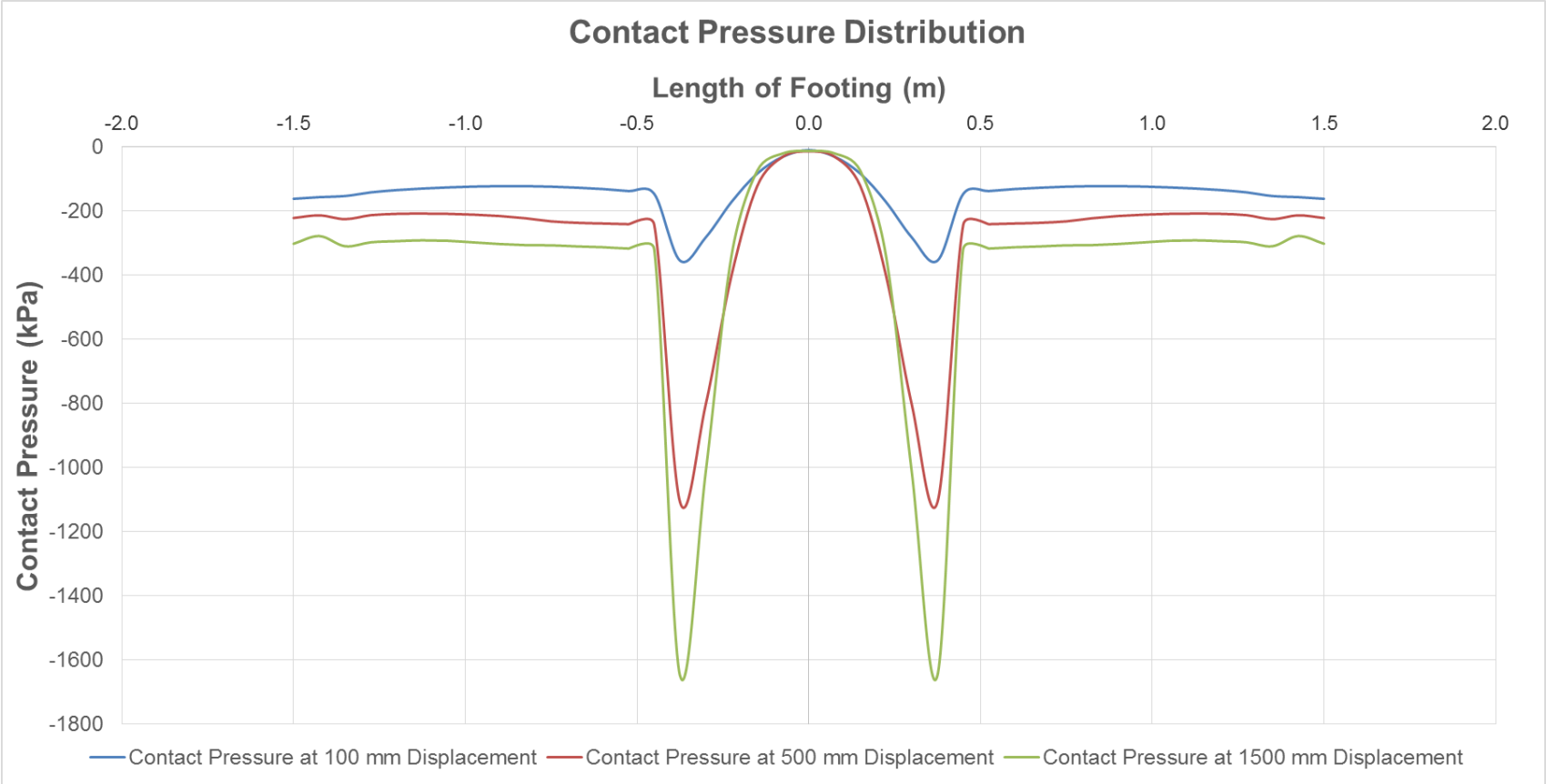


*Figure E-25: Contact pressure distribution (single 4.8 m long, 0.6 m wide trench in 40 kPa native clay; 3 m embedment depth)*

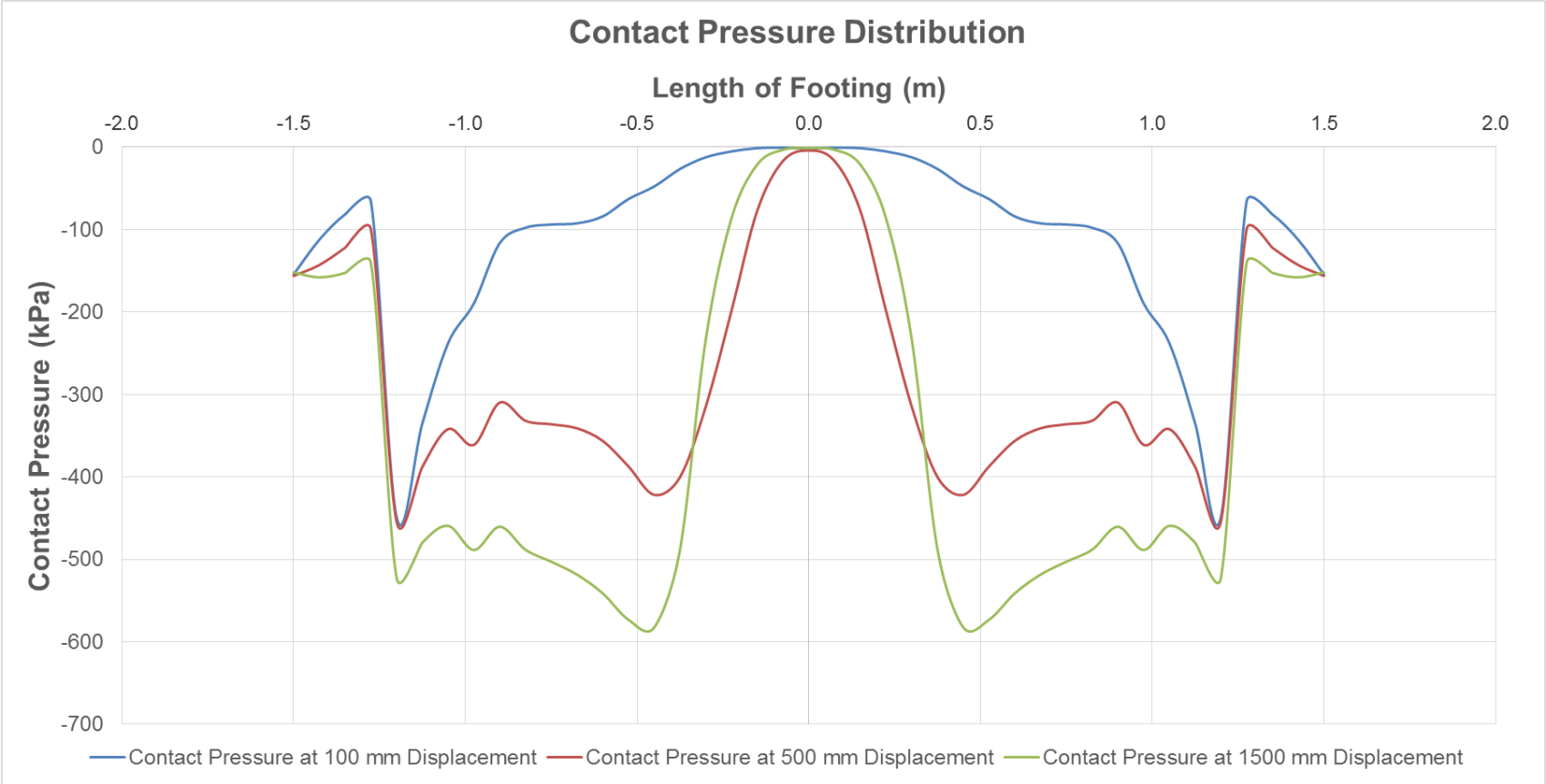


*Figure E-26: Contact pressure distribution (single 4.51 m long, 2.26 m wide trench in 40 kPa native clay; no embedment depth)*

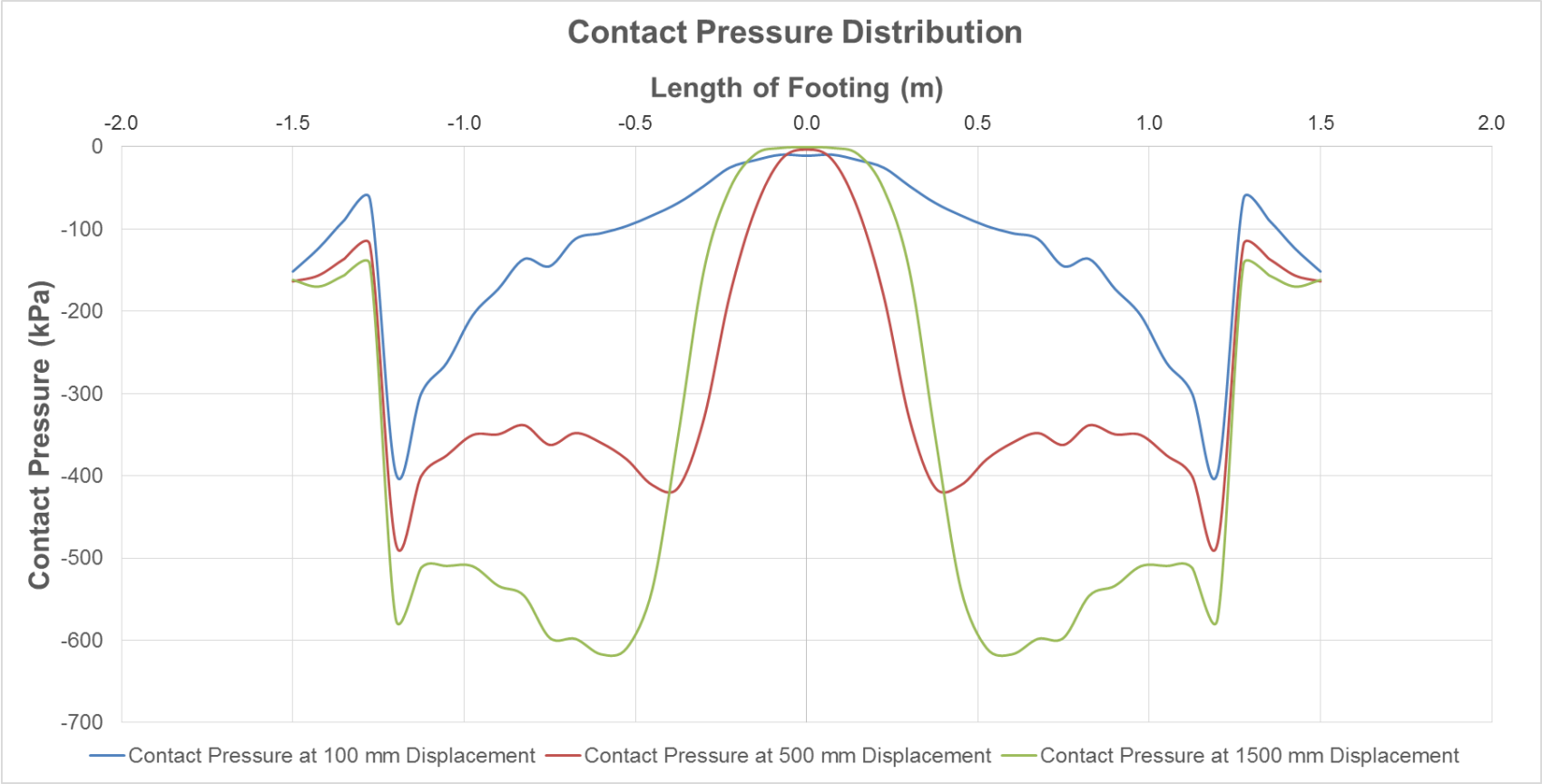


*Figure E-27: Contact pressure distribution (single 4.51 m long, 2.26 m wide trench in 40 kPa native clay; 1 m embedment depth)*

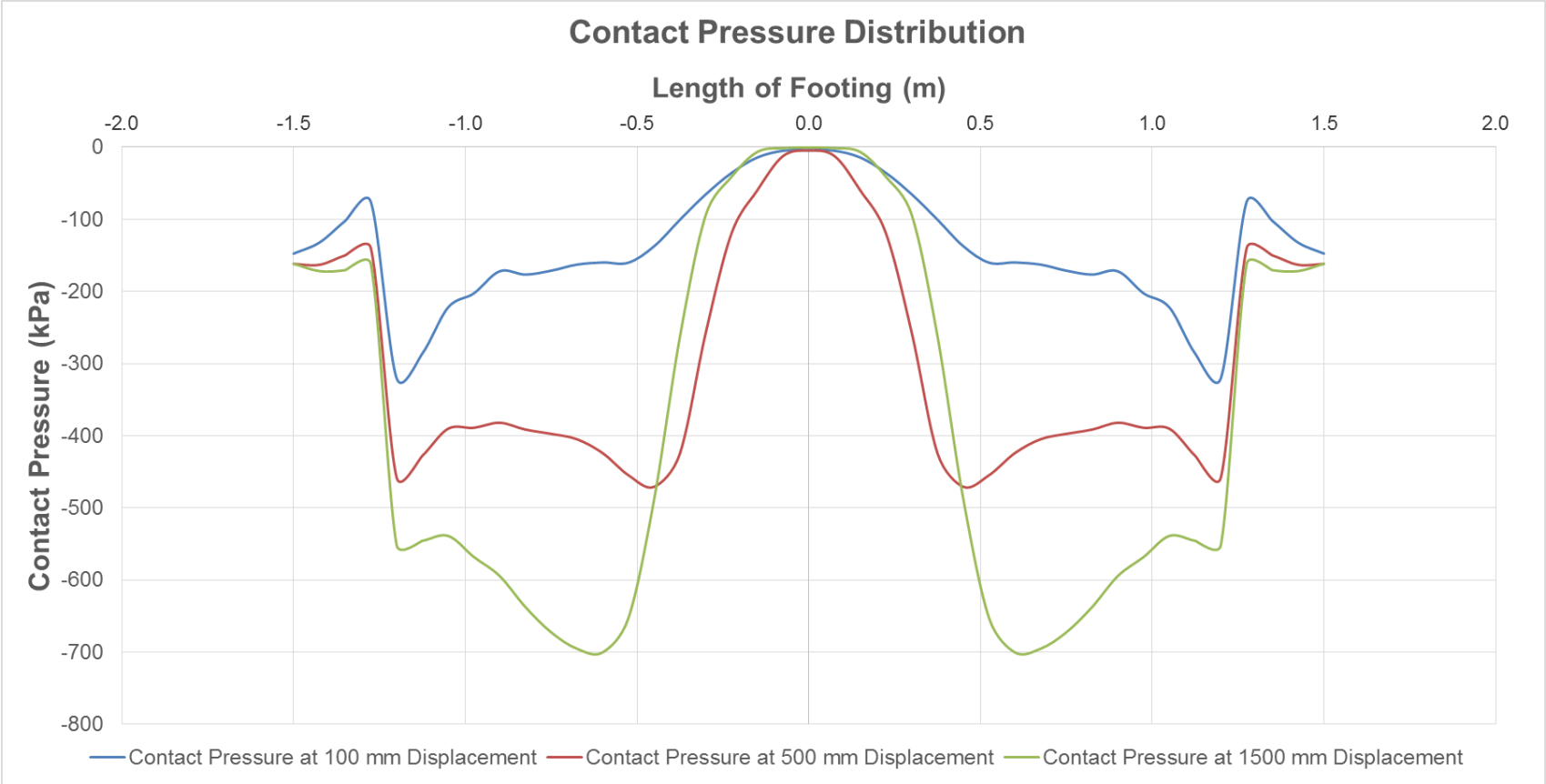


*Figure E-28: Contact pressure distribution (single 4.51 m long, 2.26 m wide trench in 40 kPa native clay; 2 m embedment depth)*

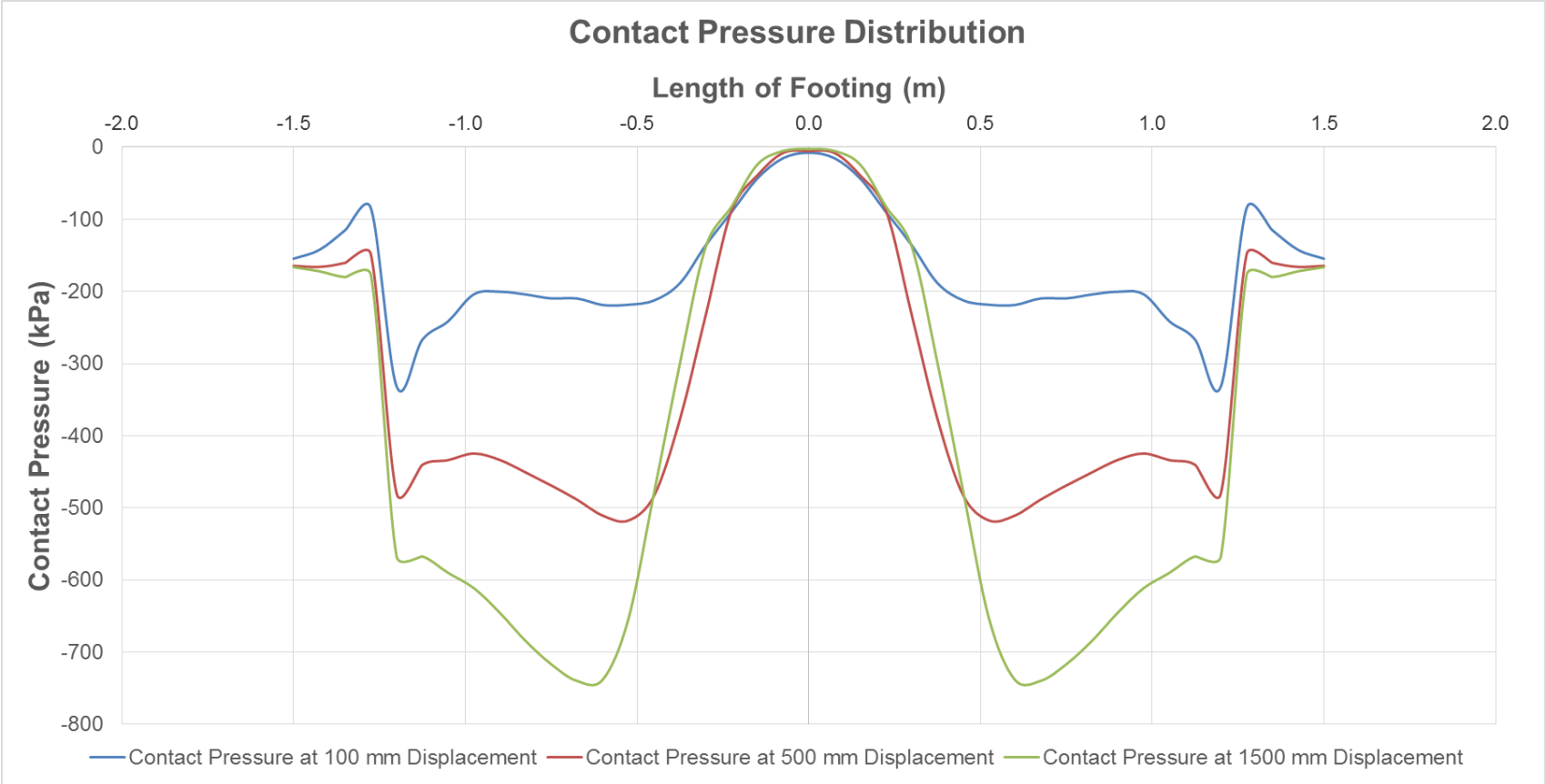


*Figure E-29: Contact pressure distribution (single 4.51 m long, 2.26 m wide trench in 40 kPa native clay; 3 m embedment depth)*

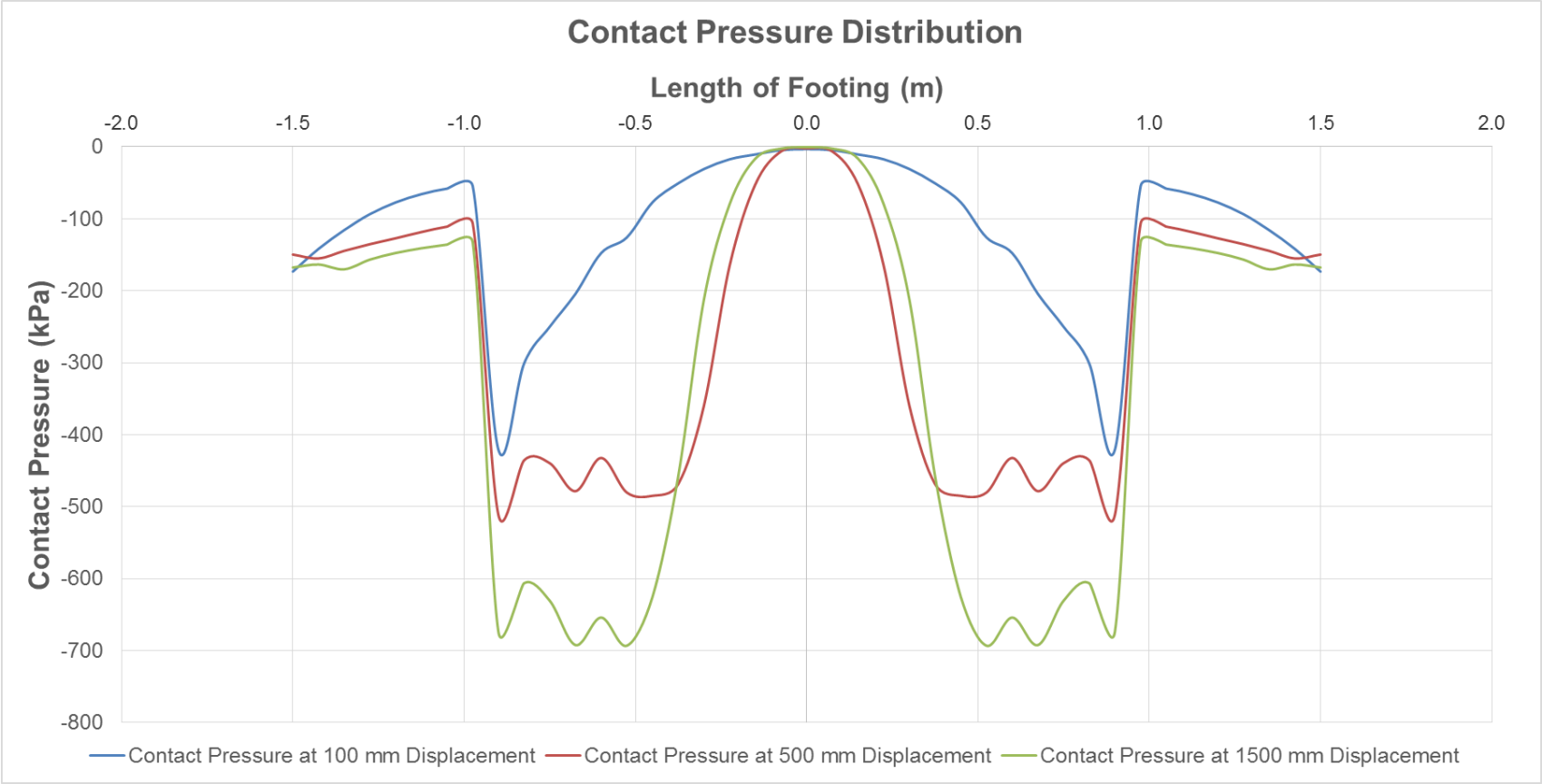


*Figure E-30: Contact pressure distribution (single 4.5 m long, 1.5 m wide trench in 40 kPa native clay; no embedment depth)*

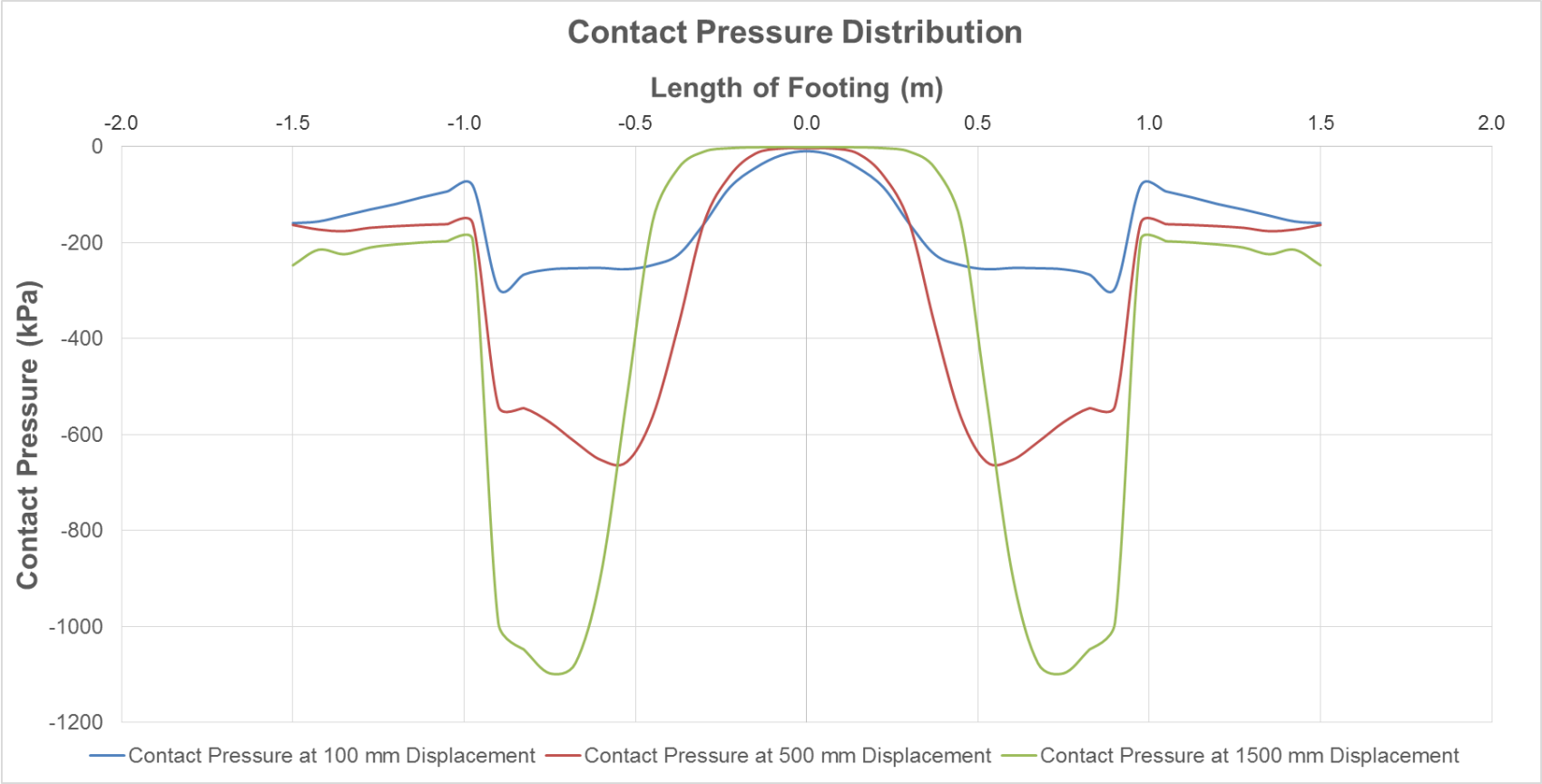


*Figure E-31: Contact pressure distribution (single 4.5 m long, 1.5 m wide trench in 40 kPa native clay; 3 m embedment depth)*

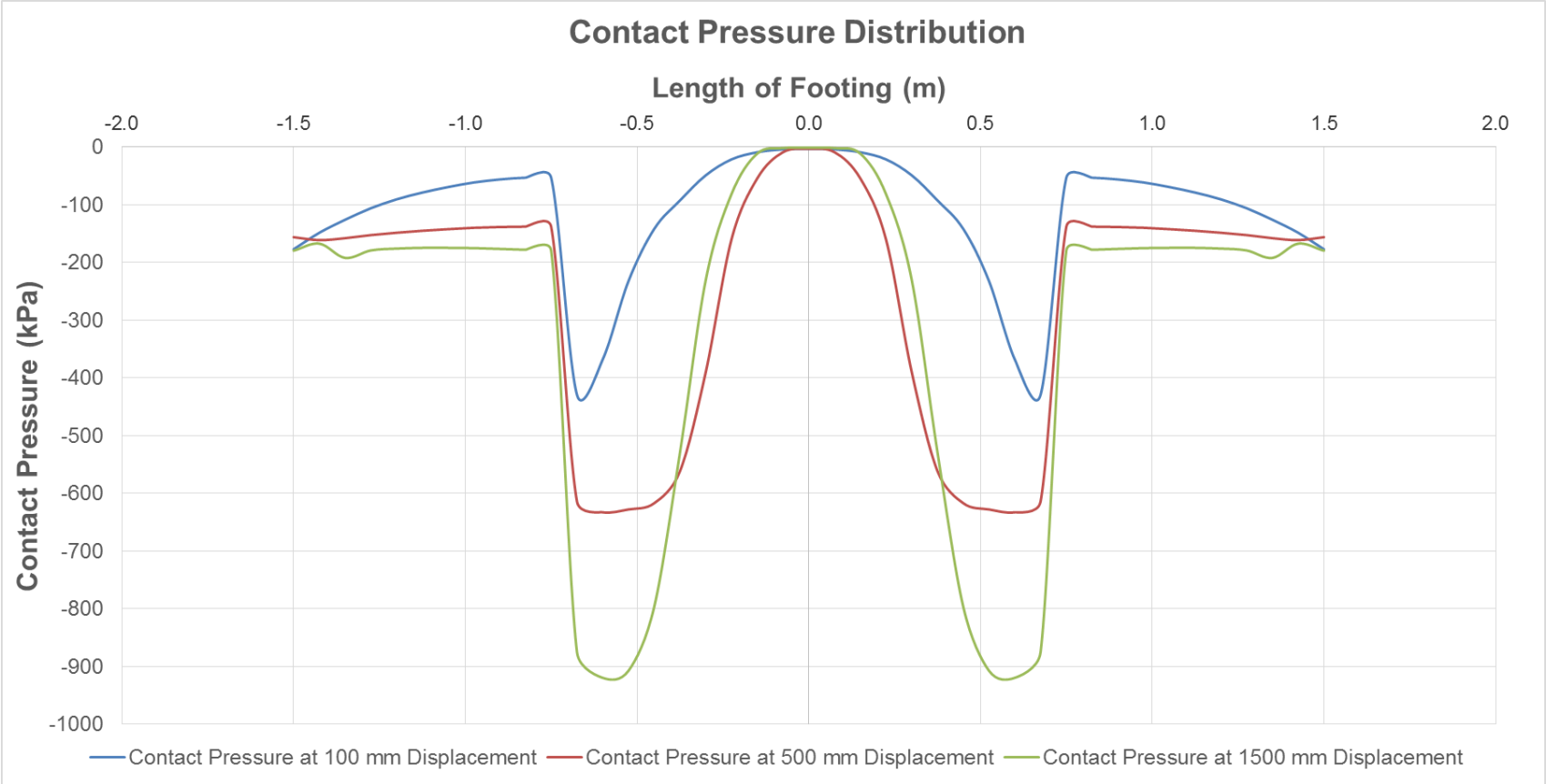


*Figure E-32: Contact pressure distribution (single 4.5 m long, 0.9 m wide trench in 40 kPa native clay; no embedment depth)*

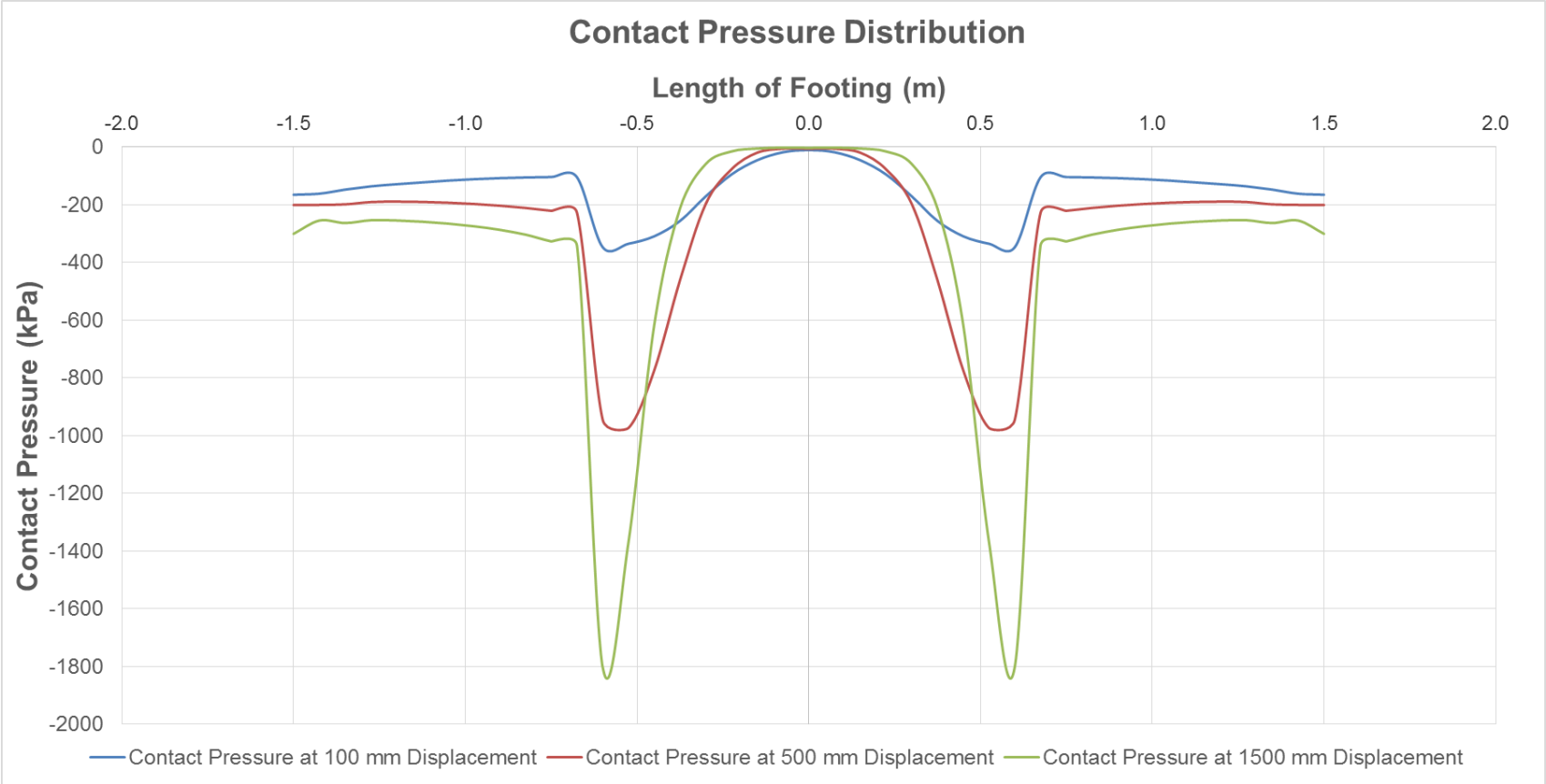


*Figure E-33: Contact pressure distribution (single 4.5 m long, 0.9 m wide trench in 40 kPa native clay; 3 m embedment depth)*

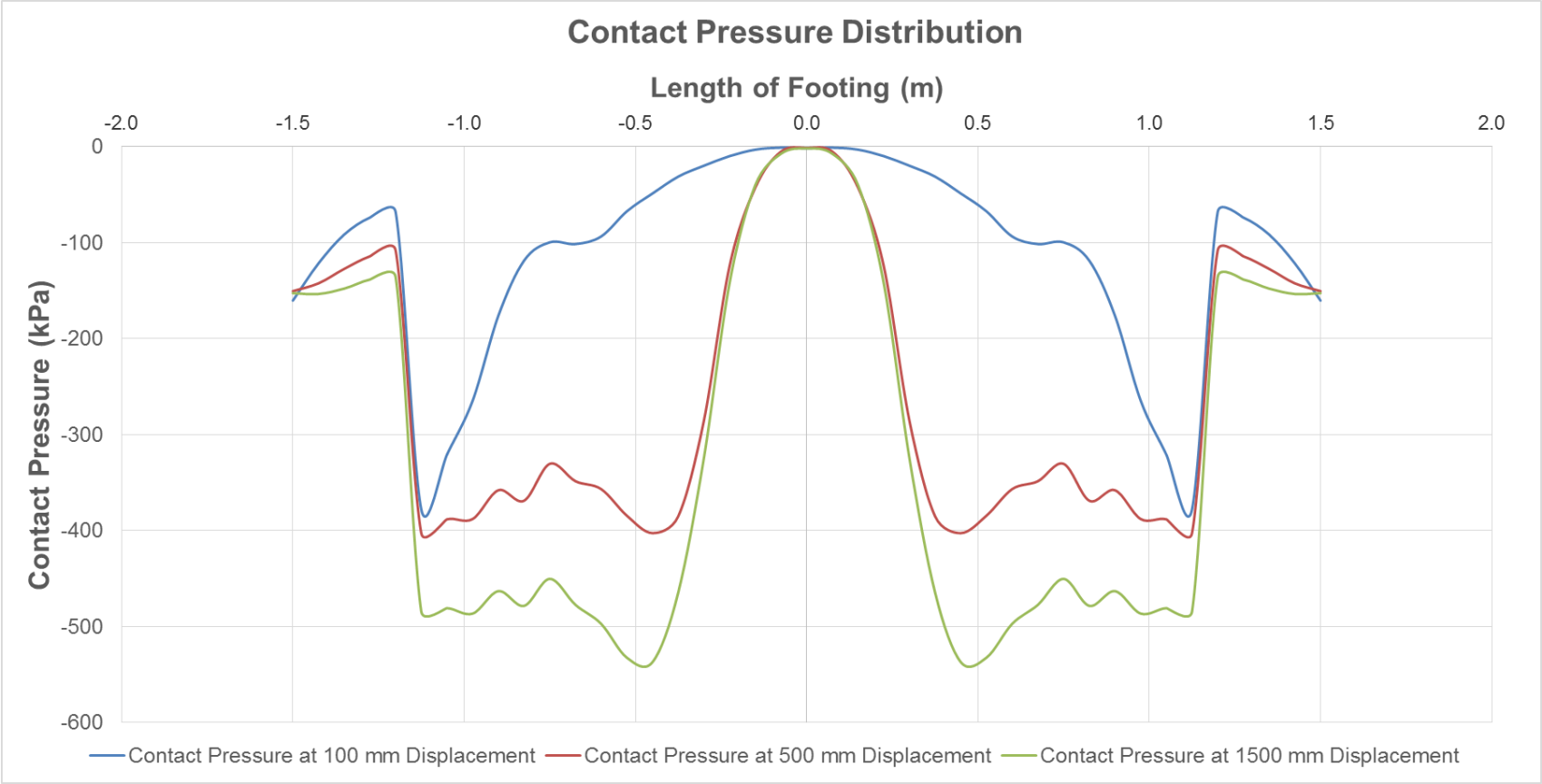


*Figure E-34: Contact pressure distribution (single 4 m long, 2 m wide trench in 40 kPa native clay; no embedment depth)*

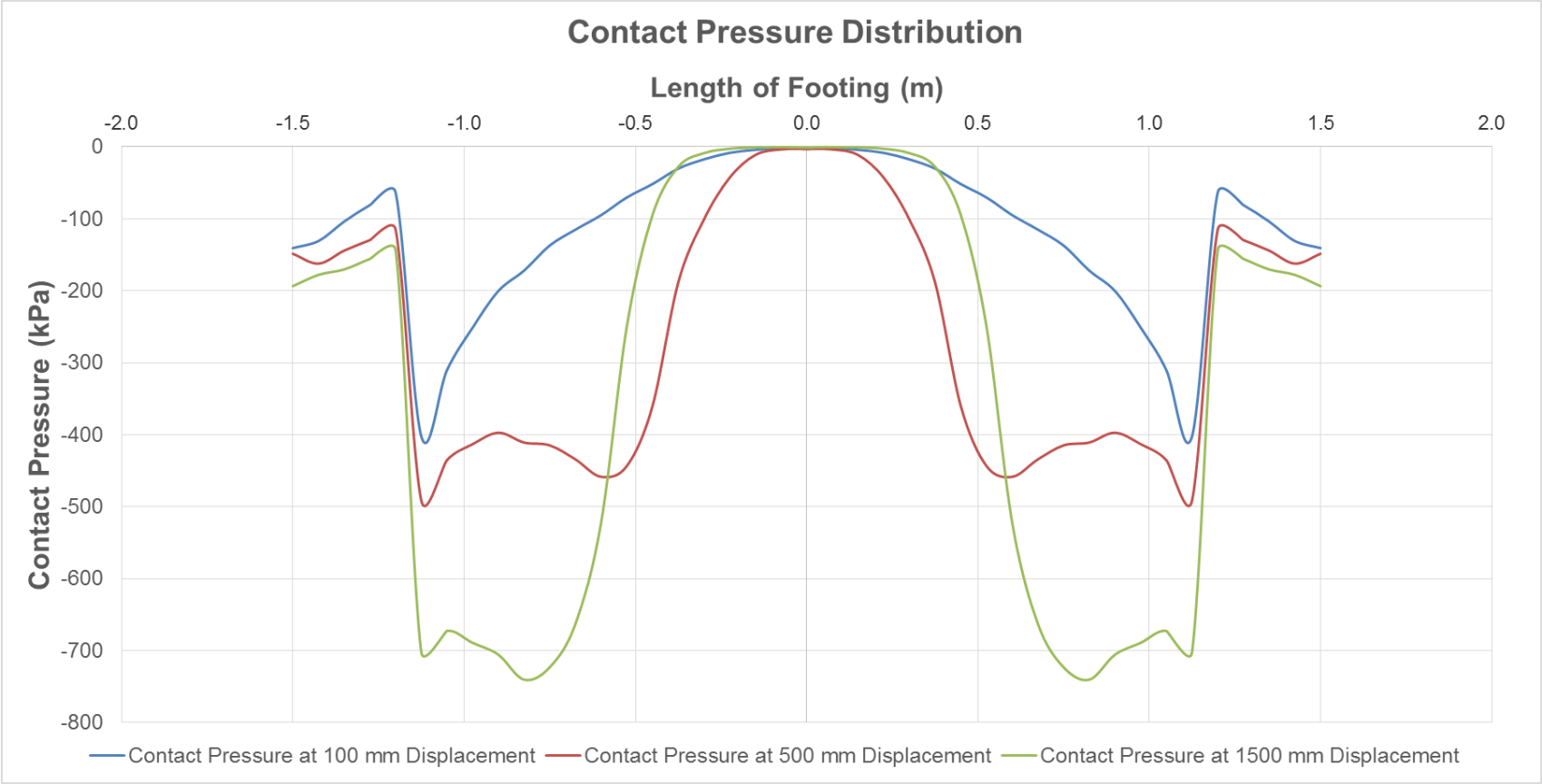


*Figure E-35: Contact pressure distribution (single 4 m long, 2 m wide trench in 40 kPa native clay; 1 m embedment depth)*

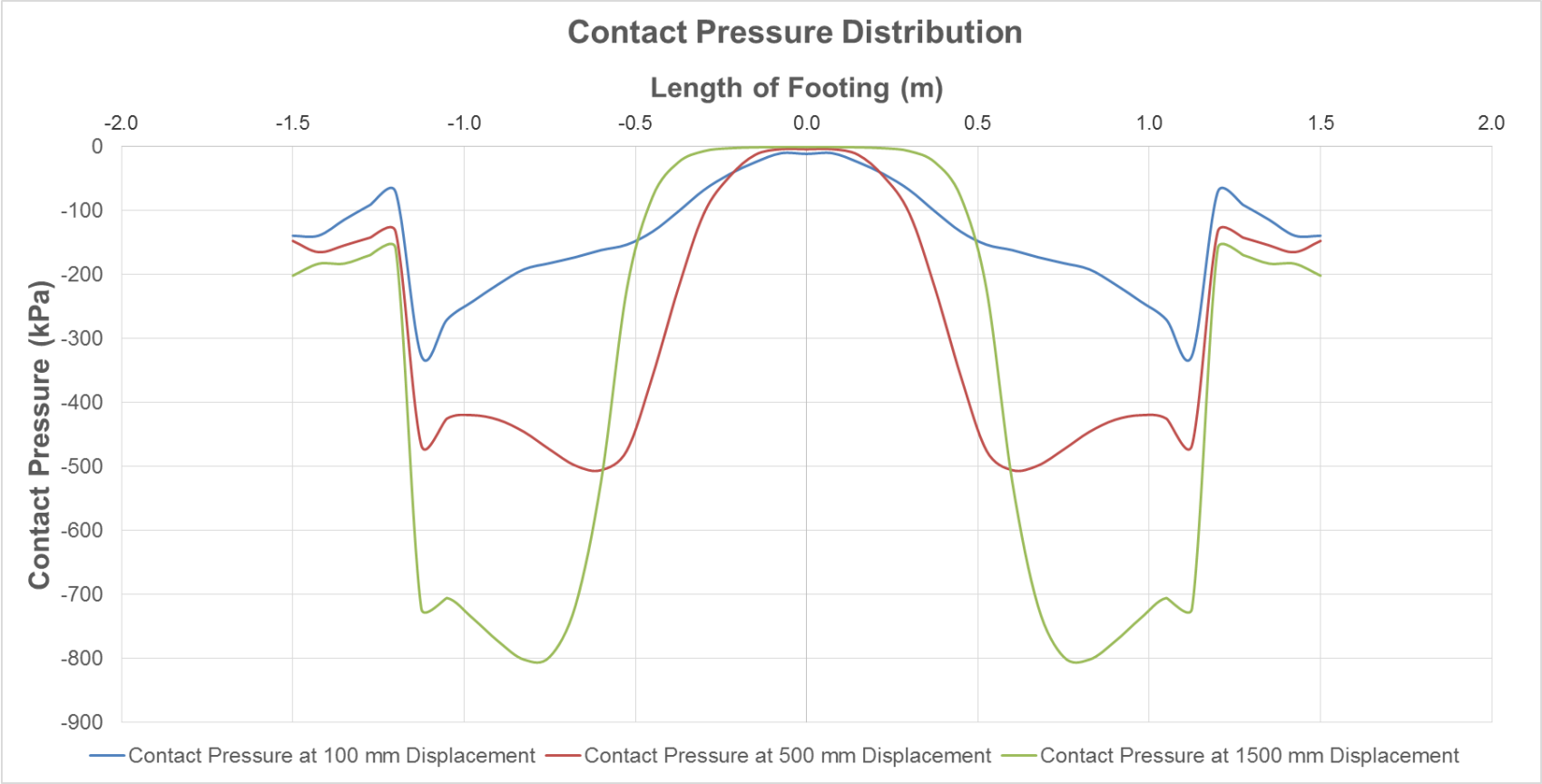


*Figure E-36: Contact pressure distribution (single 4 m long, 2 m wide trench in 40 kPa native clay; 2 m embedment depth)*

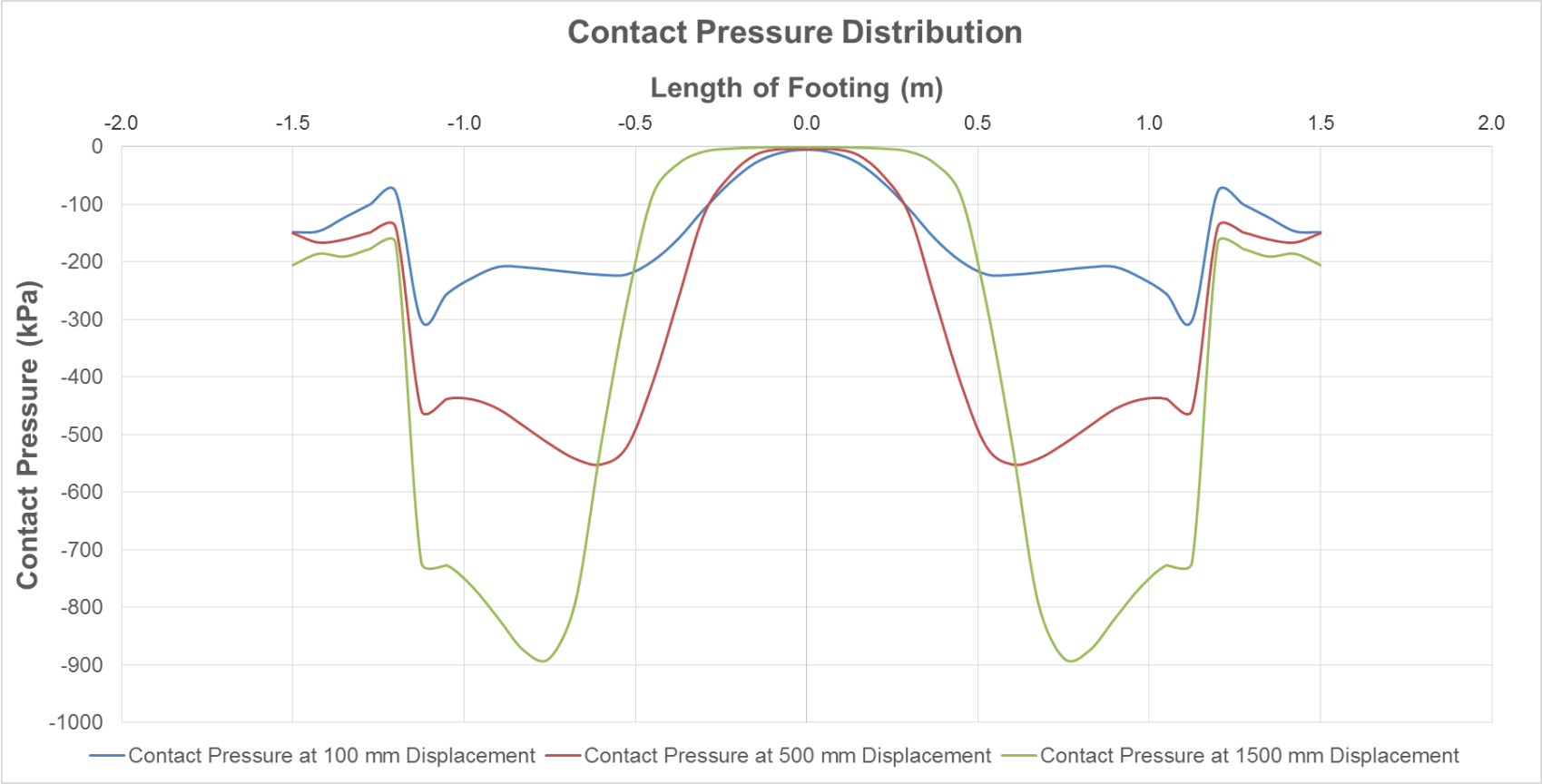


*Figure E-37: Contact pressure distribution (single 4 m long, 2 m wide trench in 40 kPa native clay; 3 m embedment depth)*

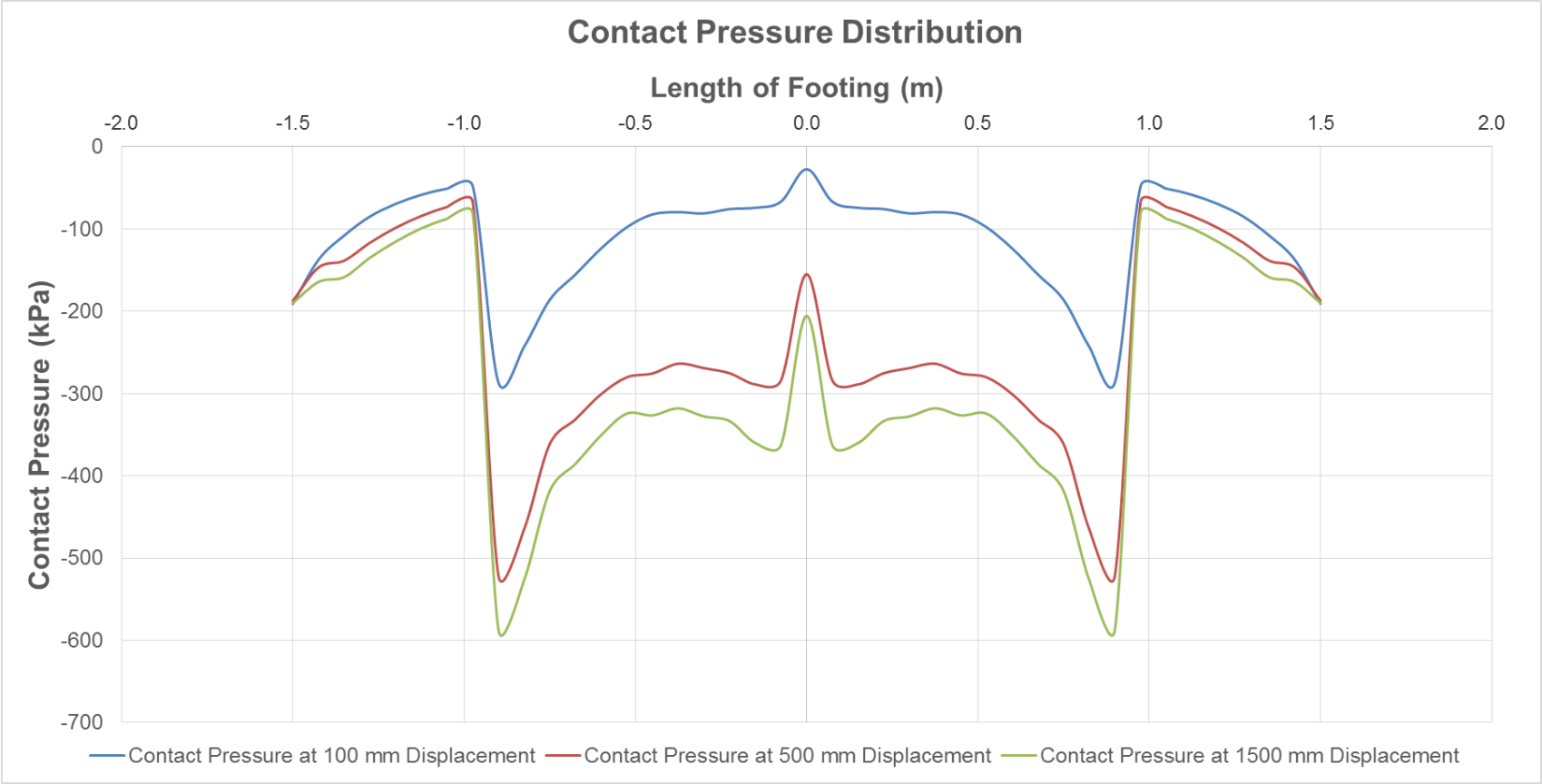


*Figure E-38: Contact pressure distribution (single 3 m long, 1.5 m wide trench in 40 kPa native clay; no embedment depth)*

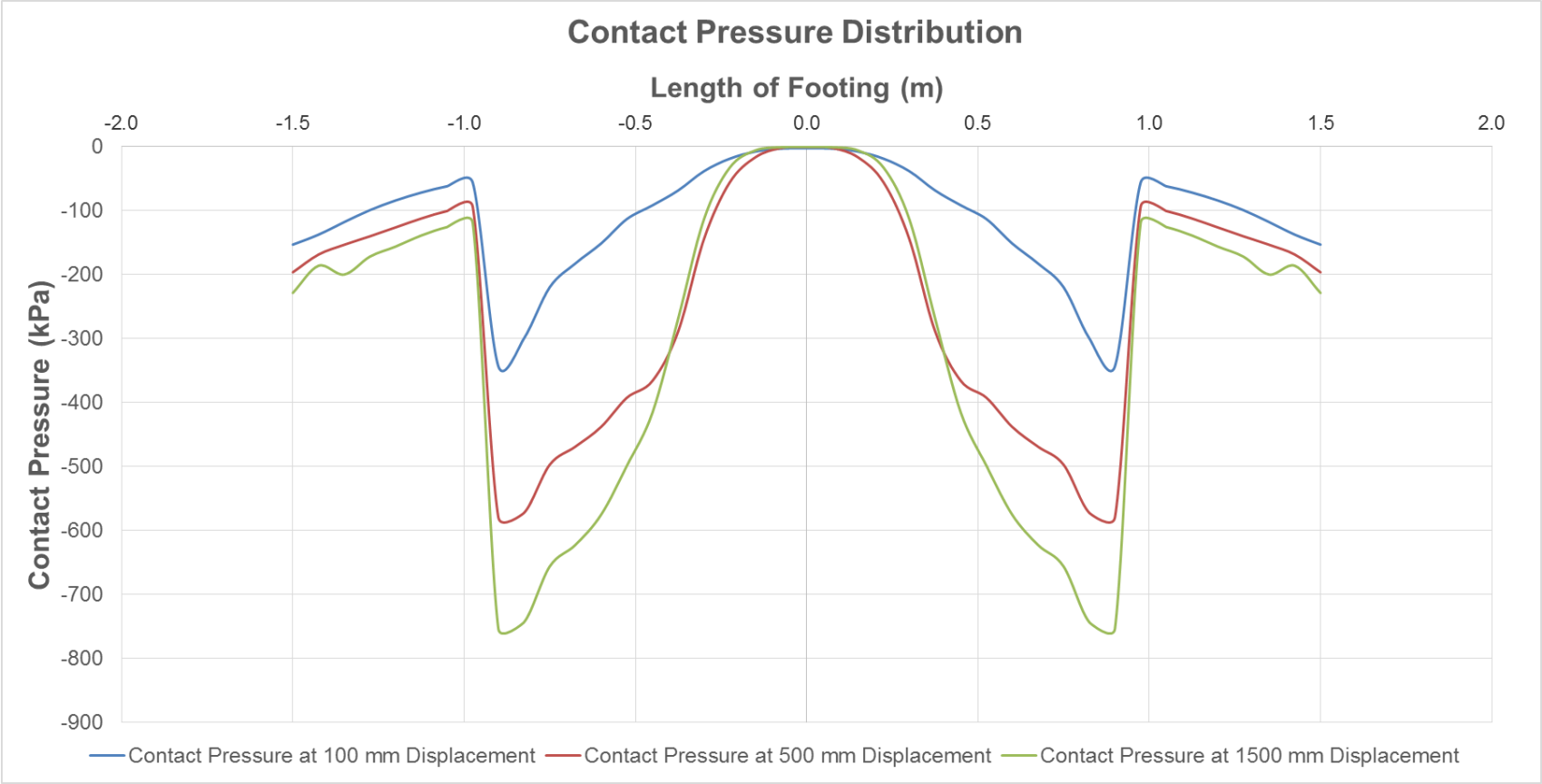


*Figure E-39: Contact pressure distribution (single 3 m long, 1.5 m wide trench in 40 kPa native clay; 1 m embedment depth)*

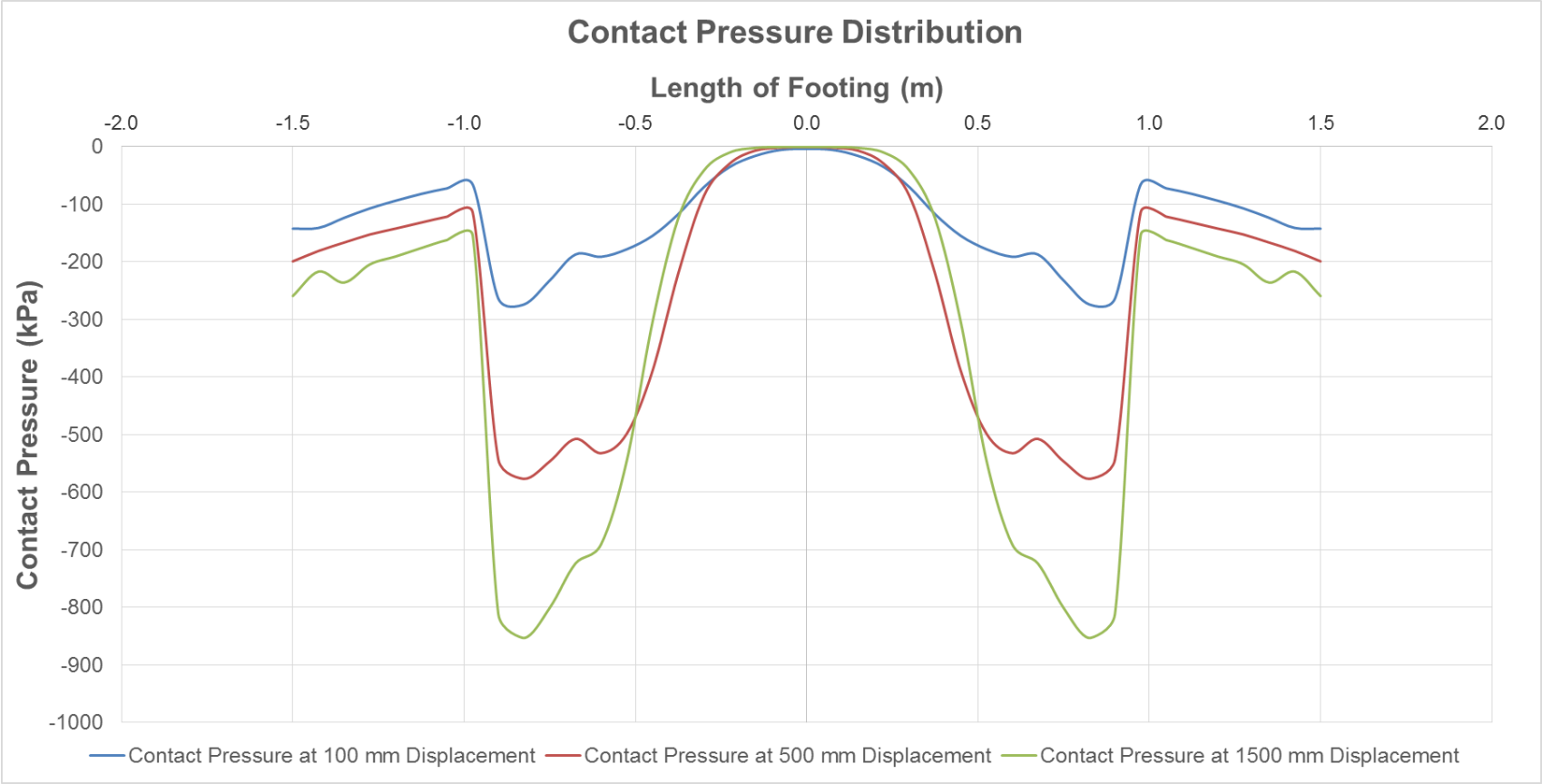


*Figure E-40: Contact pressure distribution (single 3 m long, 1.5 m wide trench in 40 kPa native clay; 2 m embedment depth)*

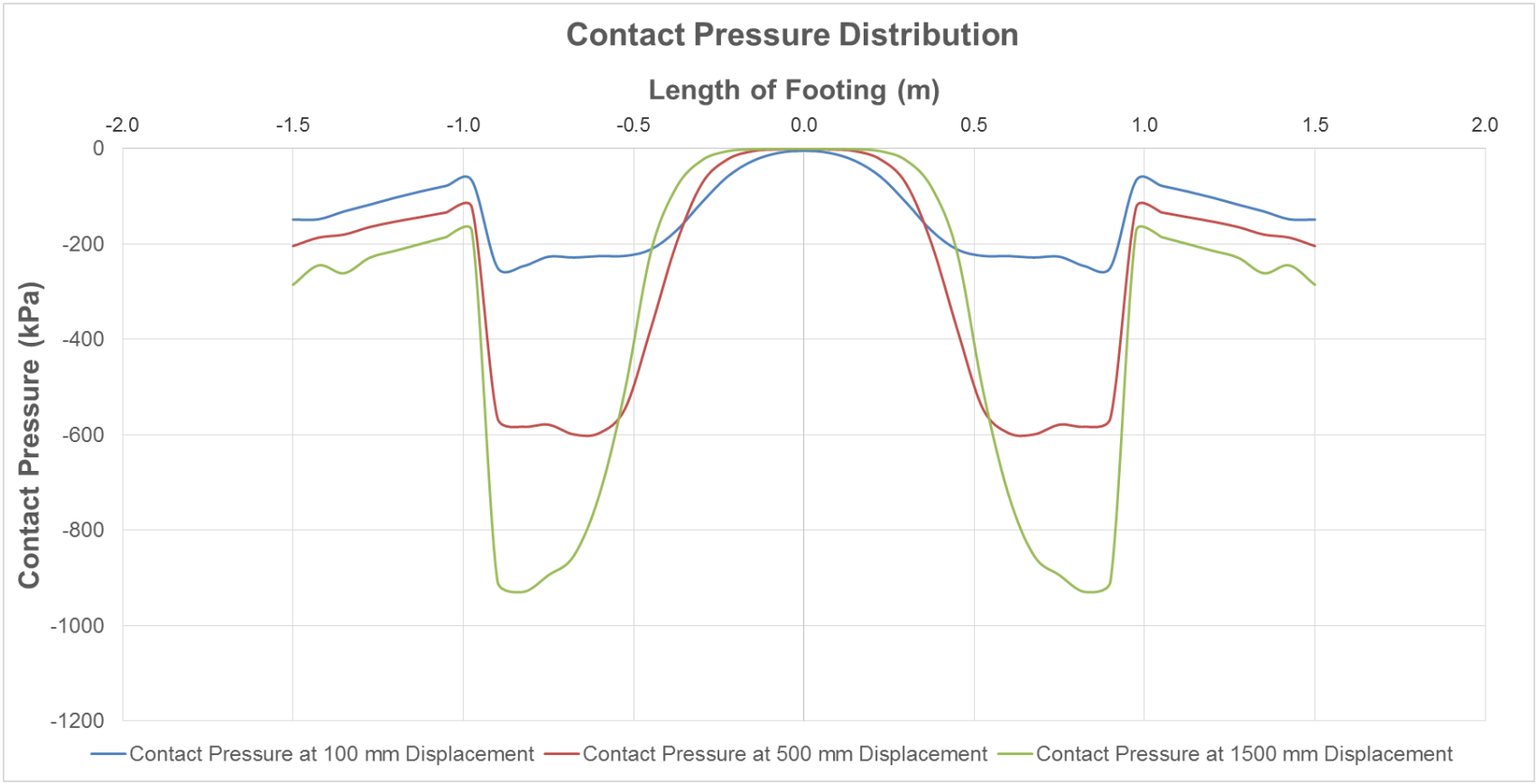


*Figure E-41: Contact pressure distribution (single 3 m long, 1.5 m wide trench in 40 kPa native clay; 3 m embedment depth)*

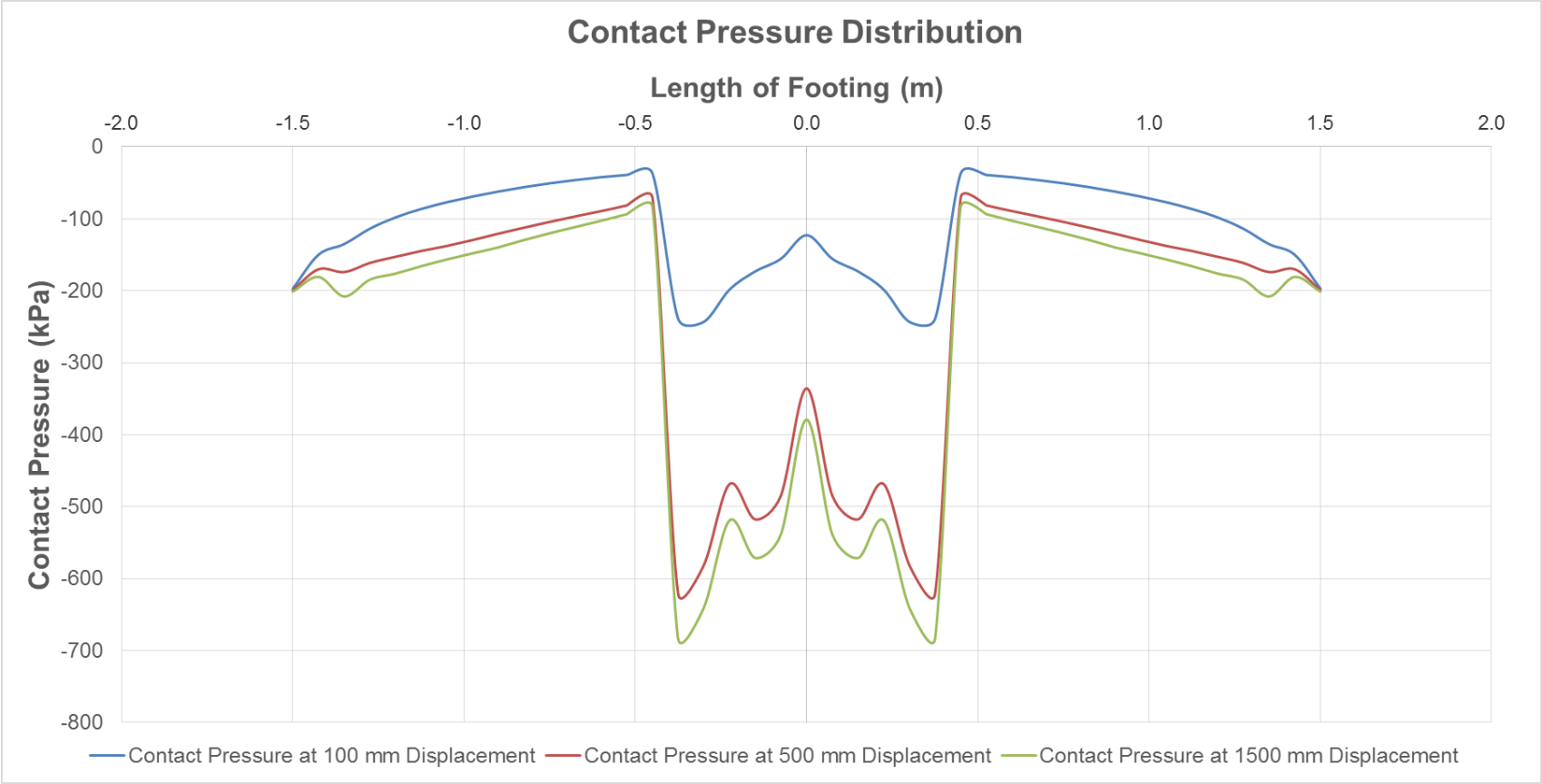


*Figure E-42: Contact pressure distribution (single 3 m long, 0.6 m wide trench in 40 kPa native clay; no embedment depth)*

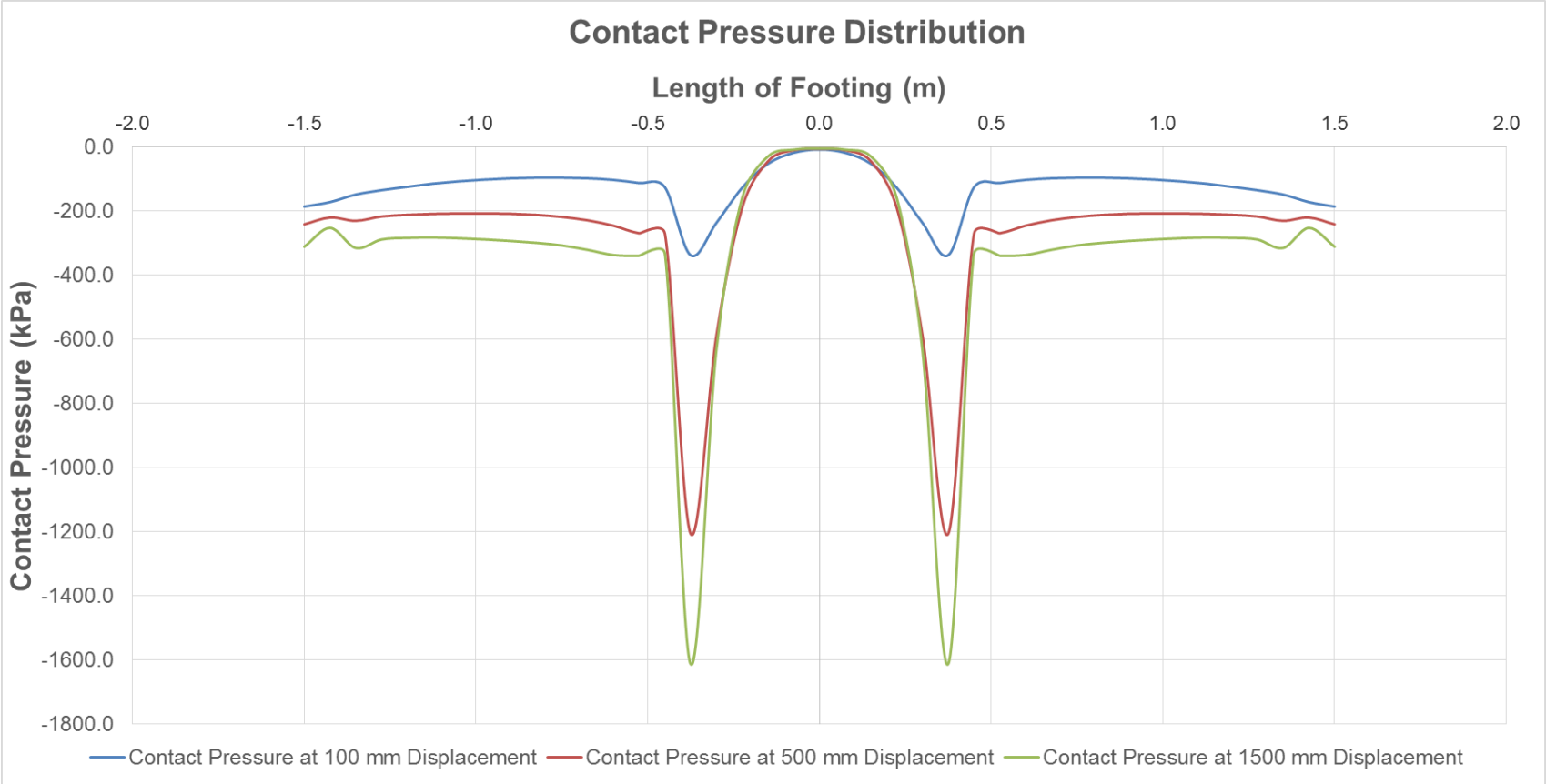


*Figure E-43: Contact pressure distribution (single 3 m long, 0.6 m wide trench in 40 kPa native clay; 3 m embedment depth)*

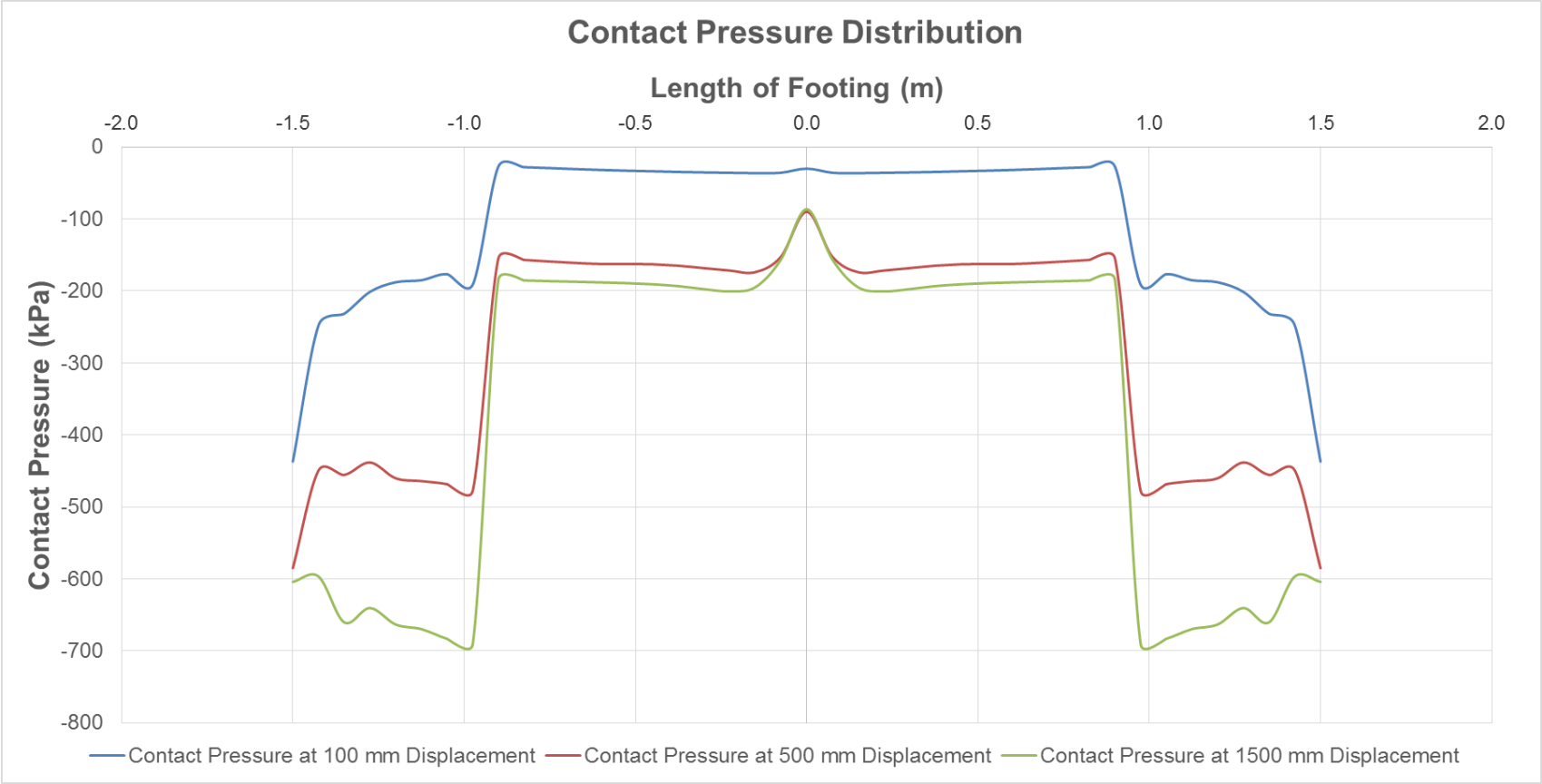


*Figure E-44: Contact pressure distribution (two 6 m long, 0.75 m wide trenches in 40 kPa native clay; no embedment depth)*

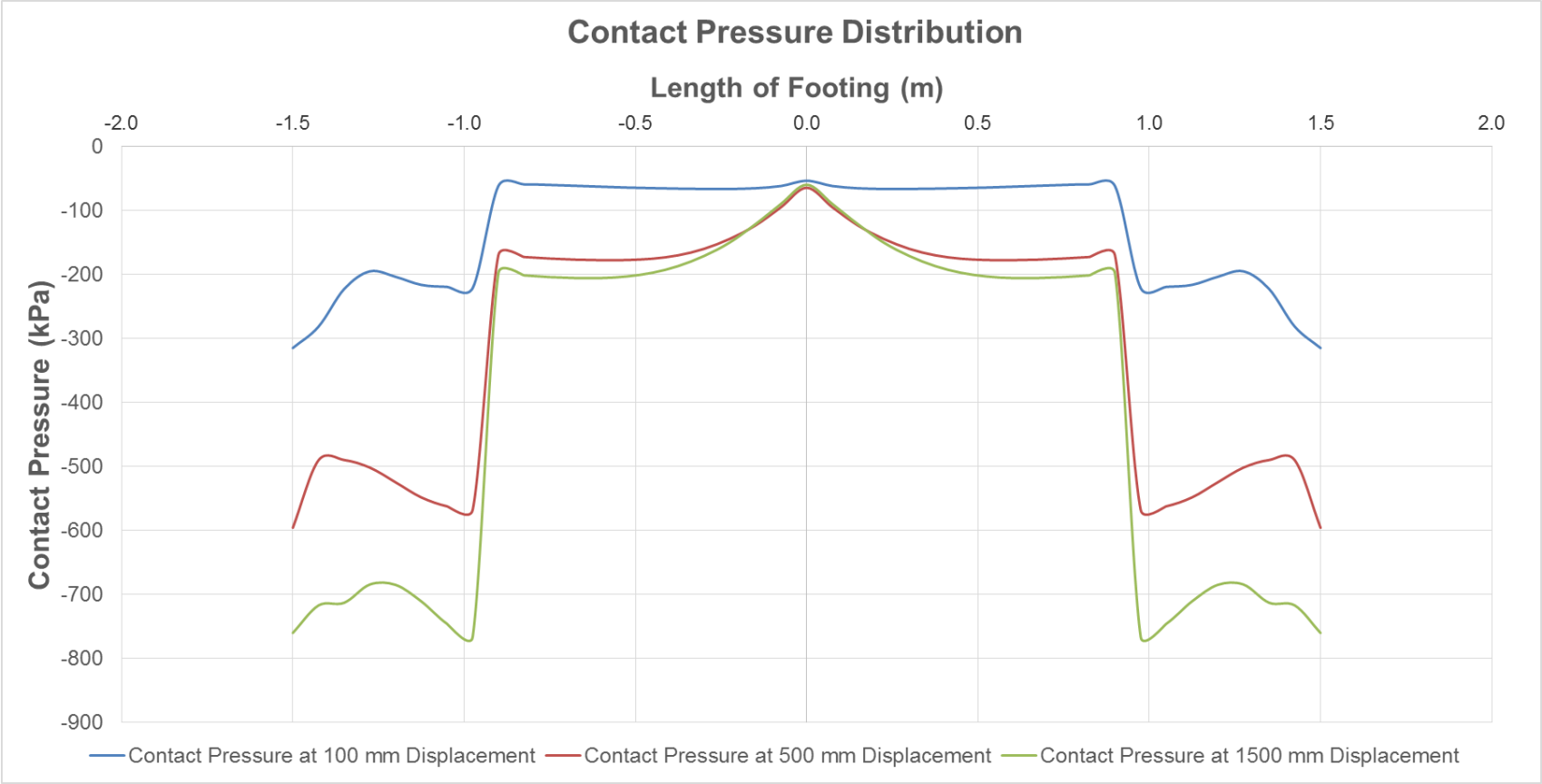


*Figure E-45: Contact pressure distribution (two 6 m long, 0.75 m wide trenches in 40 kPa native clay; 1.5 m embedment depth)*

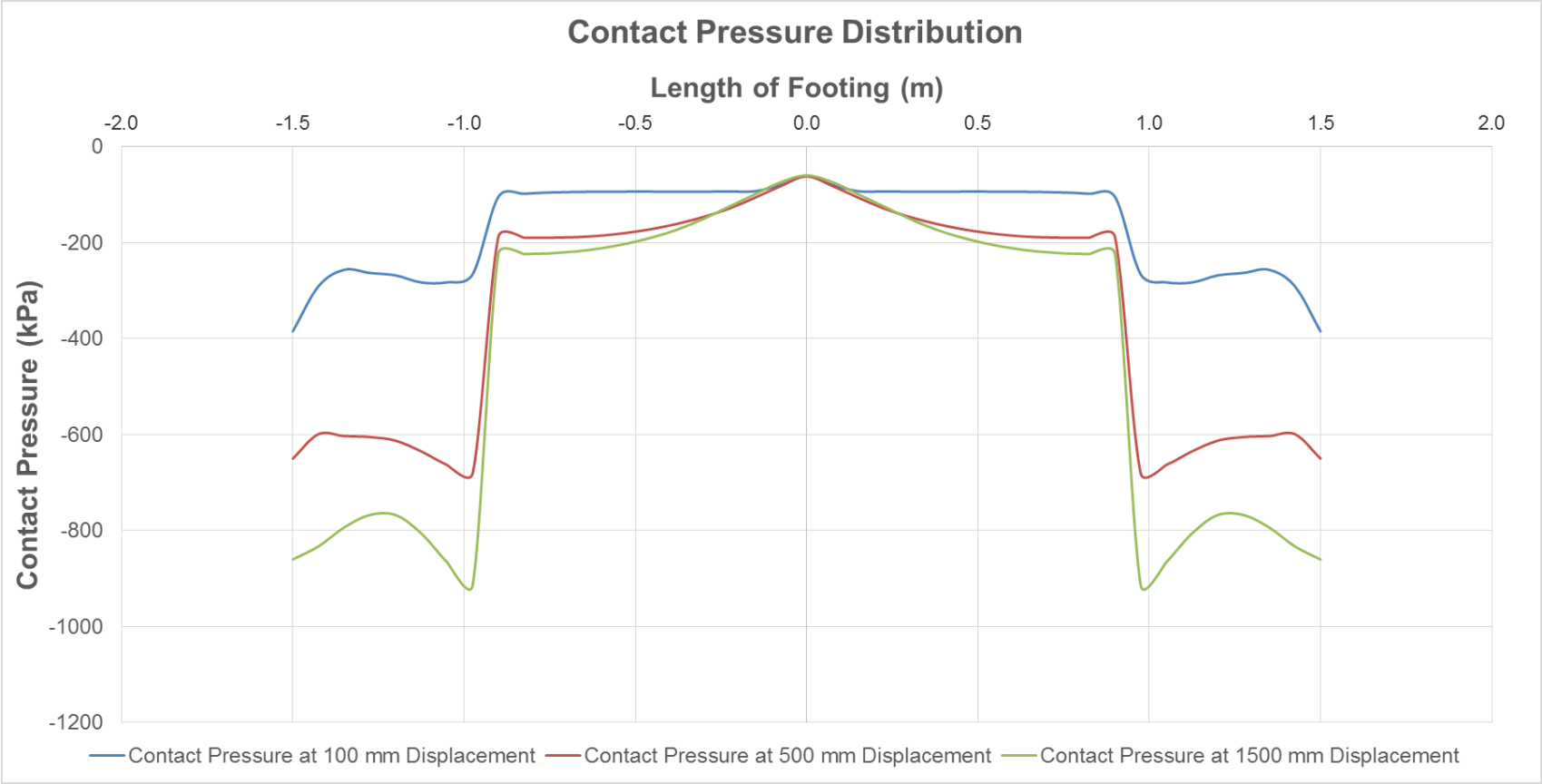


*Figure E-46: Contact pressure distribution (two 6 m long, 0.75 m wide trenches in 40 kPa native clay; 3 m embedment depth)*

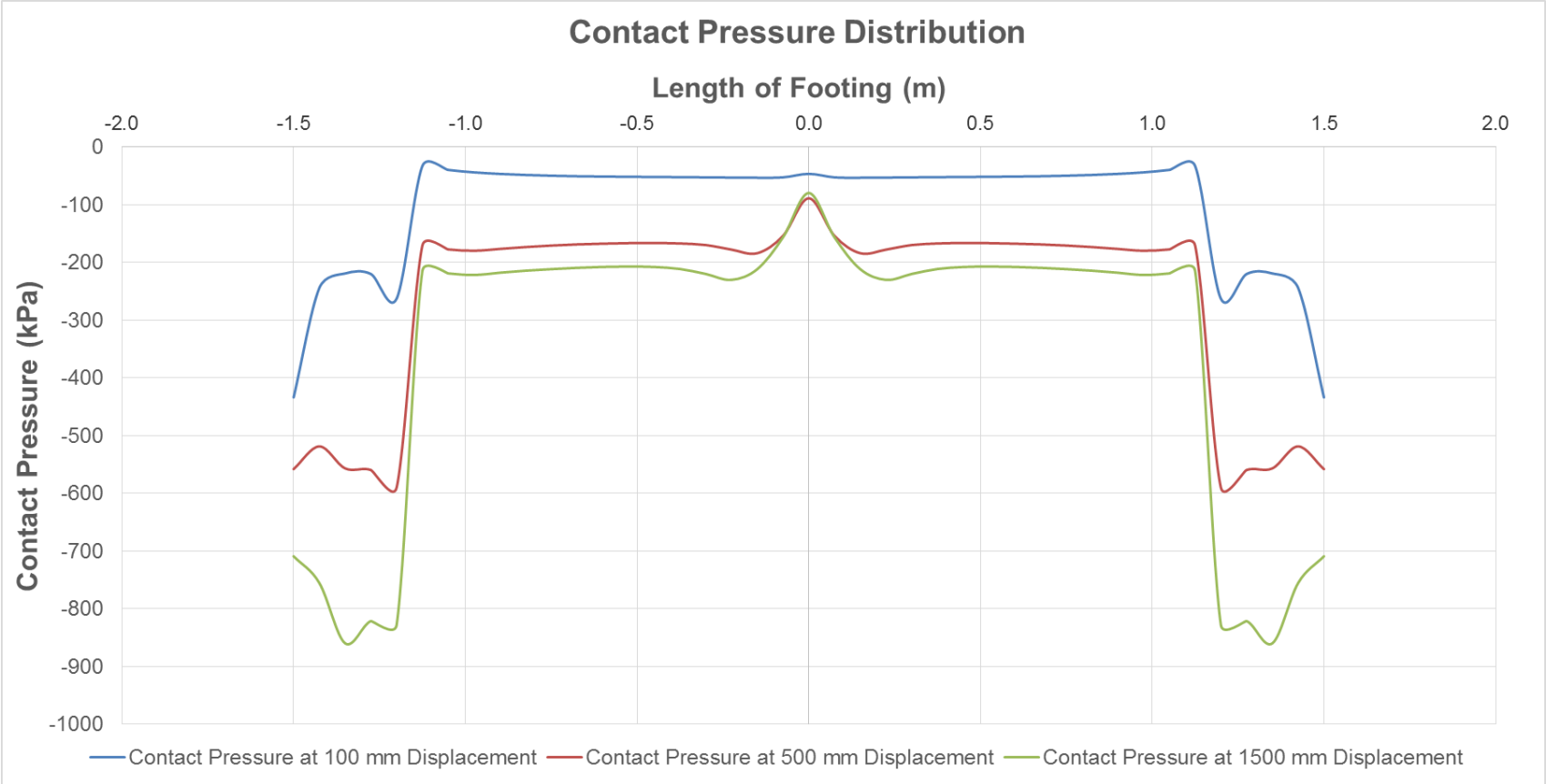


*Figure E-47: Contact pressure distribution (two 6 m long, 0.45 m wide trenches in 40 kPa native clay; no embedment depth)*

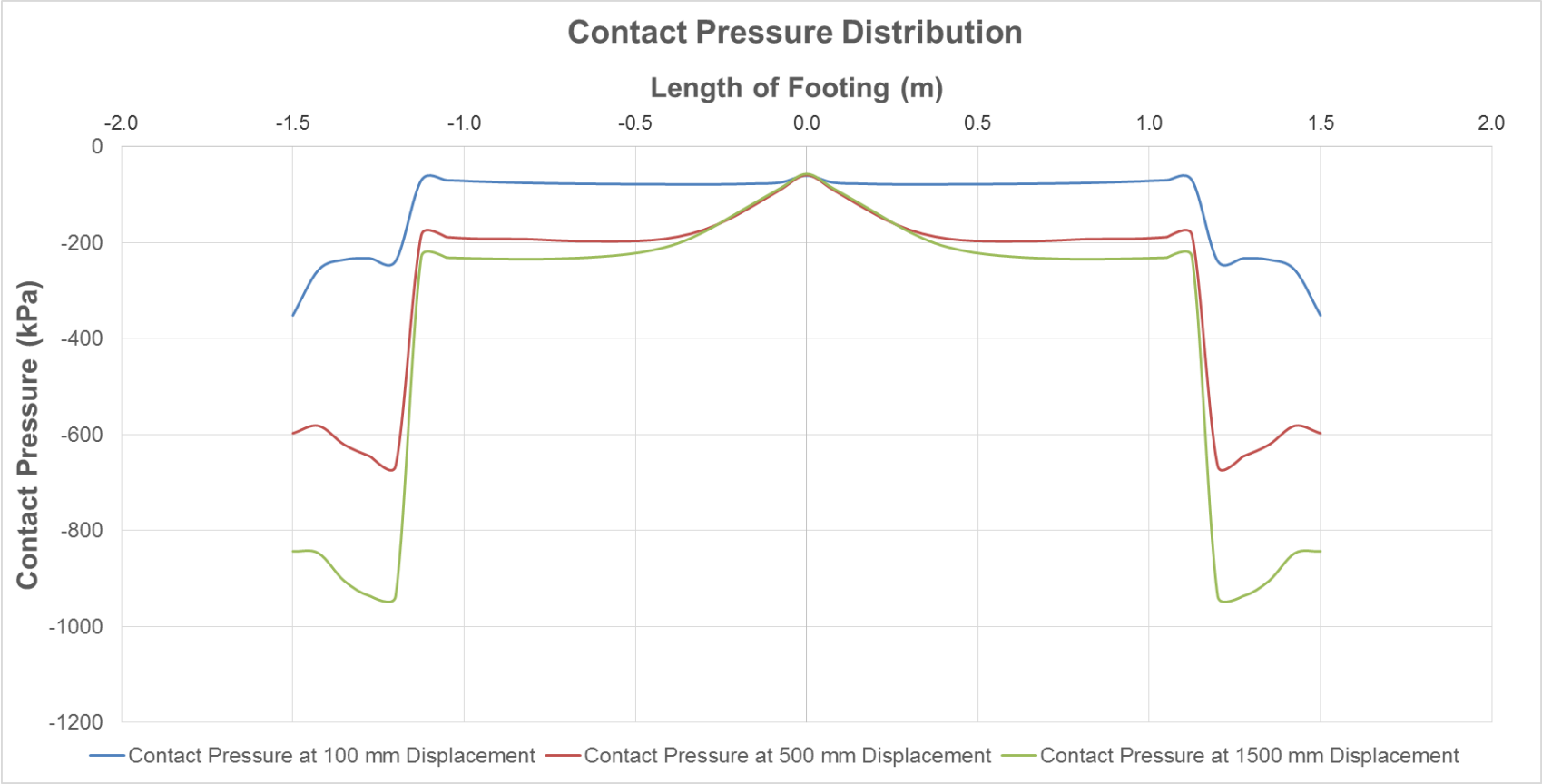


*Figure E-48: Contact pressure distribution (two 6 m long, 0.45 m wide trenches in 40 kPa native clay; 1.5 m embedment depth)*

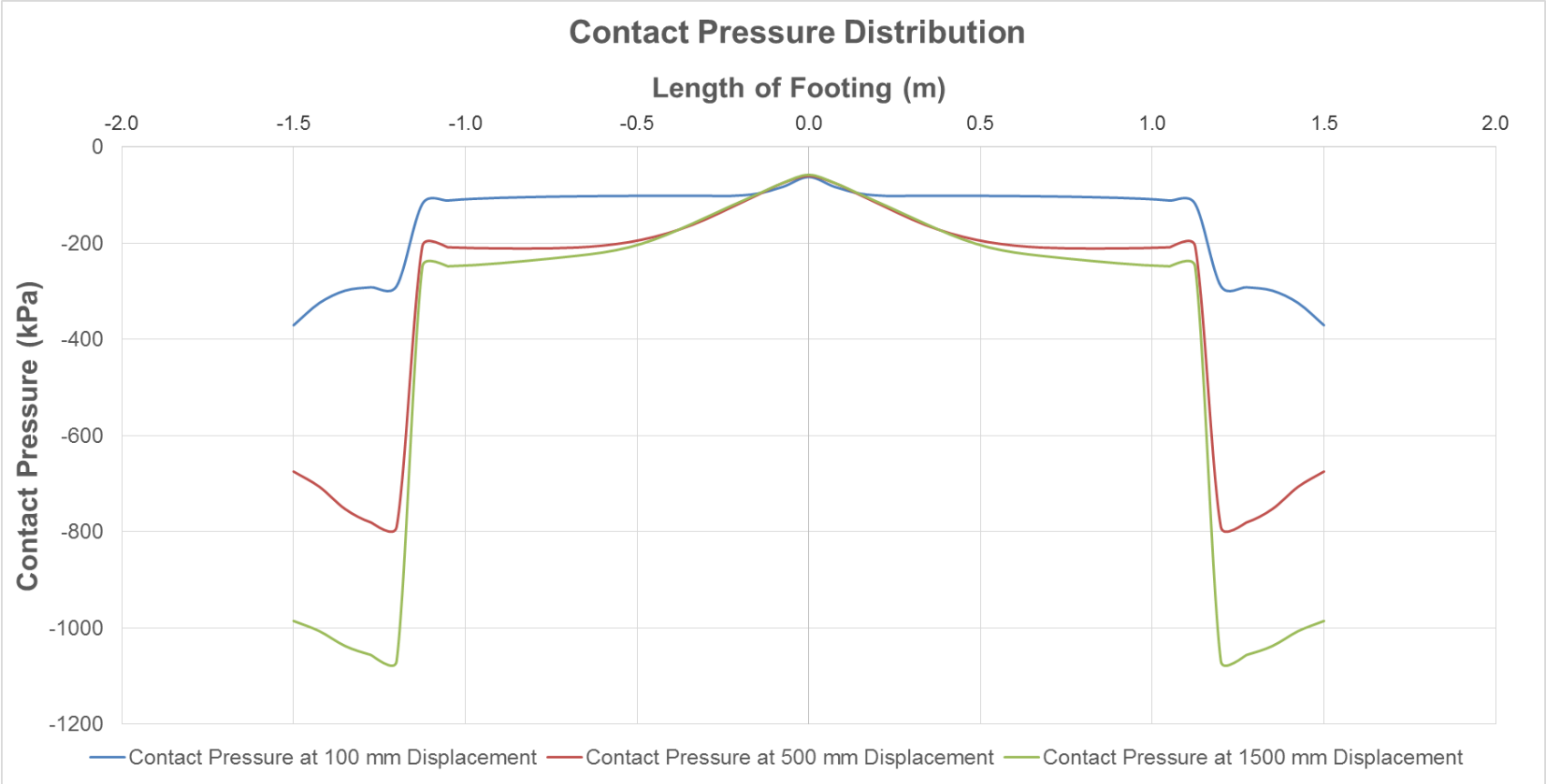


*Figure E-49: Contact pressure distribution (two 6 m long, 0.45 m wide trenches in 40 kPa native clay; 3 m embedment depth)*

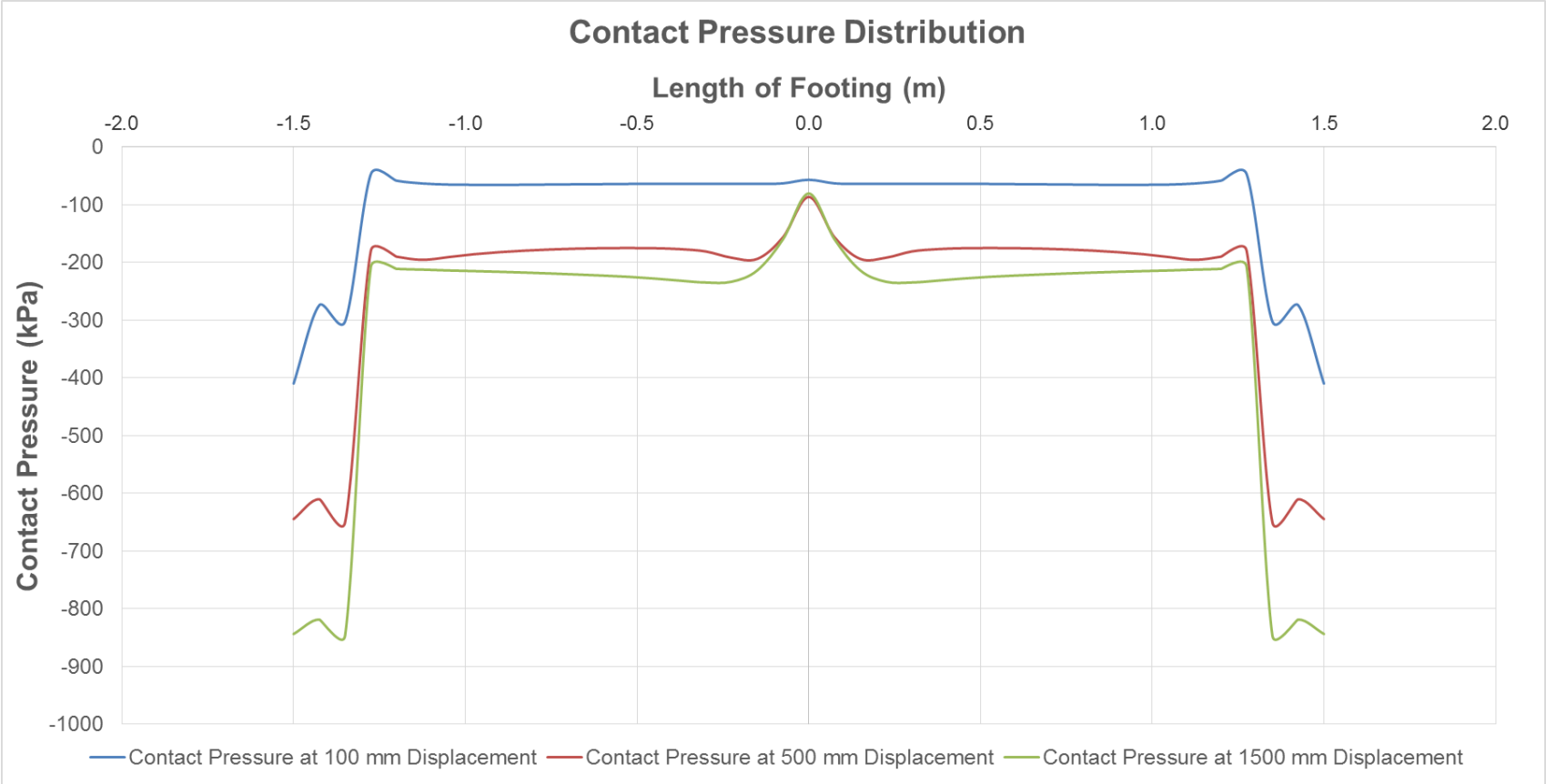


*Figure E-50: Contact pressure distribution (two 6 m long, 0.3 m wide trenches in 40 kPa native clay; no embedment depth)*

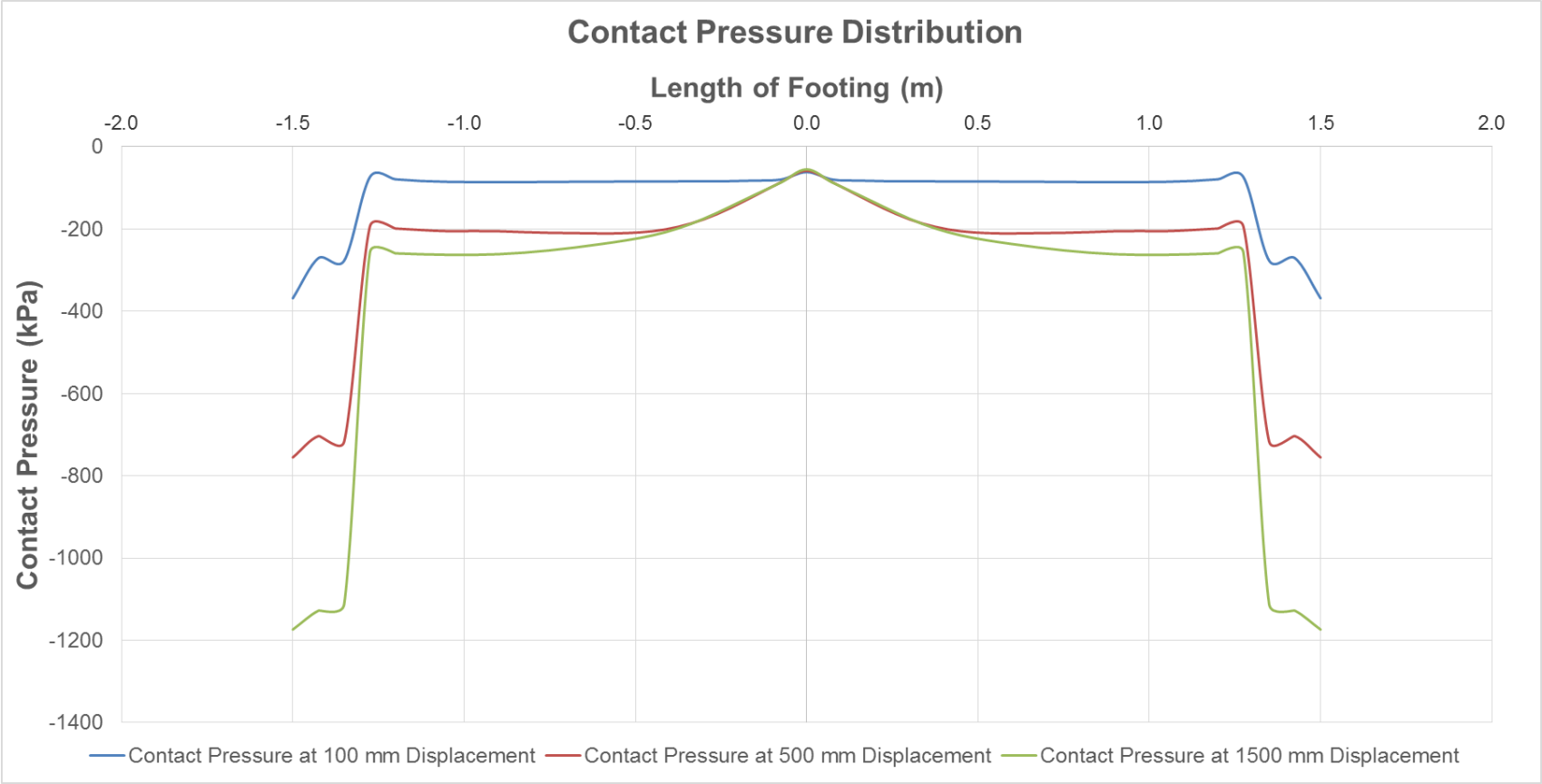


*Figure E-51: Contact pressure distribution (two 6 m long, 0.3 m wide trenches in 40 kPa native clay; 1.5 m embedment depth)*

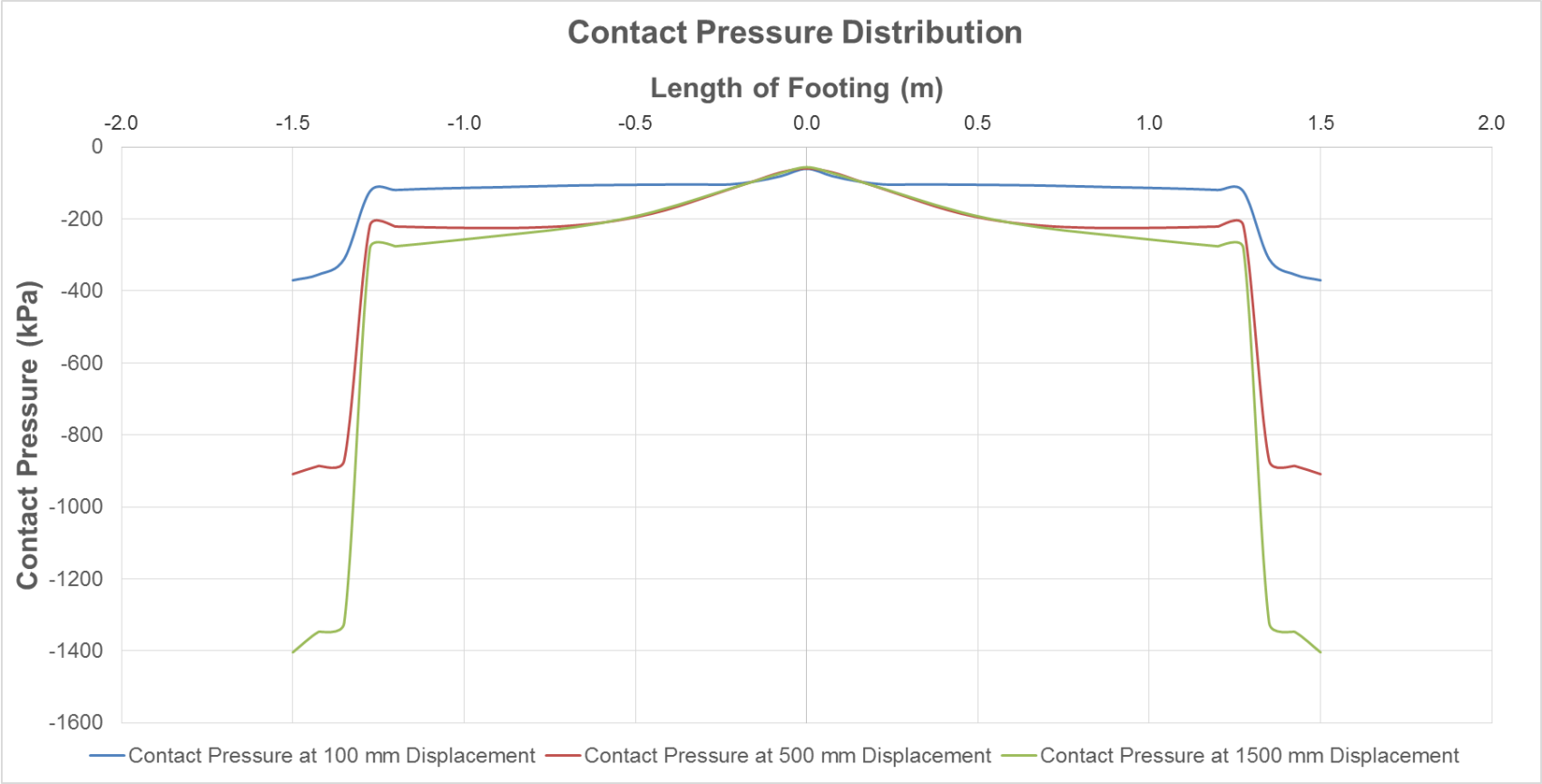


*Figure E-52: Contact pressure distribution (two 6 m long, 0.3 m wide trenches in 40 kPa native clay; 3 m embedment depth)*

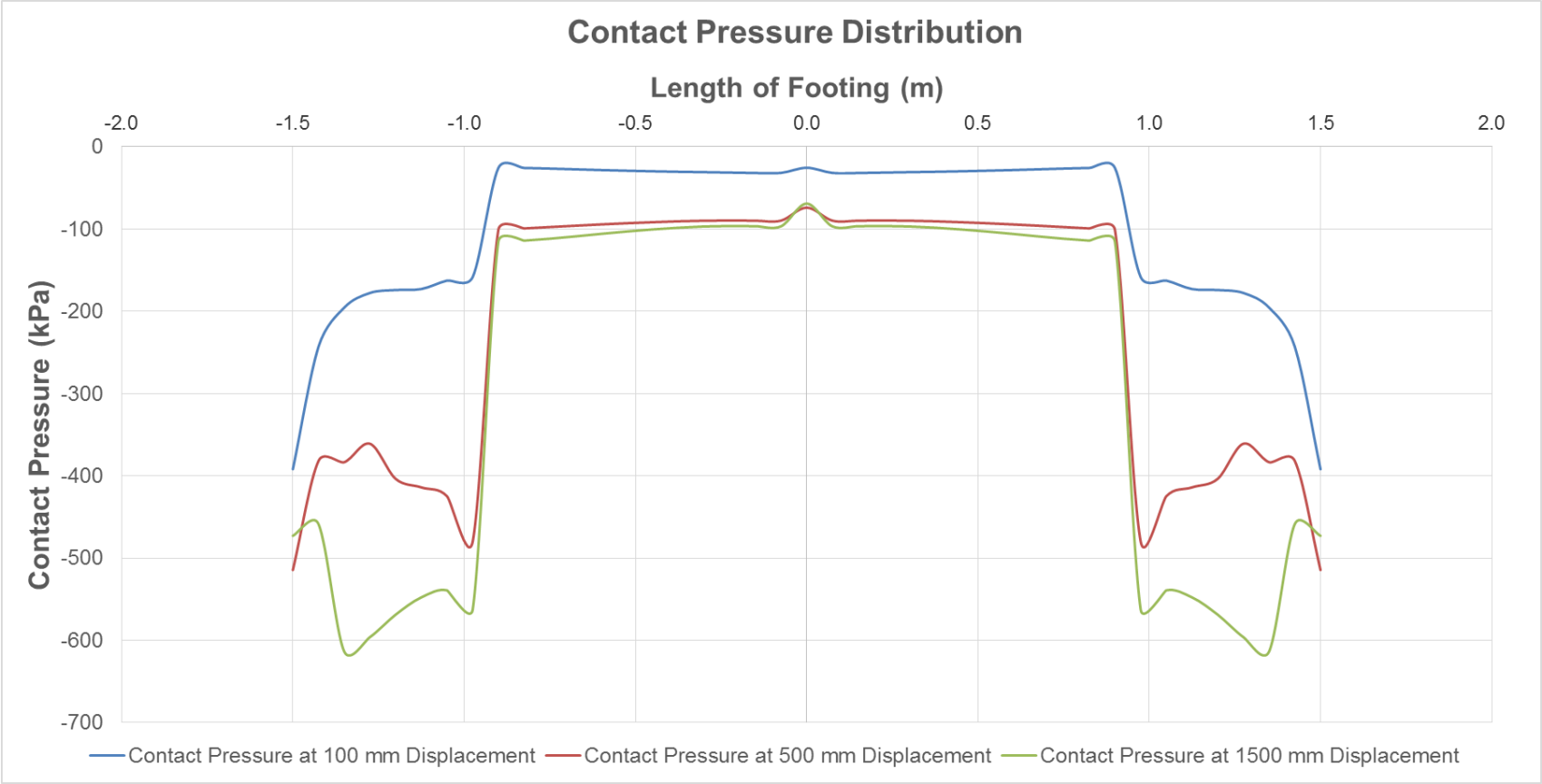


*Figure E-53: Contact pressure distribution (two 3 m long, 0.75 m wide trenches in 40 kPa native clay; no embedment depth)*

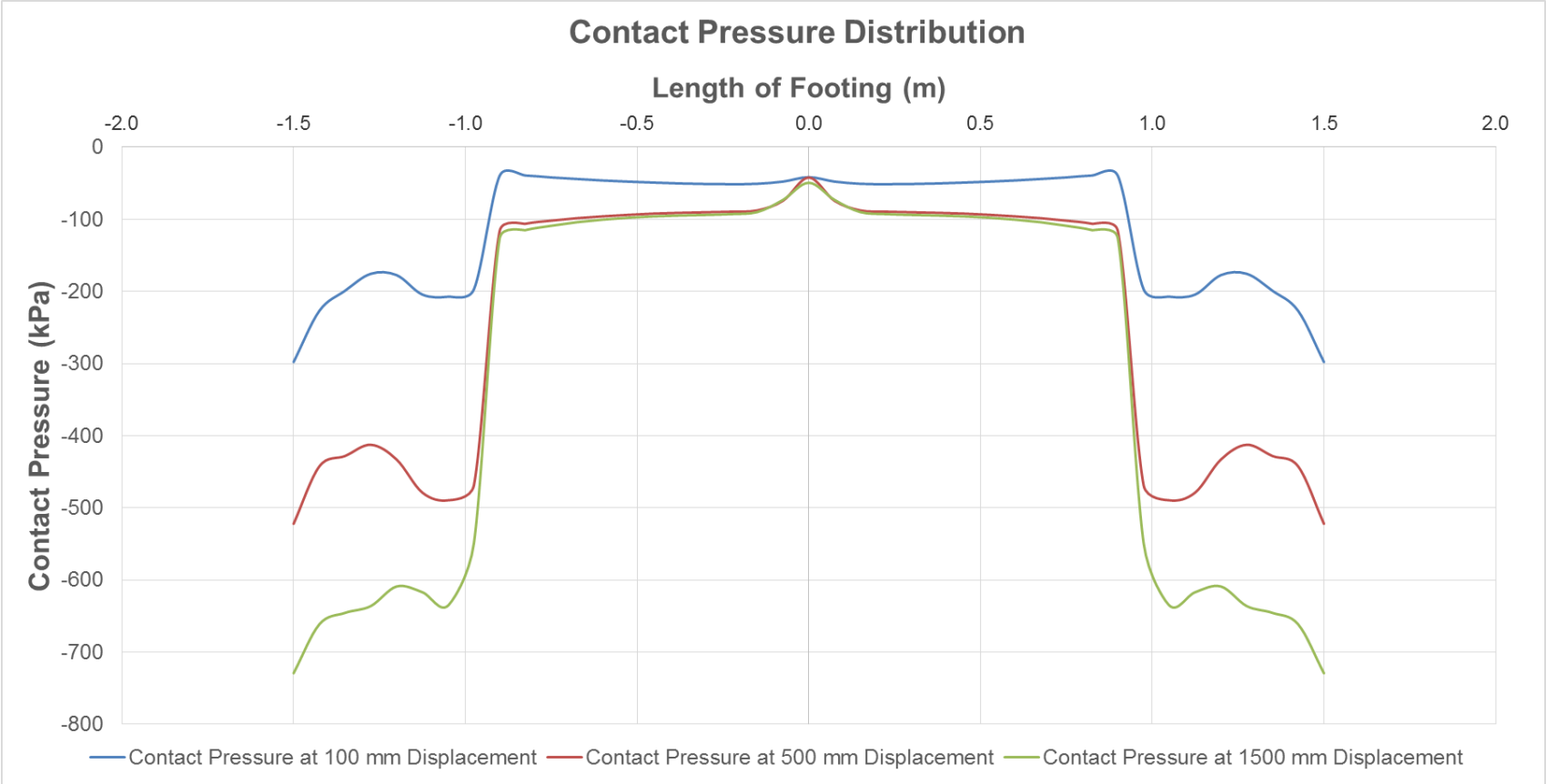


*Figure E-54: Contact pressure distribution (two 3 m long, 0.75 m wide trenches in 40 kPa native clay; 1.5 m embedment depth)*

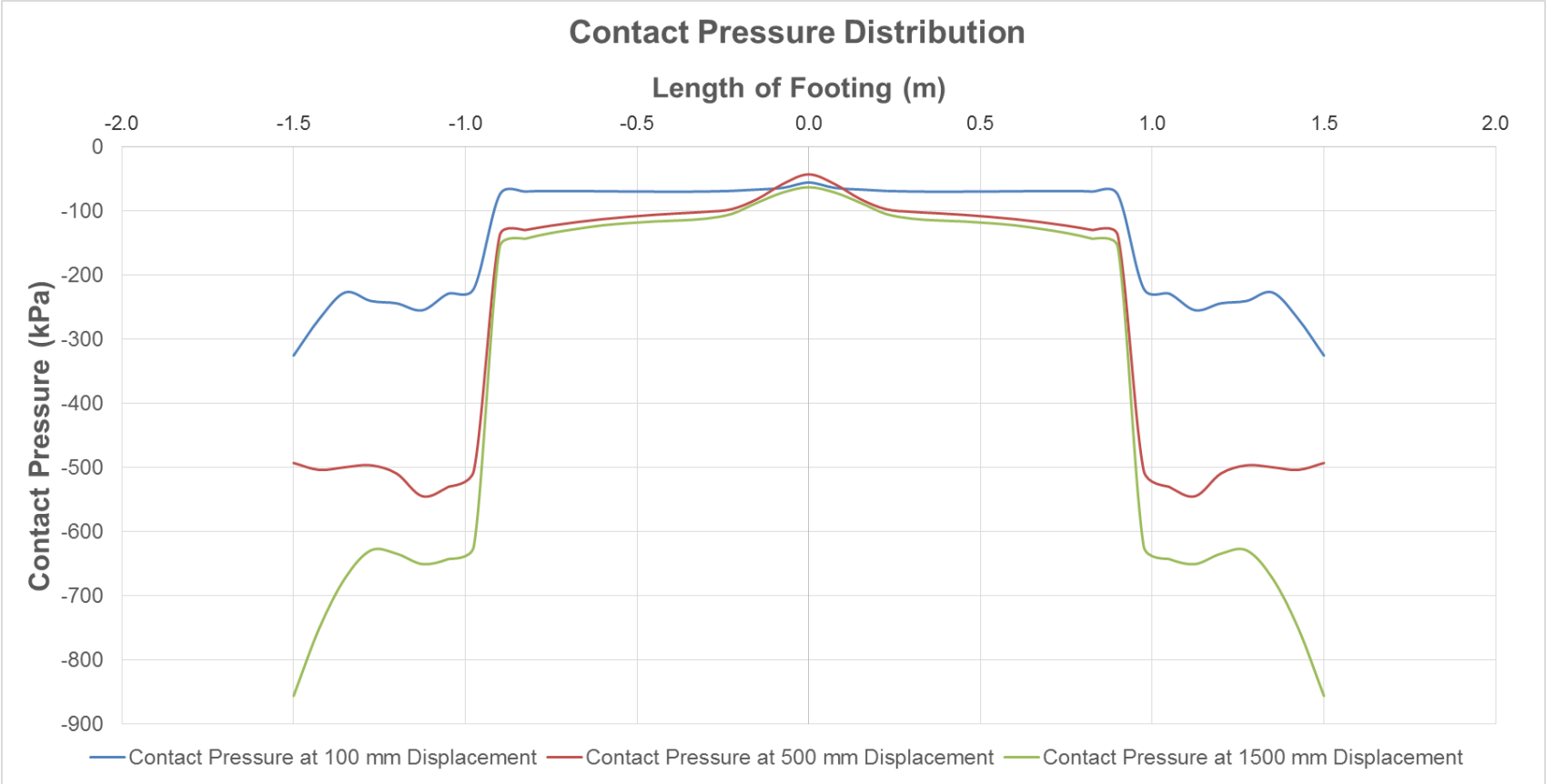


*Figure E-55: Contact pressure distribution (two 3 m long, 0.75 m wide trenches in 40 kPa native clay; 3 m embedment depth)*

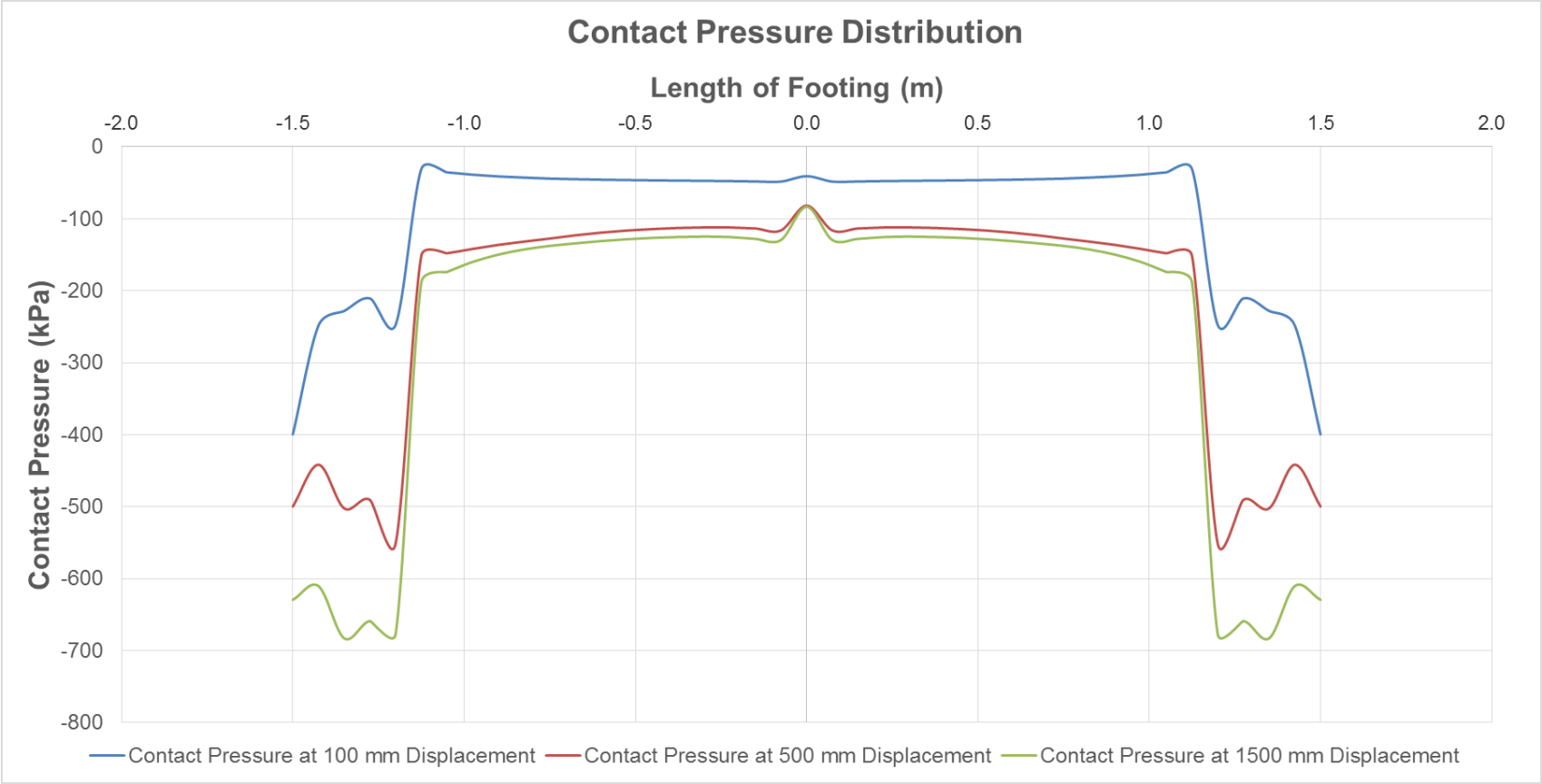


*Figure E-56: Contact pressure distribution (two 3 m long, 0.45 m wide trenches in 40 kPa native clay; no embedment depth)*

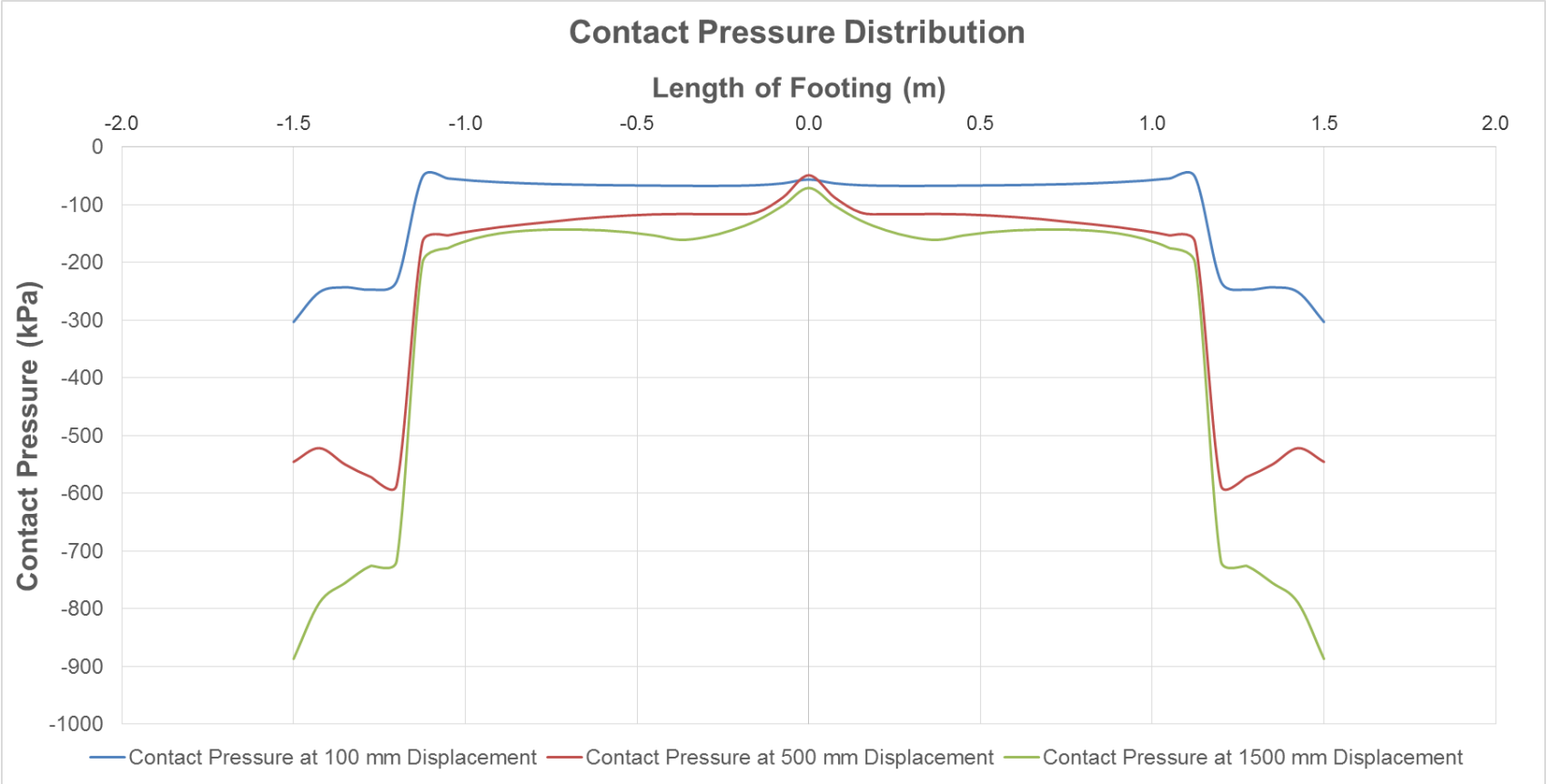


*Figure E-57: Contact pressure distribution (two 3 m long, 0.45 m wide trenches in 40 kPa native clay; 1.5 m embedment depth)*

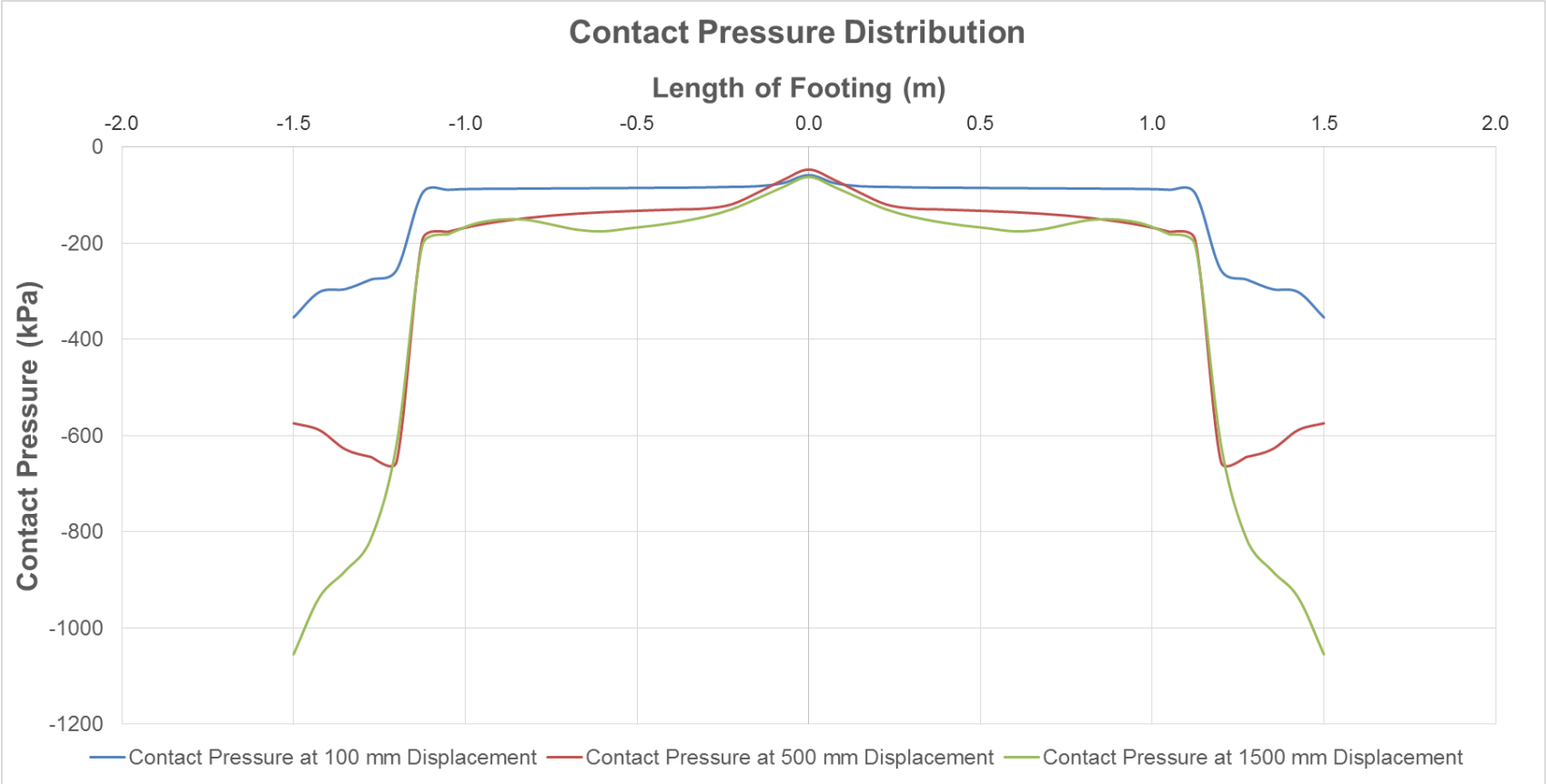


*Figure E-58: Contact pressure distribution (two 3 m long, 0.45 m wide trenches in 40 kPa native clay; 3 m embedment depth)*

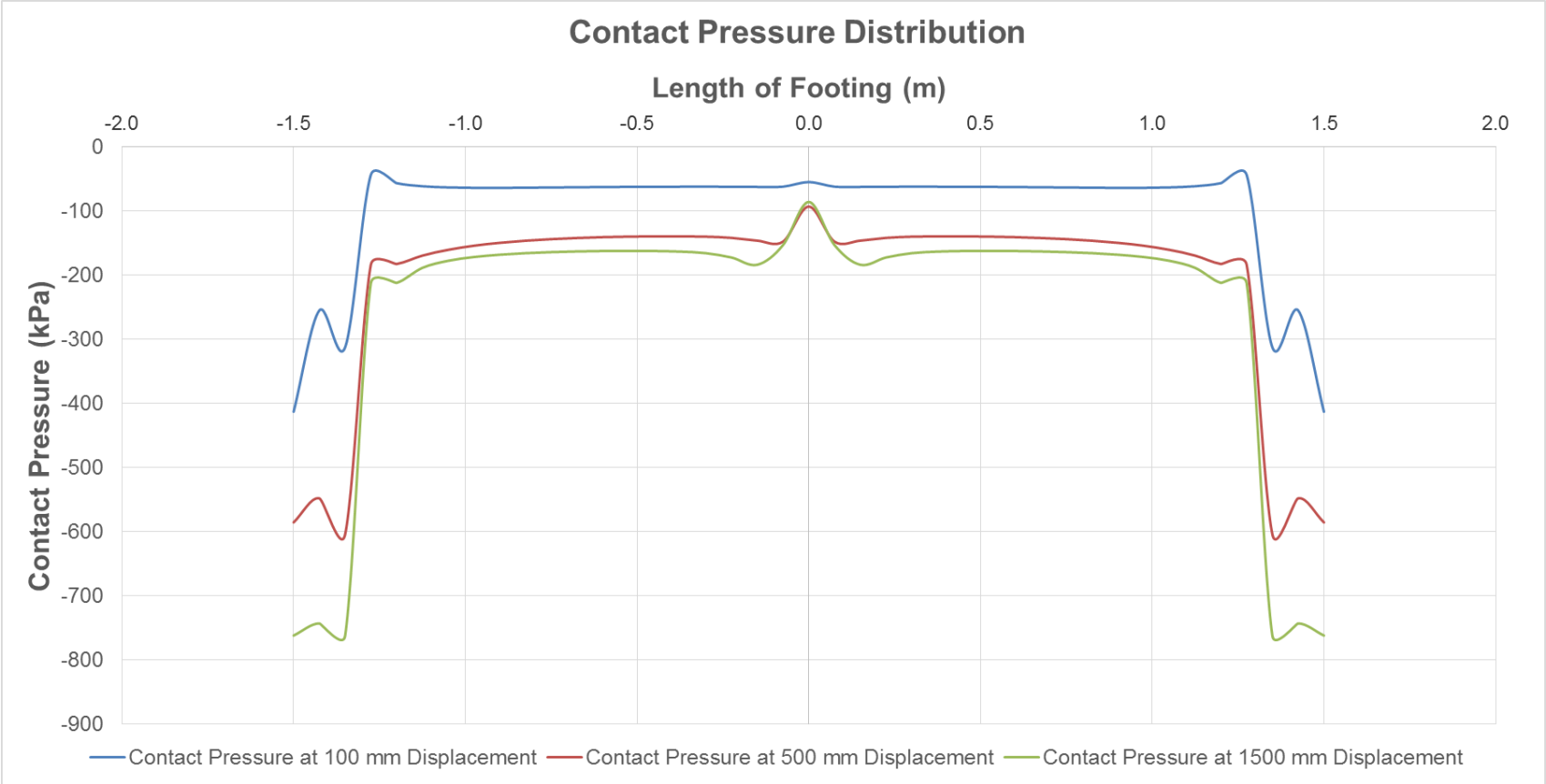


*Figure E-59: Contact pressure distribution (two 3 m long, 0.3 m wide trenches in 40 kPa native clay; no embedment depth)*

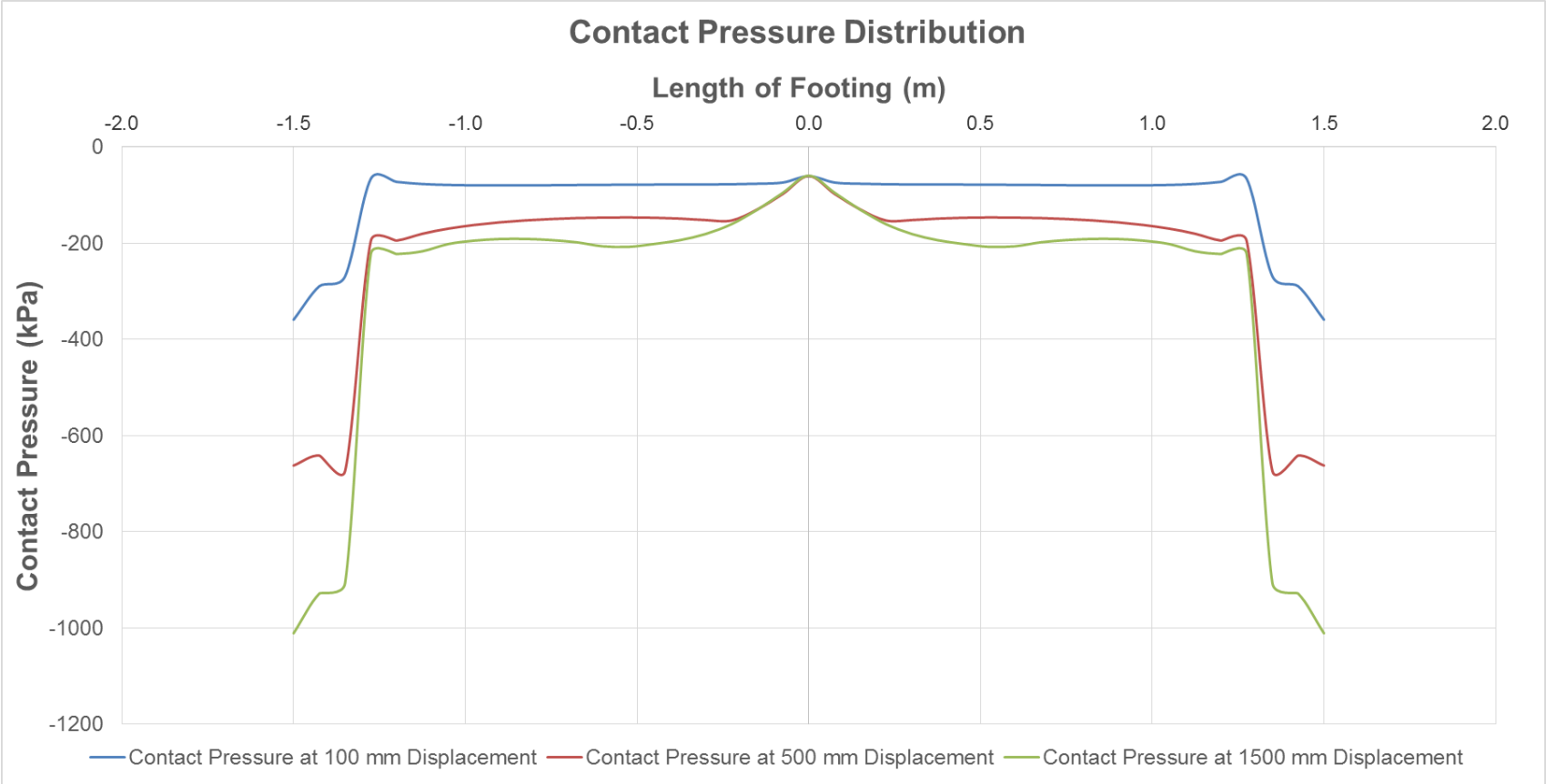


*Figure E-60: Contact pressure distribution (two 3 m long, 0.3 m wide trenches in 40 kPa native clay; 1.5 m embedment depth)*

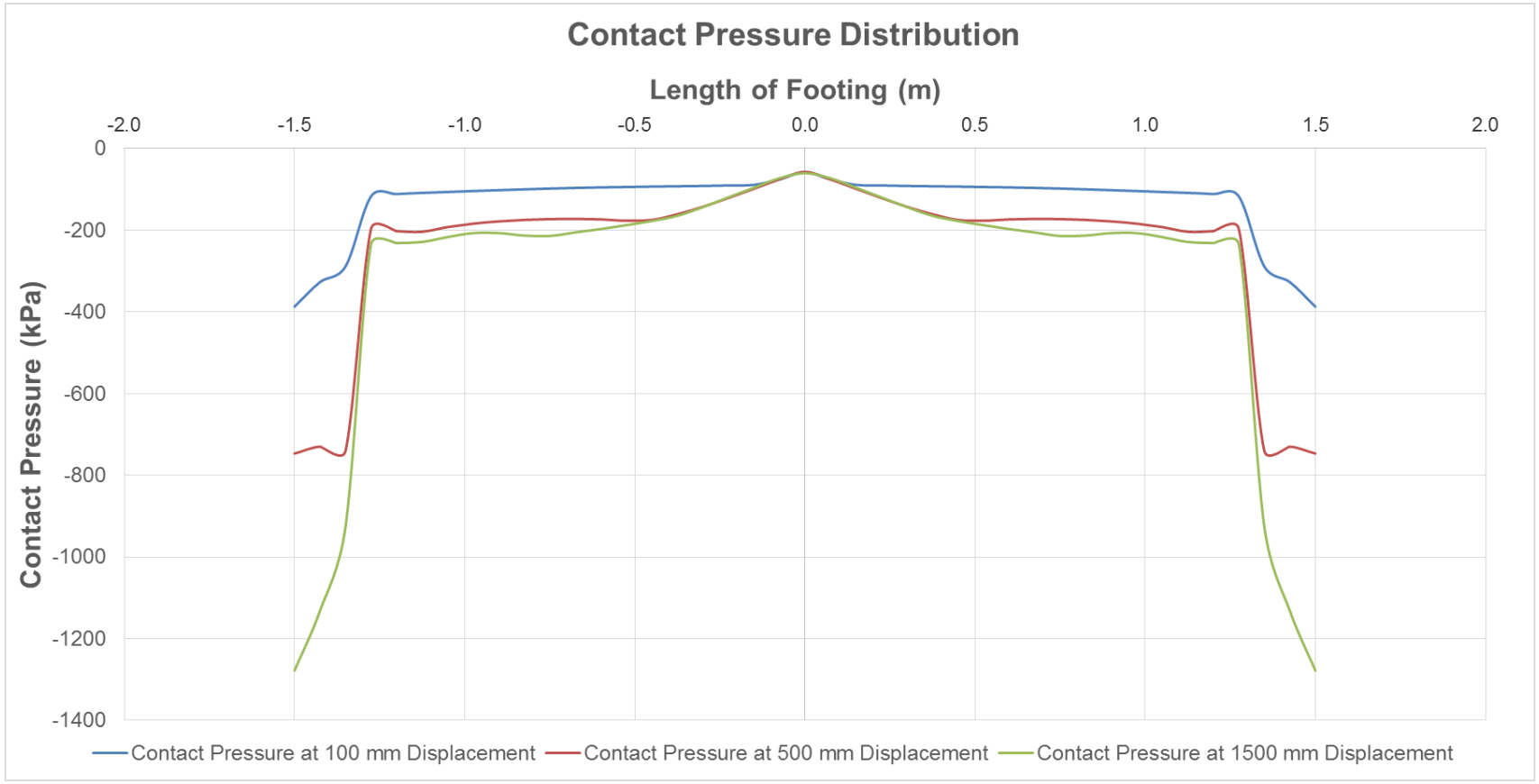


*Figure E-61: Contact pressure distribution (two 3 m long, 0.3 m wide trenches in 40 kPa native clay; 3 m embedment depth)*